2’-Deoxy-6-Thioguanosine: Synthesis of Monomer, Oligomers and Long DNA, and their Binding with Metal Ions

Samira Hribesh

Newcastle University

A thesis submitted for the degree of
Doctor of Philosophy

School of Chemistry

2013

Abstract

The formation of one-dimensional (1D) coordination polymers using thiolated DNA nucleosides and nucleotides with transition metals was investigated. 2'-Deoxy-6-thioguanosine was successfully synthesised and characterized by ^{1}H-NMR, ^{13}C-NMR, IR, MS and UV spectroscopy. Subsequently, the binding of several transition metal ions to 2'-deoxy-6-thioguanosine and 6-thioguanosine was studied. The binding ratio of thio-monomer with metal ions was shown to be three ligands to one metal in the case of cobalt (II) and nickel (II), whilst in the case of the cadmium (II)-complex with the thio-monomer, the results suggested that a 1D coordination polymer might be formed, although no crystal data was obtained to confirm this structure. Therefore, the oligonucleotides containing the thiolated monomer were synthesised to extend this study. The preparation of thiolated homo-guanosine oligomers involved standard solid phase synthesis of oligo-guanosine followed by on-column conversion of guanosine to 6-thioguanosine. The thiolated reaction was the same as that used for the monomer and yielded 2-, 3-, 4- and 5-mer thio-oligomers in good yield. The thio-oligomers were purified by HPLC and were fully characterized by mass spectrometry and UV. The interaction of thio-oligomers with cadmium (II) ions was investigated. For the dimer and tetramer, the binding ratio was two thio-bases bound to one cadmium, whereas for the trimer and pentamer the binding ratio showed more than one binding species in solution. In order to synthesise a long thiolated DNA polymer, an enzymatic slippage reaction was performed, where a short primer-template of poly (**dG**)$_{10}$-poly (**dC**)$_{10}$ was extended up to 300 bp using Klenow exo^{-} polymerase and nucleosides triphosphate (**d-tGTP** and **d-CTP**). The addition of cadmium ions to thio-modified DNA suggested a structure resembling M-DNA as coordination polymer is obtained according to UV titration data.

Acknowledgements

First of all, profusely all thanks for God, who helped me to achieve this work.
I would like to express my thanks to my supervisor **Dr. Andrew R Pike** who gave me the chance to work with him and for close supervisor, guidance, advice, courteous supports and helpful comments throughout all stages of this work. Many thanks to Dr Eimer Tuite and Prof. Andrew Houlton who helped me to understand some difficult information that related to this work.

I would like to express my thanks to Faculty of Science and Chemistry Department of Newcastle University for offering me the opportunity to submit this project.

I would like to express my thanks to Dr. Majid Al Nakeeb, Dr. David Smith and Dr Sarah Upson who offered me a helping hand throughout writing my thesis. Many thanks to staff members of Nano LAP Science for their support and helpful
Last but not least, I am not going to forget my husband, my mother, my family and my friends, to them I express my sincere gratitude.

Table of Contents

Chapter 1 Introduction

1.1 Nanotechnology

Recently, significant advances have been made in the application of nanotechnology in a wide range of industries.[1-4] In particular, nanobioelectronics (bionanotechnology) which integrates elements of nanomaterials and molecular biology has led to the development of novel biosensors and medical devices.[5,6]

Nanotechnology is a technology which handles objects that have dimensions on the order of several nanometers (1 nm = 10-9 m). Recently, researchers have been using the bottom-up technique to fabricate nanomaterials via the directed assembly of the material to produce structures of a high order.[7] In addition, these nanomaterials can exhibit improved optical, electronic and chemical properties, due to their unique nanometer dimensions. These materials can be zero dimensional (0-D) including nanoparticles and nanoclusters,[8,9] one dimensional (1-D), including nanorods, nanofibers,[10,11] nanotubes and nanowires,[12] or two dimensional (2-D) which are films and sheets[13,14] with nanometer thick layers. Three dimensional (3-D) nanostructure materials are those in which the 0D, 1D and 2D structural elements are in close contact with each other to form larger structures such as polycrystals and multilayer nanomaterials.[15]

A nanowire is one type of 1D nanomaterial which exhibits electrical conductivity; it can also act as a sensing object because of its high surface-to-volume ratio.[4,16-19] Since the 1990s there have been advances in semi-conductive nanowires.[20,21] These nanowires are rod-like structures that have diameters less than 100 - 200 nm. Different fabrication techniques have been investigated to grow nanowires, for example, by epitaxial crystal growth (where the wire can be grown by seeding metals),[22] or by template based methods, which rely on biological macromolecules such as DNA (Deoxyribonucleic acid).[23]

DNA has been used as a construction tool since it is has nanoscale dimensions, is able to self-assemble, self-organise and can be functionalised for different applications.[24] Therefore, in this project, a novel approach will be employed using an enzymatic method to grow a functional DNA duplex of high macromolecular weight, and

subsequently functionalize it with metal ions to produce a conductive 1D-material which can act as a nanowire. The following sections review the importance of the fundamental structure of DNA.

1.2 DNA structure

DNA has an essential role in biology as the genetic storage material in all living organisms, due to its ability for high density information encoding.[25] The structure of DNA, in several secondary forms, has been well described since the double-helix was first proposed in 1953.[26,27] DNA usually exists as a double helix – two single-stranded species twisted about each other. The structure of a polymeric DNA single strand is composed of monomeric units of nucleotides. The nucleotide unit consists of a sugar, a nucleobase and a phosphate group as shown in Figure 1. The DNA sugar is 2'-deoxyribose and its OH group on the 1'-carbon is substituted by one of four nitrogenous nucleobases. The four nucleobases of DNA are two purine bases [adenine (A) and guanine (G)] which are attached to the sugar at N(9), and two pyrimidine bases [thymine (T) and cytosine (C)] which are bonded to the sugar at N(1), as shown in Figure 2. The structure of the DNA duplex consists of two anti-parallel single strands composed of polynucleotides which are associated with each other *via* hydrogen bonding between the bases to form a double helix as shown in Figure 3.

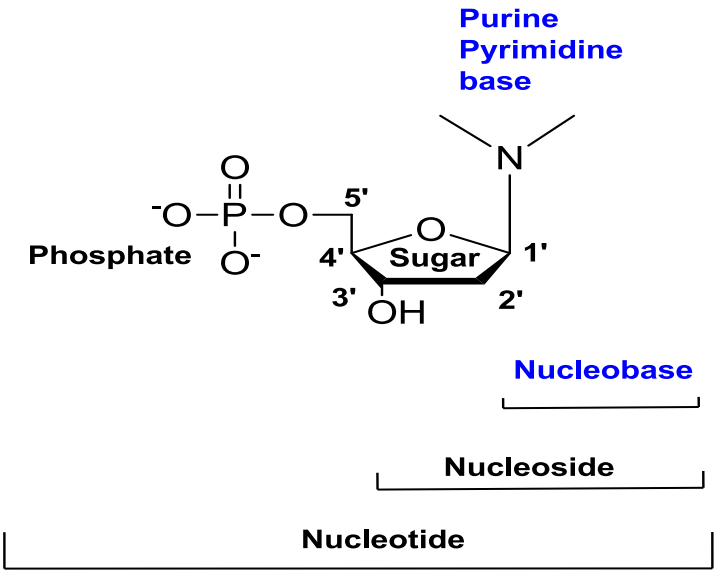

Figure 1. The structure of nucleoside and nucleotide.

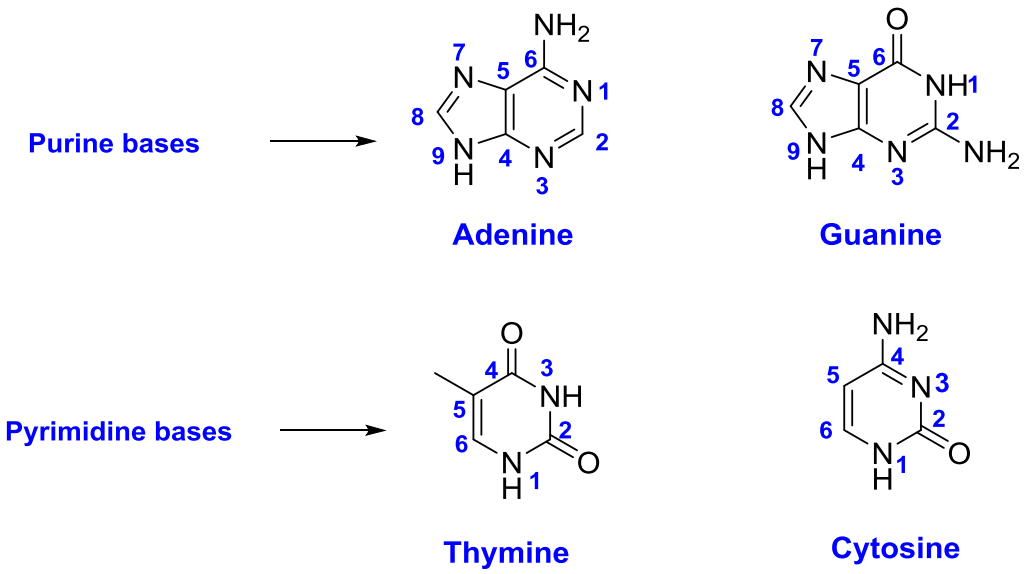

Figure 2. DNA bases, purine bases (adenine and guanine) and pyrimidine bases (thymine and cytosine).

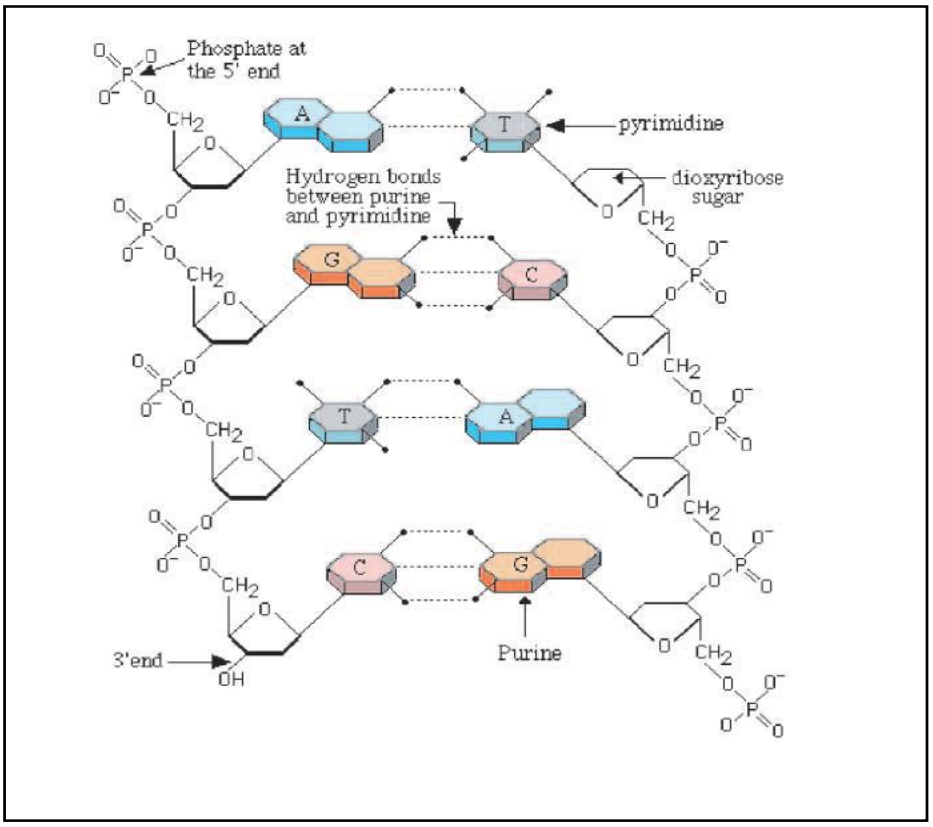

Figure 3. Schematic structure of double stranded DNA, showing covalent and hydrogen bonds.[28]

This double helix of DNA was first proposed from fibre X-ray diffraction by Watson and Crick in 1953 who suggested that intermolecular hydrogen bonds were formed between specific base pairs.[27] This was confirmed in high resolution structures in subsequent years. In Watson-Crick base pairing, adenine (A) pairs only with thymine (T) whereas guanine (G) pairs only with cytosine (C) in the DNA duplex, as shown in Figure 4.

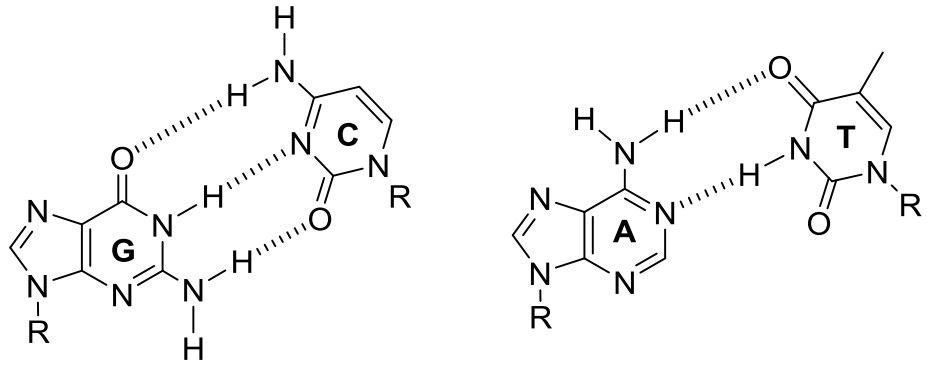

Figure 4. The Watson-Crick base-pairing for AT and GC base pairs.

The DNA duplex structure is defined by the comparative conformations of the bases in the base-pairs and the orientations of the adjacent base-pairs relative to one another. As a result all of this flexibility, DNA can adopt a diversity of conformations, such as B-DNA, A-DNA and Z-DNA. B-DNA is the most common secondary structure in solution and in cells.[27] B-DNA is a right handed double helix with a diameter approximately 2 nm. It has a base separation of 0.34 nm along the helical axis and a helical twist of helix of 36° per base. This result is in a complete turn every 3.4 nm; therefore, there are about 10 base pairs per turn. The base pairs are located towards the central axis of the helix. Moreover, the external structure of the helix consists of two grooves, the major and minor grooves. Consequently, DNA can interact and bind with some small molecules through the space between stacked bases (intercalators) or in the grooves (groove binding molecules).[27,29,30]

1.3 DNA as a tool for nanotechnology

In recent years, DNA has been used as a tool to fabricate nanomaterials, particularly nanowires. This process of material templating is based on bottom-up approaches and can be used to give DNA new properties. Recently researchers have been using the bottom-up techniques to fabricate nanomaterials that depend on their self-assembly in the presence of DNA.[7] DNA is an appropriate polymer for templated nanofabrication as it can create intra- and intermolecular hybridization and can be controlled by the size, shape, length and sequence. Furthermore, DNA has highly specific chemical interactions with other nanomaterials.[7,31] This is largely due to the self-complementary nature of the double helix and its relative stability. One particular structural property of DNA that has been exploited is its nanoscale dimensions; 2 nm wide but many micrometres in length. It has a very high aspect ratio and because of base pair stacking and fixed sugar conformation the DNA duplex is relatively rigid. Therefore, it has a large persistence length, *ca* 150 nm, and adopts a more linear conformation in solution compared with other synthetic polymers that form higher order random coils. Thus its role in the fabrication of conductive nanowires has been a topic of much interest.[32] However, DNA itself acts as an insulator rather than a conductor, even though the debate about this property has been continuing for the last 20 years.[33,34] As a result, DNA in its natural form is not suited to the field of nanoelectronics, but DNA has many properties that allow it to be suitable as starting material that can be used after molecular level modifications. The phosphate groups of the DNA backbone have a negative charge and hence form a polyanionic backbone; therefore DNA can interact with charged species through electrostatic interactions, such as metal ions and conducting polymers.[35] The simplest concept is that DNA acts as a guide or a template for the association of nanoscale materials along the helix.

1.3.1 Exploiting DNA as a template for nanomaterials

The use of DNA as a template has been considered for nanoscale electronic materials. This approach transforms the insulating DNA into a nanowire that has conductivity. One way in which this can be achieved is by covering DNA with metals.[29,36,37] DNA can act as a template where an electrostatic interaction between the negative charge of the

phosphate group of the double strand of DNA and cations such as metal ions has been exploited.[37]

One method of electroless plating for metallizing DNA utilizes a sequence of three major steps. The first step generates the reactive metal sites *via* binding of metal ions or metal complexes to the DNA template. This can be achieved by ion-exchange into the DNA strands[29] or the incorporation of a metallic complex between the nitrogenated bases of DNA.[38,39] Secondly, the manipulation of the activation steps with reducing agents as shown in Figure 5. The third step is the use of catalysts to selectively deposit the metal along the DNA backbone.[29] However, the disadvantage of this construction method is the uncontrolled growth of the metal deposited along the DNA strands.[29]

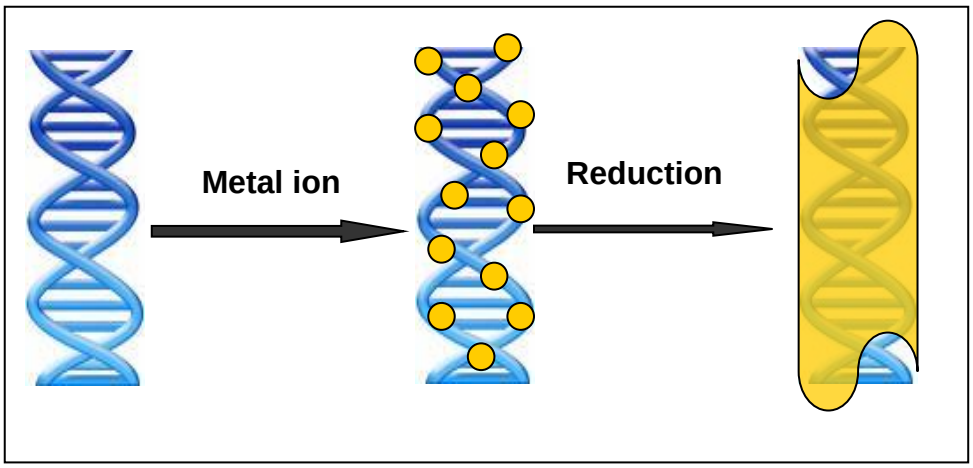

Figure 5. Schematic representation of the route to DNA-metal hybrids *via* metal ion depostion and subsequent reduction to the metal.

The most common approach to metallize a DNA template is the ion–exchange technique. For instance, Braun *et al.*[29] used this technique to fabricate a Ag nanowire. They reported that silver metal Ag was localized along a strand of lambda (λ)-DNA through ion exchange of sodium for silver cations localized along the phosphate backbone. The chemical reduction of the silver ions *via* hydroquinone led to the aggregation of silver metal on the DNA template. Initially the formation of Ag nanoparticles along the DNA template was observed, which led to the deposition of metallic silver on the dsDNA to produce a semiconducting wire immobilized between gold electrodes approximately 100 nm in length.[4] Several groups have developed DNA nanowires based on ion-exchange with other metals and are summarized below.

Richter and co-workers used a similar method to Braun *et al*. [29] to metallize DNA with palladium metal. A surface of a glass coverslip was prepared to immobilize DNA by the evaporation of small drop of DNA on the surface.

Then aqueous palladium acetate was added to the surface for two hours, to allow palladium ions Pd^{2+} to associate with DNA. The reduction of Pd^{2+} to Pd metal was achieved through treatment with sodium citrate, dimethylamine borane and lactic acid. As a result, the formation of chains of nanoparticles of palladium on λ-DNA that led to the fabrication of a palladium wire, which was 20 nm in diameter, as seen in Figure 6. However, the conductivity of the wire was not investigated.[40] Moreover, other metals have been studied using the metallization method such as the deposition of gold on the negative charge of double strand DNA by electrostatic interactions.[41,42] Other approaches have been used for the metallization of Pt [39,43,44] and Pd *via* complexes with the bases of DNA.[45]

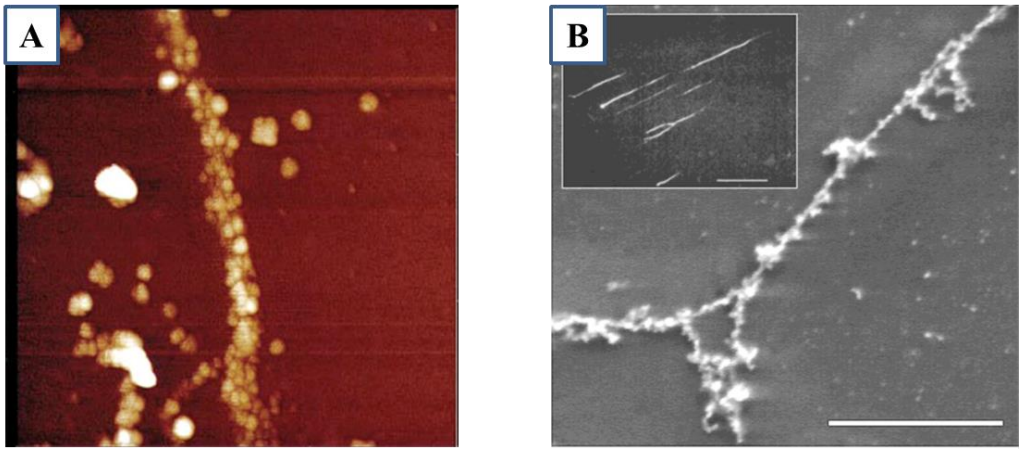

Figure 6. A) AFM image of silver DNA template produced by Braun *et al.* showing a diameter of 100 nm.[29] B) SEM image of Pd-metalized DNA.[40]

This area of work has been recently developed by the Chemical Nanoscience Laboratory in Newcastle University who found that the deposition of Ag along DNA can be controlled by first templating 2-(thiophen-2-yl)-1H-pyrrole (**TP)** onto a DNA template. This was achieved by the polymerisation of the **TP** monomer using $FeCl_3$ as an oxidant in the present of λ-DNA. Subsequent additional of Ag^+ ($AgNO_3$) on the conductive polymer was influenced by the alkynyl group. Therefore, the fabrication of uniform silver nanowires was achieved,[46] as shown in Figure 7.

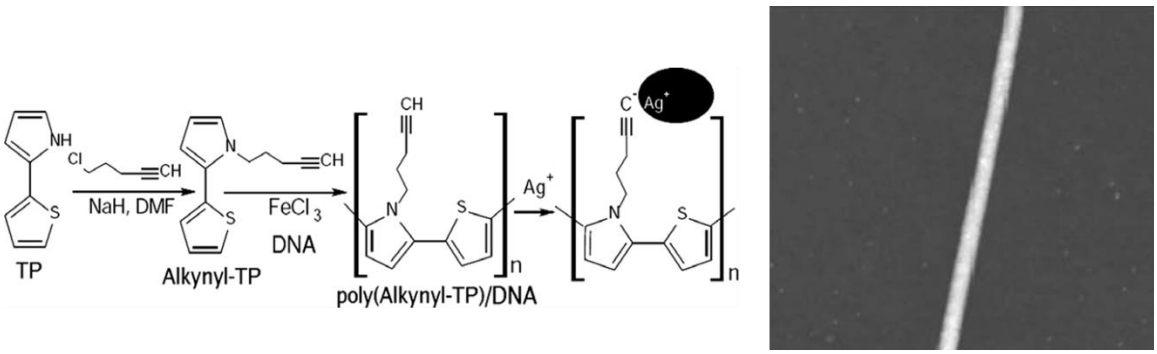

Figure 7. Tapping mode AFM image of a DNA nanowire on SiO_2/Si. Ag/poly (alkynyl-**TP**)/DNA.[46]

In other work, Houlton *et al.* were able to control the templating of CdS on DNA to make either continuous uniform nanowires as seen in Figure 8 or chains of monodispersed quantum-confined particles.[47]

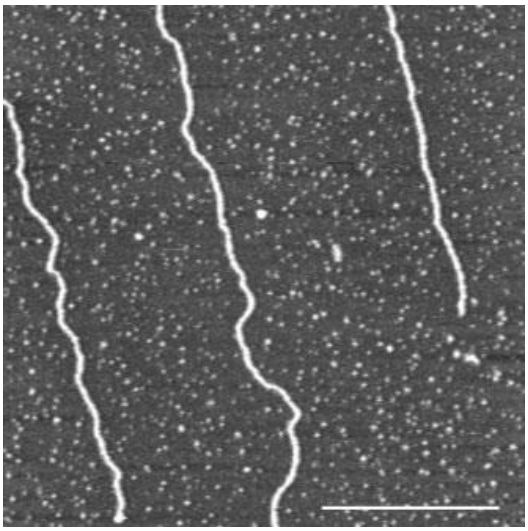

Figure 8. AFM characterization of CdS nanowires formed in DNA containing solutions after standing for 48 h. Scale bars: 500 nm; the height scale is 3 nm.[47]

However, templated synthesis lacks control with regards to the amount of material that is deposited along the dsDNA template. As a result, DNA hybrids such as DNA templated nanowires do not have a precisely known composition.[29] Therefore, other possible modifications that utilise covalent bonds are also attractive approaches to building highly regular nanostructures.

1.3.2 Exploiting DNA as a molecular scaffold

As mentioned above, DNA templating relies on the electrostatic interaction between the binding sites on DNA (negative charge of the phosphate group) and the templating material. Conversely, scaffolding is the method to incorporate a material that is directly integrated into the DNA structure by covalent binding. DNA has been used as a scaffold for a range of functional groups.[48] This has been achieved by the covalent modification of nucleosides and their incorporation into DNA *via* solid-phase DNA synthesis. Oligonucleotides can be modified at the sugar, phosphate and nuclebase positions as seen in Figure 9.

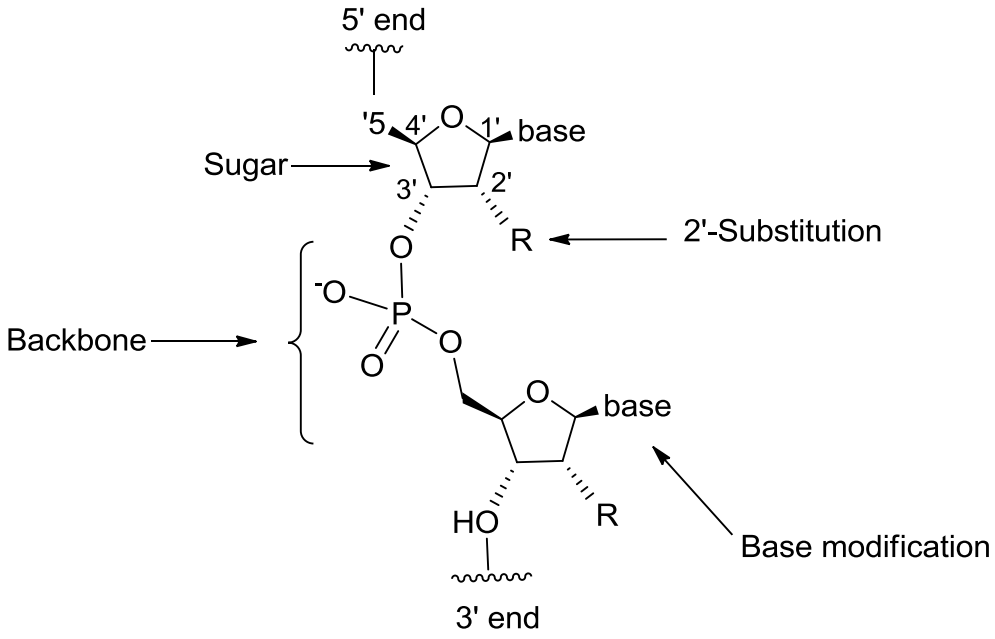

Figure 9. The chemical modified oligonucleotides sites.

1.3.2.1 Sugar modification

The 2'-deoxyribose ring in DNA can be modified to synthesise oligonucleotides that have stability toward enzymatic degradation. Therefore, these synthetic oligonucleotides can be utilised in RNA interference as well as antisense technology.[49-52] 2'-Deoxy-2'-fluororibonucleosides are examples of sugar modifications that might be suitable as antisense agents. In addition, they can increase the affinity of oligonucleotides for the complementary RNA strand.[53-55] The modification of

2’-deoxyribose can also be introduced to investigate hammerhead ribozymes where the hydroxyl group is replaced by amino, methoxy, and 2’-*C*-allyl groups.[56-59] There is another possible modification of the ribose sugar, where the oxygen in the ribose ring is substituted by nitrogen or sulphur. Haraguchi and his group have reported the resourceful synthesis of a range of 4’-thionucleosides in the study of their activity toward antitumor and antiviral treatments.[60] Fox *et al*. reported that in order to develop the stability of the DNA triple helix, the synthesis of oligonucleotides that bear amino groups on the sugar or base have been performed. They reported one of the most efficient of these oligonucleotides to be bis-amino-U that has a 2’-aminoethoxy and a 5-propargylamino modification.[61]

1.3.2.2 Backbone modification

Previous studies have shown that the modification of the backbone of oligonucleotides could raise their stability for pharmaceutical uses. A general modification is the use of phosphorothioate linkages where one of the non-linkage oxygens is substituted with sulphur. There have been several reports on the phosphorothioate bridges synthesis through the use of transfer reagents containing sulphur. For instance dimethylthiarum disulphide, dibenzoyl tetrasulfide, 3*H*-1, 2-benzodithiol-3-one-1, 1-dioxide (Beaucage reagent), and phenylacetyl disulfide (PADS)**.**[62-65] Stec and his group have reported the replacement of the oxygen of the phosphate linker by a selenolinker.[66] They also reported the design of an associated phosphoroselenate internucleotide linker which might probably be utilized to examine function and structure *via* X-ray crystallography due to multi wavelength anomalous dispersion.[66] Rozners and his co-workers have synthesized a range of oligoribonucleotides with amide linkages.[67] Caruthers *et al*. have established the synthesis of oligodeoxynucleotides with phosphonoformate bridges. They used these for participating in binding of antisense without degradation by cellular nucleases.[68] Nielsen and his group have used ring-closing metathesis to produce different internucleotide linkages in addition to the phosphate linker. This modification can lead to the stabilised secondary structure of nucleic acids, for example three-way junctions and bulges.[69]

Obika and his co-workers have introduced different amino alkyl moieties to the sulphur group of stereodefined phosphorothioate oligonucleotides. One of the amino alkyl

conjugated isomers of phosphorothioate show enhancement in the stability of the DNA duplex whereas other isomers destabilized DNA duplex.[70]

1.3.2.3 Base modification

The purine and pyrimidine bases offer complementary hydrogen bonding functional groups in DNA. The structure of modified bases should be carefully designed when introduced into oligonucleotides, as it can provide information on the important specificity of a functional group in the normal base. The most informative positions for nucleoside base substitution are those sites that are exposed to solvents in the major groove of the DNA duplex such as the C(6)-site and N(7)-site of purines and the (C4)-site and C(5)-site of pyrimidines[71] as shown in Figure 10.

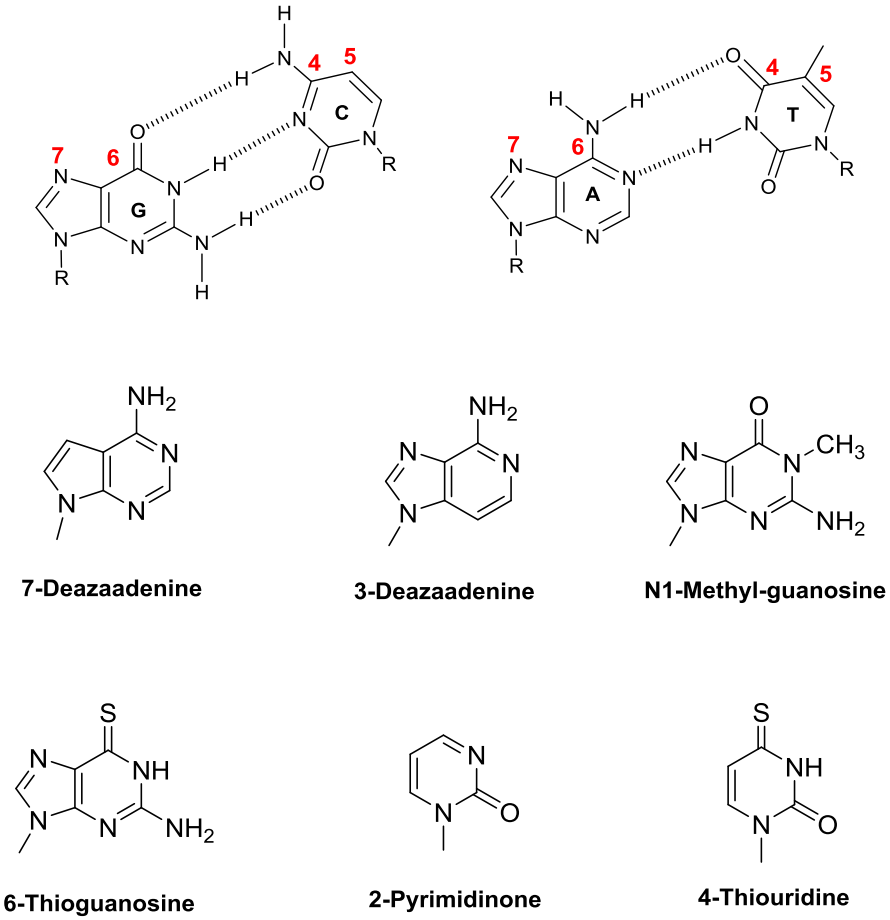

Figure 10. Positions for nucleoside base substitution sites that are exposed to solvents in the major groove of the DNA duplex (top). Some examples of purine and pyrimidine bases modification (bottom).

In the purine nucleosides, the imine nitrogen at position N(7) is located in the DNA major groove. In addition it can work as a possible hydrogen bond acceptor position in recognition. For instance, 7-deazapurine nucleosides, which lose their N(7) nitrogen atom, are useful for examining the role of N(7) in recognition. These modified bases can simply be inserted into oligonucleotides by automated solid phase synthesis or *via* enzymatic reaction.[72-74] 7-deazaadenine and 7-deazaguanine were used to investigate restriction enzyme–DNA interactions and protein-DNA interactions.[75-78] Other examples that have utilized modified 7-deazapurines are the examination of DNA-DNA interactions in homologous recombination.[79] The N(3) site of purines is positioned in the DNA minor groove and is indirectly involved in the formation of base pair hydrogen bonding. On the other hand, 3-deazaadenosine inserted into the hammerhead ribozyme significantly decreases its efficient catalysis.[80] Another example for purine modification is N1-methylguanosine, which when replaced in the centre area of the hammerhead ribozyme, totally prevents its catalytic activity.[81] The 6-position of purine bases can be modified as well to give bases such as 6-mercaptopurine and 6-thioguanine. Yoshida *et al* reported that an antimetabolite nucleoside 2'-deoxy-6-thioguanosine triphosphate can be efficiently incorporated into DNA *via* DNA polymerase α.[82] However, there is another method to synthesis the oligonucleotides containing 2'-deoxy-6-thioguanosine, the automated solid-phase phosphoramidite approach.[83] This synthesis requires special protection of the thione functional group from hydrolysis and oxidation *via* the use of the cyanoethyl protecting group.[83]

The 2-pyrimidinone and 4-thiouridine ribonucleosides have been reported to improve catalysis by the hammerhead ribozyme.[84] Harvey *et al.* have modified DNA oligomers by functionalising the 4-amino group of cytosine with N-(2-aminoethyl) aniline to create a conductive polymer.[85] The modified DNA was treated with horseradish peroxidase and H_2O_2 to polymerise the aniline along the DNA double strands. However, they found that in the region of the oligoaniline, the Watson-Crick hydrogen bonds of the duplex are broken and the positions of the nucleobases are distorted. Nevertheless, the flanking regions of the supporting duplex were not damaged. Therefore, the combination of conductive polymers with DNA may be useful in electronic applications.[85] Carell and his colleagues have used the "click" reaction which involves the copper catalysed reaction of alkynes with azides to modify pyrimidine triphosphates as seen in Scheme 1.[86] Click chemistry can provide high conversion rates; more than 90% of fragments of DNA produced by PCR are modified.[78]

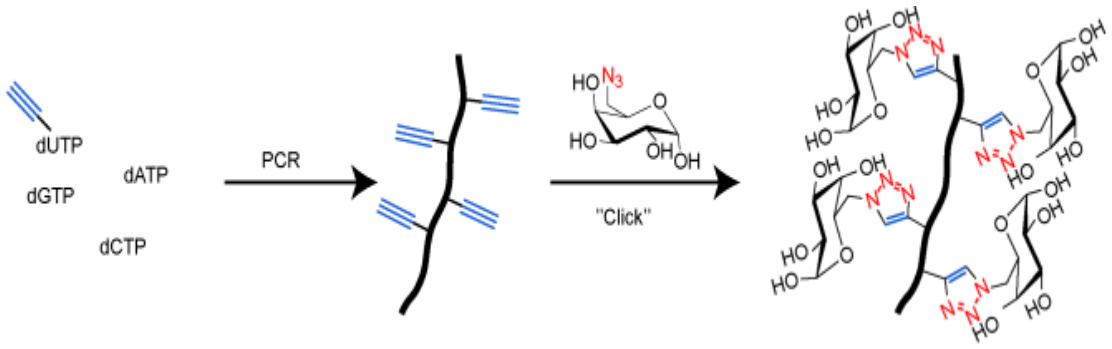

Scheme 1. Schematic illustration of the post-synthetic functionalization of DNA strands by using click chemistry.[86]

Sakthivel and Barbas have used 5-(E-3-aminopropenyl)-2'-deoxyuridine triphosphate as substrate for DNA polymerases *via* PCR.[87] Benner and his colleagues have reported the synthesis of some new 2'-deoxycytidine derivatives that bear functional amino and thiol groups. They also achieved the amplification of DNA to incorporate these nucleosides after conversion into triphosphates.[88]

1.4 Metallized DNA

The templating of metals by DNA has already been discussed above, and another approach to metallize DNA is to form metal complexes within DNA. Metal salts which interact with unnatural DNA bases were extensively studied before the secondary structures of the duplex DNA were explored.[89] Later, the DNA complexes with metal ions were called M-DNA. M-DNA studies can be divided into reports on the creation of non-canonical base pairs from the natural nucleobases under metal ions participation, and the replacement of the hydrogen bonding atoms involved in the Watson-Crick base pairing by metal ions.[90]

Metal ion binding between DNA double strands was found by Katz for thymine-rich sequences with Hg(II) salts. He proposed a structure of binding (**T**–Hg–**T** metal–base pair), in which the proton at N(3) position is removed for every thymine base,[91,92] as seen in Figure 11.

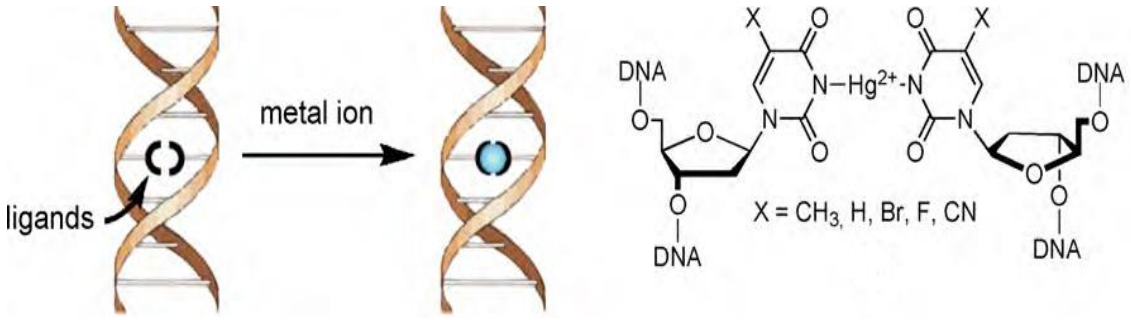

Figure 11. Formation of T-Hg-T base pairs from the simple trinucleotide 5'-d(T3)-3' upon addition of Hg^{2+} ions**.**[33]

Marzilli and Buncel, later proved this observation of Hg (II) binding to a thymine pair bases by NMR spectroscopy, CD and UV titration.[93,94] Later, Ono *et al*. found that upon addition of Ag^{+} to a DNA duplex containing cytosine-cytosine mismatches, a metal-base pair C-Ag-C formed.[95] These findings of a C-Ag-C formation were later confirmed by Muller and his group by UV and CD experiments.[96] Lee *et al.* have found that the addition of divalent metal ions Zn^{2+}, Ni^{2+} and Co^{2+} to duplex DNA forms a complex at pH above 8, they called M-DNA,[97,98] as shown in Figure 12.

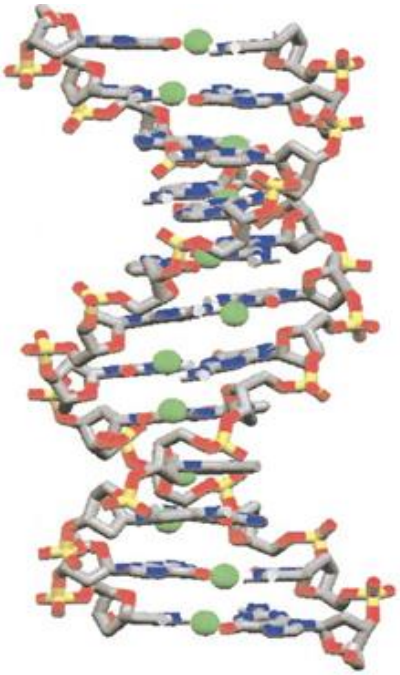

Figure 12. Modelled structure of M-DNA, zinc ions are shown as green spheres and are buried in the centre of the helix.[98]

They reported that the formation of M-DNA depends on the concentration of metal ions, DNA and the pH conditions. Moreover, the addition of EDTA to M-DNA can cause the reformation of B-DNA and removal of the metal ions. Furthermore, they have explained the structure of M-DNA by NMR that illustrated the imino protons of the base pair have been removed and replaced with divalent metal ions as shown in Scheme 2. As metal ions have free orbitals they can bind to the bases of B-DNA by coordination bonding. Recently it was found that M-DNA has some electronic properties and could behave as a molecular wire.[99]

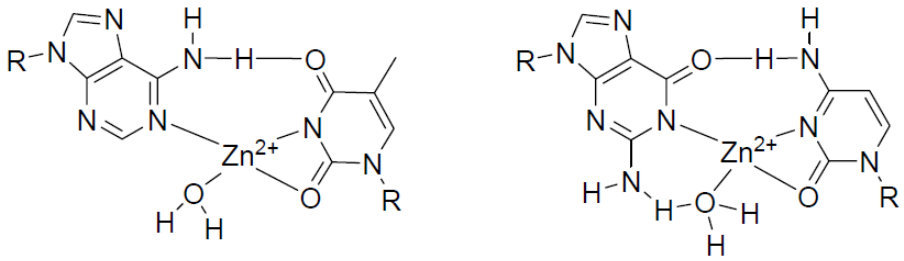

Scheme 2. Suggested structure of the Zn^{2+}-coordinated **AT** and **GC** base pairs in M-DNA.

It was found that, the normal nucleobases were capable of binding only limited amounts of metal ions. Therefore, designed, synthetic nucleobases that bind to metals were developed for novel metal-base paring.[33] Tanaka and Shionoya first reported the synthesis of an artificial nucleobase ligand, which might be suitable for chemical coordination of metal ions inserted into the double helix of DNA as shown in Figure 13.[100]

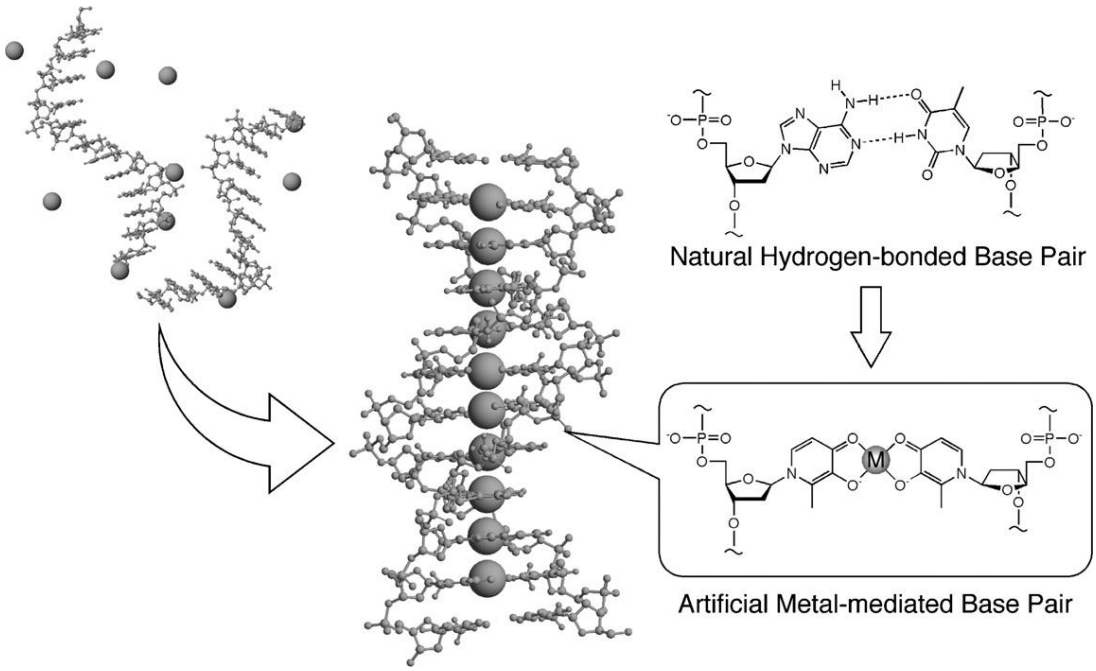

Figure. 13. Artificial DNA which has metallo-base pairs instead of hydrogen-bonded pairs.[101]

A complex of *o*-phenylenediamine–palladium in solution was synthesized; however, the insertion of these modified nucleosides into oligonucleotides was not yet established at that time.[100] In 2000, Meggers and his colleges reported the first successful synthesis of metal-base pairing that depend on modified ligands as a replacement for normal nucleobases incorporated into DNA.[102] A mixture of a pyridine (Py) nucleoside and a ligand of planar tridenate [pyridine-2,6-dicarboxylate (Dipic)] were inserted into the self-complementary dodecamer sequence [d(5'-CGCG**Dipic**AT**P**CGCG)$_2$]. The copper base pair-Dipic-Py complex was formed when the Cu (II) ion was added, which makes DNA strands significantly more stable. Later, Shionoya *et al.* reported the incorporation of five copper–hydroxypyridone base pairs into a DNA double strand.[103] The copper ions were coordinated in the middle of the DNA helix and supposedly stack on top of each other as shown in Figure 14.

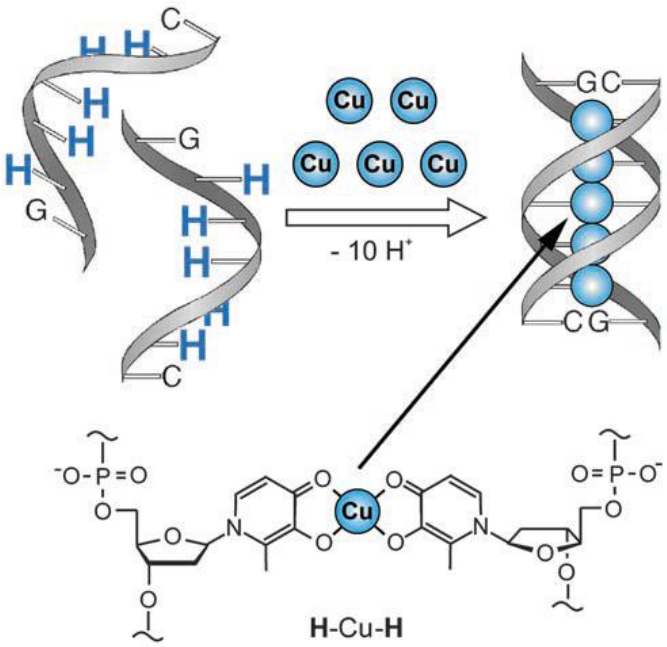

Figure 14. Schematic depiction of the assembly of a duplex containing five stacked Cu^{2+} consisting of a short palindromic oligonucleotide containing five consecutive hydroxypyridone ligands flanked by only one natural nucleobase on both ends.[104]

This new M-DNA was characterized by ESI mass spectrometry, EPR spectroscopy and UV and CD titrations.[103] Recently, Carell and his group reported the crystal structure of a DNA duplex consisting of a salen-type base pair (Sal-Cu^{2+}(en) Sal) inside a Bst DNA polymerase.[105]

The transition metal complexes incorporated into DNA could result in a new type of material in which the nanoscale rigidity and programmability of DNA, and the required functionality and properties of metal complexes are combined. For instance, in cases of DNA assembly, metal complexes have different distinct geometries, and these may be used to build branching or junctions of DNA with diverse spatial arrangements that would be difficult to reach by other methods. The binding of metal complexes to double stranded DNA can also modulate the DNA stability, generating the reversible and robust structures of DNA for nanomaterials. The metal complexes can have catalytic electronic or photochemical properties, and this may be relevant for materials science and biotechnology applications.[106] Another clever way to metallize DNA is *via* the formation of 1D-coordination polymers.

1.5 Coordination polymers

Coordination polymers (CP) are compounds which can be considered as the extended nature of a coordinated compound toward polymerisation. A CP has three important properties associated with metal-ligand linkers: self-recognition, reversible coordination bonds and self-assembly. The formation process of a CP happens by the self-assembly of two building blocks; metal ion (nodes) with organic ligands (linker), to create the infinite system.[107] Transition metals are usually utilised for the formation of a CP as they can offer geometric, conductive and magnetic properties.[108] The simple synthesis of coordination polymers involves the combination of two building blocks in solution by using an emulsion or template, as shown in Figure 15. More complicated procedures include the use of poor solvents, temperature, slow diffusion, thermal techniques, microwaves and ultrasound.[107,109]

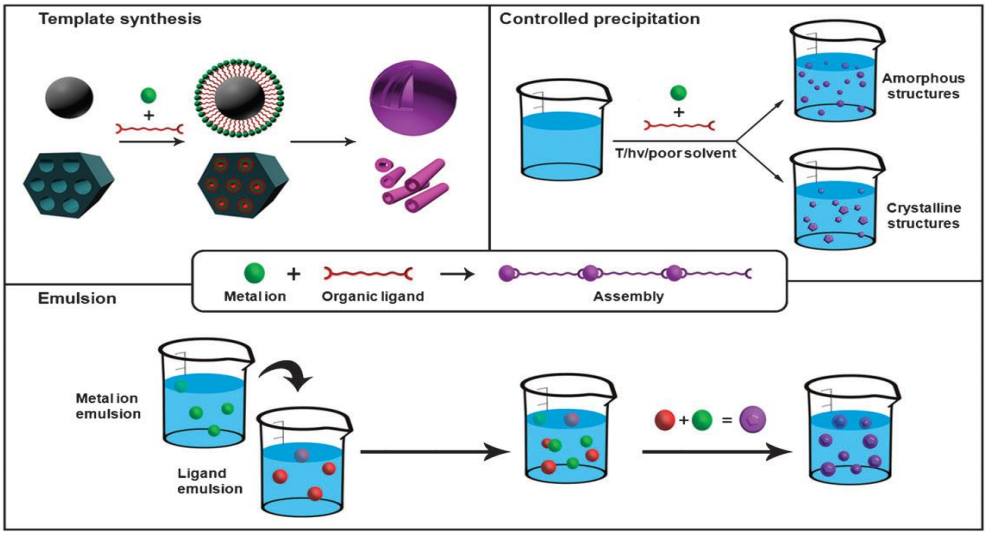

Figure 15. Schematic representation of the principal synthetic strategies used for synthesizing 1-D metal–organic nanostructures [109]

The characterisation of synthetic coordination polymers is conducted primarily by X-ray diffraction studies. Other techniques such as NMR, IR, and elemental analysis can be used to further characterise the CP structure. There are different types of conformation of CP such as linear, zigzag, ladder, rotaxane and ribbon/tape polymers,[110] as shown in Figure 16.

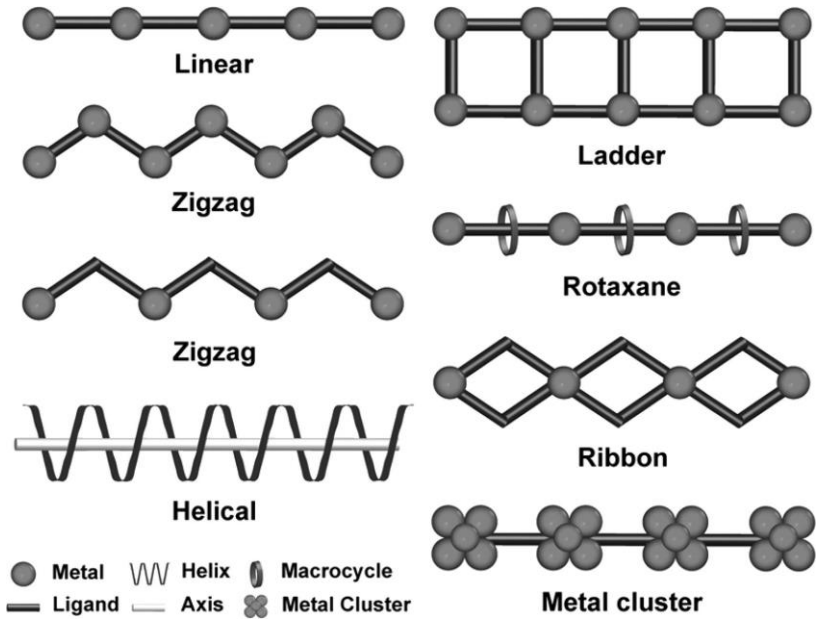

Figure 16. Different types of coordination polymer.[110]

The focus of this thesis is on the synthesis and characterisation of 1D-linear polymers, taking inspiration from Zamora *et al's* work on the complex $[Cd(6\text{-}MPH)_2.2H_2O]_n$ (6-MPH = 6-mercaptopurinate in the monoanionic form).[111] This 1D polymer was prepared by the direct reaction between 6-MPH and cadmium nitrate in methanol leading to dimer complex formation $[Cd_2\ (6\text{-}MPH)_4(NO_3)_2]\ (NO_3)_2$. When this complex was stirred in water, the coordinated nitrate was substituted by water molecules resulting in a new dimer complex $[Cd_2(6\text{-}MPH)_4(H_2O)_2](NO_3)_4$. Deprotonation of the ligands of the new dimer complex in an aqueous basic solution lead to self-assembly of the dimetallic subunits into a 1D-coordination polymer as shown in Figure 17.[111]

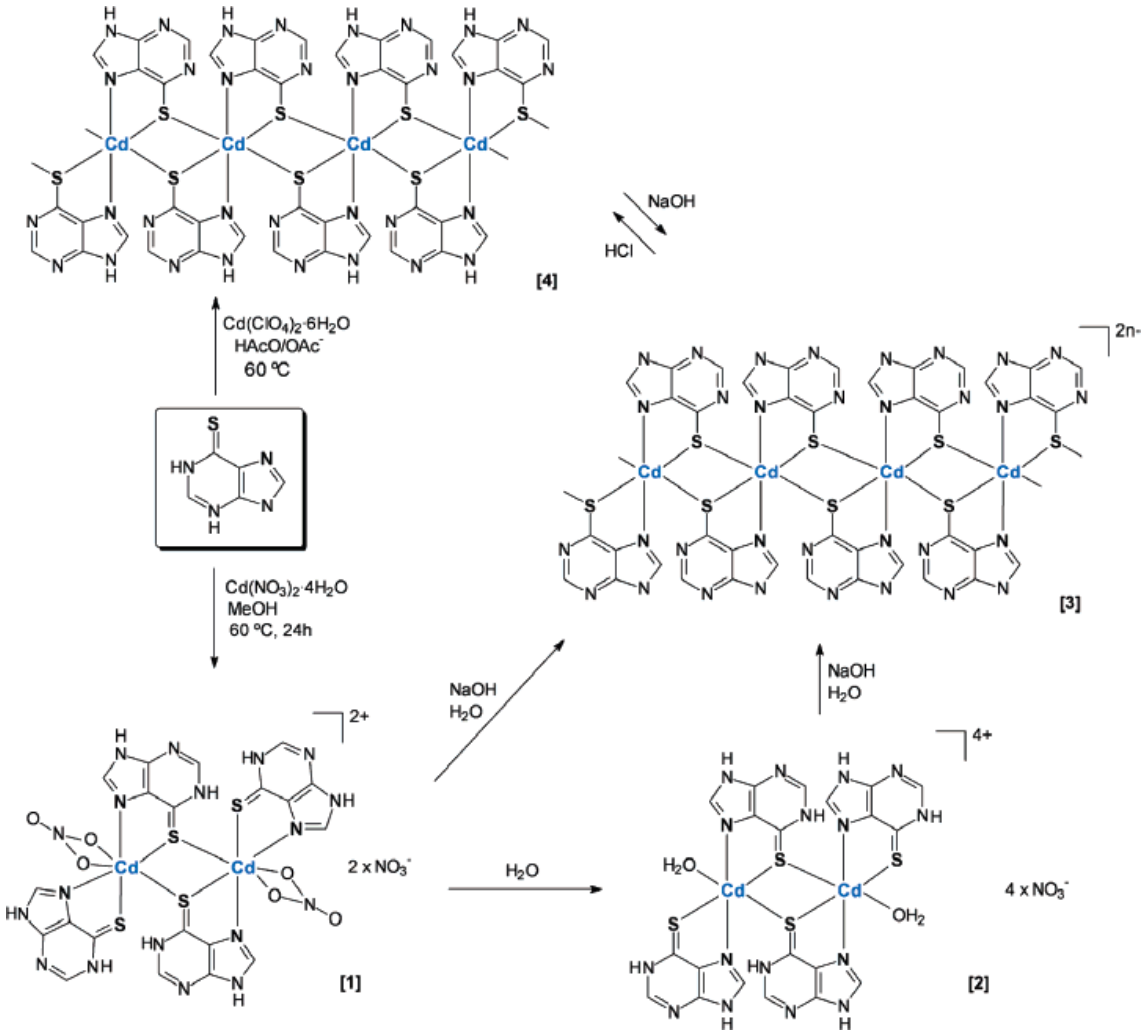

Figure 17. Represented scheme of the routes employed in the synthesis of as $[Cd(6\text{-}MPH)_2.2H_2O]_n$.[111]

Other examples of CPs are {[Co (ox)$(Htr)_2$.$2H_2O$] (ox = oxalate, Htr = 1,2,4-triazole) which was prepared by the reaction of $Co(NO_3)_2$, $H_2C_2O_4$ and Htr in an aqueous media.[112,113] In addition, there are other examples of CPs for instance [Mn(μ-ox) (4atr $_2]_n$, [Pd(OAc) $_2$(L1)]$_n$, $[Pt_2I(\mu\text{-}S_2CR)_4]_n$ and $[Ru_2Br(\mu\text{-}O_2CEt)_4]_n$.[113-116]

An extensive range of promising properties can be achieved for the multiple organic and inorganic building blocks which can be joined to organize metal-organic materials on the nanoscale. They can also be used to develop new nanomaterials for drug delivery systems such as nanoscale coordination polymers for platinum (IV), Fe (III) and Zn (II) based anticancer drugs.[117-119] In addition, their applications as encapsulating materials, contrast agents, and sensors have been reported.[120-122]

1.6 Aims of project

In light of the work reviewed above, this thesis describes the work performed to syntheise 2'-deoxy-6 thioguanosine (monomer) and then to incorporate it into oligonucleotides. For this, 2, 3, 4 or 5 thioguanosine units were linked together by phosporamidite chemistry to make short oligomers. Thioguanosine was also incorporated into DNA enzymatically with the hope of achieving modified DNA containing up to 10,000 basepairs. Subsequently, the binding of these different species with metal ions is described and the overall aims of the work summarized in Scheme 3.

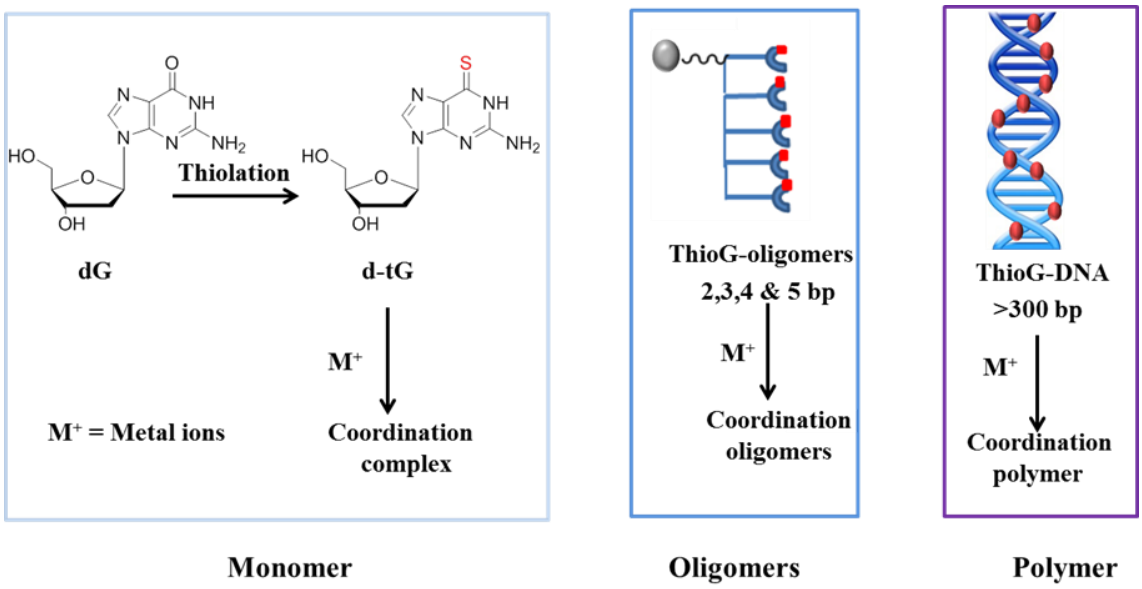

Scheme 3. Schematic routes for thesis outline.

In order to achieve these objectives, the synthesis of 2'-deoxy-6thioguanosine from 2'-deoxyguanosine *via* the thiolation reaction is required. In chapter 2, the binding properties of various metal ions with the monomer are reported.

Chapter 3 describes a way to incorporate 2'-deoxy-guanosine into short DNA oligomers *via* solid phase DNA synthesis, using phosphoaramidite chemistry, followed by conversion into the thio-guanosine through the thiolation reaction developed in Chapter 2. The ability of these thio-oligomers to act as multiple metal binding sites (ligands) that can coordinate metal ions to form Cd-S-Cd bridged polymers was also investigated.

Chapter 4 investigates the synthesis and characterisation of the thio-modified triphosphate, **d-tGTP** and its incorporation into DNA using an enzymatic slippage extension reaction. This approach introduced multiple metal binding sites into long strands of DNA. The thio-modified DNA was then treated with metal ions that can bind between two thio-sites on neighboring nucloebases in order to create a metal / DNA coordination polymer.

References

(1) West, J. L.; Halas, N. J. *Current Opinion in Biotechnology* **2000**, *11*, 215.

(2) Gordon, R.; Losic, D.; Tiffany, M. A.; Nagy, S. S.; Sterrenburg, F. A. S. *Trends in Biotechnology* **2009**, *27*, 116.

(3) Sozer, N.; Kokini, J. L. *Trends in Biotechnology* **2009**, *27*, 82.

(4) Paull, R.; Wolfe, J.; Hebert, P.; Sinkula, M. *Nat Biotech* **2003**, *21*, 1144.

(5) Merkoçi, A. *Electroanalysis* **2007**, *19*, 739.

(6) Cavalcanti, A.; Shirinzadeh, B.; Zhang, M.; Kretly, L. *Sensors* **2008**, *8*, 2932.

(7) Becerril, H. A.; Woolley, A. T. *Chemical Society Reviews* **2009**, *38*, 329.

(8) Kruis, F. E.; Fissan, H.; Peled, A. *Journal of Aerosol Science* **1998**, *29*, 511.

(9) Collier, C. P.; Vossmeyer, T.; Heath, J. R. *Annual Review of Physical Chemistry* **1998**, *49*, 371.

(10) Hurst, S. J.; Payne, E. K.; Qin, L.; Mirkin, C. A. *Angewandte Chemie International Edition* **2006**, *45*, 2672.

(11) Sun, Z.; Zussman, E.; Yarin, A. L.; Wendorff, J. H.; Greiner, A. *Advanced Materials* **2003**, *15*, 1929.

(12) Hu, J. T.; Odom, T. W.; Lieber, C. M. *Accounts of Chemical Research* **1999**, *32*, 435.

(13) Bune, A. V.; Fridkin, V. M.; Ducharme, S.; Blinov, L. M.; Palto, S. P.; Sorokin, A. V.; Yudin, S. G.; Zlatkin, A. *Nature* **1998**, *391*, 874.

(14) Schliehe, C.; Juarez, B. H.; Pelletier, M.; Jander, S.; Greshnykh, D.; Nagel, M.; Meyer, A.; Foerster, S.; Kornowski, A.; Klinke, C.; Weller, H. *Science* **2010**, *329*, 550.

(15) Buzea, C.; Pacheco, I.; Robbie, K. *Biointerphases* **2007**, *2*, MR17.

(16) Appenzeller, T. I. M. *Science* **1991**, *254*, 1300.

(17) Murray, C. B.; Kagan, C. R.; Bawendi, M. G. *Annual Review of Materials Science* **2000**, *30*, 545.

(18) Mazzola, L. *Nat Biotech* **2003**, *21*, 1137.

(19) Yogeswaran, U.; Chen, S.-M. *Sensors* **2008**, *8*, 290.

(20) Al-Mawlawi, D.; Liu, C. Z.; Moskovits, M. *Journal of Materials Research* **1994**, *9*, 1014.

(21) Yan, P.; Xie, Y.; Qian, Y.; Liu, X. *Chem. Commun.* **1999**, *0*, 1293.

(22) Thelander, C. A., P ; Brongersma, S ; Eymery, J; Feiner, L.F ; Forchel, A ; Scheffler, M ; Riess, W ; Ohlsson, B. J ;Gosele, U ; Samuelson, L. *Mater. Today* **2006**, *9*, 28.

(23) Lakhno, V. D. *International Journal of Quantum Chemistry* **2008**, *108*, 1970.

(24) Csáki, A.; Maubach, G.; Born, D.; Reichert, J.; Fritzsche, W. *Single Molecules* **2002**, *3*, 275.

(25) Goldman, N.; Bertone, P.; Chen, S.; Dessimoz, C.; LeProust, E. M.; Sipos, B.; Birney, E. *Nature* **2013**, *advance online publication*.

(26) Wilkins, M. H. F.; Stokes, A. R.; Wilson, H. R. *Nature* **1953**, *171*, 738.

(27) Watson, J. D.; Crick, F. H. C. *Nature* **1953**, *171*, 737.

(28) Braun , E.; Keren, K. *Advances in Physics* **2004**, *53*, 441.

(29) Braun, E.; Eichen, Y.; Sivan, U.; Ben-Yoseph, G. *Nature* **1998**, *391*, 775.

(30) Liu, X.; Diao, H.; Nishi, N. *Chemical Society Reviews* **2008**, *37*, 2745.

(31) Condon, A. *Nat Rev Genet* **2006**, *7*, 565.

(32) Wang, Z.; Liu, J.; Zhang, K.; Cai, H.; Zhang, G.; Wu, Y.; Kong, T.; Wang, X.; Chen, J.; Hou, J. *The Journal of Physical Chemistry C* **2009**, *113*, 5428.

(33) Clever, G. H.; Shionoya, M. *Coordination Chemistry Reviews* **2010**, *254*, 2391.

(34) Porath, D.; Bezryadin, A.; de Vries, S.; Dekker, C. *Nature* **2000**, *403*, 635.

(35) Houlton, A.; Pike, A. R.; Angel Galindo, M.; Horrocks, B. R. *Chem. Commun.* **2009**, *0*, 1797.

(36) Richter, J. *Physica E: Low-dimensional Systems and Nanostructures* **2003**, *16*, 157.

(37) Monson, C. F.; Woolley, A. T. *Nano Letters* **2003**, *3*, 359.

(38) Lund, J.; Dong, J. C.; Deng, Z. X.; Mao, C. D.; Parviz, B. A. *Nanotechnology* **2006**, *17*, 2752.

(39) Macquet, J. P.; Theophanides, T. *Biopolymers* **1975**, *14*, 781.

(40) Richter, J.; Seidel, R.; Kirsch, R.; Mertig, M.; Pompe, W.; Plaschke, J.; Schackert, H. K. *Advanced Materials* **2000**, *12*, 507.

(41) Maubach, G.; Born, D.; Csáki, A.; Fritzsche, W. *Small* **2005**, *1*, 619.

(42) Kumar, A.; Pattarkine, M.; Bhadbhade, M.; Mandale, A. B.; Ganesh, K. N.; Datar, S. S.; Dharmadhikari, C. V.; Sastry, M. *Advanced Materials* **2001**, *13*, 341.

(43) Ford, W. E.; Harnack, O.; Yasuda, A.; Wessels, J. M. *Advanced Materials* **2001**, *13*, 1793.

(44) Seidel, R.; Colombi Ciacchi, L.; Weigel, M.; Pompe, W.; Mertig, M. *The Journal of Physical Chemistry B* **2004**, *108*, 10801.

(45) Deng, Z.; Mao, C. *Nano Letters* **2003**, *3*, 1545.

(46) Farha Al-Said, S. A.; Hassanien, R.; Hannant, J.; Galindo, M. A.; Pruneanu, S.; Pike, A. R.; Houlton, A.; Horrocks, B. R. *Electrochemistry Communications* **2009**, *11*, 550.

(47) Dong, L.; Hollis, T.; Connolly, B. A.; Wright, N. G.; Horrocks, B. R.; Houlton, A. *Advanced Materials* **2007**, *19*, 1748.

(48) Bell, N. M.; Micklefield, J. *ChemBioChem* **2009**, *10*, 2691.

(49) Buchini, S.; Leumann, C. J. *Current Opinion in Chemical Biology* **2003**, *7*, 717.

(50) Kurreck, J. *European Journal of Biochemistry* **2003**, *270*, 1628.

(51) Braasch, D. A.; Corey, D. R. *Biochemistry* **2002**, *41*, 4503.

(52) Manoharan, M. *Current Opinion in Chemical Biology* **2004**, *8*, 570.

(53) Uesugi, S.; Miki, H.; Ikehara, M.; Iwahashi, H.; Kyogoku, Y. *Tetrahedron Letters* **1979**, *20*, 4073.

(54) Guschlbauer, W.; Jankowski, K. *Nucleic Acids Res.* **1980**, *8*, 1421.

(55) Kawasaki, A. M.; Casper, M. D.; Freier, S. M.; Lesnik, E. A.; Zounes, M. C.; Cummins, L. L.; Gonzalez, C.; Cook, P. D. *Journal of Medicinal Chemistry* **1993**, *36*, 831.

(56) Olsen, D. B.; Benseler, F.; Aurup, H.; Pieken, W. A.; Eckstein, F. *Biochemistry* **1991**, *30*, 9735.

(57) PiekenWA, O. D., Benseler F, Aurup; H, E. F. *Science* **1991**, *253*, 314.

(58) Paolella G, S. B., Lamond AI *EMBO J.* **1992.**, *11*, 1913.

(59) Jarvis, T. C.; Wincott, F. E.; Alby, L. J.; McSwiggen, J. A.; Beigelman, L.; Gustofson, J.; DiRenzo, A.; Levy, K.; Arthur, M.; Matulic-Adamic, J.; Karpeisky, A.; Gonzalez, C.; Woolf, T. M.; Usman, N.; Stinchcomb, D. T. *Journal of Biological Chemistry* **1996**, *271*, 29107.

(60) Haraguchi, K.; Shiina, N.; Yoshimura, Y.; Shimada, H.; Hashimoto, K.; Tanaka, H. *Organic Letters* **2004**, *6*, 2645.

(61) Cardew, A. S.; Brown, T.; Fox, K. R. *Nucleic Acids Res.* **2012**, *40*, 3753.

(62) Song, Q.; Wang, Z.; Sanghvi, Y. S. *Nucleosides, Nucleotides and Nucleic Acids* **2003**, *22*, 629.

(63) Rao, M. V.; Reese, C. B.; Zhao, Z. *Tetrahedron Letters* **1992**, *33*, 4839.

(64) Iyer, R. P.; Egan, W.; Regan, J. B.; Beaucage, S. L. *Journal of the American Chemical Society* **1990**, *112*, 1253.

(65) Ravikumar, V. T.; Andrade, M.; Carty, R. L.; Dan, A.; Barone, S. *Bioorganic & Medicinal Chemistry Letters* **2006**, *16*, 2513.

(66) Du, Q.; Carrasco, N.; Teplova, M.; Wilds, C. J.; Egli, M.; Huang, Z. *Journal of the American Chemical Society* **2001**, *124*, 24.

(67) Xu, Q.; Katkevica, D.; Rozners, E. *The Journal of Organic Chemistry* **2006**, *71*, 5906.

(68) Yamada, C. M.; Dellinger, D. J.; Caruthers, M. H. *Journal of the American Chemical Society* **2006**, *128*, 5251.

(69) Sharma, P. K.; Mikkelsen, B. H.; Christensen, M. S.; Nielsen, K. E.; Kirchhoff, C.; Pedersen, S. L.; Sorensen, A. M.; Ostergaard, K.; Petersen, M.; Nielsen, P. *Organic & Biomolecular Chemistry* **2006**, *4*, 2433.

(70) Rahman, S. M. A.; Baba, T.; Kodama, T.; Islam, M. A.; Obika, S. *Bioorganic & Medicinal Chemistry* **2012**, *20*, 4098.

(71) Verma, S.; Eckstein, F. *Annual Review of Biochemistry* **1998**, *67*, 99.

(72) Seela, F.; Kehne, A. *Biochemistry* **1985**, *24*, 7556.

(73) Seela, F.; Tranthi, Q. H.; Franzen, D. *Biochemistry* **1982**, *21*, 4338.

(74) Seela, F.; Driller, H. *Nucleic Acids Res.* **1986**, *14*, 2319.

(75) Zhang XL, G. P. *Biochemistry* **1993**, *32*, 11374.

(76) Duggan LJ, H. T., Wu S, Garrison K,; Zhang XL, G. P. *J. Biol. Chem.* **1995**, *270*, 28049.

(77) Lesser DR, K. M., Jen-; L., J. *Science* **1990**, *250*, 776.

(78) Aiken CR, G. R. *Methods Enzymol* **1991**, *208*, 433.

(79) Kim MG, Z. V., Jernigan RL,; RD., C.-O. *J. Mol. Biol.* **1995**, *247*, 874.

(80) Bevers S, X. G., McLaughlin LW. *Biochemistry* **1996**, *35*, 6483.

(81) Limauro S, B. F., McLaughlin LW *Bioorg. Med. Chem. Lett* **1994**, *4*, 2189.

(82) Yoshida, S.; Yamada, M.; Masaki, S.; Saneyoshi, M. *Cancer Res.* **1979**, *39*, 3955.

(83) Christopherson, M. S.; Broom, A. D. *Nucleic Acids Res.* **1991**, *19*, 5719.

(84) Murray JB, A. C., Arnold JRP,; PG., S. *Biochem. J.* **1995**, *311*, 487.

(85) Datta, B.; Schuster, G. B.; McCook, A.; Harvey, S. C.; Zakrzewska, K. *Journal of the American Chemical Society* **2006**, *128*, 14428.

(86) Gierlich, J.; Gutsmiedl, K.; Gramlich, P. M. E.; Schmidt, A.; Burley, G. A.; Carell, T. *Chemistry – A European Journal* **2007**, *13*, 9486.

(87) Sakthivel, K.; Barbas Iii, C. F. *Angewandte Chemie International Edition* **1998**, *37*, 2872.

(88) Roychowdhury, A.; Illangkoon, H.; Hendrickson, C. L.; Benner, S. A. *Organic Letters* **2004**, *6*, 489.

(89) Hammersten, E. *Biochem.Z.* **1924**, *144*, 383.

(90) Wettig, S. D.; Wood, D. O.; Lee, J. S. *Journal of Inorganic Biochemistry* **2003**, *94*, 94.

(91) Katz, S. *Journal of the American Chemical Society* **1952**, *74*, 2238.

(92) Katz, S. *Biochim. Biophys. Acta* **1963**, *68*, 240.

(93) Buncel, E.; Boone, C.; Joly, H.; Kumar, R.; Norris, A. R. *Journal of Inorganic Biochemistry* **1985**, *25*, 61.

(94) Kuklenyik, Z.; Marzilli, L. G. *Inorganic Chemistry* **1996**, *35*, 5654.

(95) Ono, A.; Cao, S.; Togashi, H.; Tashiro, M.; Fujimoto, T.; Machinami, T.; Oda, S.; Miyake, Y.; Okamoto, I.; Tanaka, Y. *Chem. Commun.* **2008**, *0*, 4825.

(96) Megger, D. A.; Müller, J. *Nucleosides, Nucleotides and Nucleic Acids* **2009**, *29*, 27.

(97) Lee, J. S.; Latimer, L. J. P.; Reid, R. S. *Biochemistry and Cell Biology* **1993**, *71*, 162.

(98) Aich, P.; Labiuk, S. L.; Tari, L. W.; Delbaere, L. J. T.; Roesler, W. J.; Falk, K. J.; Steer, R. P.; Lee, J. S. *Journal of Molecular Biology* **1999**, *294*, 477.

(99) Aich, P.; Skinner, R. J. S.; Wettig, S. D.; Steer, R. P.; Lee, J. S. *Journal of Biomolecular Structure & Dynamics* **2002**, *20*, 93.

(100) Tanaka, K.; Shionoya, M. *The Journal of Organic Chemistry* **1999**, *64*, 5002.

(101) Tanaka, K.; Shionoya, M. *Coordination Chemistry Reviews* **2007**, *251*, 2732.

(102) Meggers, E.; Holland, P. L.; Tolman, W. B.; Romesberg, F. E.; Schultz, P. G. *Journal of the American Chemical Society* **2000**, *122*, 10714.

(103) Tanaka, K.; Tengeiji, A.; Kato, T.; Toyama, N.; Shionoya, M. *Science* **2003**, *299*, 1212.

(104) Clever, G. H.; Kaul, C.; Carell, T. *Angewandte Chemie International Edition* **2007**, *46*, 6226.

(105) Kaul, C.; Müller, M.; Wagner, M.; Schneider, S.; Carell, T. *Nat Chem* **2011**, *3*, 794.

(106) Yang, H.; Metera, K. L.; Sleiman, H. F. *Coordination Chemistry Reviews* **2010**, *254*, 2403.

(107) Gómez-Herrero, J.; Zamora, F. *Advanced Materials* **2011**, *23*, 5311.

(108) Batten, S. R., Neville, S. M. , Turner, D *Coordination Polymers: Design, Analysis and Applications* ,; RSC Publishing: Cambridge, UK, **2009** . Vol. 7.

(109) Carne, A.; Carbonell, C.; Imaz, I.; Maspoch, D. *Chemical Society Reviews* **2011**, *40*, 291.

(110) Wei Lee Leong and Jagadese J. Vittal, *Chem. Rev* **2011**, *111*, 688.

(111) Amo-Ochoa, P.; Rodr A-guez-Tapiador, M. I.; Castillo, O.; Olea, D.; Guijarro, A.; Alexandre, S. S.; G A mez-Herrero, J.; Zamora, F. *Inorganic Chemistry* **2006**, *45*, 7642.

(112) Olea, D.; García-Couceiro, U.; Castillo, O.; Gómez-Herrero, J.; Zamora, F. *Inorganica Chimica Acta* **2007**, *360*, 48.

(113) Welte, L.; García-Couceiro, U.; Castillo, O.; Olea, D.; Polop, C.; Guijarro, A.; Luque, A.; Gómez-Rodríguez, J. M.; Gómez-Herrero, J.; Zamora, F. *Advanced Materials* **2009**, *21*, 2025.

(114) García-Couceiro, U.; Olea, D.; Castillo, O.; Luque, A.; Román, P.; de Pablo, P. J.; Gómez-Herrero, J.; Zamora, F. *Inorganic Chemistry* **2005**, *44*, 8343.

(115) Surin, M.; Samorì, P.; Jouaiti, A.; Kyritsakas, N.; Hosseini, M. W. *Angewandte Chemie International Edition* **2007**, *46*, 245.
(116) Olea, D.; Gonzalez-Prieto, R.; Priego, J. L.; Barral, M. C.; de Pablo, P. J.; Torres, M. R.; Gomez-Herrero, J.; Jimenez-Aparicio, R.; Zamora, F. *Chem. Commun.* **2007**, *0*, 1591.

(117) Rieter, W. J.; Pott, K. M.; Taylor, K. M. L.; Lin, W. *Journal of the American Chemical Society* **2008**, *130*, 11584.

(118) Taylor-Pashow, K. M. L.; Rocca, J. D.; Xie, Z.; Tran, S.; Lin, W. *Journal of the American Chemical Society* **2009**, *131*, 14261.

(119) Imaz, I.; Rubio-Martinez, M.; Garcia-Fernandez, L.; Garcia, F.; Ruiz-Molina, D.; Hernando, J.; Puntes, V.; Maspoch, D. *Chem. Commun.* **2010**, *46*, 4737.

(120) Imaz, I.; Hernando, J.; Ruiz-Molina, D.; Maspoch, D. *Angewandte Chemie International Edition* **2009**, *48*, 2325.

(121) Rieter, W. J.; Taylor, K. M. L.; An, H.; Lin, W.; Lin, W. *Journal of the American Chemical Society* **2006**, *128*, 9024.

(122) Rieter, W. J.; Taylor, K. M. L.; Lin, W. *Journal of the American Chemical Society* **2007**, *129*, 9852.

Chapter 2 Synthesis of 2'-deoxy-6-thioguanosine and its binding with metal ions

2.1 Introduction

With the aim of investigating the possible metal binding properties of 6-thioguanine units that could be incorporated into both DNA and RNA, routes for the preparation of coordination polymers based on the corresponding deoxy- and ribonucleosides are explored in this chapter. 6-Thioguanosine is a 6-thioguanine base with ribose sugar, whereas 2'-deoxy-6-thioguanosine is a 6-thioguanine base with 2'-deoxy ribose sugar, as shown in Figure 1. These nucleosides are known as members of the thiopurine family.

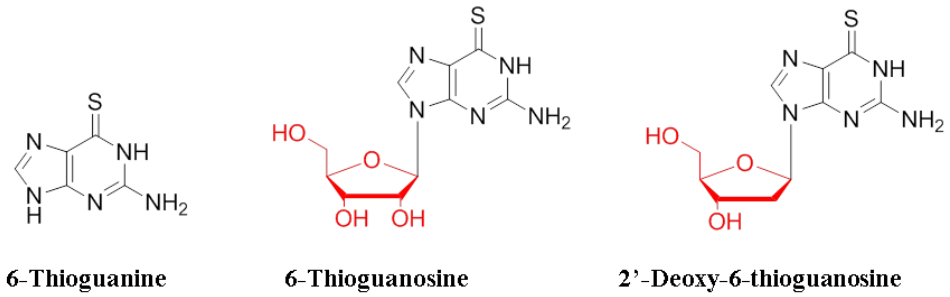

Figure 1. The structure of 6-thioguanine and its nucleoside derivatives.

Thiopurines are not naturally occuring nucleobases. Nevertheless, these compounds have been used as clinical agents for treating leukemia,[1] also as inhibitors of metabolism for immunosuppressive, antineoplastic and antitumor activity.[1-3] For instance, 6-mercaptopurine (6-MPH) is an example of a thiopurine that is most widely used in acute lymphoblast leukemia treatment regimens,[4] and 6-thioguanine is used in the treament of myelocytic leukemia.[5,6]

Despite their clinical applications, the synthesis however, of thiopurines is not a straightforward process, involving mupltiple steps and a range of different approaches.[7] Some key synthetic strategies for 6-thiopurines are summarised in Scheme 1.

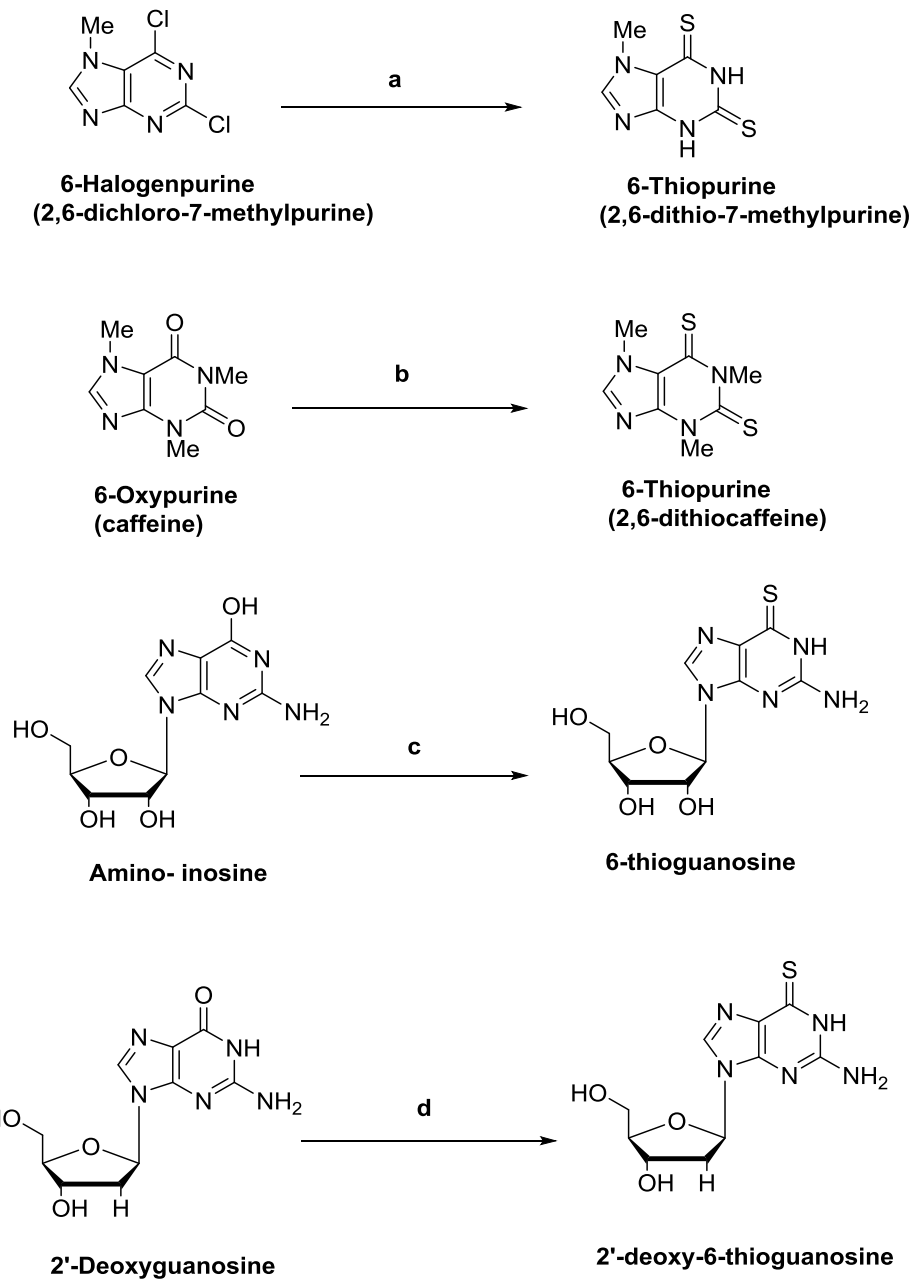

a = $(NH_4)_2S$, N_2H_4CS and SCN^-, b = P_2S_3 in kerosine at 210-220 °C, c = C_6H_5COCl in C_5H_5N, P_2S_5 in C_5H_5N and CH_3ONa, d = pyridine, $(CF_3CO)_2O$, f) NaSH in DMF.

Scheme 1. Some synthetic routes of 6-thiopurines.

6-Thiopurine derivatives have been synthesised by the multi-step conversion of 6-halogenpurine *via* the reaction of hydrosulfides and sulfides of alkali metals or ammonium with thiourea and with alkali metal rhodanides. Alternatively, the conversion of 6-oxypurine to 6-thiopurines, by the replacement of the 6-oxy group with a 6-thio group was reported.[7] This reaction involved heating caffeine with P_2S_3 at high

temperature in addition to several other steps that eventually led to the formation of 6-thiopurines.

Another example is the synthesis of 6-thioguanosine. 6-thioguanosine is generally synthesised *via* thiolation reactions of amino inosine. In one approach, amino inosine was treated with benzoyl chloride in pyridine which gave the 2,3,5-tri-O-benzoyl-D-ribofuranosyl derivative. This derivative was then thiolated by using phosphorous pentasulfide in pyridine and sodium methylate to yield the 6-thioguanosine.[8] Whereas 2'-deoxy-6-thioguanosine was synthesised by the treatment of 2'-deoxy-adenosine-N^1-oxide with cyanogen bromide in methanol, followed by treatment with methyl iodide to give 1-methoxy-6-cyano-2'-deoxy-adenosine. To offer 2'-deoxy-6-thioguanosine, 1-methoxy-6-cyano-2'-deoxy-adenosine was treated with sodium hydroxide followed by sulfhydrolysis using hydrogen sulfide.[9] Jones and his co-workers synthesised 2'-deoxy-6-thioguanosine from 2'-deoxyguanosine. 2'-Deoxyguanosine in pyridine was added to trifluoroacetic anhydride to give the pyridinium intermediate followed by the addition of sodium sulphide in anhydrous dimethyl formamide to give 2'-deoxy-6-thioguanosine.[10] In this instance the two-step reaction is performed in one-pot minimising the need for several purification steps required by the thiolation methods described for 6-thiopurines. It is apparent that the method developed by Jones is the most attractive for the synthesis of 2'-deoxy-6-thioguanosine and the work described here to study the metal binding interactions.

2.1.1 Interaction of thiopurines with metal ions

The interaction of thiopurines with metal ions has attracted considerable attention, with preliminary research mostly focussed on understanding the essential aspects of the coordination chemistry.[11] In addition, the possibilty for developing novel metal-containing drugs was studied.[12] For example, it has been found that some complexes of thiopurines with transtion metals, in particlar those of platinum and palladium have shown antitumor activity which is enhanced with respect to the free ligand.[13,14] The coordination complexes of 6-MPH with several transition metals have been reported.[15] The first crystal structure of a 6-MPH complex with Pd(II) was reported by Heitner *et al,* who found that two 6-MPH ligands chelate to Pd(II) through the S(6) and N(7) atoms.[16]

Subsequently, additional transition metal complexes with 6-MPH were described including, Hg(II), Pd(II), Cd(II) and Cu(I). The coordination systems of these complexes can be divided into two types, Type I complexes contain a ligand / metal ratio of 2:1, and Type II complexes consist of a metal / ligand ratio of 1:1. Within Type I, there are two further possibilities, Type IA, which contains only sulphur coordination bonds [17] or Type IB which has both S(6) and N(7) chelating interactions.[16,18] One further possibility is the formation of coordination polymers of the Type IC.[19] Similarly within Type II complexes, both monomer and chelating binding modes are possible, Type IIA sulphur chelated[20] or Type IIB, S(6) and N(7) coordinated,[21] as shown in Figure 2.

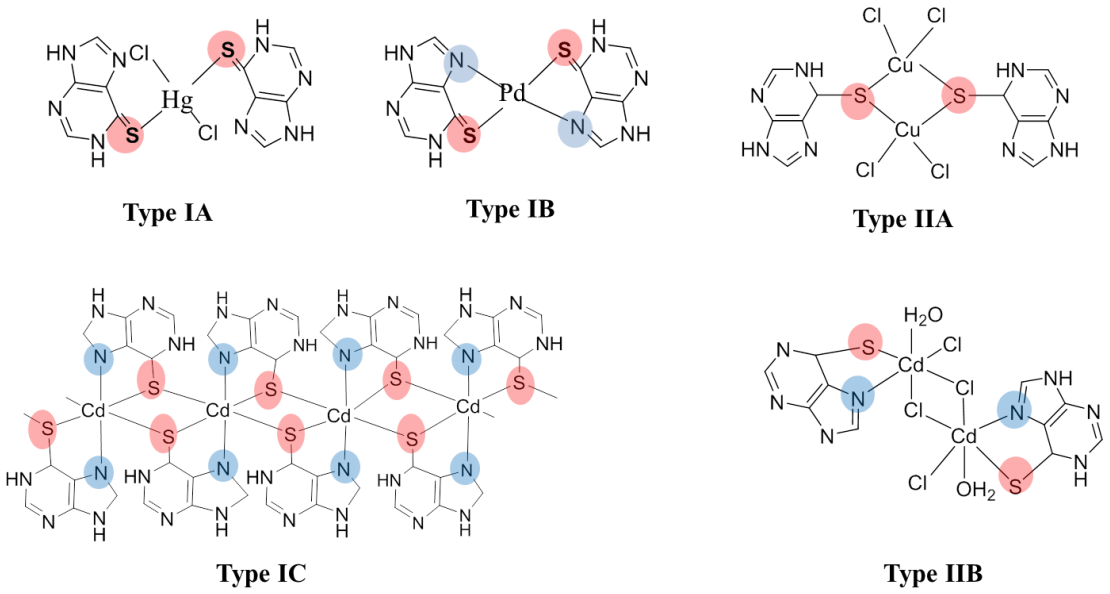

Figure 2. Different coordination types of thiopurines with metals.

Coordination polymers of the Type IC are of particular interest for possible applications of systems containing nucleobases and metal ions within the framework of designer molecular materials for nanotechnology.[22-24] Especially, the 6-mercaptopurine system offers the ability for metal ion assembly in a 1D-coordination polymer, such as [M(6-MP)$_2$] that is similar in structure to M-DNA.[25] Zamora and his group were able to form the 1D-coordination polymer [Cd(6-MP)$_2$]$_n$ from 6-MP and Cd(II) which is depicted in Figure 2 as Type IC.[19]

One property of these coordination polymers is their potential to act as nanoscale conductors; nanowires which from density functional theory **(**DFT) studies by Zamora *et al.* showed promise for enhanced electrical conduction. However, Ni(II)

1D-coordination polymers with 6-MP $[Ni(6\text{-}MP)_2]_n$ and 6-thioguanine $[Ni(6\text{-}thioG)_2]_n$ exhibit semiconducting behaviour.[24]

Therefore, Cd(II) and Ni(II) was chosen in this study to form 1D-coordination polymers with the 6-thionucleosides (6-thioguanosine and 2'-deoxy-6-thioguanosine). In addition, Co(II) was chosen as it is adjacent to Ni in the periodic table. Co is also able of adopting the necessary octahedral geometry for formation of the chain-like structure and may do so at two different levels of oxidation, +2 and +3. In addition, this introduces the probability for magnetic effects, especially for d^7 Co (II).

2.2 Results and Discussion

In order to produce 1D-coordination polymers, the synthesis of **d-tG** and its binding with metal ions was explored. The conversion of 2'-deoxyguanosine (**d-G**) to 2'-deoxy-6-thioguanosine (**d-tG**) was achieved according to the Jones procedure.[10] **d-tG** was characterized by ^{1}H-NMR, ^{13}C-NMR, IR, MS and UV spectroscopy. Then **d-tG** and the commercially available 6-thioguanosine (**tG)** were compared through binding studies with a range of metal ions Co^{2+}, Cd^{2+} and Ni^{2+}. The resulting metal complexes were characterized by MS, ^{1}H-NMR, IR spectroscopy, X-ray crystallography, magnetic susceptibility and CHN analysis.

2.2.1 Synthesis of 2'-deoxy-6-thioguanosine, d-tG

The Jones procedure was followed to synthesize **d-tG** from **d-G** as shown in Scheme 2.[10] **d-G** in pyridine was added to trifluoroacetic anhydride to give the pyridinium intermediate. Sodium sulphide in anhydrous dimethylformamide was then added to the intermediate to give crude **d-tG** in 85 % overall yield, as seen in Scheme **2**. Two techniques were used to purify **d-tG,** column chromatography and crystallization. Silica gel column chromatography yielded the compound **d-tG** by elution with methanol / chloroform (20:80). However, the yield was extremely low, less than 5 %. Purification of pure **d-tG** was also achieved by crystallization from water and methanol within 24 hour in a much improved yield of approximately 85 %.

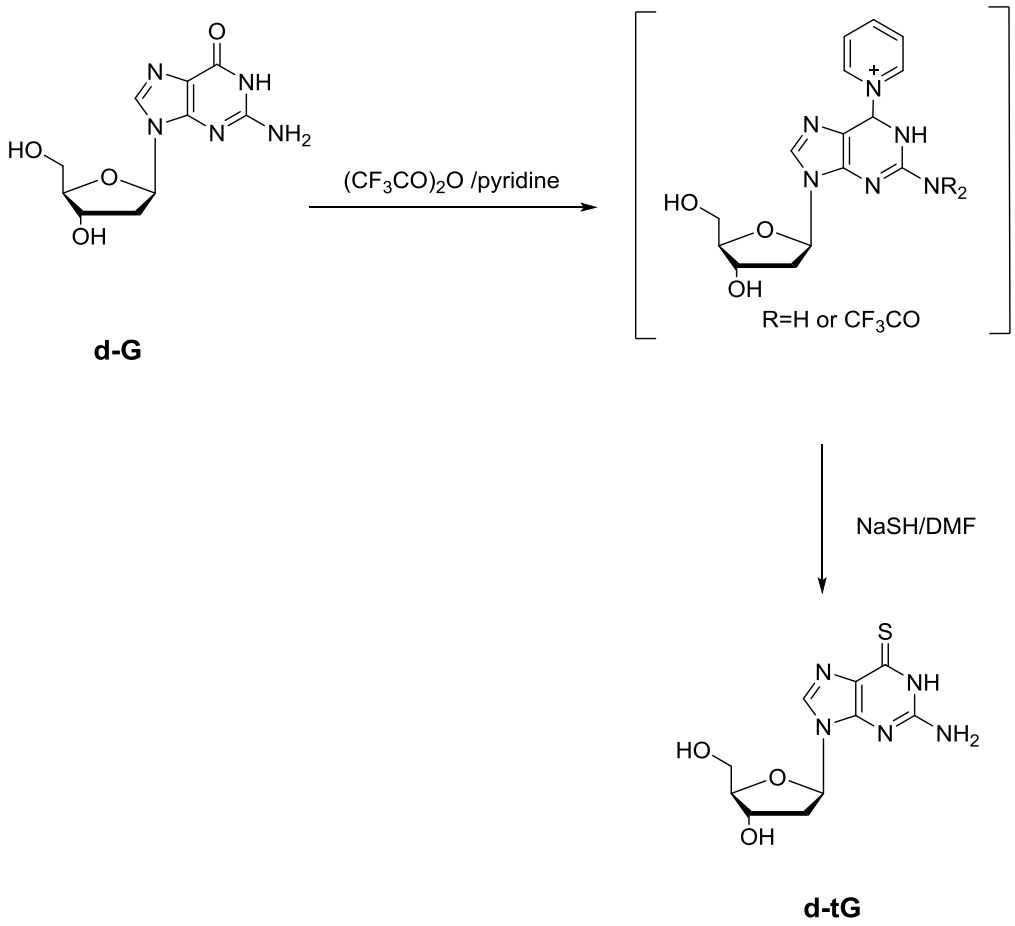

Scheme 2. Synthetic route to **d-tG** *via* the Jones route.[10]

The ^{1}H-NMR spectrum of the purified **d-tG** was compared with that of **d-G**. It was found that the N(1) proton of **d-G** appeared at 10.5 ppm while for **d-tG** it appeared at 11.9 ppm. This chemical shift of the N(1) proton of **d-tG** was the same as reported by Jones *et al*. indicating successful conversion.[10] This downfield shift of over 1 ppm is unexpected due to the higher relative electronegativity of the oxygen atom over sulphur. In addition, the H(8) and NH_2 protons were shifted as well as shown in Figure 3, however by not as much, as is expected due to their relatively larger distance from the modification at C(6).

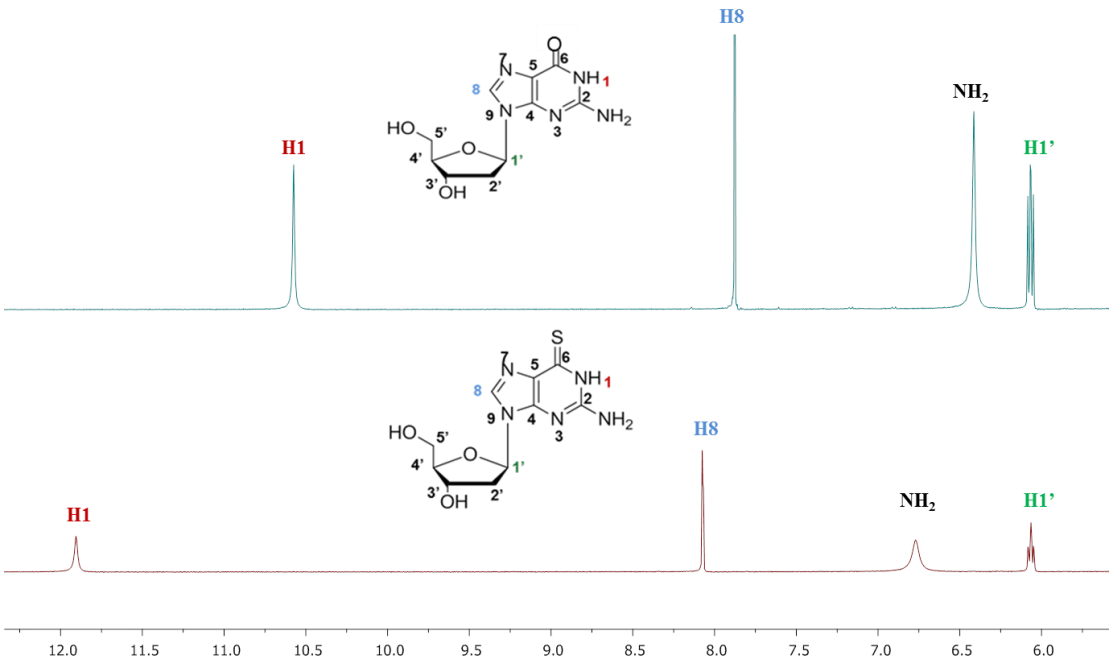

Figure 3. The comparison between the ^{1}H-NMR shifts of the N(1), H(8) and NH_2 protons in **d-G** and **d-tG**.

In addition**,** ^{13}C-NMR spectrum of **d-tG** showed nine carbon signals, however the CH_2 at the 2'-position was not seen. A DEPT experiment revealed that this peak is buried under the solvent peak as shown in Figure 4. Moreover, the ^{13}C-NMR data showed that the ^{13}C signal of C=O of **d-G** appeared at 157 ppm, whereas for **d-tG** the equivalent carbon appeared at 176 ppm, as shown in Table 1. The reason for these differences in the chemical shifts of **d-G** and **d-tG** is related to the thiol modification.

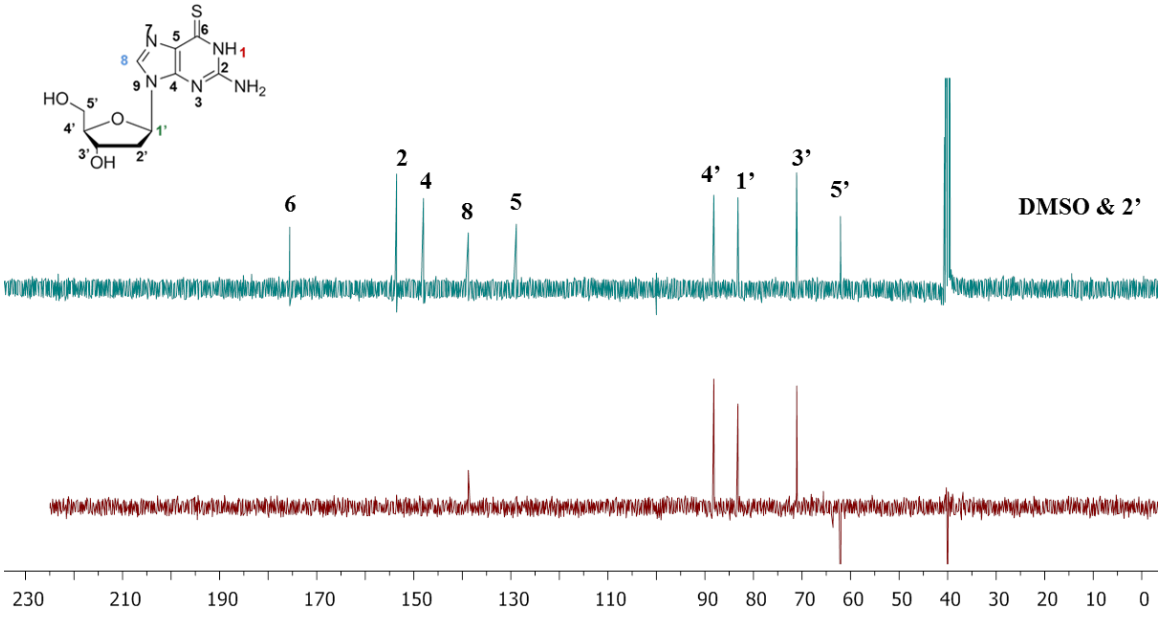

Figure 4. ^{13}C-NMR and DEPT spectra of **d-tG**.

Number of carbon	^{13}C-NMR of 2’ d-G ppm	^{13}C-NMR of d-tG ppm
2	154	154
4	151	148
5	117	129
6	157	176
8	136	139
1’	83	83
2’	30	40
3’	71	71
4’	88	88
5’	62	62

Table 1. Comparison of C signals in the ^{13}C-NMR between **d-G** and **d-tG**.

IR spectroscopy was also used to monitor the conversion of **d-G** into **d-tG.** The C=O stretch of **d-G** was evident at 1675 cm^{-1} while this peak did not appear in the **d-tG** spectrum. At the same time the band due to the C=S stretch appeared at 1200 cm^{-1}, as seen in Figure 5. In addition, the band at about 2600 cm^{-1} that relates to a thiol stretching mode was not seen, which suggests that the **d-tG** is in the thione form. These data confirm that **d-tG** was successfully synthesized.

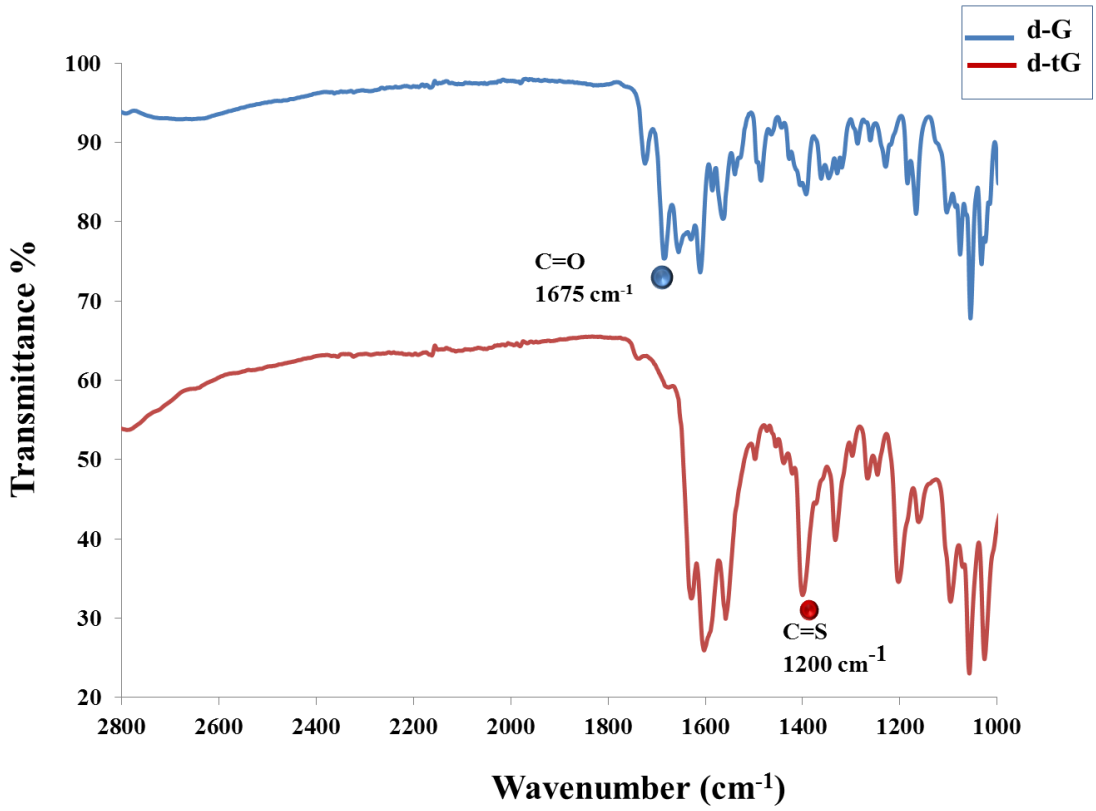

Figure 5. IR comparison between **d-G** (blue line) and **d-tG** (red line).

Further characterisation by UV-vis of an aqueous solution of the purified **d-tG** showed characteristic peaks at 260 and 345 nm.[26] Figure 6 shows a comparison of the absorption spectra of **d-tG** and **d-G,** and highlights the major difference between the two compounds due to the new peak at 345 nm. This new lower energy band is due to the substitution of the C(6) carbonyl oxygen to sulphur. Mishra and his group noted that the calculated excitation energies for 6-thioguanine showed this transition to be the $\pi-\pi^*$excitation of the thione form at 345 nm. [26]

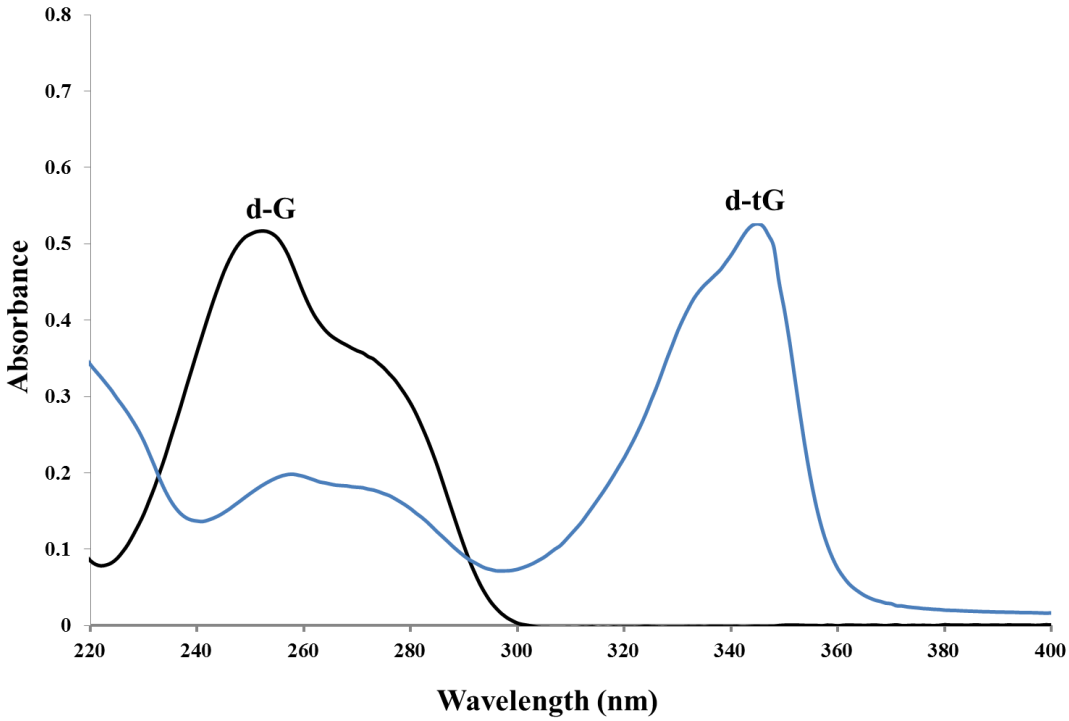

Figure 6. UV comparison between **d-G** at 43 µM (black line) and **d-tG** at 21 µM (blue line) in aqueous solution.

2.2.1.1 UV –vis spectrophotometric pH titration of d-tG

The spectroscopic characterisation of the synthesized **d-tG** suggested that the final product **d-tG** is in its thione form; however it may also exist in the thiol form, see Scheme 3.

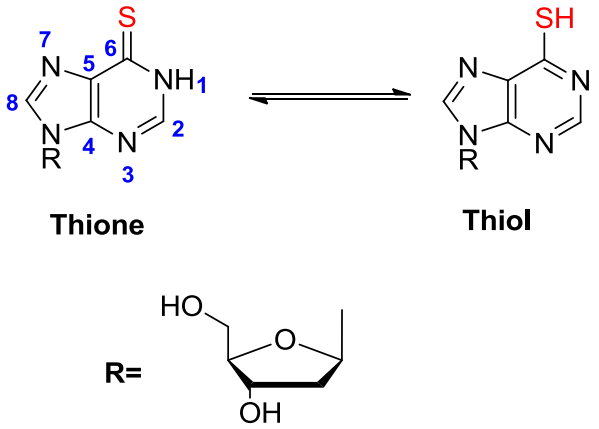

Scheme 3. Thione-thiol tautomerism of **d-tG**.

Therefore, the study of the effect of pH on its structure was examined in order to investigate the effect of protonation at N(1) on the electronic absorption spectrum, to aid in future understanding of metal ion interactions.

Figure 7 shows the effect of titration with NaOH on **d-tG** over the pH range from 6.25 to 11.80. The initial absorbance at 345 nm shifts to higher energy, 322 nm as the pH is raised with a concomitant increase in absorbance as well. This might be due to the increase in pH that leads to the deprotonation at N(1) of **d-tG.** Thus, the thione structure of **d-tG** is transformed into the thiol form, as shown in Figure 7. Similar absorbance peak shifts were noted by Mishra *et al*. for 6-thioguanine when the pH was altered from neutral to alkaline conditions.[26]

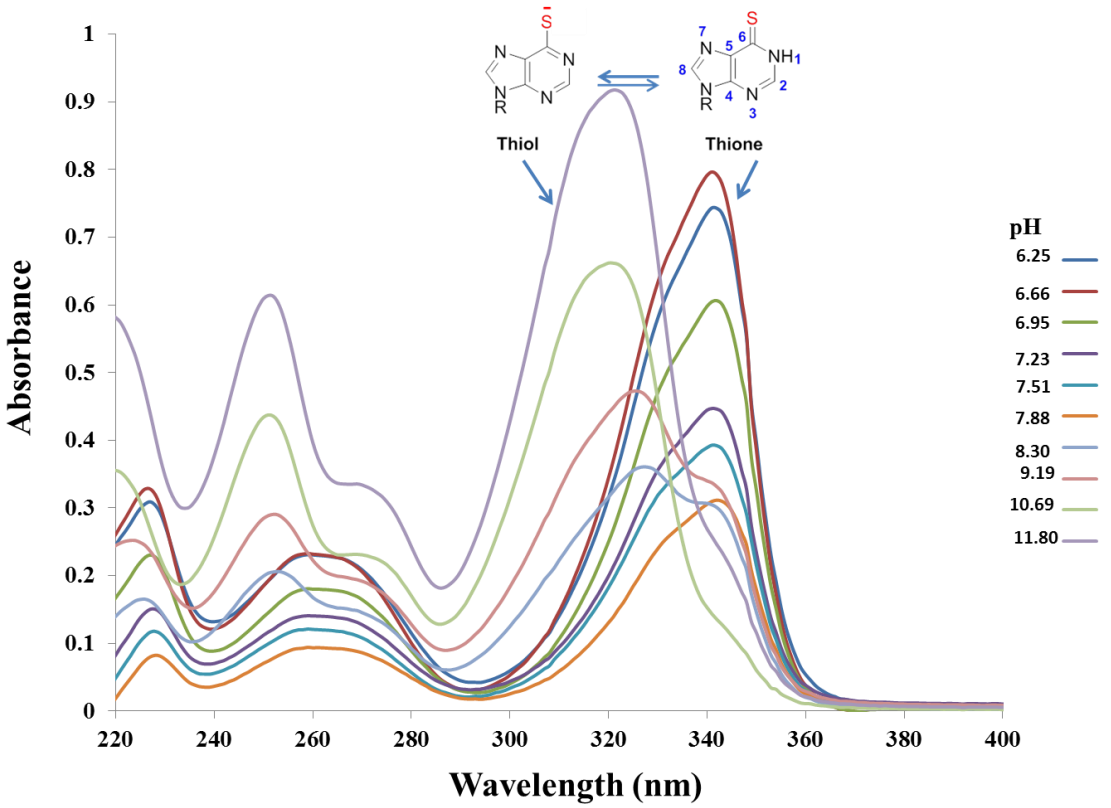

Figure 7. UV –vis spectrophotometric pH titration of **d-tG** upon the addition of NaOH.

After the synthesis of **d-tG** was achieved, the binding of several transition metal ions to 2'-deoxy-6-thioguanosine and 6-thioguanosine is explored in the next sections. Scheme 4 summarises the proposed binding of metal ions by 6-thioguanosine (**tG**) or 2'-deoxy-6-thioguanosine (**d-tG**) to form 1D coordination polymers as previously reported by Zamora.[19]

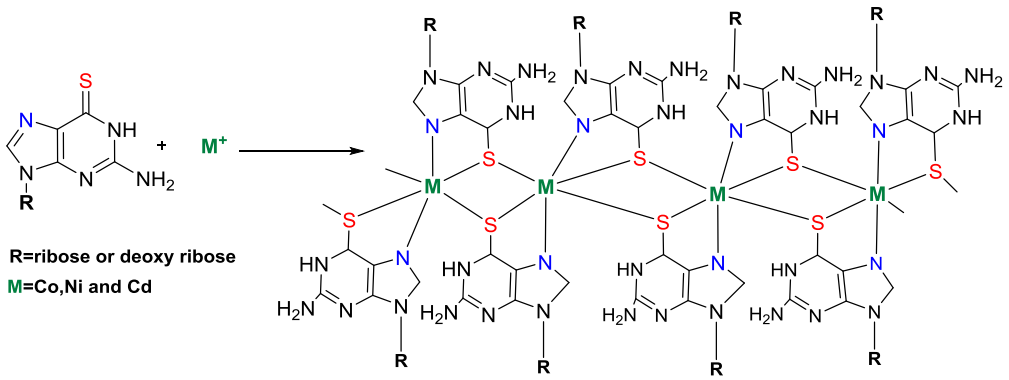

Scheme 4. Possible structure of 1-D coordination polymers of **tG** or **d-tG** with metal ions.

1Dimensional coordination polymers are however, not the only possible structures that these systems might form, there are other possible structures that deoxy- and ribonucleosides could form on treatment with metals,[18,19] as shown in Scheme 5.

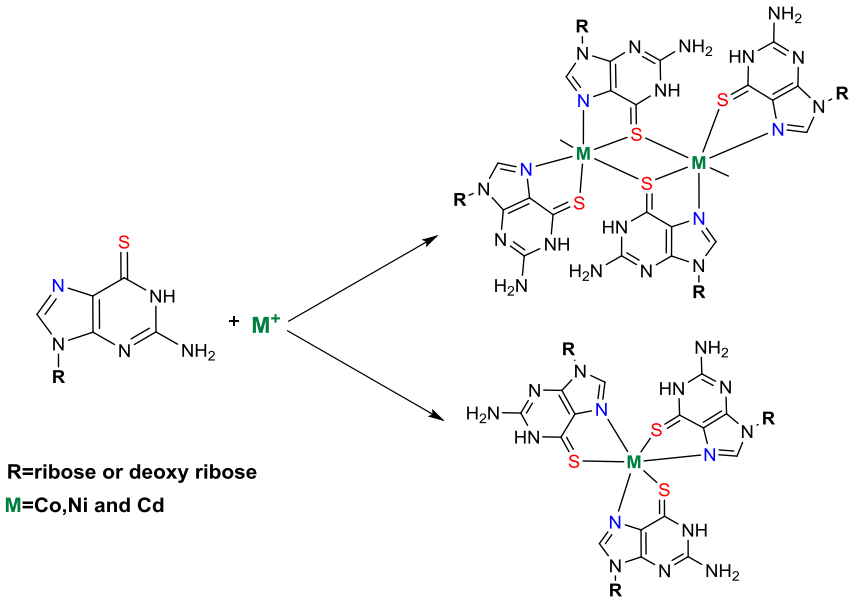

Scheme 5. Other possible structures of **tG** or **d-tG** complexes with metal ions.

2.2.2 Synthesis and characterization of cobalt complexes of d-tG and tG, 1 and 2

The synthesis and characterization of cobalt complexes with the corresponding **d-tG** and **tG** ligands was performed. $Co(NO_3)_2$ was used as the source of cobalt in all reactions however the final oxidation state of the metal in the complex varied. The two different oxidation states of the metal ion, Co^{2+} and Co^{3+} highlight two different forms in which the ligand can coordinate to the metal ions as noted in the two crystal

structures that were obtained. In the first instance, 1.3 equivalents of **d-tG** were reacted with 1 equivalent of $Co(NO_3)_2$ in refluxing MeOH, yielded green crystals of complex **1**, as shown in Scheme 6.

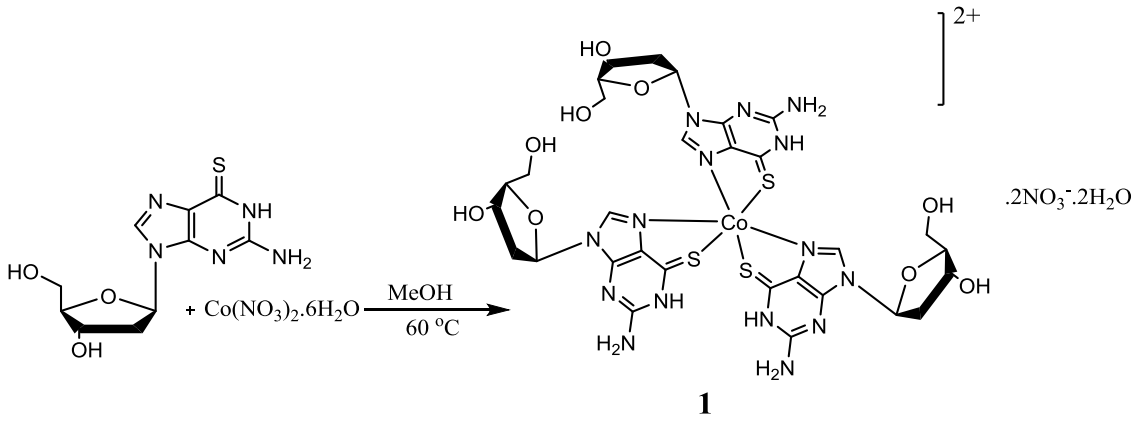

1

Scheme 6. Synthesis route to **1.**

Secondly, the reaction of 2 equivalents of **tG** were reacted with 1 equivalent of $Co(NO_3)_2$ in a refluxing 1:1 H_2O:MeOH mixture at pH 8, yielded dark green crystals of complex **2** as shown in Scheme 7.

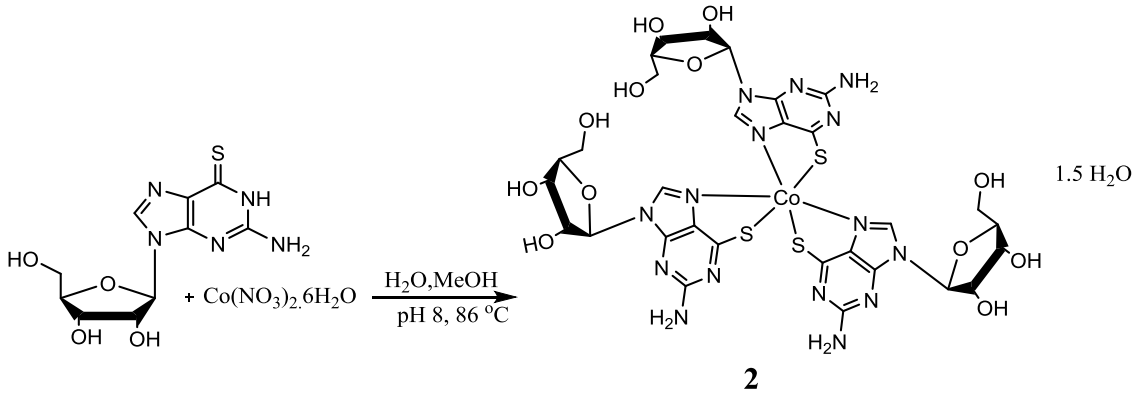

2

Scheme 7. Synthesis route to **2.**

The characterisations of cobalt complexes 1 and 2 were carried out by ES-MS, FT-IR, x-ray crystallography, ^{1}H-NMR, elemental analysis and magnetic susceptibility.

2.2.2.1 ES-MS of cobalt complexes of d-tG and tG, 1 and 2

ES-MS of cobalt complex, **1** shows the formation of a complex containing three ligands of **d-tG** coordinating to one Co^{2+} cation (m/z found 907.1469, calculated 907.1471). Likewise in the case of ES-MS of cobalt complex, **2** the complex contains three ligands of **tG** coordinating to one Co^{3+} cation (m/z found 976.1069, calculated 976.1060).

2.2.2.2 FT-IR of cobalt complexes of d-tG and tG, 1 and 2

The IR spectra of **1** and **2** were compared with those of the respective free ligands **d-tG** and **tG**. In the free nucleoside **d-tG** the absorption band of C=S is at 1200 cm^{-1} whereas in the complex **1** it is shifted to 1175 cm^{-1}. In the case of **d-tG** the bands between 1612-1555 cm^{-1} were assigned to C=C and C=N stretching modes. After complexation, these bands shifted to form one band at about 1603 cm^{-1}. This shift is indicative of N(7) of **d-tG** becoming involved in the cobalt complex. In addition, in the IR data of complex**, 1** there is a new broad band at 1319 cm^{-1} that relates to the nitrate group suggesting the involvement of the nitrate group in the complex,[27] as seen in Figure 8. The above observations show the involvement of the exocyclic sulphur C=S and N(7) in the formation of the cobalt complex.

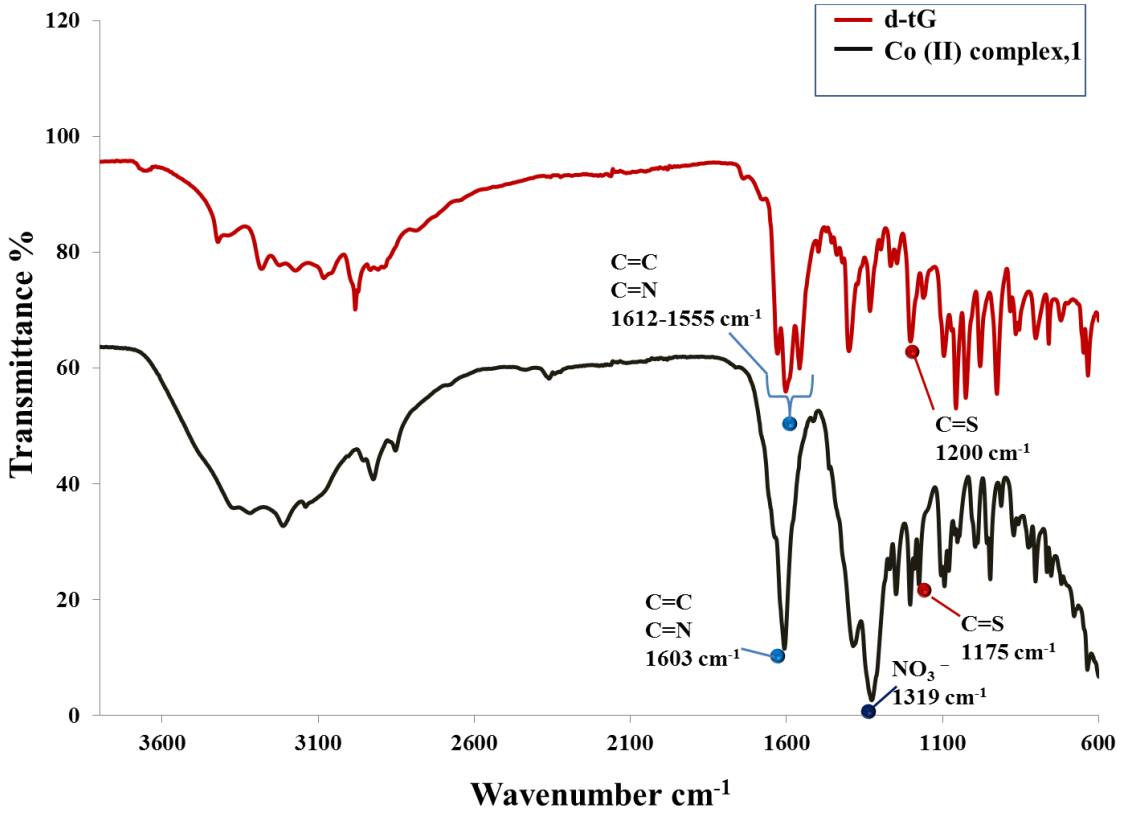

Figure 8. IR comparison between **d-tG** (red line) and cobalt complex, **1** (black line).

The IR spectrum of the cobalt complex, **2** showed similar spectral changes as the cobalt complex **1.** In particular, the band at 1207 cm^{-1} that related to C=S stretch in the free nucleoside **tG** shifted to 1192 cm^{-1} in the complex, **2.** In addition, the bands of C=C and C=N were also shifted as shown in Figure 9. These IR observations confirmed the

involvement of the cobalt metal in the complex and the interaction with the ligand was once again through both the C=S and N(7) positions. These findings correlate with Sodhis' results on the formation of a mercury complex with 6-thioguanine.[28]

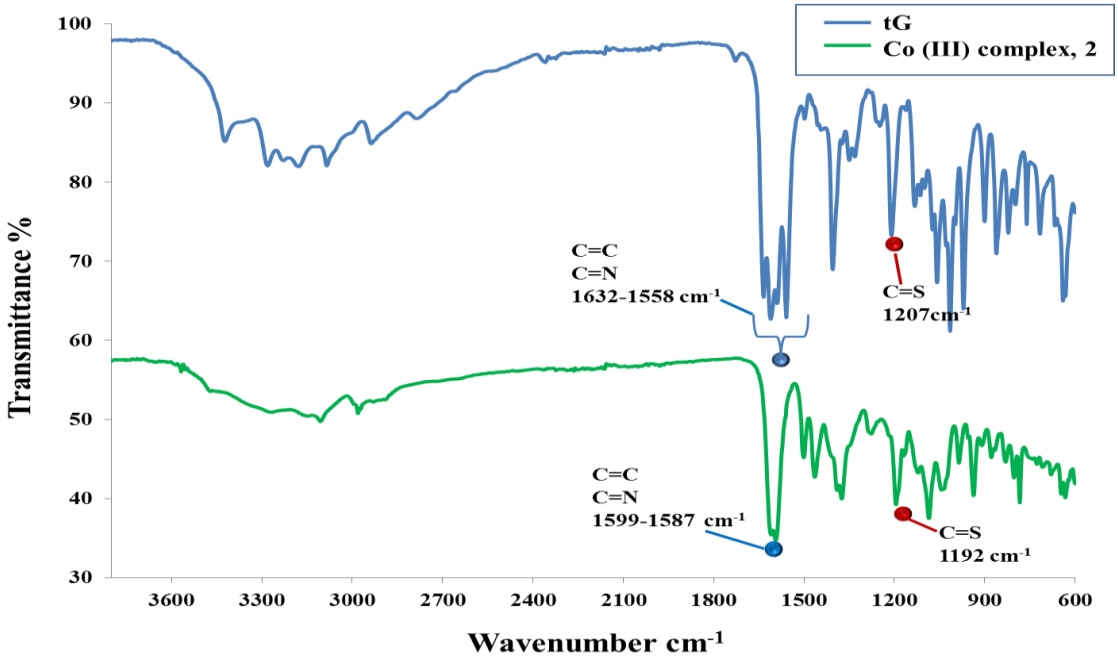

Figure 9. IR comparison between **tG** (blue line) and cobalt complex, **2** (green line).

2.2.2.3 Crystallography of cobalt complexes of d-tG and tG, 1 and 2

Due to the small size of the crystals, data were collected using synchrotron radiation at the Diamond Light Source. The crystal structures of **1** and **2,** shown in Figure 10, both exhibited a 3-fold axis of rotation about a central octahedral Co atom.

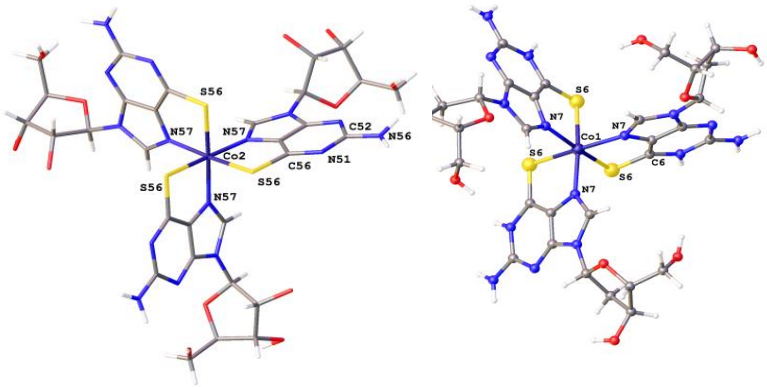

Figure 10. Molcular structure of **1** (right) and **2** (left) in a 3-fold axis of rotation about a central octahedral Co atom.

Although the only difference between the components of the complexes **1** and **2** the form of the ribose, **tG** or **d-tG,** there are some notable differences in the final structures. The Co oxidation state and the protonation state of the ligands vary and these subtle nuances of the individual structures are discussed later. In each structure, the thio-nucleoside ligands are coordinated to the metal centre through the S(6) and N(7) donor positions, giving rise to a five membered chelate ring. Also, in each complex three ligands coordinate the metal centre providing a trigonally elongated *fac*-N_3S_3 octahedral environment. However examination of the extended crystal lattice in each case gave no indication of the desired 1D coordination polymers as previously reported for 6-MPH with cadmium.[19] In complexes, **1** and **2** the monomeric entities are held together by means of complementary hydrogen bonds as seen Figure 11 and 12.

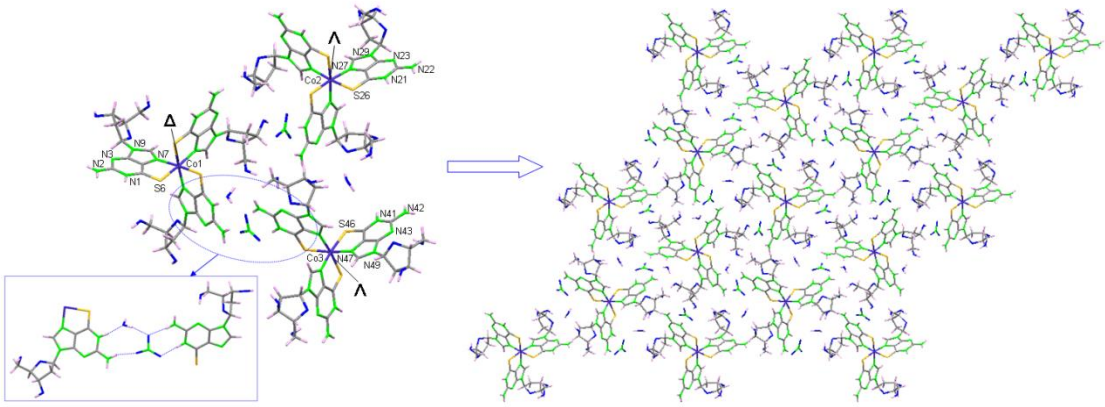

Figure 11. Crystal packing of complex, 1 entities showing the supramolecular interactions.

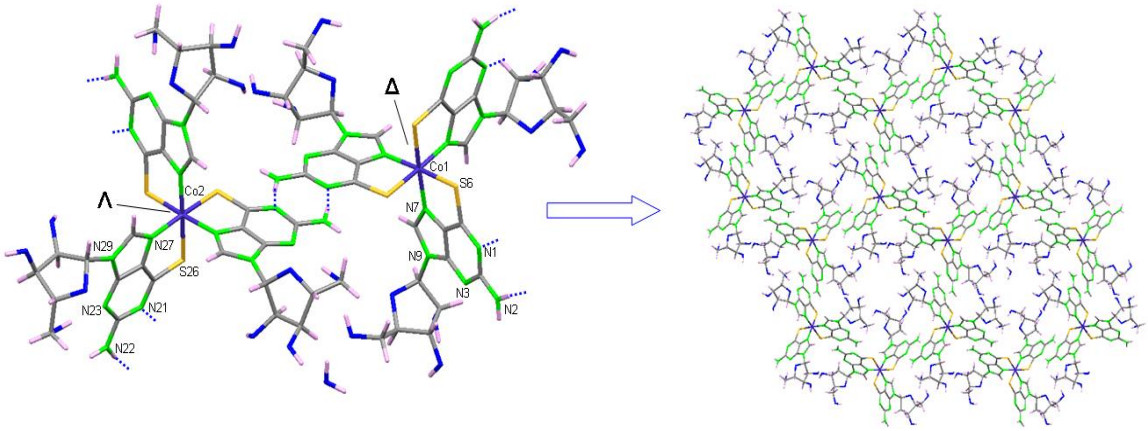

Figure 12. Supramolecular assembly of complex, 2 entities showing the presence of 1D channels running along the c axis. The crystallization water molecules placed inside the channels have been omitted for clarity.

In **1**, the nitrate anion acts as a bridging hydrogen bond acceptor between the NH_2 groups of two neighbouring ligands. The ribose units are linked *via* a hydrogen bond network involving a water molecule and also form a hydrogen bond with the exocyclic amino group.

Within **1** and **2** some noteworthy differences in the nature of the nucleoside and also the metal centre within each unit cell were observed. Complex **1** contains three independent molecules in the unit cell with composition $[Co(\mathbf{d\text{-}tG})_3](NO_3)_2.2H_2O$. The central Co atom is in an octahedral arrangement formed by the coordination of N(7) and S(6) of three **d-tG** ligands, generating the chiral CoN_3S_3 environment. Notably, N(1) of the **d-tG** ligand is protonated in all cases and each ligand is therefore neutral. The coordination sphere of the Co cation contains two nitrate anions indicating that complex **1** is based around a Co (II) centre. Considering compound **2,** $[Co(\mathbf{tG})_3]\cdot 1.5H_2O$, two independent molecules in the unit cell were observed. Here, however, the three **tG** ligands are all deprotonated at N(1), hence formally anionic, $\mathbf{tG}^-$, and indicating that the metal ion is now in the Co(III) state. The three deprotonated ligands of **tG** similarly chelate the central Co(III) cation *via* N(7) and S(6), again in octahedral geometry. A previous study has shown that the major effect of protonation and deprotonation of N(1) on the coordination complex results in a difference in the C(6)-N(1)-C(2) angle by about 4°.[29] Here the C(6)-N(1)-C(2) angles in compound **1** are 119.0(10)° to 123.6(7)°, whereas in **2** the angles are 117.1(3)° to 117.3(3)°, a difference of up to 6.5°, in support of the literature precedence.

Moreover, the C(6)-N(1) bond length of the protonated ligands in **1** range from 1.358(13) Å to 1.388(13) Å, whereas in the deprotonated complex, **2** they are between 1.321(6)Å to 1.328(6)Å, i.e. noticeably shorter (by *ca.* 0.05 Å). This indicates slightly more double bond character at this point in the heterocycle of the deprotonated complex, as would be expected. Likewise, the corresponding analysis of the average C-S bond lengths, 1.693(12) Å for **1**, and 1.737(4) Aº for **2** supports the thione and thiol tautomer structures respectively. In addition, a comparison between the S-Co bond lengths in compounds **1** and **2** indicates that the S-Co distance in compound **2** (2.315 Aº), is shorter than in compound **1** (2.443 Å). This is not unexpected due to the increased electrostatic attraction of Co^{3+} over Co^{2+} to the sulphur group. These findings imply that in compound **1** the ligand has a largely thione based structure, whereas in compound **2** it is predominantly thiol-like.

These observations indicate that both complexes **1** and **2** exhibit the same binding modes albeit to different oxidation states of the central Co; Co(II) in **1** and Co(III) in **2**. The magnetic susceptibility measurements of cobalt (III) complex, **2** indicated a negative molar magnetic susceptibility and exhibits diamagnetic properties.

2.2.2.4 ^{1}H-NMR of cobalt complexes of d-tG and tG, 1 and 2

^{1}H-NMR of **d-tG** and **tG** were examined to study their binding of cobalt ions. The ^{1}H-NMR spectrum of the cobalt (II) complex, **1** showed very broad peaks. This is because the cobalt (II) ion in the hexa-coordinated complex exhibits paramagnetic properties,[30-32] due to its high-spin through the unpaired electron in the d^{7} orbital electron configuration. The ^{1}H-NMR data of the cobalt (III) complex, **2** revealed sharp peaks as seen in Figure 13. This is probably due to the cobalt (III) ion in the hexa-coordinated complex now exhibits diamagnetic properties.[33] This is because of its low-spin d^{6} paired electron configuration. Figure 13 shows the comparison between the ^{1}H-NMR spectra of the **tG** ligand and the cobalt (III) complex, **2**. In **2** the peaks were shifted downfield compared to the free ligand. In addition, the N(1) proton (~11.98 ppm) in the free ligand **tG** disappeared in the spectrum of the complex suggesting deprotonation of the **tG** ligand during complex formation. However, there seems to be more than one species of the complex the ^{1}H-NMR spectrum, this might be due to geometrical and optical isomerism of the cobalt(III) complex in the solution, which is not observed in the solid state of the crystal structure.

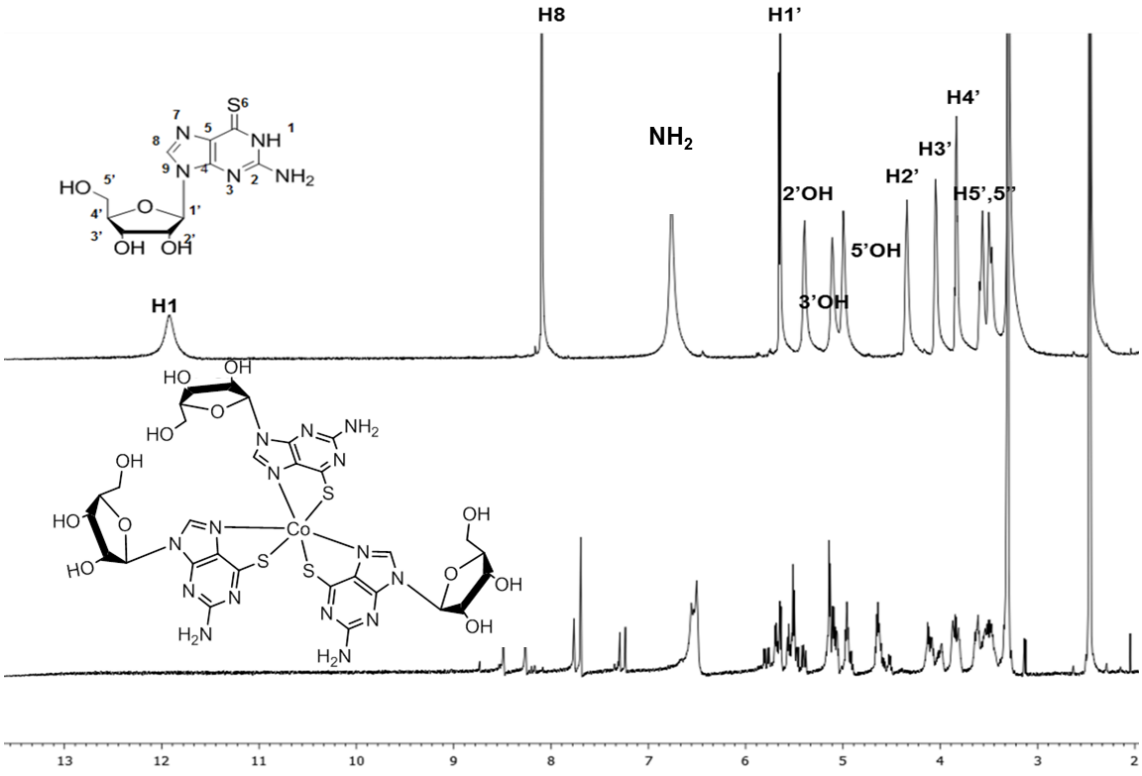

Figure 13. ^{1}H-NMR of cobalt (III) complex, **2**.

In summary, the compositional and molecular formula of the cobalt complexes **1** and **2** were determined by ES-MS spectroscopy, IR, ^{1}H-NMR and magnetic susceptibility and were confirmed by x-ray crystallography. These characterizations showed that the structure of cobalt (II) complex **1** consists of three **d-tG** ligands coordinated to a central Co^{2+} through S(6) and N(7) with two nitrate group and two water molecules in an octahedral geometry, [Co(II)(**d-tG**)$_3$].2NO_3.2H_2O as shown in Figure 14.

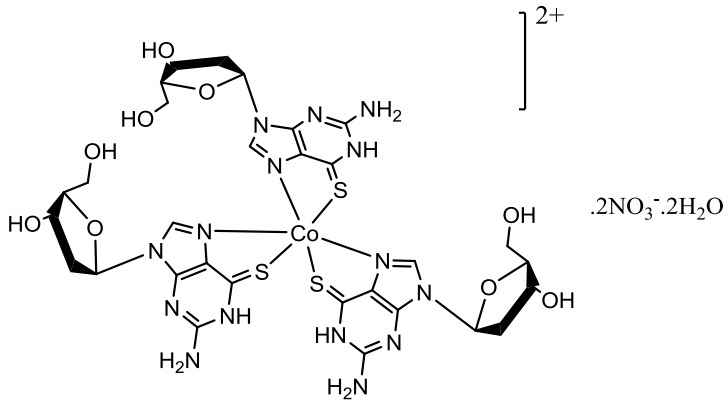

Figure 14. The molecular structure of **1** [Co(II)(**d-tG**)$_3$].2NO_3.2H_2O.

Whilst in the complex, **2** the three deprotonated **tG**$^-$ ligands chelate to Co^{3+} *via* S(6) and N(7) [Co(III)(**tG**)$_3$].1.5 H_2O, again in an octahedral geometry, as shown in Figure 15.

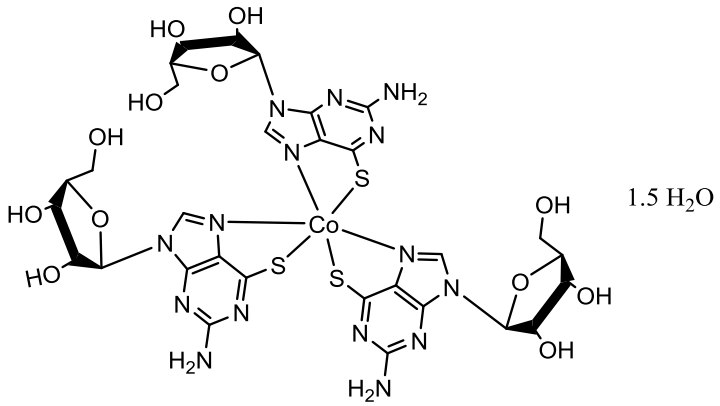

Figure 15. The molecular structure of **2** [Co(III) (**tG**)$_3$].1.5 H_2O.

2.2.3 Synthesis and characterization of nickel complexes of d-tG and tG, 3 and 4

The nickel (II) complexes, **3** and **4** were prepared according to the procedure of Zamora *et al.* [19] by the direct reaction of 1.3 equivalents of **d-tG** and **tG** respectively were reacted with 1 equivalent of nickel nitrate in methanol. A small green crystal was formed for complex **3** as shown in Scheme 8.

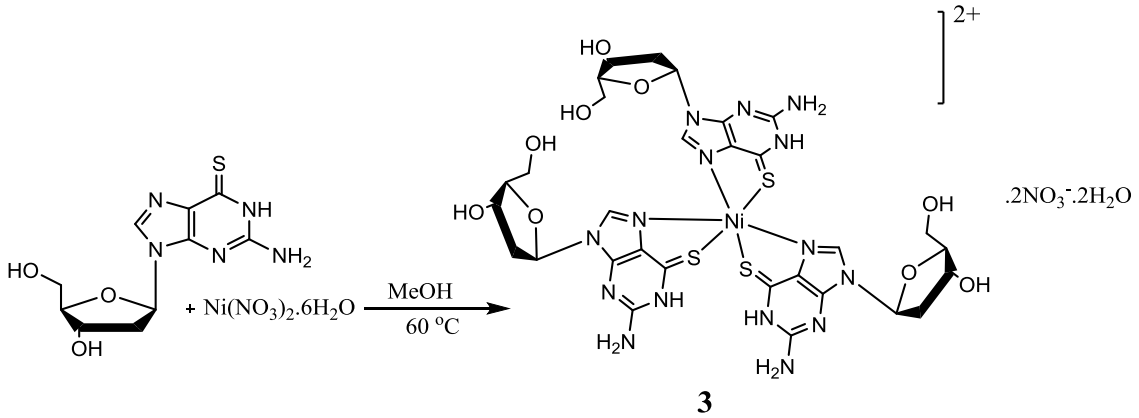

3

Scheme 8. Synthesis route to **3.**

In the case of complex, **4** a light green powder was obtained as shown in Scheme 9.

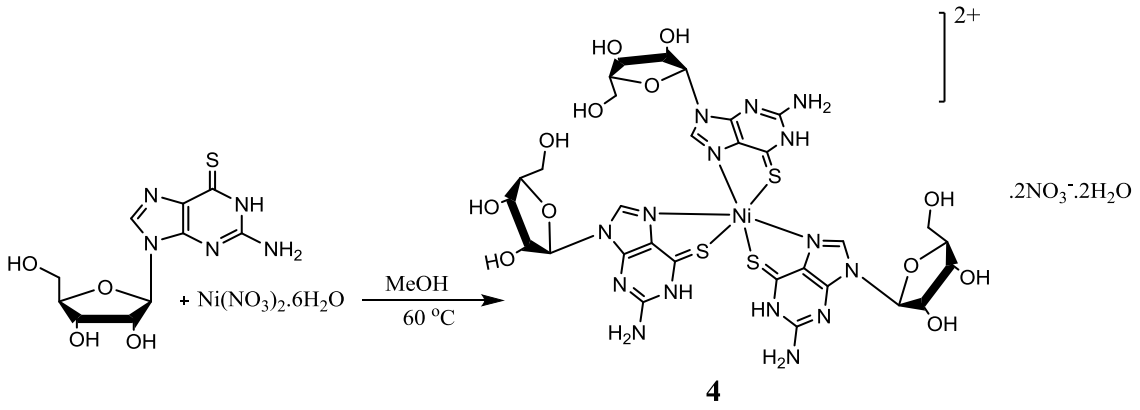

4

Scheme 9. Synthesis route to **4.**

The complexes of **3** and **4** were characterised by ES-MS, FT-IR, x-ray crystallography, ^{1}H-NMR and elemental analysis.

2.2.3.1 ES-MS of nickel complexes of d-tG and tG, 3 and 4

ES-MS of **3** shows the formation of a complex containing three ligands of **d-tG** coordinating to one Ni^{2+}cation (m/z found 906.1757, calculated 906.1492). Similarity in the case of **4**, the complex consists of three ligands of **tG** coordinating to one Ni^{2+}cation (m/z found 954.1432, calculated 954.1340).

2.2.3.2 FT-IR of nickel complexes of d-tG and tG, 3 and 4

IR assignments of nickel complexes showed similar spectral changes as the cobalt complexes that were discussed earlier in this chapter. The similarity of the IR spectra of these complexes suggests that the 6-thioguanosine ligands display the same coordination type in all these complexes. In particular, the changes were noted for the (C=S), (C=C) and (C=N) stretching modes. Figure 16 compares the IR spectra of **d-tG** (red line) and the nickel (II) complex, **3** (green line). In the free nucleoside **d-tG** the absorption frequency of C=S is at 1200 cm^{-1} whereas in **3** it is slightly shifted to 1197 cm^{-1} hinting the involvement of the exocyclic sulphur C=S in the binding of the

nickel complex. In **d-tG** the 1612 -1555 cm^{-1} bands were assigned to (C=C) and (C=N) stretching modes. After complexation these bands shifted to about 1598-1572 cm^{-1} indicative that the N(7) of **d-tG** is also involved in the binding within the nickel (II) complex. In addition, there is a strong new band at 1308 cm^{-1} in **3** assigned to the nitrate group which is therefore involved in the nickel complex, as seen in Figure 16.

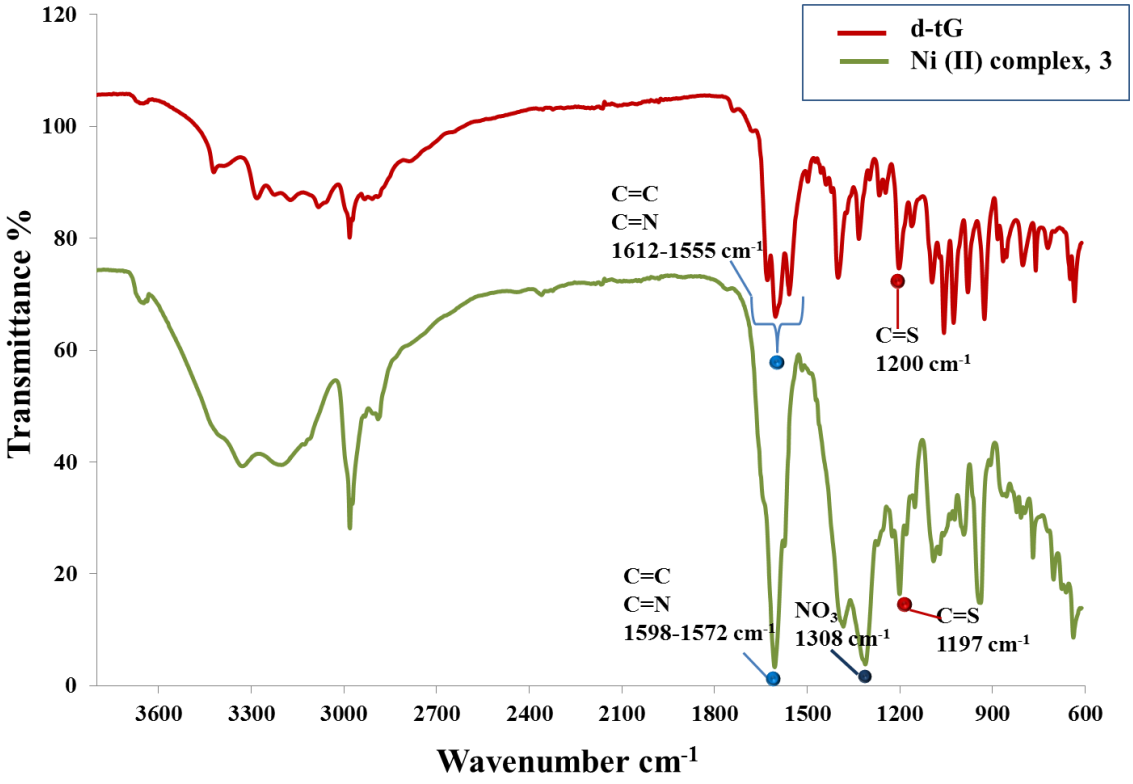

Figure 16. IR comparison between **d-tG** (red line) and nickel complex, **3** (green line).

In the case of the **4** the IR spectrum showed similar spectral variations as seen in **3**. A slight shift in the C=S band at 1207 cm^{-1} in the free nucleoside **tG** was shifted to 1194 cm^{-1} in the complex **4**. In addition, the bands of C=C and C=N were once again shifted upon complexation as shown in Figure 17. Moreover, the absorption band at 1312 cm^{-1} associated to nitrate group was also evident. These IR data confirmed the involvement of the nickel metal in the complexation during formation of **3** and **4**. These findings correlate well with Sodhis' results on the formation of a mercury complex with 6-thioguanine.[28]

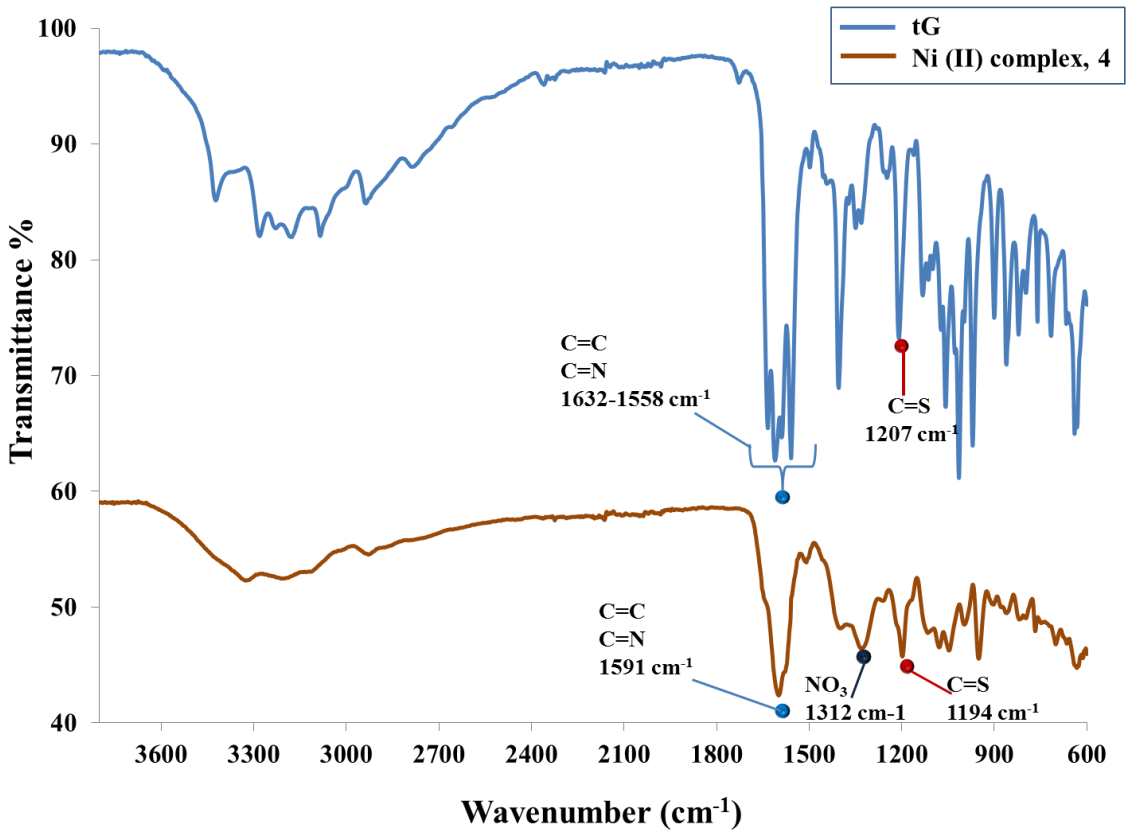

Figure 17. IR comparison between **tG** (blue line) and nickel complex, **4** (red line).

2.2.3.3 Crystallography of nickel complex of d-tG, 3

The crystal structure of **3,** see Figure 18, exhibited a 3-fold axis of rotation about a central octahedral Ni atom. In **3** the thio-nucleoside ligands are coordinated to the metal centre through the S(6) and N(7) donor positions, giving rise to a five membered chelate ring. Also, in the complex three ligands coordinate the metal centre providing a trigonally elongated *fac*-N_3S_3 octahedral environment. However, the octahedral angles range from 83.56(5)° to 90.87(6)° giving a slightly distorted octahedral geometry of the complex. The monomeric entities are held together by means of complementary hydrogen bonds.

Notably, N(1) of the **d-tG** ligand is protonated in all cases and each ligand is therefore neutral. The coordination sphere of the Ni cation contains two nitrate anions indicating that complex **3** is based around a Ni (II) centre. The bite distance of S(6)….N(7) for the free ligand is 3.334 Å,[34] whereas the bite distance for the chelating ligand here is 3.128 Å, which is shorter due to the metal ionic radius. This observed reduction in bite

distance is similar to previous studies on 6-thioguanine and 6-mercaptopurine with metal ions.[24]

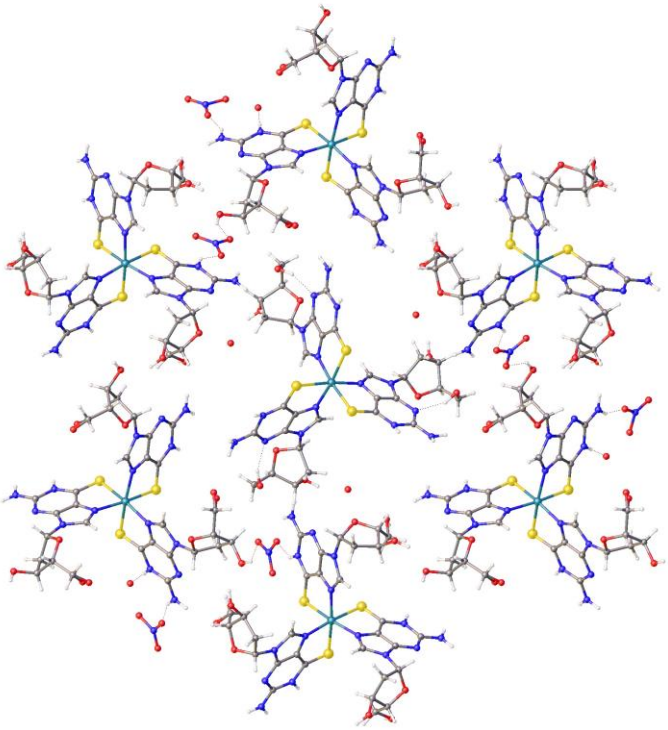

Figure 18. Molcular structure of **3** in a 3-fold axis of rotation about a central octahedral Ni atom and packing in the crystal structure of **3**, viewed down the crystallographic *c* axis.

2.2.3.4 ^{1}H-NMR of nickel complexes of d-tG and tG, 3 and 4

^{1}H-NMR spectra of the Ni(II) complexes **3** and **4**, show slightly broad peaks compared to the free ligands. In addition, there is a small downfield shift of the ligand protons in the complexes **3** and **4** compared to the free ligand, in particular NH (1), H (8) and NH_2, indicating metal ion coordination. However, it was expected the ^{1}H-NMR of the Ni^{2+} complex should exhibit very broad peaks due to its paramagnetic properties in the octahedral geometry and $3d^8$ electronic configuration.[35] Therefore the ^{1}H-NMR spectra of the complexes were measured over a wide range (from -50 to 50 ppm) to identify whether any broad peaks were observed, but none were.

In conclusion, the compositional and molecular formula of the nickel complex **3** was determined by ES-MS spectroscopy, IR and ^{1}H-NMR and was confirmed by crystal structure. These characterizations showed that the structure of nickel (II) complex **3** consists of three **d-tG** ligands coordinated to a central Ni^{2+} through S(6) and N(7) with

two nitrate group and two water molecules in a octahedral geometry, [Ni(II)(**d-tG**)$_3$].2NO$_3$.2H$_2$O as shown in Figure 19.

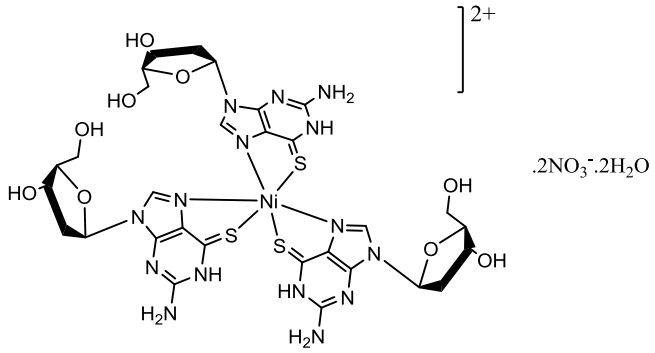

Figure 19. The molecular structure of **3** [Ni(II)(**d-tG**)$_3$].2NO$_3$.2H$_2$O.

In the case of the nickel complex, **4** a crystal suitable for x-ray analysis was not formed. Therefore, the compositional and molecular formula of nickel complex, **4** was determined by IR, ES-MS, ^{1}H-NMR and elemental analysis. IR data showed that the Ni (II) ion coordinates to the **tG** ligand *via* N(7) and S(6) due to the shift in the stretching modes (C=S, C=C and C=N) of the complex compared with the free **tG** ligand. In addition, the nitrate group was involved in the complex structure as it is clearly seen in the IR data as a strong absorption band in the nitrate group region. Further confirmation was carried out by utilizing ES-MS that showed three ligands of **tG** bound to one Ni^{2+}. According to these data and the crystal structure of complex **3,** the final proposed structure of complex **4** is that it could be similar to complex **3**, the formation of three protonated ligands coordinated to one $Ni^{2+}$with two anionic nitrate groups in an octahedral geometry [Ni(II)(**tG**)$_3$].2NO$_3$.2H$_2$O. Elemental analysis (CHN) study of the complex, **4** supports this proposed structure, C, H, N analysis formula of the complex was $C_{30}H_{39}N_{17}O_{18}S_3Ni$: Calcd (found): C, 33.44 (33.57); H, 3.37 (3.505); N, 22.10 (19.64). as shown in Figure 20.

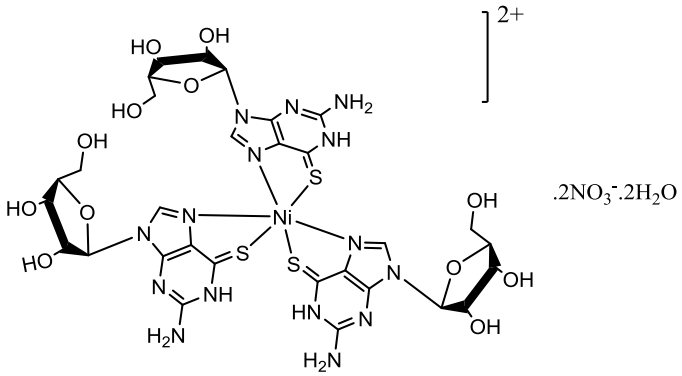

Figure 20. The molecular proposed structure of **4** [Ni(II)(**tG**)$_3$].2NO$_3$.2H$_2$O.

2.2.4 Synthesis and characterization of cadmium complexes of tG

In an attempt to extend the strategy of 6-thionucleosides as ligands to form one dimension coordination polymers, the cadmium complex of **tG** was prepared by the direct reaction of 2 equivalents of **tG** with 1 equivalents of cadmium nitrate in methanol as seen in Scheme 10 according to the procedure described by Zamora.[19]

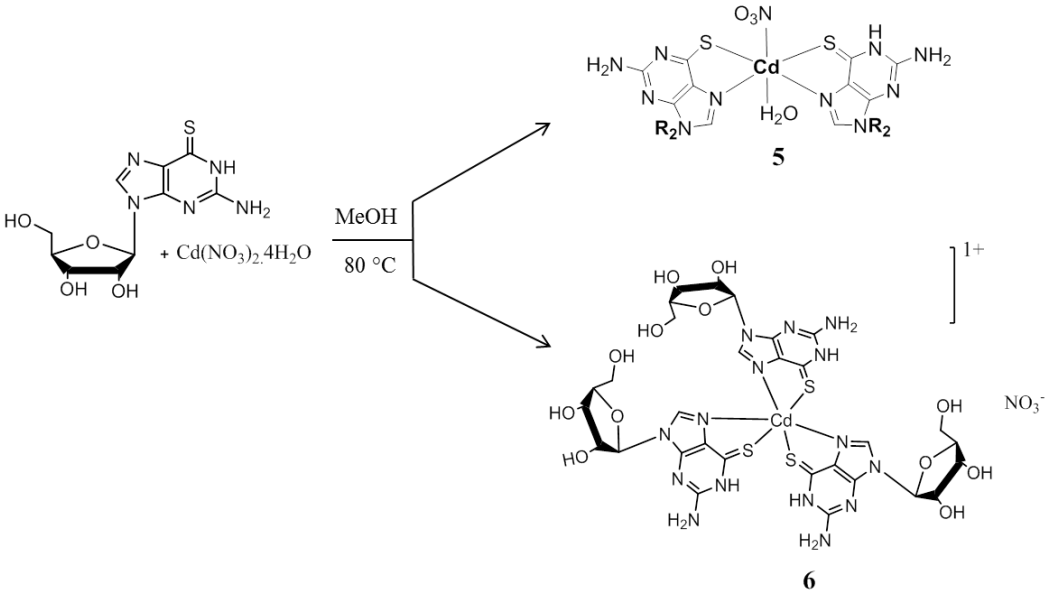

Scheme 10. Synthesis routes to **5** and **6.**

The expected product is the coordination polymer; see Figure 21 as reported by Zamora.[19] However in this instance a non-crystalline yellow powder was obtained and so it was not possible to determine the structure by x-ray diffraction. Therefore the following sections describe the structure determination of the yellow powder by, ES^- MS, IR, ^{1}H-NMR spectroscopy and elemental analysis**.**

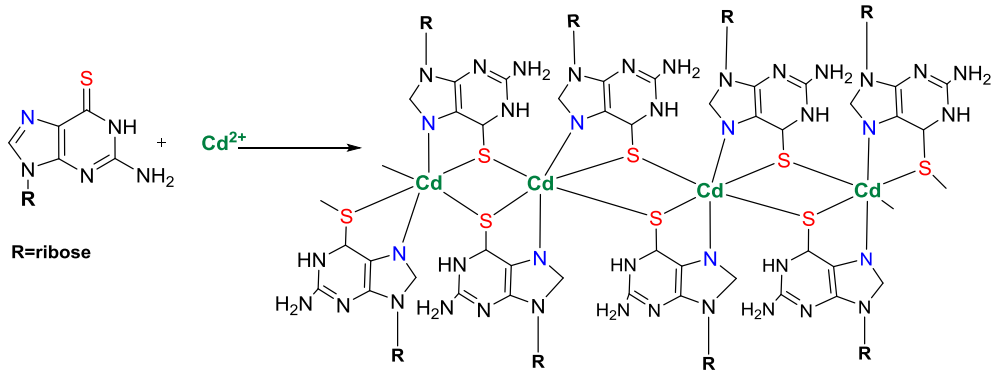

Figure 21. Proposed structure of a 1D-coordination polymer for **tG** with Cd^{2+}.

2.2.4.1 ES-MS of Cadmium complexes of tG

Spectroscopic characterization using ES-MS indicated the formation of several possible cadmium complexes with **tG** containing various combinations of ligands and metal ions, see Figure 22. The major peak corresponds to a complex of two **tG** ligands coordinating to one Cd^{2+} (complex,**5** m/z found 711.00), But also there was a peak due to the similar situation with Ni and Co, of three **tG** ligands to one Cd^{2+} (complex, **6** m/z found 1010.10). Also a small peak was observed at m/z 1419.05 related to a Cd-complex consists of four ligands chelate to two Cd^{2+} which might be an evidence of formation polymer as seen in Figure 22.

These data suggest that there could be different complexes of cadmium species in the solution, see Table 2

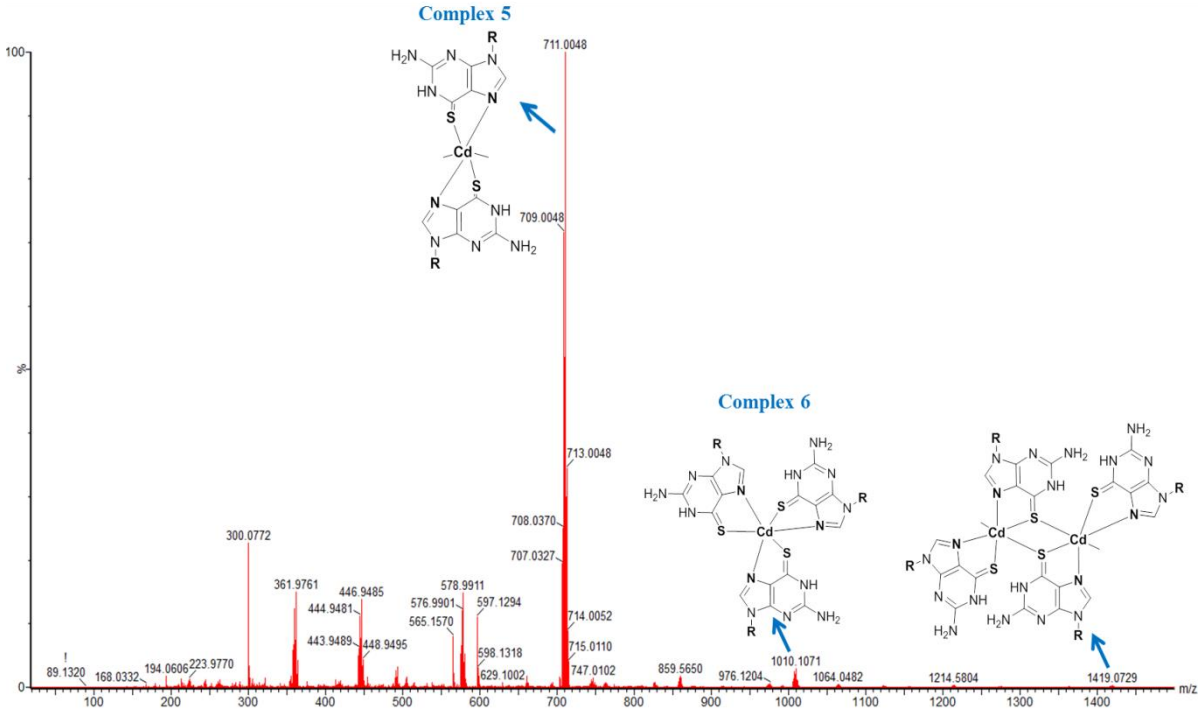

Figure 22. ES-MS of cadmium complex formation of **tG** at different ratios.

Complex formula	tG : Cd ratio	Calculated ES/MS	Found ES/MS
$C_{20}H_{25}N_{10}O_8S_2Cd$	2:1	711.0334	711.0048
$C_{30}H_{38}N_{15}O_{12}S_3Cd$	3:1	1010.1024	1010.1071
$C_{40}H_{49}N_{20}O_{16}S_4Cd_2$	4:2	1419.0592	1419.0729

Table 2. ES-MS of cadmium complex formation of **tG** at different ratios.

2.2.4.2 IR of Cadmium complexes of tG

The IR spectra of the cadmium products with **tG** were examined to propose the most likely structure of the complex; however the binding modes of **5** and **6** are equivalent and so it is impossible to determine which of these two coordination geometries are dominant. Once again IR assignments of the cadmium complexes showed similar spectral changes to the cobalt and nickel complexes that were discussed earlier in this chapter. In the possible cadmium (II) complexes, **5** and **6** the C=S band is shifted to 1194 cm^{-1} compared with free ligand **tG.** In **tG** the 1632 -1558 cm^{-1} bands were assigned to (C=C) and (C=N) stretching modes respectively. After complexation these bands shifted to about 1591-1500 cm^{-1} respectively.

These data are indicative that N(7) and C(6) of the ligand is involved in the cadmium (II) complex. In addition, in the IR data of the product from the reaction between **tG** and Cd $(NO_3)_2$ there is a new broad band at about 1304 cm^{-1} assigned to the nitrate group which suggests the involvement of the nitrate group in the complex, as seen in Figure 23. These results are similar to that observed for the Co(II) complex **1** (1319 cm^{-1}) and also Ni(II) complexes **3** and **4** (1308 and 1312 cm^{-1}).

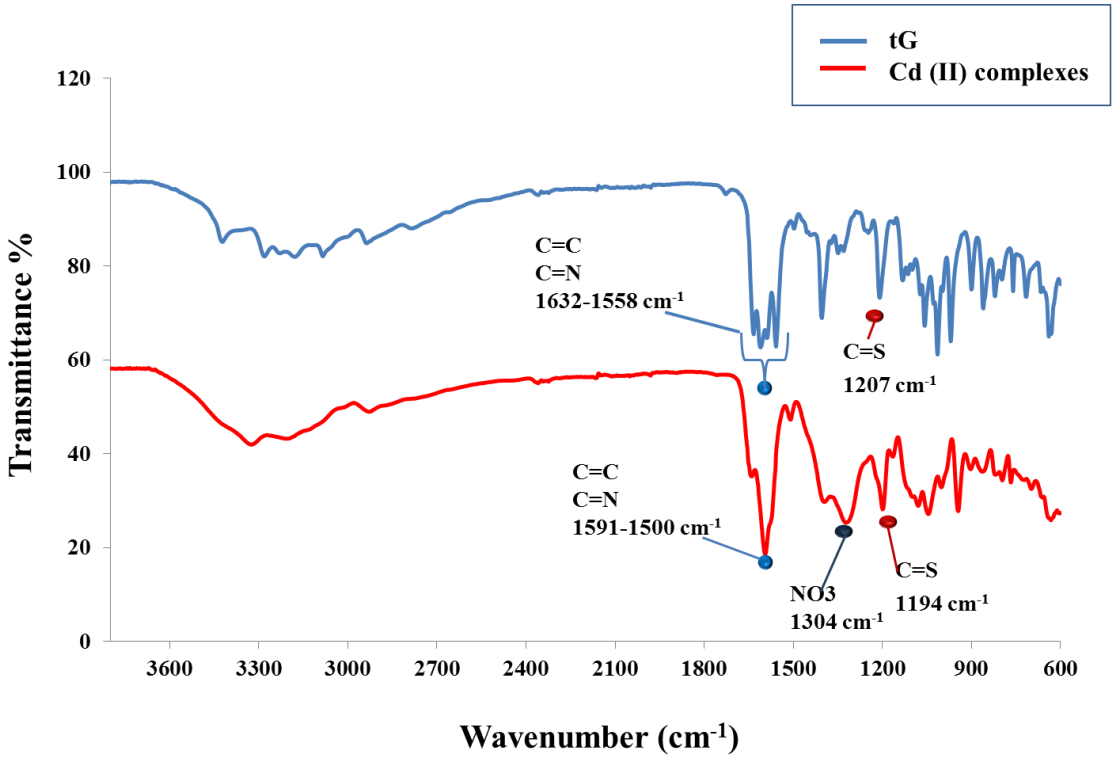

Figure 23. IR comparison between of **tG** (blue line) and Cd complexes of **tG** (red line).

2.2.4.3 ^{1}H-NMR of Cadmium complexes of tG

The ^{1}H-NMR spectrum of the cadmium (II) complex showed a general downfield shift and broadening for the protons in the complex compared to the free ligand especially for N(1) proton, H(8) and NH_2 peaks as shown in Figure 24. In the ^{1}H-NMR spectrum of the free ligand **tG,** the signal at δ 11.9 is the N(1) proton. On complexation with cadmium, this signal shifts to δ 12.7 ppm. Additionally, the H(8) and NH_2 protons in the complex, 8.1 and 6.7 ppm respectively, are shifted compared to when in the free ligand, 8.4 and 7.1 ppm. This agrees with the previously report by Zamora *et al.* for the complex of 6-MPH with cadmium.[19] Moreover, these peaks N(1) proton, H(8) and NH_2 integrated as 1:1:2 respectively in the free ligands whilst in the complexes were integrated as 1:2:4 respectively, see Figure 24. This indicates the formation of complex consisting of two ligands bound to one cadmium ion where one of the ligands is deprotonated and has the highlighted structure shown alongside the NMR spectrum in Figure 24. In other words, this complex consists of two isomeric ligands: a neutral ligand (thione isomer) and a deprotonated ligand (anionic thiol isomer).

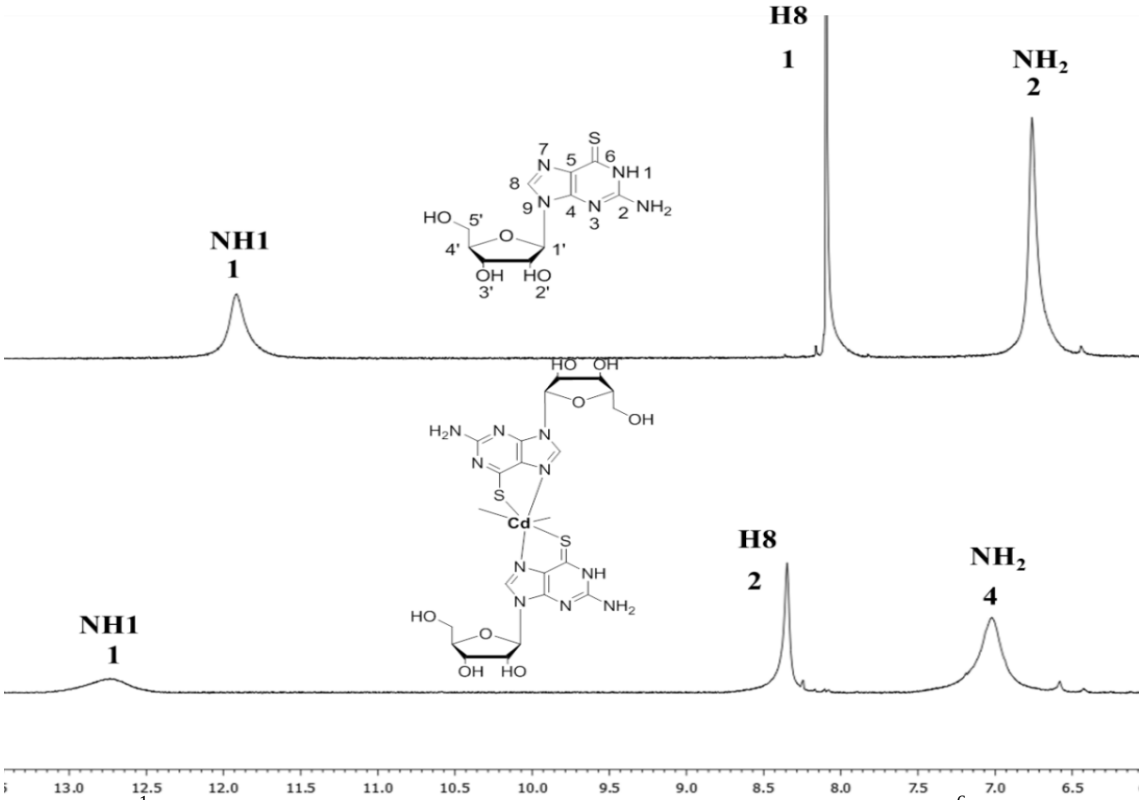

Figure 24. ^{1}H NMR comparison between **tG** and cadmium complexes of **tG** in d^{6}-DMSO.

Due to the lack of a crystal structure of the cadmium complex with **tG**, the molecular formula and structure of the complex was determined from the above discussion of the

ES-MS, IR, ^{1}H NMR and elemental analysis data. These data suggest that the cadmium complex consists of two ligands (neutral and anionic ligands) coordinated to one Cd^{2+} through N(7) and S(6). In addition, the inner sphere of the cadmium (II) complex is anionic as one of the two ligands is deprotonated (thiol form). As a result, there is one nitrate group to neutralize the complex. In a previous report the geometry for a cadmium complex with 6-MPH is octahedral arrangement.[19] Therefore it was expected that **5** will have octahedral geometry [Cd(II)(**tGH**)(**tG**)]NO_3 H_2O as shown in Figure 25. Moreover, the elemental analysis of complex, **5** is consistent with this proposed structure. The C, H, N analysis of the complex, **5** indicated the formula of the complex was $C_{20}H_{27}N_{11}O_{12}S_2Cd.2H_2O$, Calcd (found): C, 29.08 (29.05); H, 3.78 (3.09); N, 18.65 (17.12)

However it is inconclusive that the final structure exists as the non-polymeric unit, **5**, or whether the desired coordination polymer is also formed.

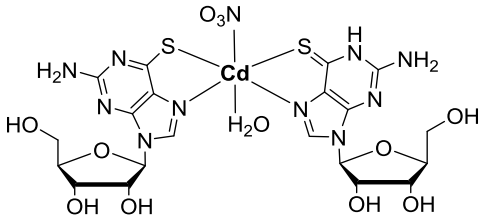

Figure 25. The proposed molecular structre of Cd (II) complex, **5.**

Overall, the binding of **tG** and **d-tG** with metal ions was explored. The reaction conditions (pH and solvent), ligands (**tG** or **d-tG**) and metal salts, Co^{2+}, Ni^{2+} and Cd^{2+} were varied. Two crystal structures with Co (three ligands (**tG** or **d-tG**) to one Co) and one crystal structure with Ni (three **d-tG** ligands to one Ni) were obtained. Whereas in the case of Cd(II) two complexes of **tG** were formed. Table 3 summarise the complex structures for the products of **tG** and **d-tG** with these metals.

Ligand	Metal salt	Complexes structure	
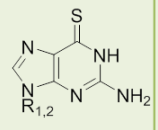	$Co(NO_3)_2.6H2O$	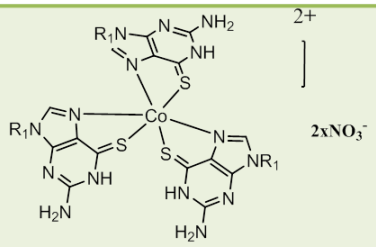 Complex 1	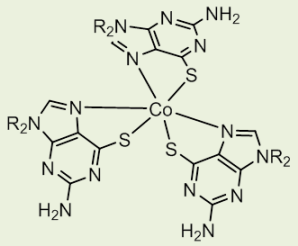 Complex 2
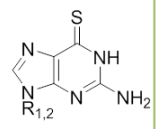	$Ni(NO_3)_2.6H2O$	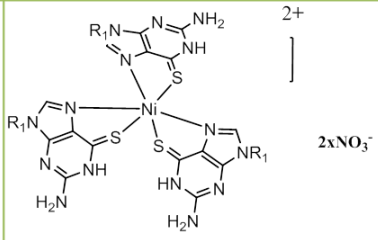 Complex 3	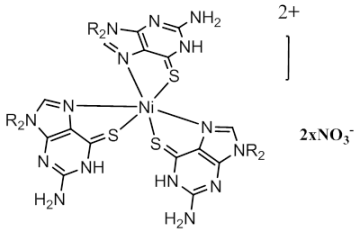 Complex 4
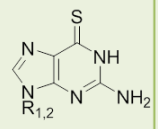	$Cd(NO_3)_2.4H2O$	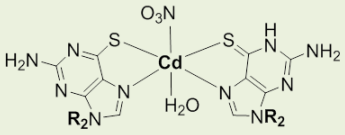 Complex 5	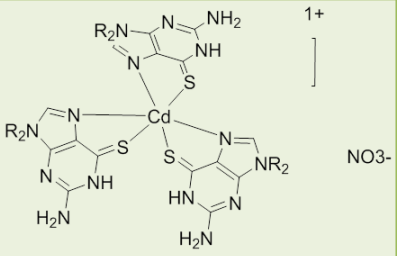 Complex 6

Table 3. Summary of the complex structures of **tG** and **d-tG** with metal ions (Co^{2+},Ni^{2+} and Cd^{2+}) where R_1= deoxy-ribose sugar and R_2= ribose sugar.

2.3 Conclusion

This chapter set out to form 1D-coordination polymers using thiolated DNA nucleosides. The results in this chapter discussed the approach taken to create 1D-coordination polymers based on **tG** and **d-tG** with Ni, Co and Cd. First, the synthesis of **d-tG** as indicated by data from ^{1}H-NMR, ^{13}C-NMR, IR, MS and UV was achieved. Second, the comparison of **d-tG** with **tG** as ligands for the binding of a range of metal ions (Co^{2+}, Ni^{2+} and Cd^{2+}) was performed. The formation of complexes was characterized by x-ray crystallography, IR, ES-MS, ^{1}H-NMR and CHN. In the case of Co^{2+} and Ni^{2+} the binding ratio of monomer (thio-nucleoside ligands) with Co^{2+} and Ni^{2+} ions was shown to be three ligands to one metal in both cases. Whereas, in the case of Cd^{2+}, the binding ratio was shown to be two ligands to one metal. However, ES-MS of the Cd-complex did show another possible binding ratio of three ligands to one Cd^{2+}

and also evidence of a larger extended structure containing four ligands and two Cd^{2+} centres. This supports that the Cd-complex with **tG** may form the desired 1D coordination polymer, similar to the reported cases for the equivalent nucleobase system.[19] Therefore, the next chapter considers the binding of cadmium ions by DNA oligomers which contain multiple thio-nucleosides.

2.4 Experimental

NMR spectra were measured on a 400 MHz Delta Jeol. IR analysis was performed on a Varian 800 FT-IR and ESI-MS was performed on a Waters LCT-Premier mass spectrometer. For elemental analysis a Carlo-Erba CE1108, configured for % CHN was used. UV–visible spectra were measured on a Cary.100 Bio Spectrometer. Crystal data were collected using synchrotron radiation at station I19, Diamond Light Source. Magnetic susceptibility measurements were performed on Magnetic Susceptibility Balance of Johnson Matthey (JM) PLC, York Way Royston. All chemicals were purchased from Sigma-Aldrich.

Synthesis of 2'-deoxy-6-thioguanosine (d-tG)

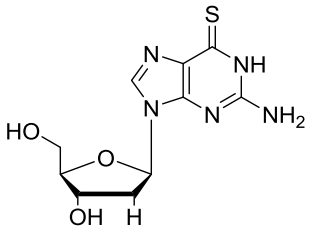

2'-deoxyguanosine (0.20 g 0.75 mmol) was added to 15 ml of dry pyridine, which was cooled in an ice bath under a nitrogen atmosphere. Trifloroacetic anhydride 0.9 ml (6.3 mmol) was added drop wise and stirred for 40 min. After that, a suspension of 1.3 g (23 mmol) of NaSH in 22.6 ml of anhydrous dimethylformamide was added and stirred. After 24 h, 38 ml of 0.16 M ammonium bicarbonate was poured into the reaction mixture with vigorous stirring. The mixture was concentrated to dryness then was dissolved in methanol and filtered. The filtrate was concentrated to dryness and 0.1 M of triethylammonium acetate (TEAA) was added. The product was crystallized from water and methanol to give a yellow crystal (0.18 g, 85% yield). ^{1}H-NMR (399.78 MHz, DMSO-*d*6) δ 11.89 (s, 1H, NH), 8.05 (s, 1H, H_8), 6.75 (br, 2H, NH_2), 6.04 (dd, 1H, J_1=6.33 Hz, J_2= 7.29 Hz $H_{1'}$), 5.23 (d, 1H, J=3.30 Hz, 3'-OH), 4.95 (t, 1H, J=4.94 Hz , 5'-OH), 4.27 (m, 1H, $H_{3'}$), 3.75 (m, 1H , $H_{4'}$), 3.46 (m, 2H, $H_{5',5''}$), 2.45 & 2.34 (m & m, 1H & 1H, $H_{2'}$ & $H_{2''}$). ES-MS: m/z (positive mode) 306.063 (calcd for $C_{10}H_{13}N_5O_3S$ (M+Na) 306.062).

Synthesis of $[Co(d\text{-}tG)_3](NO_3)_2 \cdot 2H_2O$ (1)

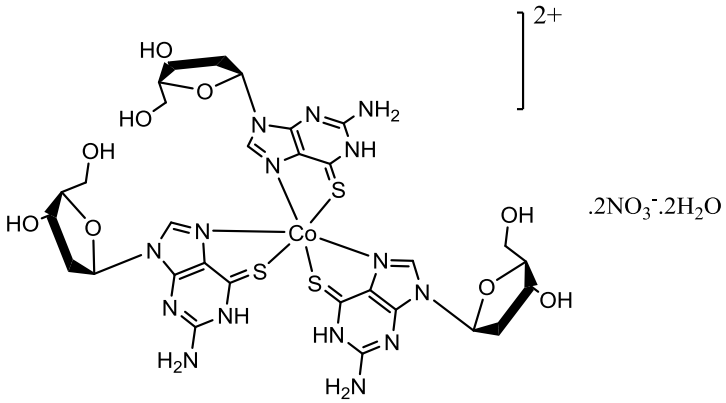

2'-Deoxy-6-thioguanine **(d-tG)** (86.03 mg, 0.304 mmol) was dissolved in methanol (10 mL), and a solution of cobalt nitrate $Co(NO_3)_2 \cdot 6H_2O$ (68 mg, 0.234 mmol) also in methanol (3 mL) was added and the mixture was refluxed, with stirring, at 60 °C overnight. After 24 h the solution was filtered and left to crystallize at room temperature by slow evaporation. After 5 days a crystalline precipitate was isolated by filtration (65 mg, 31 % yield), from which a small green single crystal of **1** suitable for X-ray structure determination was obtained. Anal. Calcd. (found) for $C_{30}H_{44}N_{18}O_{20}S_3Co$: C, 31.83 (31.81); H, 3.92 (3.94); N, 22.27 (22.14). IR selected data (cm^{-1}): 3300 (w), 3200 (m), 2916 (m), 2845 (w), 1603 (s), 1375 (m), 1319 (s), 1246 (m), 1202 (m), 1175 (m), 1092 (m), 1045 (w), 988 (m), 947 (m), 800 (m).723 (w), 603 (w). ES-MS: m/z (positive mode) 907.1469 (calcd for $[Co(6\text{-}MP)_3]^+$ 907.1471).

Synthesis of $[Co(tG)_3] \cdot 1.5H_2O$ (2)

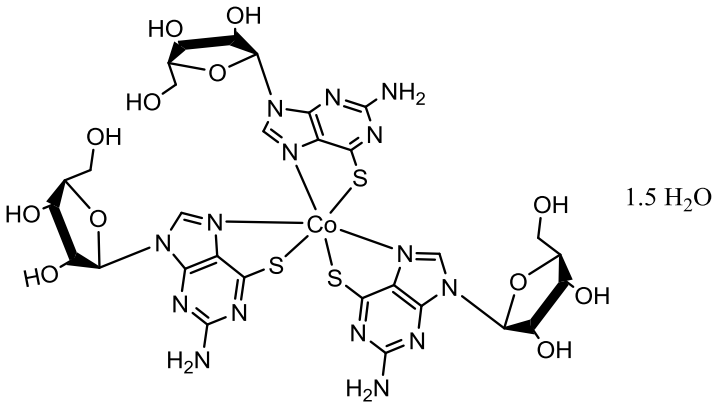

6-Thioguanosine (**tG**) (74.4 mg, 0.248 mmol) was dissolved in a mixture of water (10 mL) and methanol (10 mL); then 10 mL of an aqueous solution of $Co(NO_3)_2 \cdot 6H_2O$

(36.1 mg, 0.124 mmol) was added to the mixture. The mixture was refluxed and stirred at 86 °C for 3 h. After that, the pH of the solution was adjusted to 8 with NaOH and refluxed again for 3 h. After cooling, the solution was filtered and kept at room temperature to afford (57 mg 48 % yield) of dark green crystals suitable for X-ray structure determination. Anal. Calcd. (found) for $C_{30}H_{39}N_{15}O_{13.5}S_3Co \cdot 0.5NaOH$: C, 36.00 (36.59); H, 3.98 (3.22); N, 20.99 (19.96). IR selected data (cm^{-1}): 3248 (s), 3130 (s), 2972 (m), 2889 (s), 1599 (s), 1587 (s), 1371 (s), 1267 (s), 1192 (s), 1082(s), 982 (m), 935 (s), 873 (m), 630 (m). ES-MS: m/z (positive mode) 976.1069 (Calcd. for $[Co(6\text{-}MP)_3]Na^+$ 976.1060).

Synthesis of $[Ni(d\text{-}tG)_3](NO_3)_2 \cdot 2H_2O$ (3)

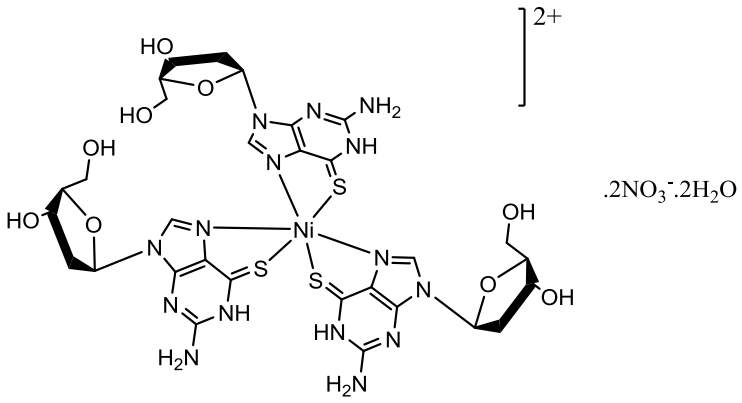

d-tG (166 mg, 0.587 mmol) was dissolved in methanol (10 ml), and a solution of nickel nitrate $Ni(NO_3)_2.6H_2O$ (131 mg, 0.45 mmol) in methanol was added. The mixture was stirred at 60 °C for 24 h and then filtered. Green crystals were obtained after 4 days at room temperature. (120 mg, 24 %). Anal. Calcd (found) for $C_{30}H_{43}N_{17}O_{17}S_3Ni$: C, 33.71 (33.26); H, 4.06 (4.14); N, 22.28 (22.23). IR selected data: 3635 (s), 3330 (s), 3205 (s), 2981 (m), 2889 (s), 1598 (s), 1572 (s), 1383 (s), 1308 (s), 1197 (s), 1151 (w), 993 (m), 943 (s), 866 (m), 676 (m). ^{1}H-NMR (399.78 MHz, DMSO-*d*6): δ 11.86 (s, 1H, NH), 8.03 (s, 1H, H_8), 6.73 (br, 2H, NH_2), 6.01 (br, 1H, $H_{1'}$), 5.20 (br, 1H, 3'-OH), 4.86 (br, 1H, 5'-OH), 4.26 (br, 1H, $H_{3'}$), 3.72 (br, 1H , $H_{4'}$), 3.46 (m, 2H, $H_{5',5''}$), 2.45 & 2.34 (m & m, 1H & 1H, $H_{2'}$ & $H_{2''}$). ES-MS: m/z (positive mode) 906.1757 (calcd for $[Ni(\mathbf{d\text{-}tG})_3]^+$ 906.1492).

Synthesis of $[Ni(tG)_3](NO_3)_2$ (4)

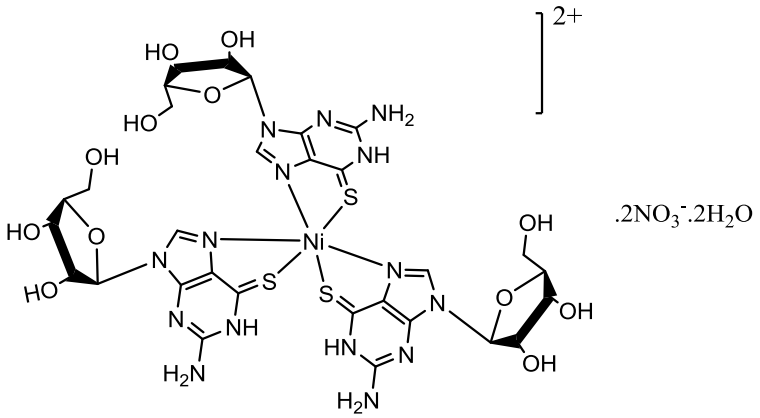

tG (332 mg, 1.110 mmole) was dissolved in methanol (10 ml), and a solution of nickel nitrate $Ni(NO_3)_2.6H_2O$ (262 mg, 0.90 mmole) was added in the same solvent. The mixture was stirred at 60 °C for 24 h and then filtered. A light green powder was obtained (260 mg, 26 %). Anal. Calcd (found) for $C_{30}H_{39}N_{17}O_{18}S_3Ni$: C, 33.44 (33.57); H, 3.37 (3.505); N, 22.10 (19.64). IR selected data: 3321 (s), 3179 (s), 3086 (s), 2903 (m), 2801 (s), 1591 (s), 1499 (s), 1368 (s), 1312 (s), 1194 (s), 1045 (w), 945(s), 866 (m), 673 (m). ^{1}H-NMR (399.78 MHz, DMSO-*d*6): δ 11.90 (s, 1H, NH), 8.08 (s, 1H, H_8), 6.76 (br, 2H, NH_2), 5.64 (br, 1H, $H_{1'}$), 5.39 (br, 1H, 2'-OH), 5.01 (br, 1H, 3'-OH), 4.96 (br, 1H, 5'-OH), 4.33 (br, 1H, $H_{3'}$), 4.03 (br, 1H , $H_{4'}$), 3.46 (m, 2H, $H_{5',5''}$), 3.56 (m, 1H, $H_{2'}$). ES-MS: m/z (positive mode) 954.1432 (calcd for $[Ni(\mathbf{tG})_3]^+$ 954.1340).

Synthesis of $[Cd(tGH)(tG)]NO_3\,H_2O$ (5)

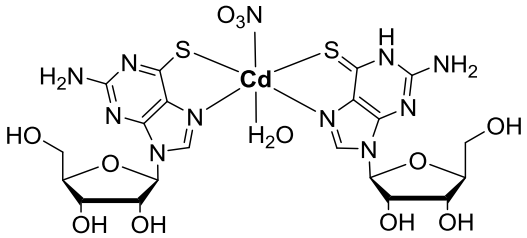

tG (56 mg, 0.2 mmole) was dissolved in 10 ml methanol, and a solution of cadmium nitrate $Cd(NO_3)_2.4H_2O$ (30 mg, 0.1 mmole) was added in the same solvent. The mixture was stirred at 80 °C for overnight. After 24 h, a yellow powder was obtained and filtered and was dried at room temperature (33 mg, 42 %). Anal. Calcd (found) for $C_{20}H_{27}N_{11}O_{12}S_2Cd.2H_2O$: C, 29.08 (29.05); H, 3.78 (3.09); N, 18.65 (17.12). IR

selected data: 3294 (s), 3181 (w), 3115 (s), 2966 (m), 2876 (s), 1591 (s), 1500 (s), 1371 (s), 1304 (s), 1194 (s), 1038(w), 941(s), 854 (m), 630 (m). ^{1}H-NMR (399.78 MHz, DMSO-*d*6): δ 12.74 (br, 1H, NH), 8.40 (s, 1H, H_8), 7.11 (br, 2H, NH_2), 5.69 (d, 1H, J=5.01 Hz,, $H_{1'}$), 5.47 (br, 1H, 2'-OH), 5.18 (br, 1H, 3'-OH), 5.06 (br, 1H, 5'-OH), 4.41 (br, 1H, $H_{3'}$), 4.07 (br, 1H , $H_{4'}$), 3.87 (m, 2H, $H_{5',5''}$), 3.52 (m, 1H, $H_{2'}$). ES-MS: m/z (positive mode) 711.0048 (calcd for $[Cd(\mathbf{tG})_2]^+$ 711.0334).

UV-vis spectrophotometric pH titration

A 10 mM solution of 2'-deoxy-6-thioguanosine in water was titrated in a 10 mm path length absorption cell by successive additions of sodium hydroxide. The small volume of a 60 mM stock solution of NaOH was added. The absorbance was monitored between 200 and 500 nm after each addition.

References

(1) Elion, G. B. *Science* **1989**, *244*, 41.

(2) Aubrecht, J.; Goad, M. E. P.; Schiestl, R. H. *Journal of Pharmacology and Experimental Therapeutics* **1997**, *282*, 1102.

(3) Kasende, O. E. *Spectrochimica Acta Part a-Molecular and Biomolecular Spectroscopy* **2002**, *58*, 1793.

(4) Evans, W. E.; Relling, M. V. *Science* **1999**, *286*, 487.

(5) Freund, M.; Poliwoda, H.; Bodenstein, H.; Eisert, R. *Onkologie* **1985**, *8*, 150.

(6) Wiernik, P. H.; Glidewell, O. J.; Hoagland, H. C.; Brunner, K. W.; Spurr, C. L.; Cuttner, J.; Silver, R. T.; Carey, R. W.; Delduca, V.; Kung, F. H.; Holland, J. F. *Medical and Pediatric Oncology* **1979**, *6*, 261.

(7) Aleksandrova, E. V. *Pharmaceutical Chemistry Journal* **2003**, *37*, 645.

(8) Fox, J. J.; Wempen, I.; Hampton, A.; Doerr, I. L. *Journal of the American Chemical Society* **1958**, *80*, 1669.

(9) Tohru Ueda, K. M. a. T. K. *chem.Pharm.Bull* **1978**, *26*, 2122.

(10) Kung, P.-P.; Jones, R. A. *Tetrahedron Letters* **1991**, *32*, 3919.

(11) Dubler, E. *Metal Ions in Biological Systems* **1996**, *32*, 301.

(12) Lippert, B. *Cisplatin*; Wiley-VCH: Weinheim: Germany, 1999.

(13) Kirschner, S. W., Y. K.; Francis, D.; Bergman, J. G *J. Med. Chem* **1969**, *9*, 369.

(14) Das, M.; Livingstone, S. E. *British Journal of Cancer* **1978**, *38*, 325.

(15) Cheney, G. E.; Freiser, H.; Fernando, Q. *Journal of the American Chemical Society* **1959**, *81*, 2611.

(16) Heitner, H. I.; Lippard, S. J. *Inorganic Chemistry* **1974**, *13*, 815.

(17) Lavertue, P.; Hubert, J.; Beauchamp, A. L. *Inorganic Chemistry* **1976**, *15*, 322.

(18) Schmalle, H. W.; Gyr, E.; Dubler, E. *Acta Crystallographica Section C-Crystal Structure Communications* **2000**, *56*, 957.

(19) Amo-Ochoa, P.; RodrÃ-guez-Tapiador, M. I.; Castillo, O.; Olea, D.; Guijarro, A.; Alexandre, S. S.; GÃ³mez-Herrero, J.; Zamora, F. *Inorganic Chemistry* **2006**, *45*, 7642.

(20) Caira, M. R.; Nassimbeni, L. R. *Acta Crystallographica Section B-Structural Science* **1975**, *31*, 1339.

(21) Griffith, E. A. H.; Amma, E. L. *Journal of the Chemical Society-Chemical Communications* **1979**, 1013.

(22) Houlton, A. In *Advances in Inorganic Chemistry*; Academic Press: **2002**; Vol. 53, p 87.

(23) Zamora, F.; Pilar Amo-Ochoa, M.; Sanz Miguel, P. J.; Castillo, O. *Inorganica Chimica Acta* **2009**, *362*, 691.

(24) Amo-Ochoa, P.; Castillo, O.; Alexandre, S. S.; Welte, L.; de Pablo, P. J.; Rodriguez-Tapiador, M. I.; Gomez-Herrero, J.; Zamora, F. *Inorganic Chemistry* **2009**, *48*, 7931.

(25) Wettig, S. D.; Wood, D. O.; Aich, P.; Lee, J. S. *Journal of Inorganic Biochemistry* **2005**, *99*, 2093.

(26) Santhosh, C.; Mishra, P. C. *Spectrochimica Acta Part a-Molecular and Biomolecular Spectroscopy* **1993**, *49*, 985.

(27) Amo-Ochoa, P.; Alexandre, S. S.; Hribesh, S.; Galindo, M. A.; Castillo, O.; Gómez-García, C. J.; Pike, A. R.; Soler, J. M.; Houlton, A.; Zamora, F. *Inorganic Chemistry* **2013**, *52*, 5290.

(28) Ahluwalia, V. K.; Kaur, J.; Ahuja, B. S.; Sodhi, G. S. *Journal of Inorganic Biochemistry* **1991**, *42*, 147.

(29) Dubler, E.; Gyr, E. *Inorganic Chemistry* **1988**, *27*, 1466.

(30) Lloret, F.; Julve, M.; Cano, J.; Ruiz-García, R.; Pardo, E. *Inorganica Chimica Acta* **2008**, *361*, 3432.

(31) Podgajny, R. C., S.; Nitek, W.; Budziak, A.; Rams, M.; Gomez-Garcia, C. J.; Oszajca, M.; Lasocha, W.; Sieklucka, B *Cryst Growth Des* **2011**, *11*, 3866.

(32) Benmansour, S.; Setifi, F.; Triki, S.; Gómez-García, C. J. *Inorganic Chemistry* **2012**, *51*, 2359.

(33) Lippard, S. J. *Progress in Inorganic Chemistry*; John Wiley & Sons, Inc: Canda, 1976.

(34) Gartland, G. L. a. B., C.E *Acta Crystallographica Section B-Structural Science* **1977**, *B33*, 3678.

(35) Suh, M. P.; Kang, S. G. *Inorganic Chemistry* **1988**, *27*, 2544.

Chapter 3 On column conversion of dG-oligomers to d-tG-oligomers and their binding with metal ions

3.1 Introduction

Chapter 2 described the investigation into the synthesis and characterisation of **d-tG** (monomer) *via* the conversion of **d-G** according to the procedure reported by Jones.[1] Subsequently, the binding of a range of different metal ions by **d-tG** and **tG** was compared. The binding ratio of thio-monomer (ligand) with metal ions was shown to be three ligands to one metal in the case of Co(II) and Ni(II), which was contrary to the work of others,[2] where the formation of a 1D coordination polymer of the nucleobase 6-meracuptopurine with cadmium was reported. However, in the case of the Cd(II)-complex with the **tG** monomer, the results hinted that the formation of a 1D coordination polymer was likely eventhough no crystal data was obtained to confirm this structure. Therefore in order to realize this goal, the synthesis of uniform thio modified guanosine-oligomers containing 2, 3, 4 and 5 thio-nucleobase were synthesised, and the addition of cadmium ions to these thio-guanosine oligonucleotides performed in order to assess the metal binding properties of thioguanosine units pre-assembled *via* phosphoramidite chemistry, see Scheme 1.

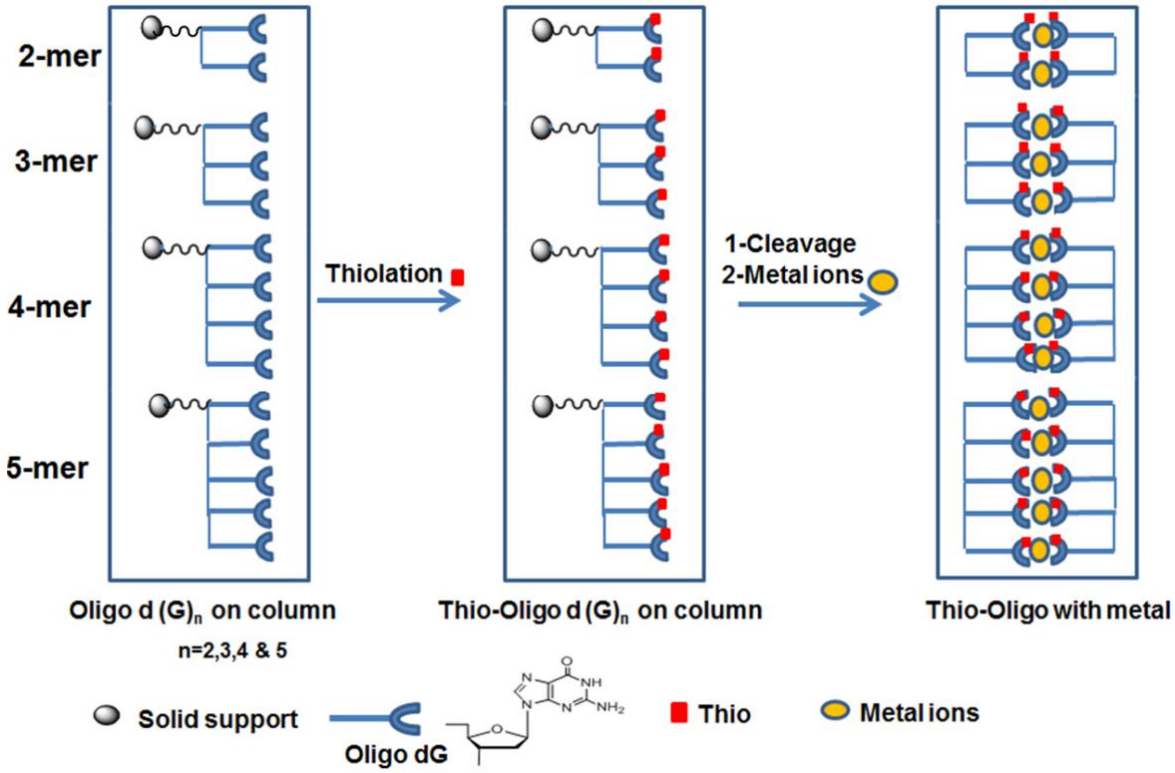

Scheme 1. Schematic routes for the synthesis of thio-functionalized oligomers for metal binding coordination polymers.

Although, the overall aim of this project was to produce a 1D coordination polymer from thio-guanosine units and metal ions, the synthesis of thioguanosine oligomers has been studied for other reasons. For example, previous reports have showed that oligonucleotides containing a thiol or thione substituted base, such as 6-thioguanine, are very useful tools in the fields of cancer research and biology.[3-7] In addition, their ability for photochemical cross-linking has been utilized for probing RNA-RNA interactions or RNA proteins at the atomic level.[3-6] Moreover, they have been used in the post-synthetic modification as intermediates to synthesize other artificial oligonucleotides.[8-11] The sulphur atom of 6-thioguanosine is highly nucleophilic, and because of this property 6-thioguanosine has been utilized as a site modification of oligodeoxynucleotides (ODN).[7,12,13] Interestingly, these thionucleotides have long wavelength UV absorption (330-360 nm), which is well removed from the normal maximum absorption of the nucleic acids (260 nm) and proteins (280 nm)[14] Therefore, these interesting properties of thio-**dG** oligomers were the driving force behind research efforts into their synthetic routes. The following section describes the various routes employed for the synthesis of thio-**dG** containing oligomers.

3.1.1 Phosphoaramidite synthesis

Recently advances in the biological molecular and nucleic acid structures have been a direct result of the developments that have taken place in the synthesis of oligonucleotides.[15] There are two major improvements to the synthesis of oligonucleotides over the last decade. First, the use of solid supports in the synthesis of oligonucleotides.[16] This method is simple to purify and the oligonucleotide synthesis is carried out on an automated DNA synthesizer. Second, chemical techniques have been developed for the formation of the phosphodiester bonds.[17] In addition, the yield of the synthesis at each nucleotides step is now approaching 99.99 %. In this synthesis, the first nucleoside is already attached to the 3′-terminus of the solid support (beads of borosilicate glass), and is deprotected to offer a free 5-hydroxyl group (activated nucleoside) that will react with the second nucleoside. It is necessary to protect the 5′-hydroxyl position of the second nucleoside in order to prevent self-polymerization. After that the two nucleosides are coupled to give a dimer. During this reaction, any unreacted activated nucleoside bound to the solid support must be protected in a capping step. After the formation of the phosphorous linkage in the coupling step, the phosphorus(III) is oxidized to phosphorus(V) to give a phosphate group. This cycle of reactions steps is repeated several times until the desired oligonucleotide is formed, see Figure 1.

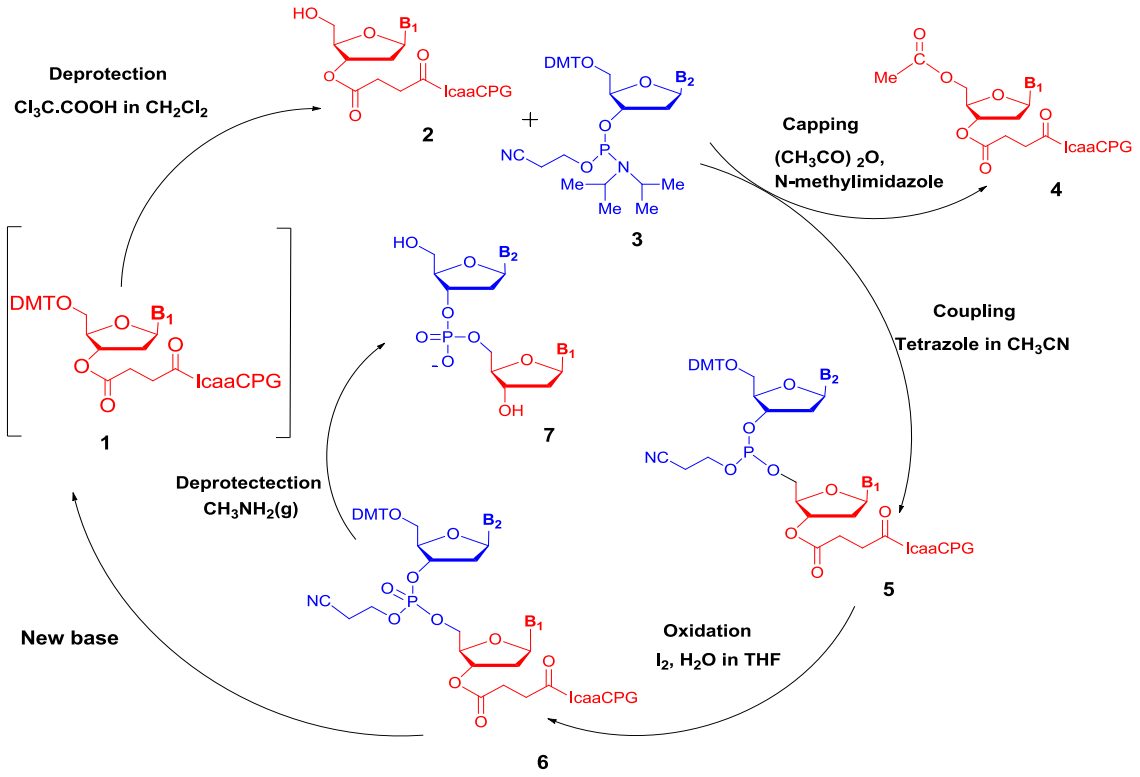

Figure 1. A schematic diagram of the chemical reactions involved in the solid phase oligodeoxynucleotide synthesis of an automated DNA synthesizer.

On completion of the desired oligonucleotide, it is cleaved from the solid support and the protecting groups are removed. The 4`,4`-dimethoxytrityl group is removed by 3% trichloroacetic acid in dichloromethane and concentrated aqueous ammonia is used to deprotect the other groups (for 5 hours at 55 °C) and cleave the oligonucleotide from the solid support. The cleaved oligonucleotide is dissolved in water, separated from the **CPG** beads, and then purified by reverse-phase HPLC.[17] The maximum length of DNA that can be obtained by this technique is around 100 bases, but normally only 40 bases are feasible.

3.1.2 Synthetic approaches towards d-tG oligomers

As discussed in chapter 1, there are several approaches to oligonucleotide modification; here we focus on the conversion of guanosine oligomers, into thio-guanosine oligomers. A number of studies have described the incorporation of thioguanosine into oligonucleotides *via* the automated DNA synthesis of oligomers using modified phosphoramidites., For example, Bronstein reported in 1988 the synthesis of an octamer

containing 6-thioguanosine synthesised from the 6-thiodG phosphoramidite.[18] In the same year, Rappaport claimed the incorporation of **d-tG** into dodecamers using the same approach, once again without using a protecting group on the thione (C=S).[19] In his method, the synthesis was time-consuming and problematic; and also there was no conclusive proof that the thione group was not oxidised during the deprotection and cleavage steps. This synthetic route to oligomers containing **d-tG** without utilizing any thione protecting group was also filed as a patent by Richardson.[20]

In 1991, Broom and his group[21] developed a new approach for the synthesis of oligonucleotides containing **d-tG** at predetermined sites.[21] This involved the synthesis of a protected **d-tG** phosphoramidite using an automated DNA synthesizer to insert **d-tG** into DNA oligomers at certain positions. This strategy prevents the **d-tG** from any possible side reactions or degradation during the cycle of DNA synthesis and also prevents any hydrolysis and oxidation of the thione function group. They synthesized an 8-mer 5'-d(ApApApCptGpTpTpT)-3' oligonucleotide containing a single **tG** bearing a phenoxyacetyl (PAc) protecting group on the exocyclic amino site of **tG**. In addition, the cyanoethyl group was used to protect the 6-thiocarbonyl function of **tG.** These protection groups are useful as they can be removed easily in concentrated ammonium hydroxide whilst also being stable during the cycle of reactions involved in the automated DNA synthesizer.[22-24] The characterisation of this thio-olignucleotide was carried out by ^{1}H-NMR and UV-vis experiments. Other researchers used automated solid-phase synthesis to create thio-oligonucleotides by using different protecting groups on the thione site such as the 2,4-dinitorophenyl group,[14,22] or the 2-ethylhexylpropionate group,[25] as seen in Figure 2.

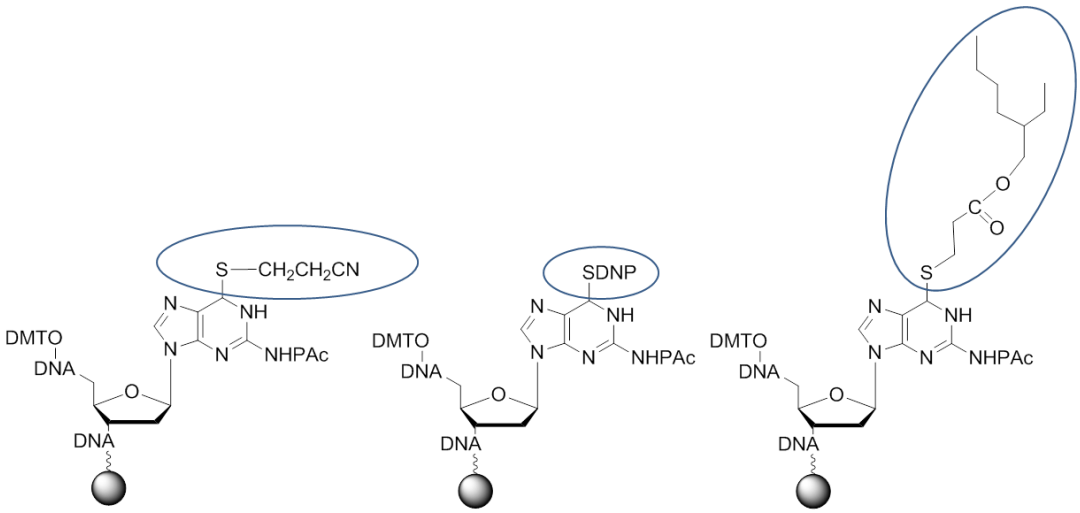

DNP = 2,4-dinitorophenyl, **PAc** = phenoxyacetyl.

Figure 2. Different protection of thione group on guanosine oligomers, for solid-phase DNA synthesizer.

One report by Zheng *et al.* highlighted how thio-guanosine oligomers undergo on-column conjugation, as shown in Scheme 2.[8] This approach leads to the introduction of diverse structures on the thione function at group of 6-thioguanosine **d-tG**. The incorporation of **d-tG** with a chemical labile-trigger at the thione position into oligonucleotides *via* phosphoramidtie chemistry is reported. This is useful as only a single phosphoramidite needs to be prepared. Moreover, as the oligonucleotides are still on the solid support during the conjugation reaction, the separation of the products from other reactants is straight-forward. Conversely; there are probable disadvantages of this method, as in some situations further purification stages are essential. Furthermore, it is time consuming as there are many steps involved in the synthesis.[8] However this work does highlight the possibility of working with thio-**dG** oligomers whilst they are still attached to the solid CPG support of a DNA synthesis column. The following section details some other reports on on-column modification of oligonucleotides.

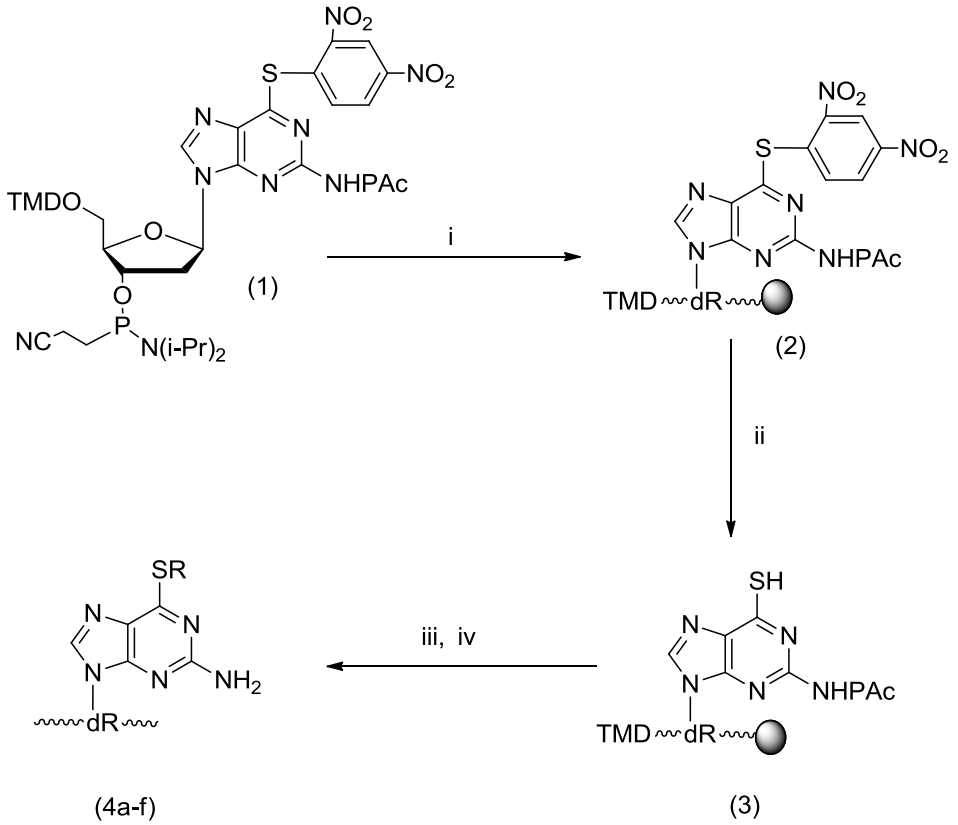

4a: R =CH_3; 4b: R =CH_3CH_2; 4C: R = $HOCH_2CH_2$; 4d: R = $(CH_3)_2CH$; 4e: R = $PhCH_2$; 4f: R = p-CH_3OPhCH_2; i: automated DNA synthesis; ii: $OHCH_2CH_2SH/CH_3CN/(i\text{-}Pr)_2NCH_2CH_3$; iii: RX; iv: 0.5 M NaOH(aq).

Scheme 2. Post-synthetic modification of oligonucleotides on-column.[8]

3.1.3 On column modification

Early examples of on–column oligonucleotide modification were developed by Grinstaff and Beilstein,[26] who reported that 5-iodo-2'-deoxyuridine phosphoramidite can be inserted at the required modification site of an oligonucleotide *via* automated solid phase synthesis. The column was removed from the synthesizer after addition of the iodo-modified nucleobase. Then ferrocenoyl propargylamide was added to the CPG beads in dimethylformamide-triethanolamine (DMF-TEA) at room temperature and allowed to react *via* a Pd catalysed before the solid support was dried and returned to the automated synthesizer. The cycle of the synthesis was continued until further ferrocenoyl propargylamide labelled nucleotides were to be inserted, and the modification repeated. A key advantage for this on-column modification strategy is that no further protection groups are required. In addition**,** it was envisaged to be

straight-forward to purify the oligomer as any unreacted materials will be simply removed from the column during the washing and purification steps.

3.2 Results and discussion

In order to produce one dimension coordination polymers that have possible applications in electronics[2], this chapter describes a route to the incorporation of **d-tG** into short DNA oligomers *via* solid phase DNA synthesis, using phosphoaramidite chemistry. Firstly, their conversion into thio-guanosine oligomers is detailed. These thio-oligomers work as multiple metal binding sites (ligands) that can coordinate metal ions such as cadmium (II) ions to create Cd-S-Cd bridged polymers. The following sections describe the synthetic work and metal binding studies.

3.2.1 On column synthesis of thio guanosine oligomers, $(d\text{-}tG)_n$

Having established in Chapter 2 the synthetic procedure for the conversion of **d-G** into **d-tG,** here the same reaction was performed on a **G** containing oligomer which is still bound to the **CPG** solid support as shown in Scheme 3.

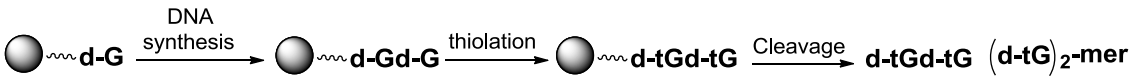

Scheme 3.Schematic synthesis of **$(d\text{-}tG)_2$**.

CPG based oligomer synthesis is a cyclic stepwise protocol for the synthesis of sequence specific short DNA oligomers. Therefore, the oligomer content can be controlled and purification is straightforward. Initially the synthesis of the two base oligomer, **$(d\text{-}tG)_2$** was performed. The guanosine-guanosine oligomer **$(d\text{-}G)_2$**, was synthesized as shown in Scheme 4. The first guanosine nucleoside is already attached to the 3′- terminus of the solid support and was deprotected to offer a free 5-hydroxyl group that will react with the second guanosine nucleoside.

Following the cycle of reactions steps, a-d in Scheme 4, the protected **G-G** dimer remains bound to the **CPG** support throughout the synthesis. On completion, the

column was removed from the synthesizer and the **CPG** beads were treated with sodium sulphide in anhydrous dimethylformamide as described previously.[1] The on-column synthesis of modified nucleotides has already been described by Grinstaff and has clear advantages in a simplified working up.[26] After reaction of 5 days, the column was then washed several times with water and ethanol and dried for 24 hours under vacuum. In previous work concentrated aqueous ammonia has been used to deprotect and cleave the oligonucleotides from the solid support, however, here we used anhydrous gaseous CH_3NH_2. This method of deprotection has been previously used in the synthesis of modified oligomers.[27] The cleaved **(d-tG)$_2$** was dissolved in water, separated from the **CPG** beads, and then purified by reverse-phase HPLC.

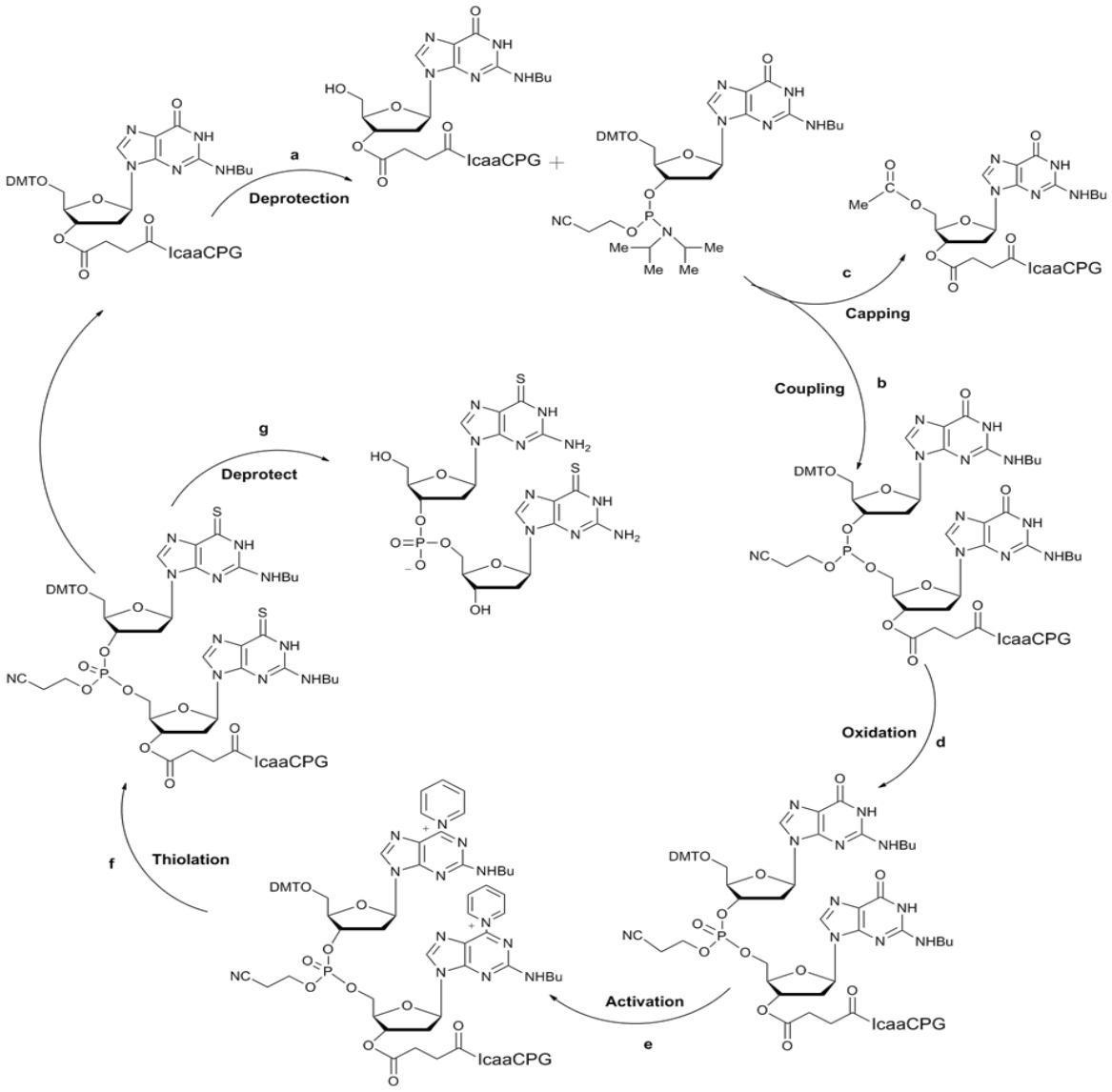

Scheme 4. Synthesis of the **(d-G)$_2$** column and its conversion to **(d-tG)$_2$**. a) $Cl_3C.COOH$ in CH_2Cl_2, b) Tetrazole in CH_3CN, c) $(CH_3CO)_2O$, N-methylimidazole, d) I_2, H_2O in THF, e) pyridine, $(CF_3CO)_2O$, f) NaSH in DMF, g) $CH_3NH_{2(g)}$ anhydrous.

3.2.2 Purification by HPLC

Short DNA oligomers are routinely purified by HPLC and analysed by LC-MS. The modified thioguanosine dimer **(d-tG)$_2$** was compared to **d-G** and the thiol 2'-deoxy-guanosine monomer by HPLC.[14] **d-G** and **d-tG** eluted at different retention times as seen in Figure 3, **d-G** was eluted after 8 min compared with **d-tG** which eluted after 11 min. This is due to different polarities of the nucleoside after the oxygen on C(6) of **d-G** was replaced by sulphur.

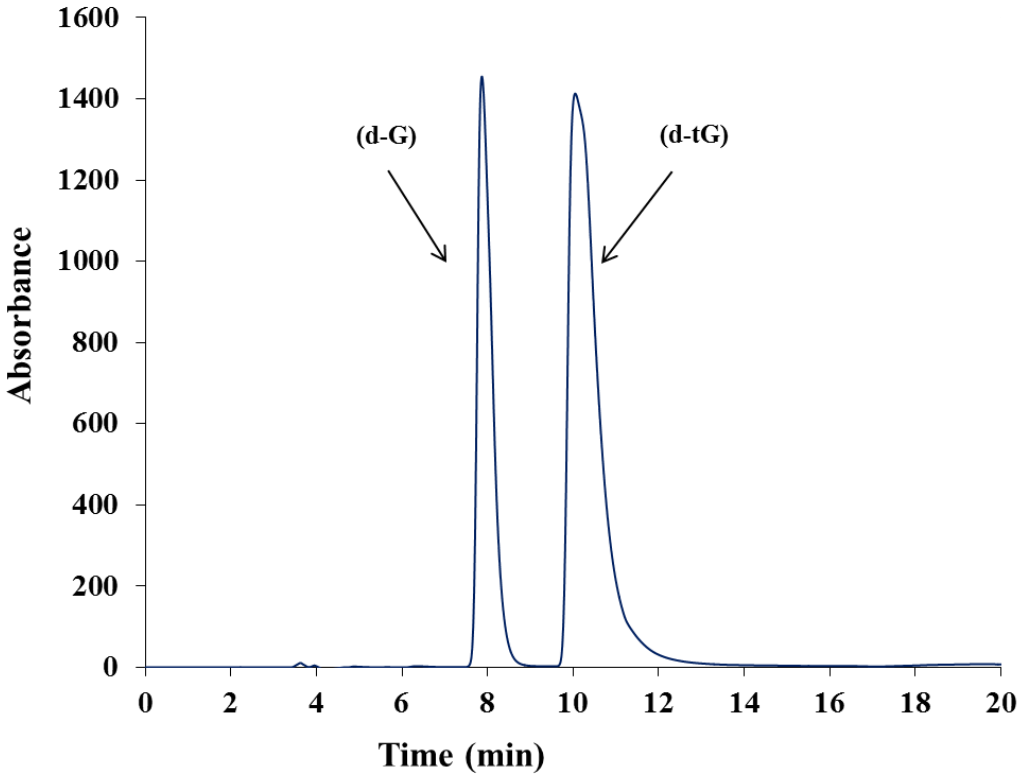

Figure 3. HPLC comparison between **d-G** and **d-tG.**

The chromatogram indicates that HPLC can easily be used to distinguish between two monomers **d-G** and **d-tG**. Therefore, the integrity of the synthesis of the **$(d\text{-}tG)_2$** was analysed by reverse-phase HPLC. During the synthesis it is possible to have five different compounds upon completion of the solid-phase cycles and the thiol conversion. These are: failed coupling and conversion: guanosine monomer **d-G**, failed coupling and successful conversion: thioguanosine monomer **d-tG**, successful coupling and failed conversion: guanosine dimer **$(d\text{-}G)_2$,** successful coupling and half conversion: thioguanosine-guanosine dimer **d-tGdG** and successful coupling and full conversion: thioguanosine dimer **$(d\text{-}tG)_2$.** These possibilities are shown in Figure 4.

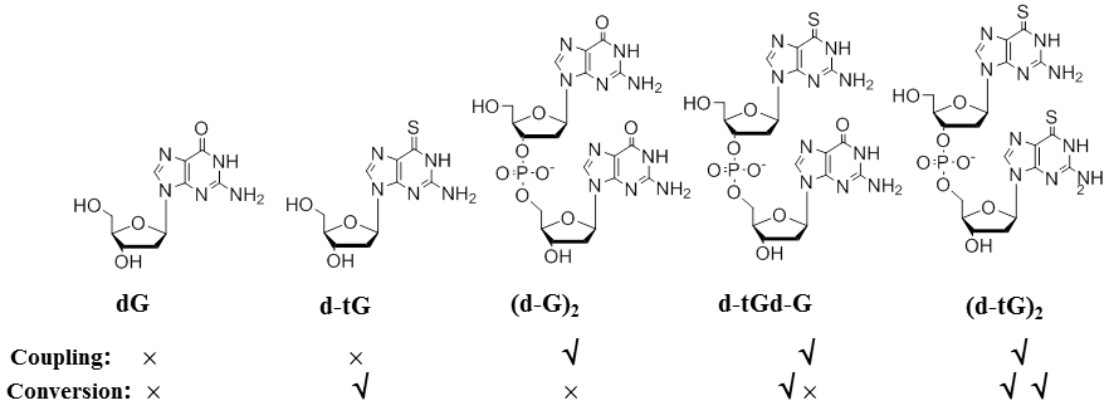

Figure 4. The structure of failed and successful coupling and conversion: guanosine dimer to thioguanosine dimer. (√) is related to successful coupling and conversion, (×) is related to failed successful coupling.

Therefore, it could be expected to see at least five species in a HPLC chromatogram. The crude product was analysed on a C_{18} HPLC reverse phase column using a mobile phase of 65% acetonitrile in 0.1 M triethyl ammonium acetate (TEAA) at (pH 6.5). Two major peaks were detected, as shown in the chromatogram in Figure 5. Both peaks were UV active at the monitored wavelengths of 260 nm and 345 nm. As only the **d-tG** unit absorbs at the longer wavelength, both these major compounds must contain at least one **d-tG** unit. This result suggests that the first peak at 4.5 min is attributed to **d-tG** whereas the second peak at ~8.2 min resulted from either the **(d-tG)$_2$** or **d-tGdG**, as shown in Figure 5. Several other smaller peaks (~ 3 min, 6 min, 8 min and 19 min) indicated that the reaction was not quantitative and these smaller impurities are most likely due to the unprotected species of each possible product.

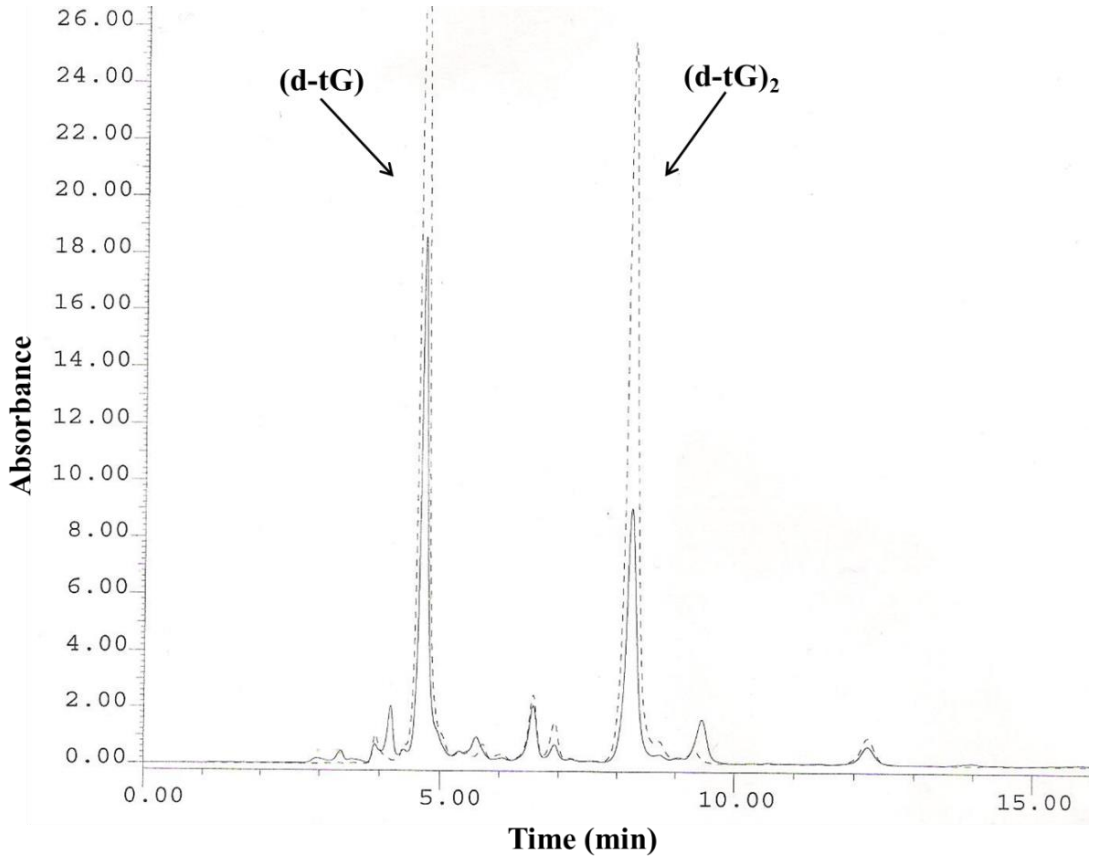

Figure 5. HPLC chromatogram of the crude reaction mixture of on-column synthesis of **(d-tG)$_2$** peak at ~ 4.5 min is attributed to **d-tG** and peak at ~ 8.2 min is attributed to **(d-tG)$_2$**. The bold line indicates monitoring at 260 nm and the dash line indicates monitoring at 345 nm.

Based on the known longer retention time of **d-tG** compared to **d-G**, and that the **(d-tG)$_2$** absorbs at 345 nm, the peak at ~8.2 min was collected and then re-analysed for purity using a different HPLC system, see Figure 6. This showed a single peak at 12.8 min which on comparison to other data using this system confirmed that the sample was now pure **(d-tG)$_2$**.

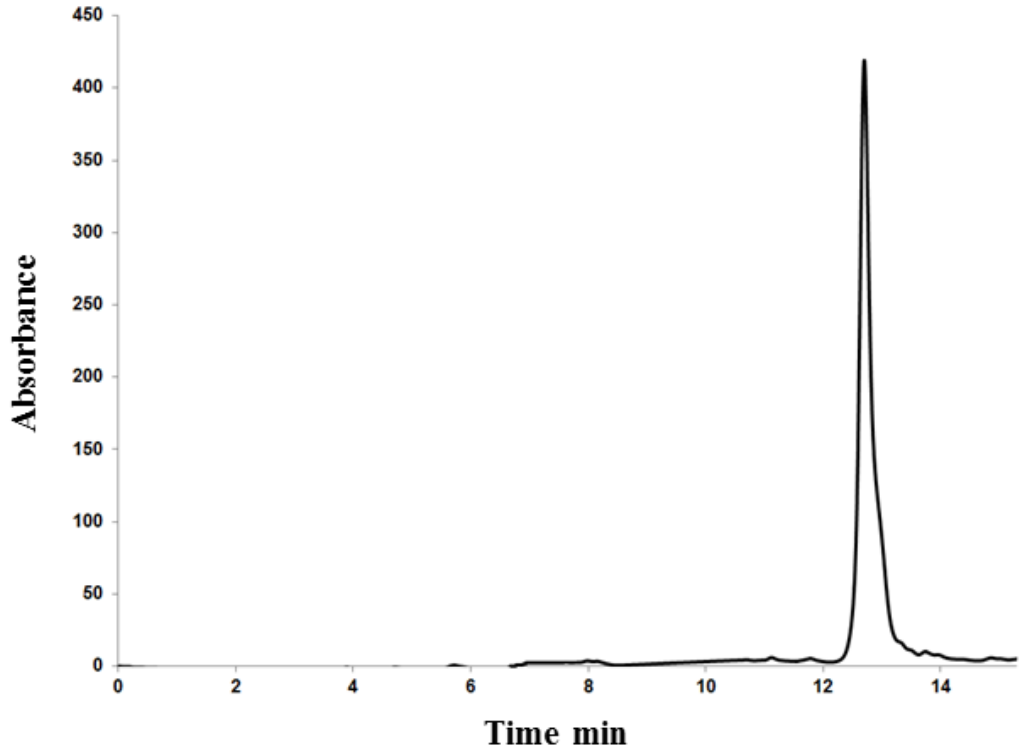

Figure 6. HPLC of pure **(d-tG)$_2$.**

3.2.3 Molecular mass determination of (d-tG)$_2$ obtained by LC-MS

Molecular mass information has been used to analyse the composition of DNA oligomers and in particular those that contain modified bases.[28] The positive and negative ion modes of electrospray ionisation mass spectrometry (ESI-MS) have both been utilized, however the negative mode provides an intensely high signal.[29] Therefore, in this study, the negative ion LC-MS (ES^-) was used to analyse the purified **(d-tG)$_2$**. The major peak was found at 627.0949; which compares to a m/z calculated for $C_{20}H_{24}N_{10}O_8S_2P$ (M^-) of 627.0958 as seen in Figure 7. The molecular peak for **d-tGd-G** $C_{20}H_{24}N_{10}O_9SP$ (M^-) at 611.11915 was not observed. This confirms the formation and isolation of the pure **(d-tG)$_2$** dimer, as the major species from the on-column synthesis and thiolation.

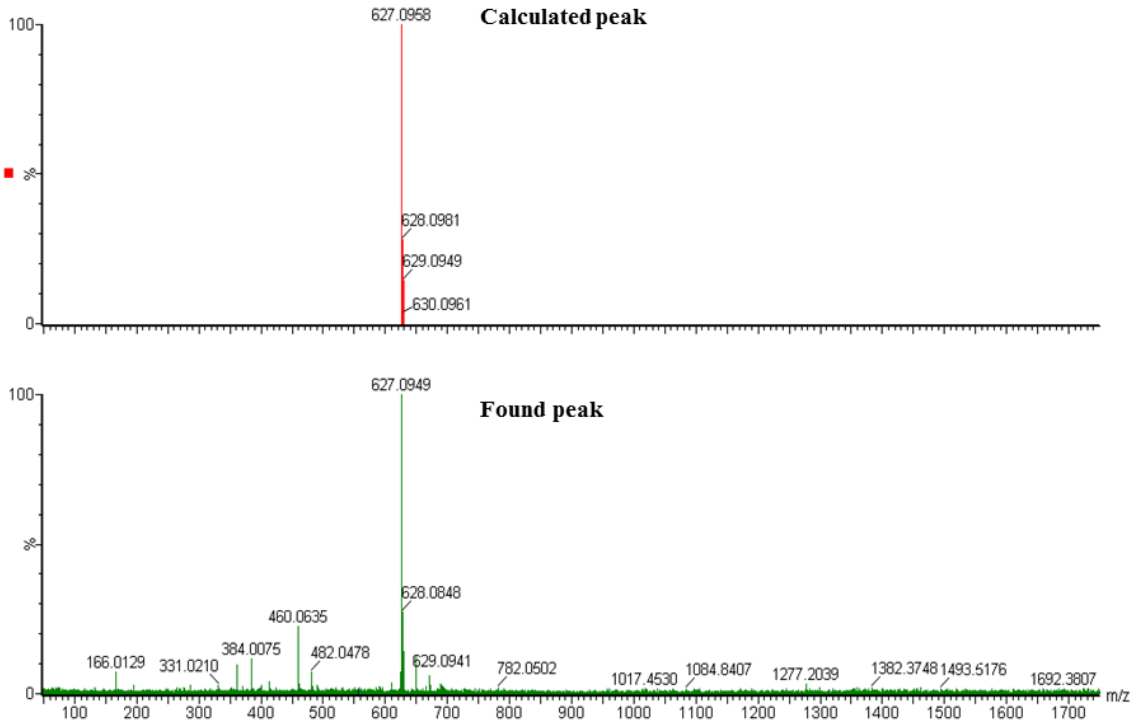

Figure 7. MS (ES^-) of purified **$(d\text{-}tG)_2$** : m/z calcl $C_{20}H_{24}N_{10}O_8S_2P$ (M^-) is 627.0958 (in the top); the found peak is 627.0949 (in the bottom).

3.2.4 UV-visible of $(d\text{-}tG)_2$

Further characterisation by UV-visible of an aqueous solution of the purified **$(d\text{-}tG)_2$** showed the characteristic peaks at 260 and 345 nm.[30] Figure 8 shows a comparison of the absorption spectra of **$(d\text{-}G)_2$** and **$(d\text{-}tG)_2$,** and highlights the difference, the new peak at 345 nm, already discussed in chapter 2 is due to the substitution of the C(6) carbonyl oxygen to a sulphur.

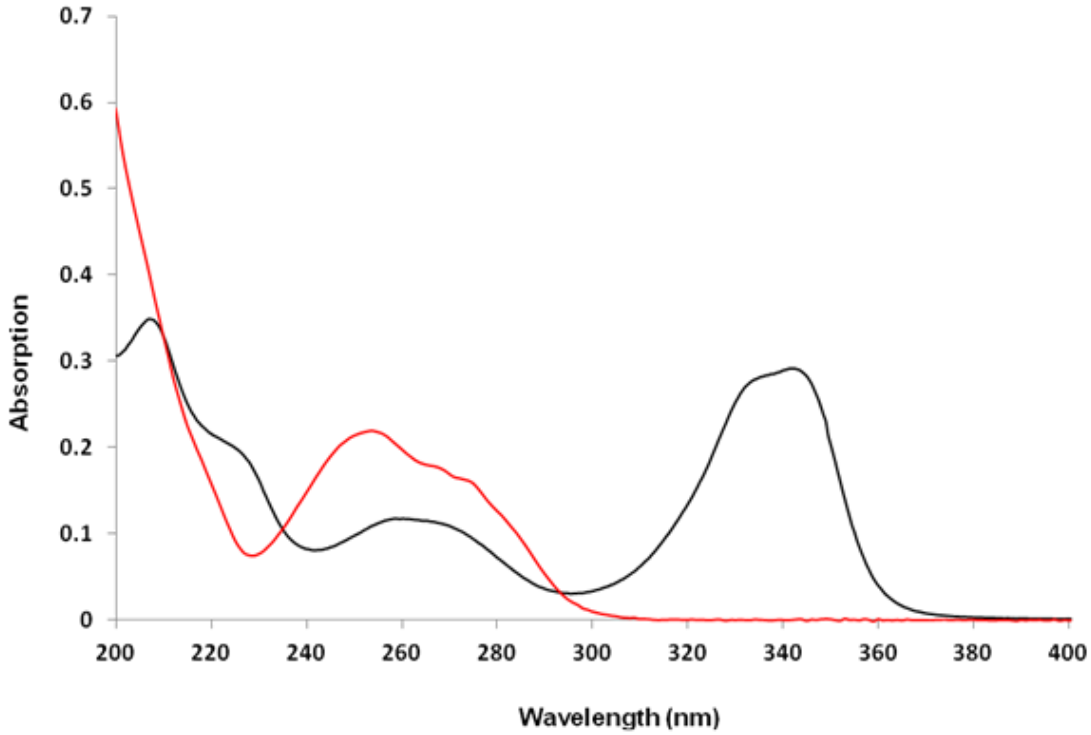

Figure 8. UV comparison between **(d-G)$_2$** (red) and **(d-tG)$_2$** (black) in water.

3.2.5 Synthesis of (d-tG)$_3$, (d-tG)$_4$ and (d-tG)$_5$

In light of the data detailing the successful synthesis of **(d-tG)$_2$** reported above, the same on-column reaction conditions and purification steps were applied to the synthesis of longer oligomers; **(d-tG)$_3$, (d-tG)$_4$** and **(d-tG)$_5$** as shown in Figure 9.

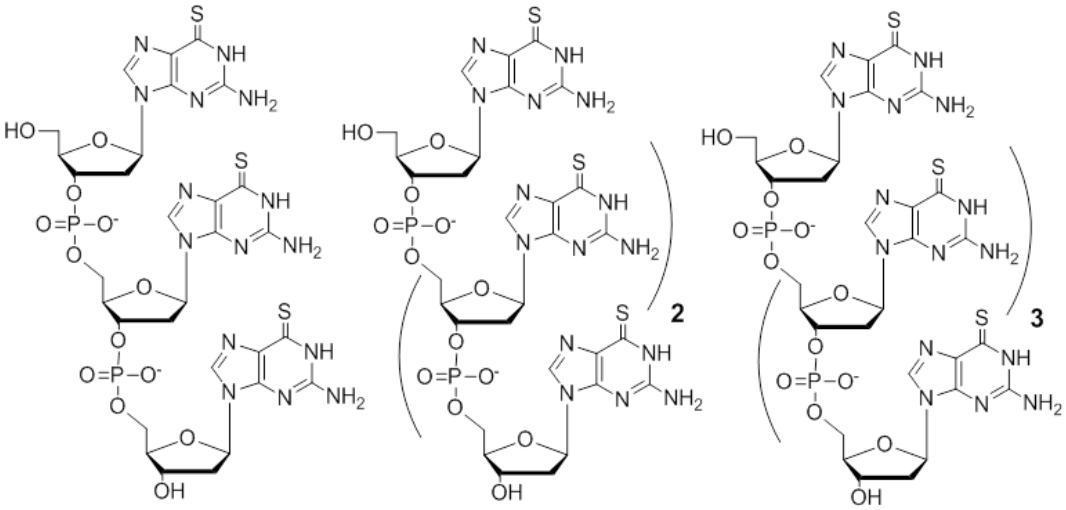

Figure 9. The structure of **(d-tG)$_3$** left, **(d-tG)$_4$** centre**,** and **(d-tG)$_5$** right.

These three thio-guanosine oligomers were purified by HPLC using the same conditions for the **(d-tG)$_2$** purification, the chromatograms of, **A**, **B** and **C** respectively are shown in Figure 10. The HPLC data indicated that the retention time of thio-ganosine oligomers increased as the molecular weight of the oligomers increases. In Figure 10**,** the retention time of the peak assigned to **(d-tG)$_4$** appears around 12.5 min whereas in the case of **(d-tG)$_5$** the major peak appeared at 16.5 min. As expected, the longer 5-oligomer is retained on the column longer than the 4-oligomer due to its increased size. However, the **(d-tG)$_3$** was purified on an alternative HPLC system and so its observed retention time of around 14.5 min is not comparable to the data of **(d-tG)$_4$** and **(d-tG)$_5$**.

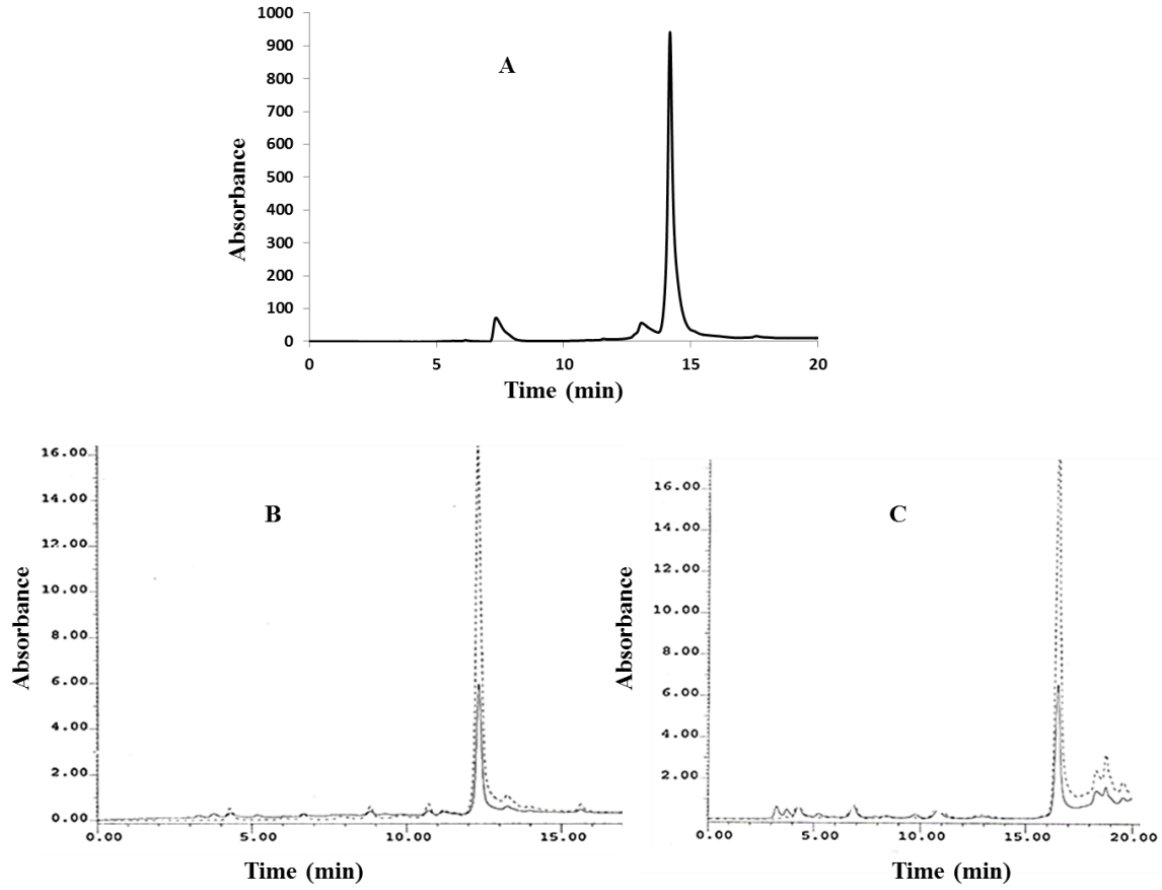

Figure 10. HPLC of **(d-tG)$_3$ A**, **(d-tG)$_4$ B**, and **(d-tG)$_5$ C.** Chromatogram **A** was recorded on **Varian** and chromatograms **B** and **C** on **Gilson**, both using a solvent gradient of 0-25 % over 30 min, solvent A is a TEAA buffer, solvent B is a 65% of acetonitrile.

LC-MS was used to confirm the composition of the purified HPLC fractions for each of the modified oligomers. It was found that the peaks at 14.5, 12.5 and 16.5 were indeed the 3-, 4-, and 5-thio-oligmers respectively. These findings are summarised in Table **1**.

Oligomer	**HPLC retention time (min)**		**Mass spectroscopy MS (ES^-)**	
			Calcd. Peak	**Found peak (M^-)**
	Gilson HPLC	**Varian** HPLC		
†$(d\text{-}tG)_2$	8.2	12.8	627.095	627.094
†$(d\text{-}tG)_3$		14.5	972.1254	972.1223
$(d\text{-}tG)_4$	12.5		1317.1552	1317.2863
$(d\text{-}tG)_5$	16.5		1662.1848	1662.3939

Table 1. Comparison of HPLC retention times and molecular masses obtained by ES^- mass spectroscopy of **$(d\text{-}tG)_n$** oligomers where n is = 2, 3, 4 and 5. **†$(d\text{-}tG)_2$** and **$(d\text{-}tG)_3$** were purified on different HPLC systems to 2, 4 and 5.

Further characterisation of the 3, 4 and 5 thio-**G** oligomers were carried out by UV-visible spectroscopy and showed similar spectra to **$(d\text{-}tG)_2$** with an absorption maximum at 345 nm.

Having demonstrated the synthesis, purification and characterisation of short single strands of thio-DNA oligomers, **$(d\text{-}tG)_2$**, **$(d\text{-}tG)_3$**, **$(d\text{-}tG)_4$** and **$(d\text{-}tG)_5$,** attention was then turned towards investigations into the metal ion binding properties of these thio-oligomers.

3.3 Metal binding and characterisation

In Chapter 2 the metal binding capabilities of **d-tG** (monomer) were discussed and in particular the binding of Cd(II) was investigated in detail. Therefore here we will look at how the uniform oligomers, **$(d\text{-}tG)_2$**, **$(d\text{-}tG)_3$**, **$(d\text{-}tG)_4$** and **$(d\text{-}tG)_5$** which all containing the thioguanosine monomer interact with Cd(II).

To the best of our knowledge, this is the first investigation on the binding of cadmium (II) ions by thio-guanosine oligomers. Previous reports on the synthesis of one dimension coordination polymers based on meracauptopurine bases utilised cadmium (II) ions to assemble the monomers through bridging coordination interactions.[2] Therefore, cadmium (II) salts were added to solutions of the thio-oligmers.

3.3.1 UV titration of $(tG)_2$ with cadmium ion

The first experimental approach that was used to investigate the binding of metal ions by the thio-modified oligomers was a UV titration experiment. The changes in the UV absorption spectra upon complexation were employed to verify Cd^{2+} binding. The UV titration of **(d-tG)$_2$** with cadmium (II) nitrate showed that during the addition of Cd^{2+}, the absorbance at 345 nm gradually decreased whereas the absorbance at 260 nm increased. This might be due to the binding of Cd^{2+} through N(7) and S(6) of the 6-thioguanosine base, in agreement with the monomer studies detailed in Chapter 2. For both of the 260 nm and 345 nm bands, the maximum wavelength blue-shifted to higher energy and also generated two isobestic points at 260 nm and 322 nm as shown in Figure 11 (A). This is consistent with equilibrium between two independent species in solution, free **d-tG** and Cd^{2+}-bound **d-tG**, by excluding the possibility that different bound species have identical spectra. To identify the ratio of Cd^{2+} to **(d-tG)$_2$** in the bound complex, the absorption data at 345 nm were plotted for a series of ligand to metal ratios. Figure 11 (B) shows that the formation of the complex between [Cd^{2+}] and the [**d-tG**] ligand is in a 1:2 (metal: thiobase) ratio.

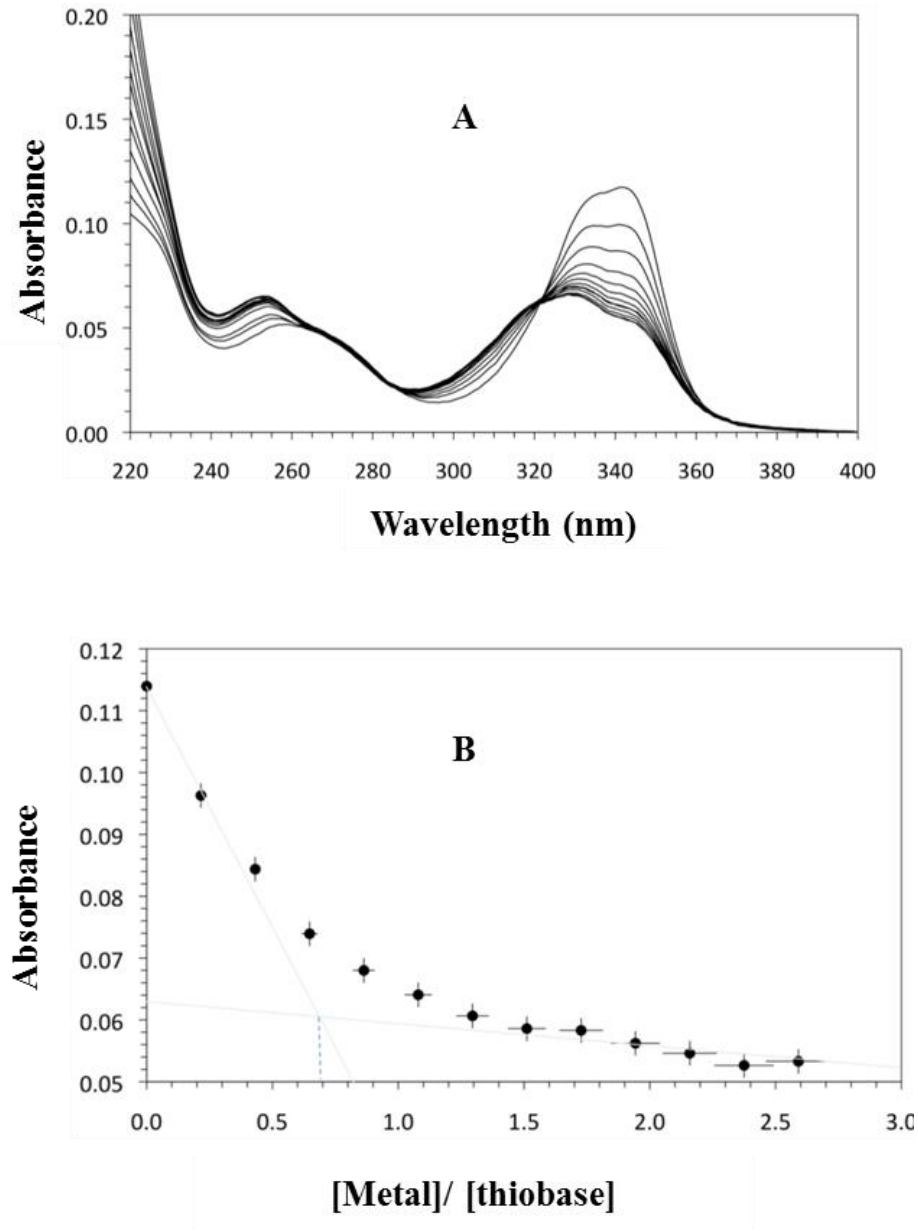

Figure 11. Absorption titration spectrum of **$(tG)_2$** with cadmium nitrate (**A**), Binding curve of complex between **$(tG)_2$** and Cd^{2+} (**B**).

3.3.2 ESI-MS of $(tG)_2$ with cadmium ion

In this study, cadmium nitrate (Cd^{2+}) was added to the **$(d\text{-}tG)_2$** dimer and then was analysed by ESI-MS. The addition of two equivalents of Cd^{2+} to the dimer resulted in the formation of a complex containing one cadmium ion bound to one oligomer. The major peak observed in the spectrum was of the form of $C_{20}H_{22}N_{10}O_8PS_2Cd$ that has an overall charge of -1, the calculated expected peak of 738.9836 was found at 738.9553, as seen in Figure **12**.

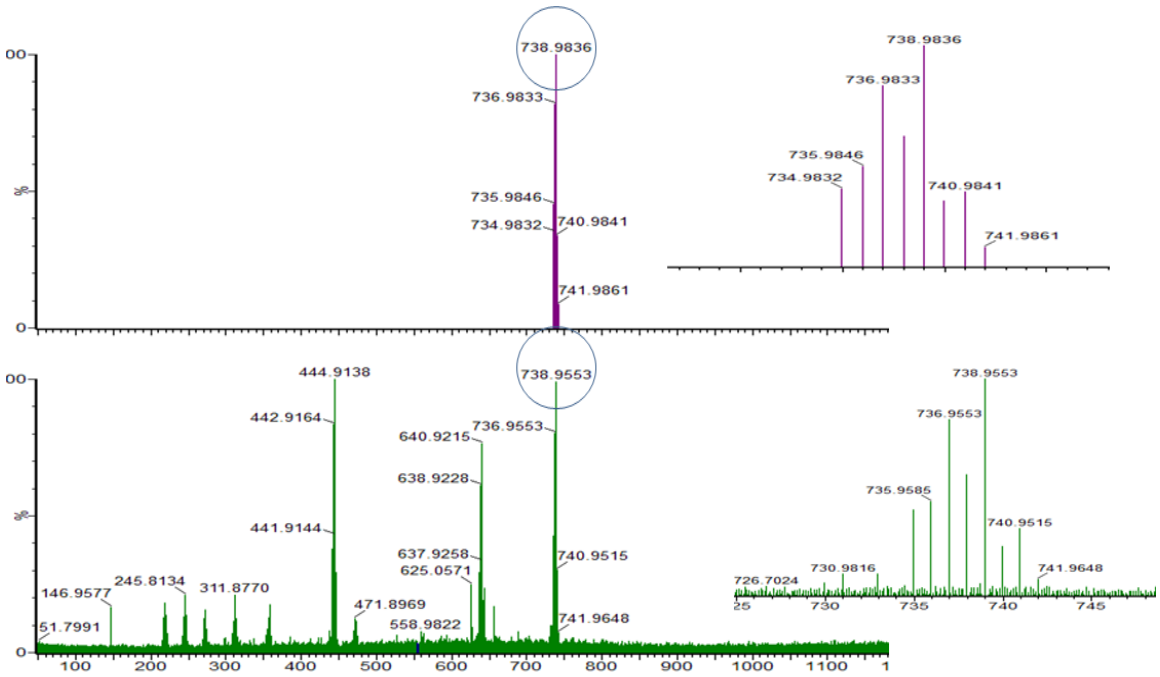

Figure 12. ESI$^-$ MS of **(d-tG)$_2$** with Cd^{2+} in methanol and water $C_{20}H_{22}N_{10}O_8PS_2Cd$ (M^-), in top is calculated peak is 738.9836 and in the bottom found peak is 738.9553.

These results from the LC-MS and UV titration studies of **(d-tG)$_2$** with Cd^{2+} confirmed the formation of a complex between metal and ligand (two-thiobases) in the ratio of 1:1. However, it was not possible to determine the exact nature of the coordination binding within the complex as two possible modes could be envisaged, **a)** bridged and **b)** chelate, as seen in Scheme 5.

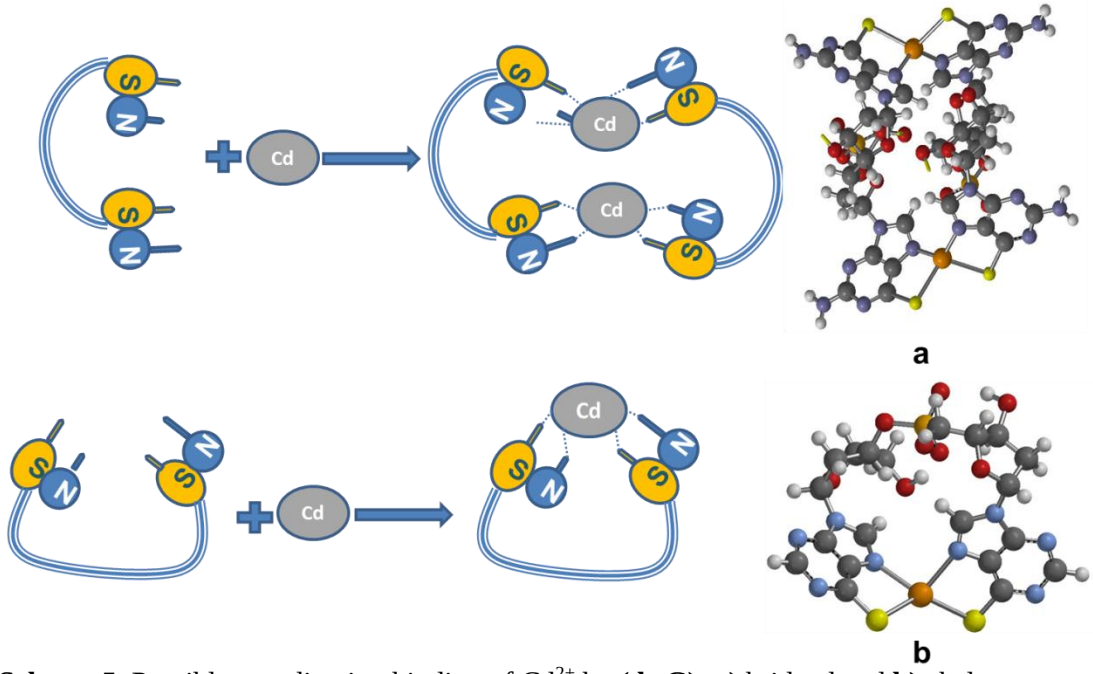

Scheme 5. Possible coordination binding of Cd^{2+} by **(d-tG)$_2$ a)** bridged and **b)** chelate.

3.3.3 UV titrations and LC-MS characterisation of 3, 4 and 5 thioguanosine-oligomers

UV titration and LC-MS studies of **(d-tG)$_3$**, **(d-tG)$_4$** and **(d-tG)$_5$** were also performed to examine their binding of cadmium ions. The UV titration experiments of **(d-tG)$_3$, (d tG)$_4$** and **(d-tG)$_5$** revealed similar changes in wavelength to the previously discussed data for **(d-tG)$_2$**. For **(d-tG)$_3$** and **(d-tG)$_5$**, during the addition of Cd^{2+} to the oligomer, the absorption at 345 nm decreases whereas the absorption at 260 nm increases, as shown in Figure 13(A and C). However, the plot of molar ratio (metal to oligomer) against absorbance (at 345 nm) for **(d-tG)$_3$** and **(d-tG)$_5$** were not simple and suggested that there were multiple binding equilibria in each case as seen in Figure 13 (B and D). The curve in Figure 13 (B) can not be filled as a single binding isotherm. Qualitatively, there appear to be three sections of the curve, with end-points about [Cd2+]:[**d-tG**] about 0.5, 1.0 and 1.5. However, further study of this system is required to conclusively determine the binding equilibria.

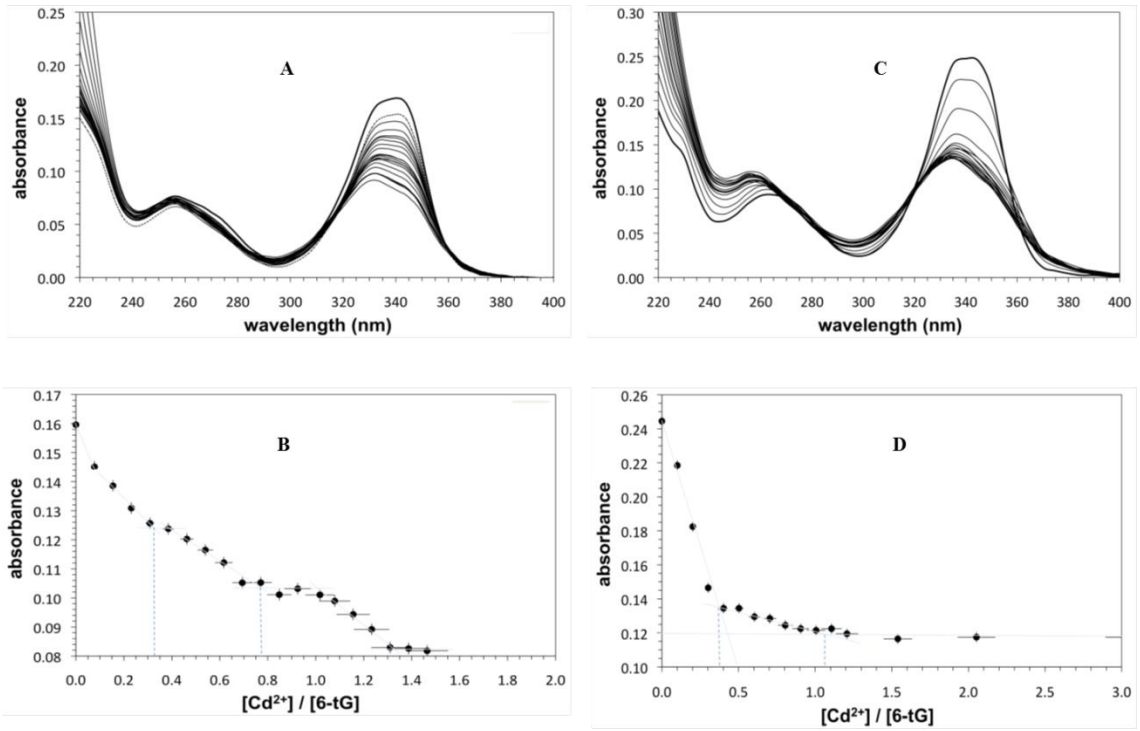

Figure 13. (A) and (C) absorption titration spectra of **(d-tG)$_3$** and **(d-tG)$_5$** with cadmium nitrate (B) and (D), binding curve of the complexes formation of **(d-tG)$_3$** and **(d-tG)$_5$** with Cd^{2+} .

While in the case of **(d-tG)$_5$**, Figure 13 (D) shows a clearer end-point at ~1 that is associated to a 1:1ratio of [Cd^{2+}] :[**d-tG].**

However, in the case of **(d-tG) $_4$**, changes in absorbance at 345 nm plotted against the ratio of [Cd^{2+}] ions to [thio base], more strongly suggested the complex consists of two Cd^{2+} coordinated to four thio bases in a 1:2 ratio, see Figure 14 (A and B).

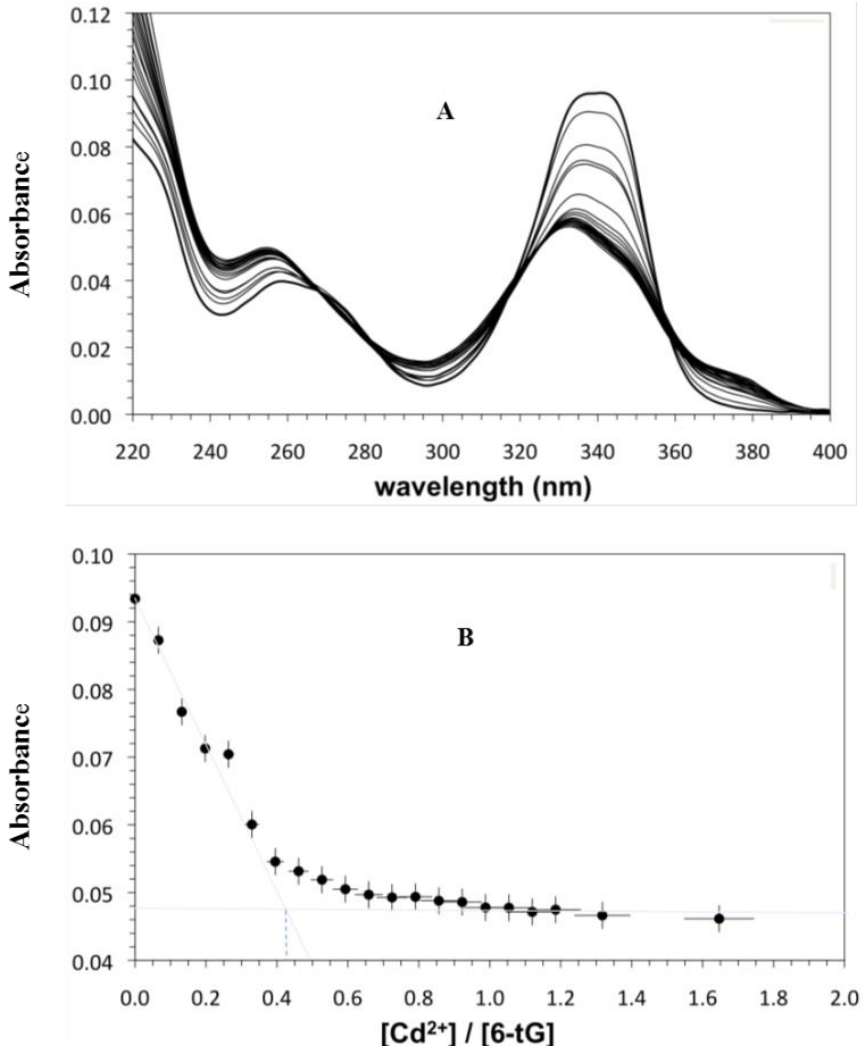

Figure 14. Titration of **(d-tG) $_4$** with cadmium nitrate (A). Binding curve of **(d-tG) $_4$** with Cd^{2+} (B).

Second, the thio oligomers were further characterized by LC-MS. It was surprising that in the LC-MS spectra of **(d-tG)$_3$** and **(d-tG)$_5$** with Cd^{2+} the expected Cd-complex peaks were not found. This could be because they might be creating a stable complex with Cd^{2+} so there is no charge to make the complex fly on the MS machine. On the other hand, in the case of **(d-tG)$_4$** the result from LC-MS showed evidence for the formation

of a complex containing two cadmium ions bound to one oligomer, in other words, two cadmium ions bound to four thio bases.

The observed major peak in the spectrum was calculated for $C_{40}H_{46}N_{20}O_{18}S_4P_3Cd_2$ (769.4656) with an overall charge of -2 and the found peak was at 769.4436 as seen in Figure 14C. These LC-MS results for the complex of **(d-tG)$_4$** with Cd^{2+} supports the findings of the UV titration experiment.

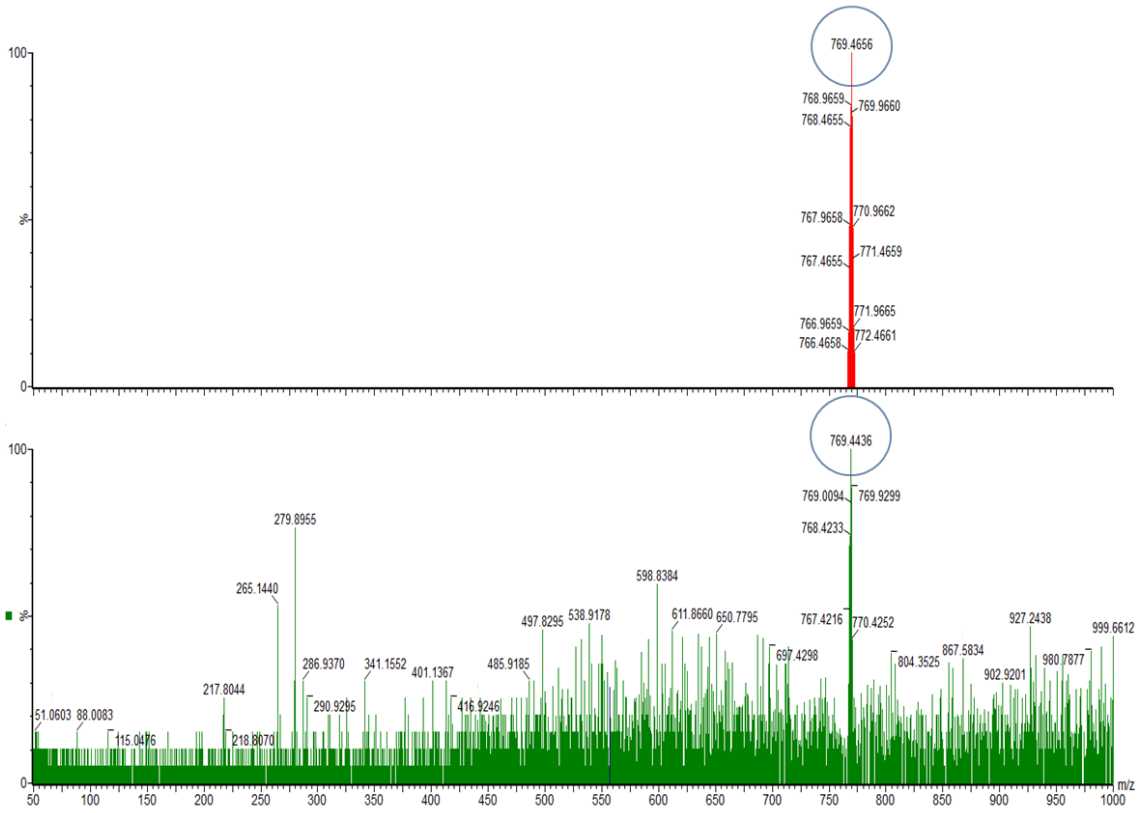

Figure 14C. ESI$^-$ MS of **(d-tG)$_4$** with Cd^{2+} in methanol and water $C_{40}H_{46}N_{20}O_{18}S_4P_3Cd_2$ (M^{2-}), in top is calculated peak is 769.4656 and in the bottom found peak is 769.4436.

Overall, these finding from the UV titration and LC-MS studies showed that when the number of thio-**G** units in the oligomer is even, such as **(d-tG)$_2$** and **(d-tG)$_4$**, the mode of binding is clear and more or less a single complex in the 1:2 ratio of [Cd^{2+}] to [thio base] forms. Whereas when the number of thio-**G** units in the oligomer is odd, such as **(d-tG)$_3$** and **(d-tG)$_5$**, the binding interaction becomes more complex.

3.3.4 Circular Dichroism (CD) measurement

To obtain information about the effect of cadmium ions on the base-base interactions for the modified thio-monomer **d-tG** and the thio-oligomers **(d-tG)$_2$** and **(d-tG)$_3$**, the

CD spectra before and after the addition of Cd^{2+} were recorded. Changes in circular dichroism were compared with changes in the isotropic absorption of the samples. In the case of **d-tG,** the addition of Cd^{2+} results in a change in absorption so that a shoulder at 331 nm becomes apparent, in addition to the maximum at 345 nm, as shown in Figure 15.

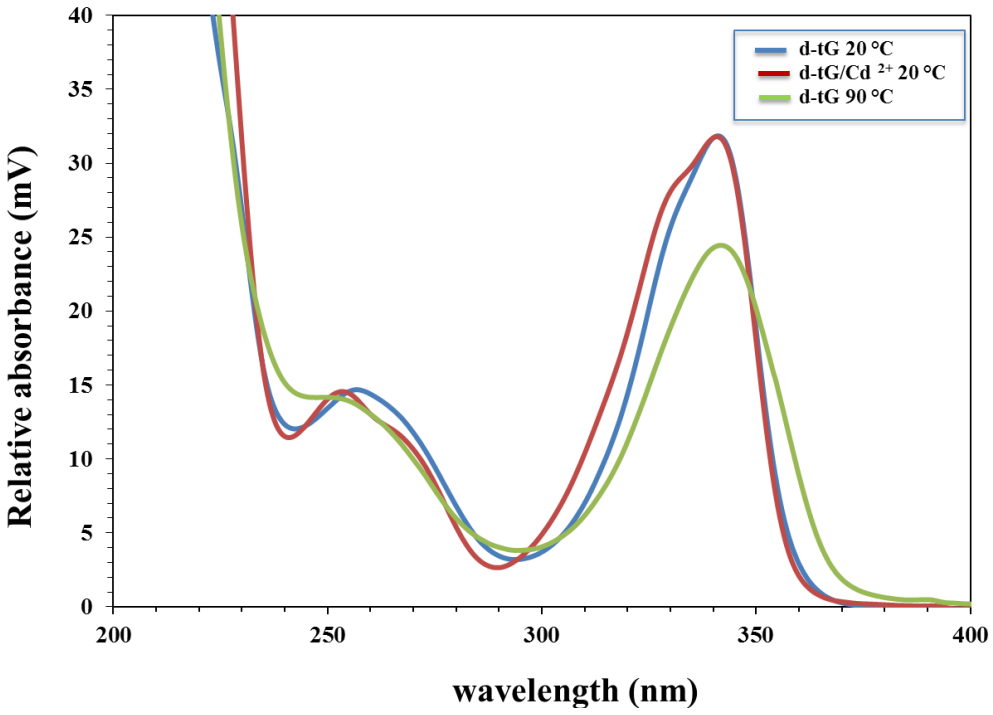

Figure 15. Isotropic absorption of **d-tG** samples in CD spectrometer.

As previously explained (Chapter 2, Figure 7), the development of a band at 331 nm indicates deprotonation of the base, which suggests that Cd^{2+} binding is coupled with deprotonation of the 6-thio group. As expected, this deprotonation causes almost no change in the CD spectrum of **d-tG.** The negative CD spectrum of **d-tG** in the 300-400 nm range agrees with the CD spectrum of **d-tG** reported by Eccleston at pH 6.5.[31] The monomer CD spectrum is dramatically changed when the temperature is raised to 90 °C with sign inversion across the whole wavelength range. Likewise, the absorption spectrum changes markedly showing a small red shift and broadening of the 345 nm band, as well as changes in the 260 nm band. On re-cooling to 20 °C, the absorbance and CD spectra revert to the original spectra. Therefore the change is physical (conformational) rather than chemical, see Figure 16. The **d-tG** spectra illustrate the expected behaviour of completely uncoupled bases.

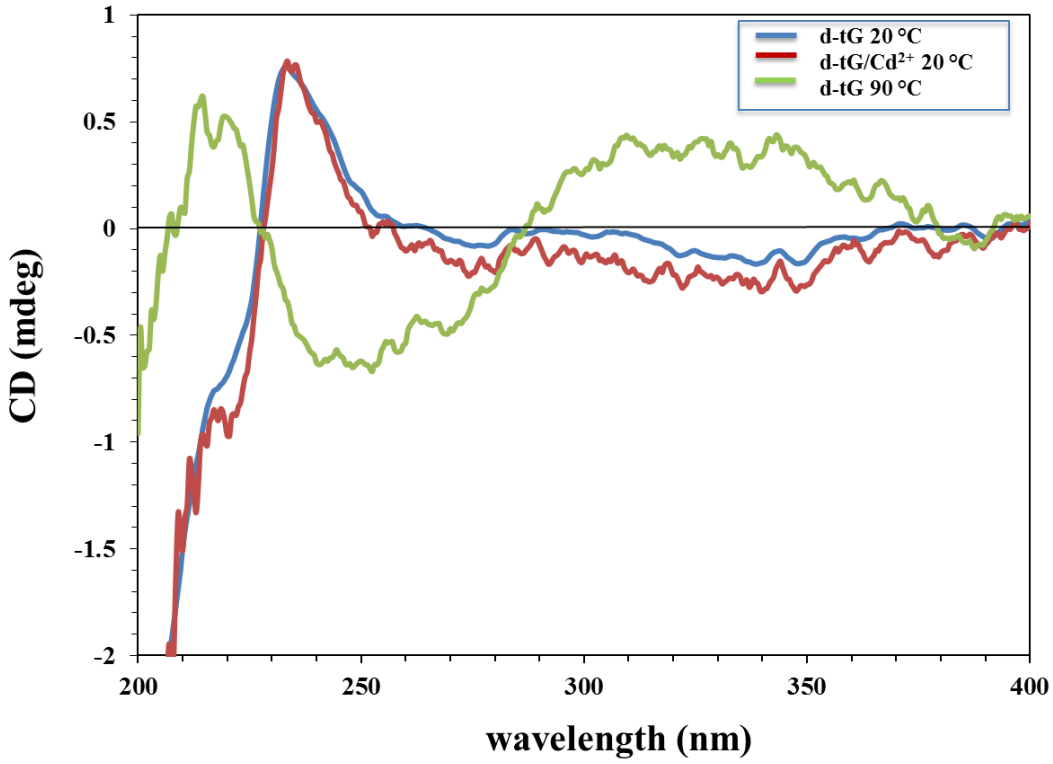

Figure 16. CD comparison between **d-tG** with and without Cd^{2+} at different temperatures.

The difference between the monomer and the oligomers is the increase in the number of the bases, and the insertion of bridging phosphate groups between adjacent bases but not at the termini. Increasing the temperature from 20°C to 90°C, and then re-cooling to 25°C, causes significant changes in both the absorption and CD spectra of **(d-tG)$_2$** see Figure 17 and 18. At 20°C, the absorption maximum appears at 322 nm with a small shoulder at 350 nm. At 90°C, the maximum blue shifts to 327 nm with reduced intensity, and the 350 nm shoulder increases in intensity. On re-cooling to 25°C, it is interesting to note that the spectrum does not revert to that observed originally. The 350 nm band remains as the main peak at long wavelengths. Likewise, the CD spectrum changes on heating to 90 °C and does not revert to the original spectrum on re-cooling to 25 °C. This indicates different configurations of the guanine bases with respect to each other before and after heating which suggests that there is more than one low energy conformation of the dimer.

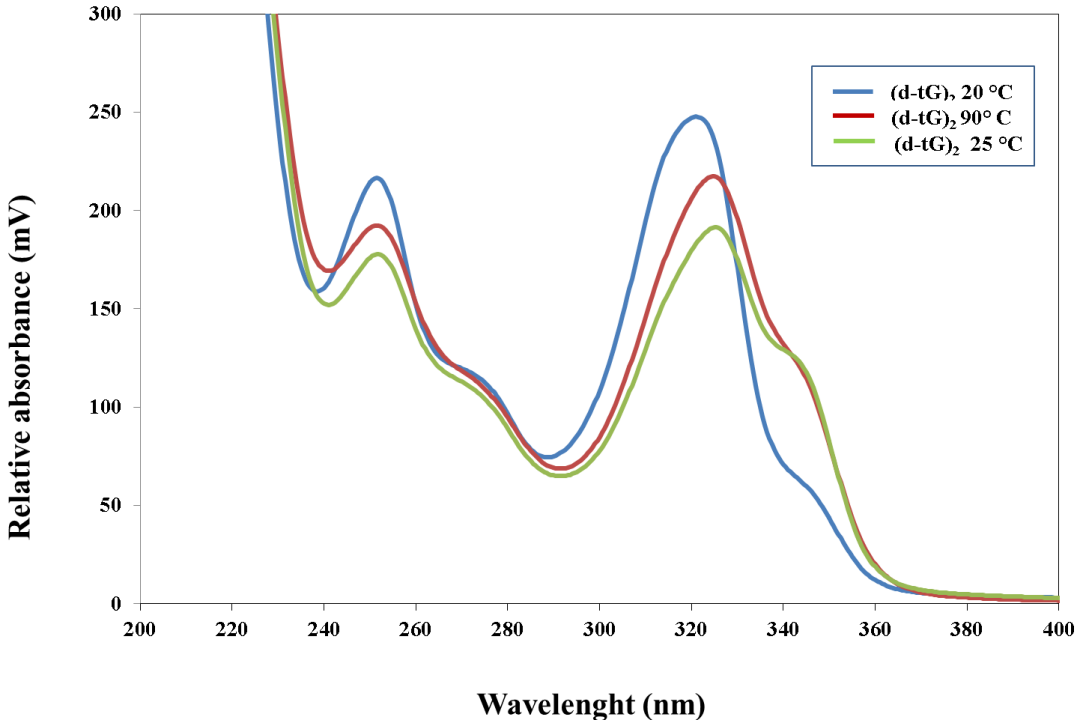

Figure 17. Isotropic absorption of (**d-tG)**$_2$ samples in CD spectrometer.

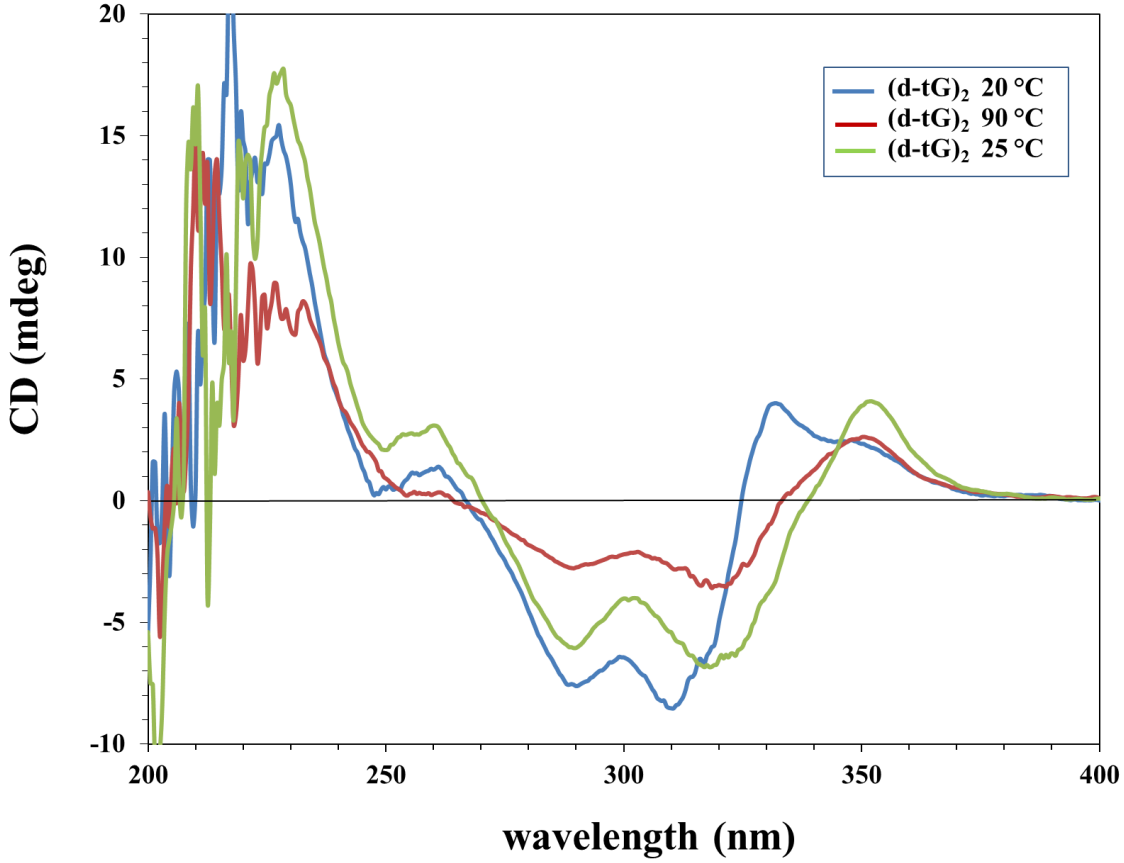

Figure 18. CD comparison of (**d-tG**)$_2$ samples at different temperatures.

At 20°C, the CD spectra with and without Cd^{2+} look completely different. Binding of Cd^{2+} to dimer at 20°C induces a large increase in the CD signal compared to dimer without Cd^{2+} as seen in Figure 19. By contrast, the absorption spectrum is greatly reduced in intensity in the long wavelength band and the shoulder at 345 nm disappears as shown in Figure 20. At 90°C, the CD spectra with and without Cd^{2+} are similar in magnitude although there is some differences in shape at long wavelengths but the absorption spectra are not the same . In fact, the absorption spectra for **(d-tG)$_2$** with Cd^{2+} are very similar at 90°C and 20°C, unlike the CD. This suggests that at high temperature, the base stacking is perturbed but Cd^{2+} remains coordinated to **d-tG** base in some form.

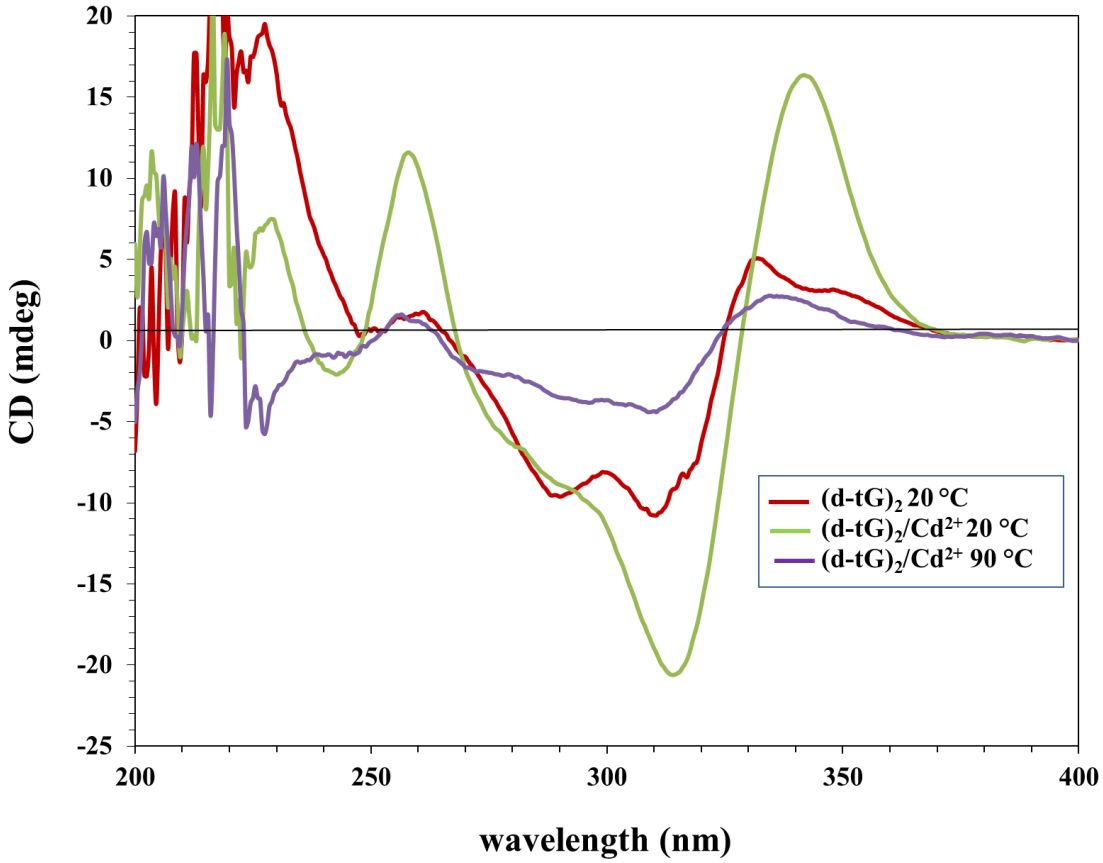

Figure 19. CD comparison between **(d-tG)$_2$** with and without Cd^{2+} at different temperatures.

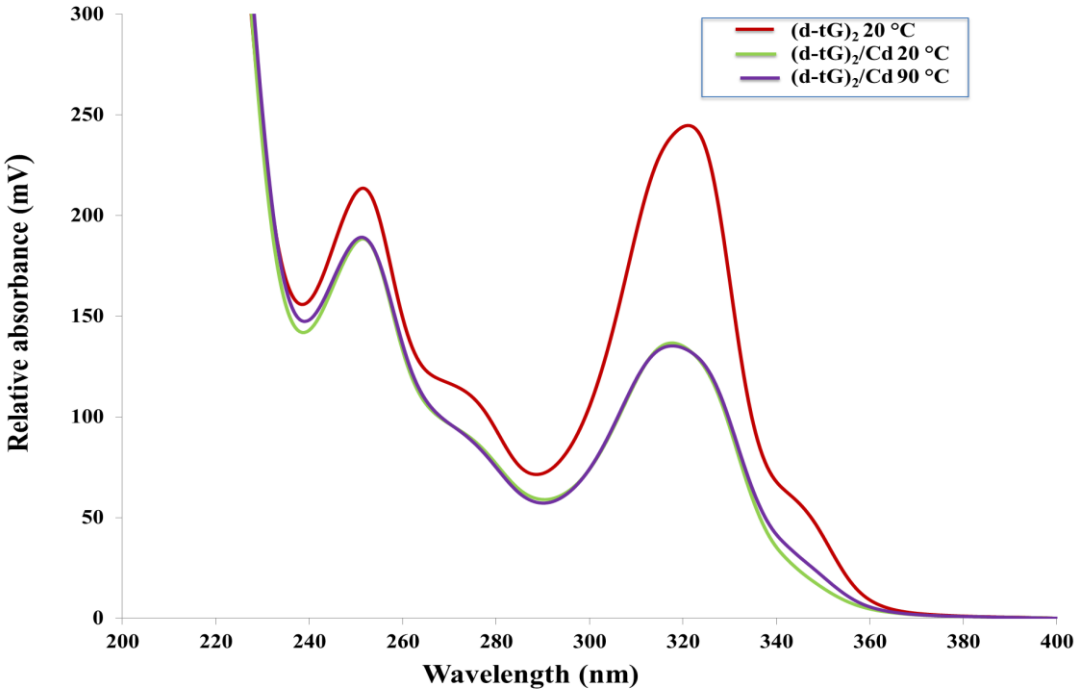

Figure 20. Isotropic absorption of **(d-tG)$_2$** samples with and without Cd^{2+} in CD spectrometer.

In the case of **(d-tG)$_3$**, the addition of Cd^{2+} causes a decrease of absorbance with changes of shape in the absorption bands centered at 340 and 260 nm as shown in Figure 21. However, the CD spectrum shows only small changes in shape, with almost no change of intensity as seen in Figure 22.

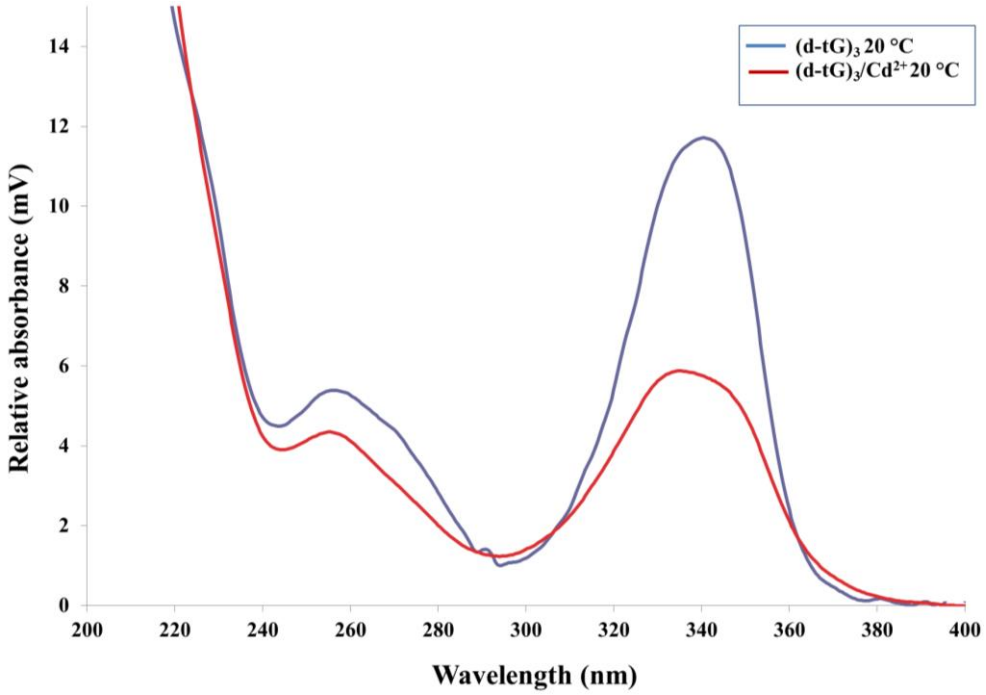

Figure 21. Isotropic absorption of **(d-tG)$_3$** samples with and without Cd^{2+} in CD spectrometer.

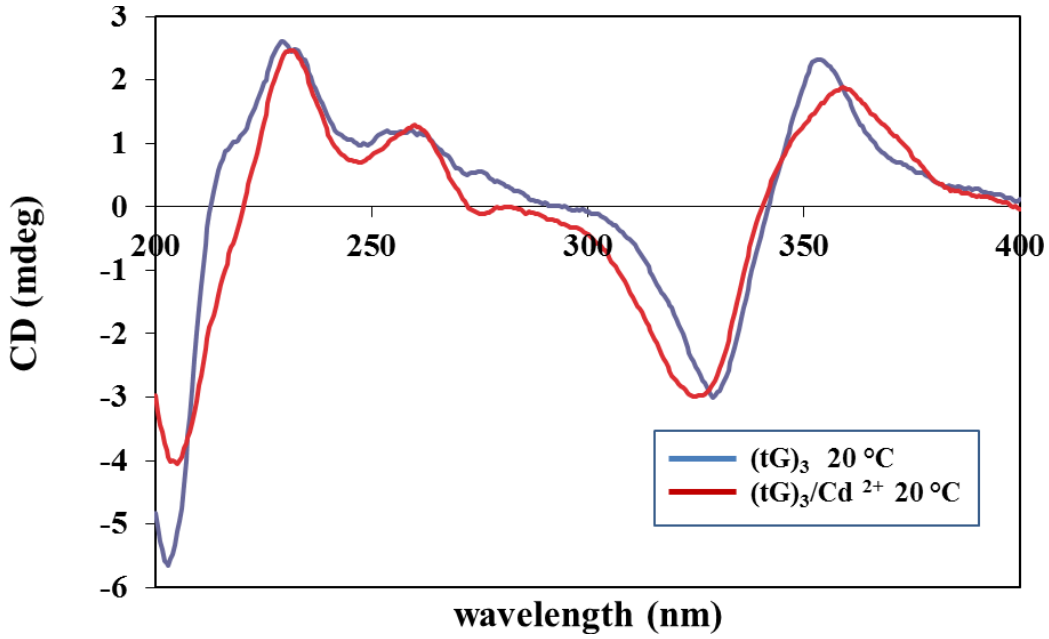

Figure 22. CD comparison between **(d-tG)$_3$** with and without Cd^{2+}.

Taken together, these results suggest that the thioguanine bases are organized in different geometries with respect to each other in the Cd^{2+} complexes with monomer, dimer, and trimer. The bases appear to be particularly well-coupled in the dimer complex.

3.3.5 Tm of thio-oligmers

In order to further assess the effect of metal ions on the formation of a complex with the thio-G oligomers, duplex melting temperatures of the free and Cd bound complex **(d-tG)$_5$** were investigated. When the complex was heated up to 95 °C, there was no significant change compared in the absorption at room temperature. Therefore the complex appears to be stable. Figure 23 shows the comparison between free **(d-tG)$_5$** and upon the addition of cadmium ions to different concentrations of **(d-tG)$_5$**. However, the structure is not known but it seems to be very thermodynamic stable. In addition, it looks like a single-strand because no transition even without cadmium is observed, therefore, it is probably an intermolecular complex but this is inconclusive.

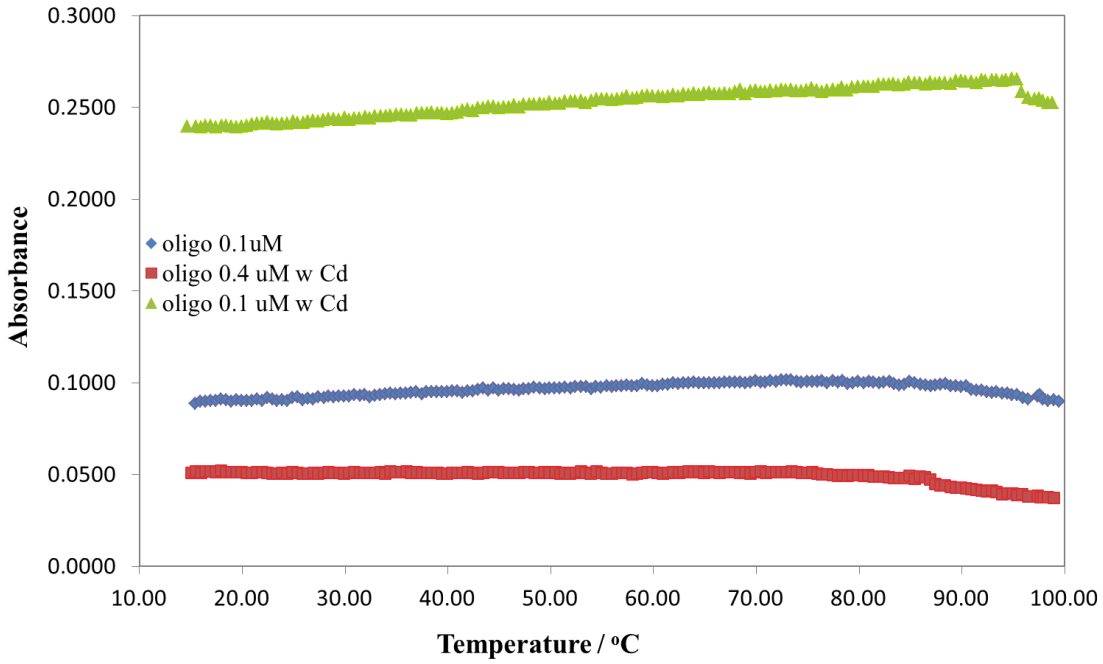

Figure 23. Melting temperature of **(d-tG)$_5$** & Cd^{+2} at different concentration.

3.4 Conclusion

The goal of this study was to form one dimension coordination polymers that have interesting properties in nanotechnology.[2] To explore this, thio-guanosine oligomers **(d-tG)$_2$, (d-tG)$_3$, (d-tG)$_4$** and **(d-tG)$_5$** were synthesised and complexed with cadmium(II) ions. Unmodified guanosine-oligomers were first synthesized by solid phase DNA synthesis, employing phosphoaramidite chemistry and then were converted to thioguanosine oligomers *via* sodium sulphide in DMF while still attached to the solid support. The HPLC, mass spectrometry and UV-visible data demonstrated the successful synthesis of thioguanosine-oligomers. The pure thioguanosine-oligomers were treated with cadmium (II) in order to study their binding properties using UV titration, MS, CD and Tm. The results of UV titration and MS spectrometry of **(d-tG)$_2$** and **(d-tG)$_4$** showed the formation of a complex containing [metal]:[thiobase] in a 1:2 ratio. From UV titrations of **(d-tG)$_3$** and **(d-tG)$_5$,** several complexes with different [metal]:[thiobase] ratios appeared to be formed. Therefore, the next chapter investigates how the cadmium ions bind to thio-modified DNA in a double stranded polymer and what type of the complex is formed.

3.5 Experimental

All chemicals to synthesize thio-guanosine oligomer were purchased from Glen Research or Sigma Aldrich, and used as received unless otherwise stated. ESI-MS was performed on a Waters LCT -Premier mass spectrometer. Modelling was carried out with the Spartan 04 package for Windows.

On column synthesis of $(tG)_2$

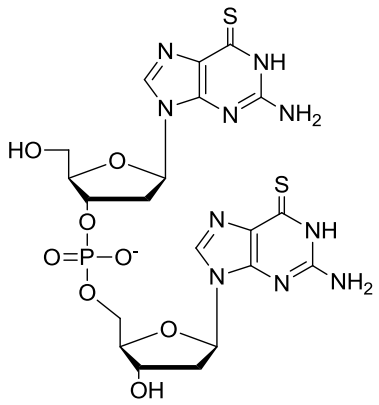

$(G)_2$ (1 μmol) was synthesized on a DNA synthesizer (EXPEDITE^{TM} Nucleic Acid System) employing bases and ultra-mild reagents and following standard phosphoramidite procedures. The column then was removed from the machine and dried under vacuum for 24 h, after which it was used to synthesise **$(tG)_2$**-oligomer using Jones procedure. **$(G)_2$ (**1 μmol) column in dry pyridine (10 ml) was added to trifluoroacetic anhydride (1 ml) to give the intermediate compound as shown in Scheme 4. Sodium sulphide (1g) in anhydrous dimethylformamide (30 ml) was then added to the intermediate to give crude **$(tG)_2$.** After 4 days the column was washed several times with water and then with ethanol and dried under vacuum for 24 hours. After drying, anhydrous CH_3NH_2 was passed through the column in order to deprotected and cleave **$(tG)_2$**. Finally, the **$(tG)_2$** yellow powder was dissolved in water and purified by HPLC. In this study, two HPLC machines were used; Gilson 715 HPLC and Varian Pro Star. In both instruments a C18 reverse phase column was used. Buffer A was 0.1 M triethyl ammonium acetate at pH 6.5 with 5% acetonitrile, and buffer B was 0.1 M triethyl ammonium acetate at pH 6.5 with 65% acetonitrile at the gradient (0-10 min 0% B, 10- 25 min 25 % B, 25-30 min 0% B). Absorbance was monitored at two wavelengths

260 nm and 345 nm. After HPLC, the pure **(tG)$_2$** was obtained (23 % yield.). ES-MS: m/z (negative mode) 627.0949 (calcd for $C_{20}H_{24}N_{10}O_8S_2P$ (M^-) 627.0958).

Synthesis of (d-tG)$_3$, (d-tG)$_4$ and (d-tG)$_5$

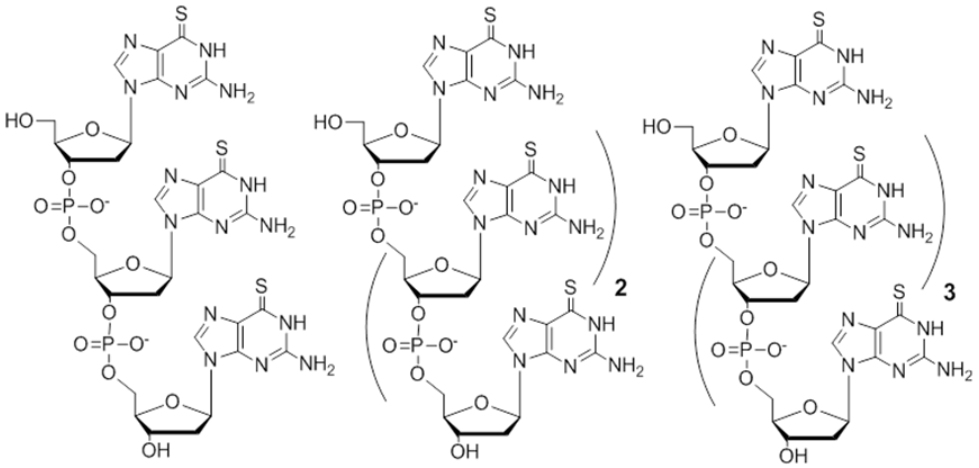

(d-tG)$_3$ **d-tG)$_4$** **d-tG)$_5$**

(tG)$_3$, **(tG)$_4$** and **(tG)$_5$** were synthesised using the same conditions and purification procedures as for the on–column synthesis of **(tG)$_2$** with the increase in the concentration of the reagents. The yield of **(tG)$_3$** is 33 %, ES-MS: m/z (negative mode) 972.1223 (calcd for $C_{30}H_{37}N_{15}O_{13}S_3P_2$ (M^-) 972.1254). The yield of **(tG)$_4$** is 29 %, ES--MS: m/z (negative mode) 1317.2863 (calcd for $C_{40}H_{49}N_{20}O_{18}S_4P_3$ (M^-) 1317.1552). The yield of **(tG)$_5$** is 26 %, ES-MS: m/z (negative mode) 1662.3939 (calcd for $C_{50}H_{61}N_{25}O_{23}S_5P_4$ (M^-) 1662.1848).

UV spectra and titrations

UV spectra and titrations were obtained with a Cary100 Bio UV-visible spectrophotometer using a 1 cm pathway quartz cuvette, and an extinction coefficient for thioguanosine of $\varepsilon = 24900$ l mol^{-1} cm^{-1}. For UV titration with Cd^{2+}, the preparation of the samples was as described in Table 2. The measurements were carried out at two wavelengths 260 nm and 345 nm.

Oligomers	Thiobase con	Cd^{2+}con	Buffer
$(d\text{-}tG)_2$	4.7 µM	150 µM	TEAA, H_2O
$(d\text{-}tG)_3$	6.9 µM	200 µM	//
$(d\text{-}tG)_4$	3.8 µM	200 µM	//
$(d\text{-}tG)_5$	10.2 µM	200 µM	//

Table 2. Preparations of samples for the different UV experiments carried out of thio-oligomers with cadmium nitrate.

Melting temperature measurement

Melting profiles were obtained with a Cary100 Bio UV-visible spectrophotometer using 1 cm pathway quartz cuvette. The measurements were carried out at different concentrations of **$(d\text{-}tG)_5$** with cadmium ions. Firstly, the measurement of free **$(d\text{-}tG)_5$** of 0.1 µM in aqueous triethyl ammonium acetate buffer at pH 6.5 heated at 95 °C at wavelength 345 nm. Then the addition of cadmium nitrate of 0.2 µM to 0.1 µM **$(d\text{-}tG)_5$** in the same buffer and heated at 95 °C. Finally, the concentration of **$(d\text{-}tG)_5$** was increased to 0.4 µM with 0.8 µM of cadmium nitrate at the same condition and temperature of previous experiment.

CD measurement

CD spectra were carried out on a Jasco J-810 spectropolarimeter using 1 cm pathway quartz cuvette. The experimental was carry out at room temperature and at 90 °C in triethylammounim acetate buffer (pH= 6.5). The concentration of the oligmer and Cd^{2+} are shown in Table 3. CD was monitored from 200-400 nm. Absorbance from 200-230 nm was very high compared to longer wavelengths and saturated the detector - so CD in this region is too high to measure, and thus appears very noisy.

DNA Sample	[DNA samples]	$[Cd^{2+}]$
d-tG monomer	**30 µM**	**45 µM**
$(tG)_2$	**24 µM**	**36 µM**
$(tG)_3$	**15.24 µM**	**61.73 µM**

Table 3. Preparations of samples for the different CD experiments carried out of thio-oligomers with cadmium nitrate.

References

(1) Kung, P. P.; Jones, R. A. *Tetrahedron Letters* **1991**, *32*, 3919.

(2) Amo-Ochoa, P.; Rodríguez-Tapiador, M. I.; Castillo, O.; Olea, D.; Guijarro, A.; Alexandre, S. S.; Gómez-Herrero, J.; Zamora, F. *Inorganic Chemistry* **2006**, *45*, 7642.

(3) de Lencastre, A.; Hamill, S.; Pyle, A. M. *Nature Structural & Molecular Biology* **2005**, *12*, 626.

(4) Christian, E. L.; McPheeters, D. S.; Harris, M. E. *Biochemistry* **1998**, *37*, 17618.

(5) Wang, Z. Y.; Rana, T. M. *Biochemistry* **1998**, *37*, 4235.

(6) Nikiforov, T. T.; Connolly, B. A. *Nucleic Acids Research* **1992**, *20*, 1209.

(7) Coleman, R. S.; Pires, R. M. *Nucleic Acids Research* **1997**, *25*, 4771.

(8) Zheng, Q. G.; Wang, Y.; Lattmann, E. *Tetrahedron* **2003**, *59*, 1925.

(9) Xu, Y. Z. *Bioorganic & Medicinal Chemistry Letters* **1998**, *8*, 1839.

(10) Coleman, R. S.; Arthur, J. C.; McCary, J. L. *Tetrahedron* **1997**, *53*, 11191.

(11) Meyer, K. L.; Hanna, M. M. *Bioconjugate Chemistry* **1996**, *7*, 401.

(12) Coleman, R. S.; Siedlecki, J. M. *Journal of the American Chemical Society* **1992**, *114*, 9229.

(13) Coleman, R. S.; Kesicki, E. A. *Journal of the American Chemical Society* **1994**, *116*, 11636.

(14) Zheng, Q. G.; Wang, Y.; Lattmann, E. *Bioorganic & Medicinal Chemistry Letters* **2003**, *13*, 3141.

(15) Vaijayanthi, B.; Kumar, P.; Ghosh, P. K.; Gupta, K. C. *Indian Journal of Biochemistry & Biophysics* **2003**, *40*, 377.

(16) Goodchild, J. *Bioconjugate Chemistry* **1990**, *1*, 165.

(17) Eckstein, F. *Oligonucleotides and analogues : a practical approach*; IRL Press at Oxford Univ. Press., Oxford [u.a.], **1991.**

(18) Bronstein, S. M.; Richardson, F. C.; Skopek, T. R.; Swenberg, J. A. *Proceedings of the American Association for Cancer Research* **1988**, *29*, 352.

(19) Rappaport, H. P. *Nucleic Acids Res.* **1988**, *16*, 7253.

(20) Richardson, F. C. a. B. S. M. In *International Patent Publication*; Publication, I. P., Ed. 19 October **1989**; Vol. #WO89/09778.

(21) Christopherson, M. S.; Broom, A. D. *Nucleic Acids Res.* **1991**, *19*, 5719.

(22) Schulhof, J. C.; Molko, D.; Teoule, R. *Nucleic Acids Research* **1987**, *15*, 397.

(23) Gloss, B.; Yeo-Gloss, M.; Meisterernst, M.; Rogge, L.; Winnacker, E. L.; Bernard, H.-U. *Nucleic Acids Research* **1989**, *17*, 3519.

(24) Ofengand, J. *Journal of Biological Chemistry* **1967**, *242*, 5034.

(25) Onizuka, K.; Taniguchi, Y.; Sasaki, S. *Nucleosides Nucleotides & Nucleic Acids* **2009**, *28*, 752.

(26) Beilstein, A. E.; Grinstaff, M. W. *Chem. Commun.* **2000**, 509.

(27) Reddy, M. P.; Hanna, N. B.; Farooqui, F. *Nucleosides Nucleotides* **1997**, *16*, 1589.

(28) McLuckey, S. A.; Habibi-Goudarzi, S. *Journal of the American Society for Mass Spectrometry* **1994**, *5*, 740.

(29) Smith, M. *Rapid Commun. Mass Spectrom.* **2011**, *25*, 511.

(30) Santhosh, C.; Mishra, P. C. *Spectrochimica Acta Part a-Molecular and Biomolecular Spectroscopy* **1993**, *49*, 985.

(31) Eccleston, J. F.; Bayley, P. M. *Biochemistry* **1980**, *19*, 5050.

Chapter 4 Synthesis of 2'-deoxy-6-thioguanosine-5'-triphosphate (d-tGTP) and its incorporation into DNA duplex by enzymatic slippage extension reaction

4.1 Introduction

The preceding chapter discussed the synthesis of short thioguanosine oligomers containing 2, 3, 4 and 5 thio-modified bases. This was achieved *via* phosphoaramidite chemistry followed by on-column conversion of guanosine to thioguanosine. Subsequently, the addition of cadmium ions to these oligomers resulted in complexes with different binding ratios of metal: thiobase. This chapter will investigate the synthesis and characterisation of the thio-modified triphosphate, **d-tGTP** and its incorporation into DNA by using an enzymatic slippage extension reaction.[1] This approach introduces multiple metal binding sites into long strands of DNA. The thio-modified DNA will then be treated with metal ions that can bind between two thio-sites on adjacent nucleobases in order to form a metal / DNA coordination polymer as seen in Scheme 1.

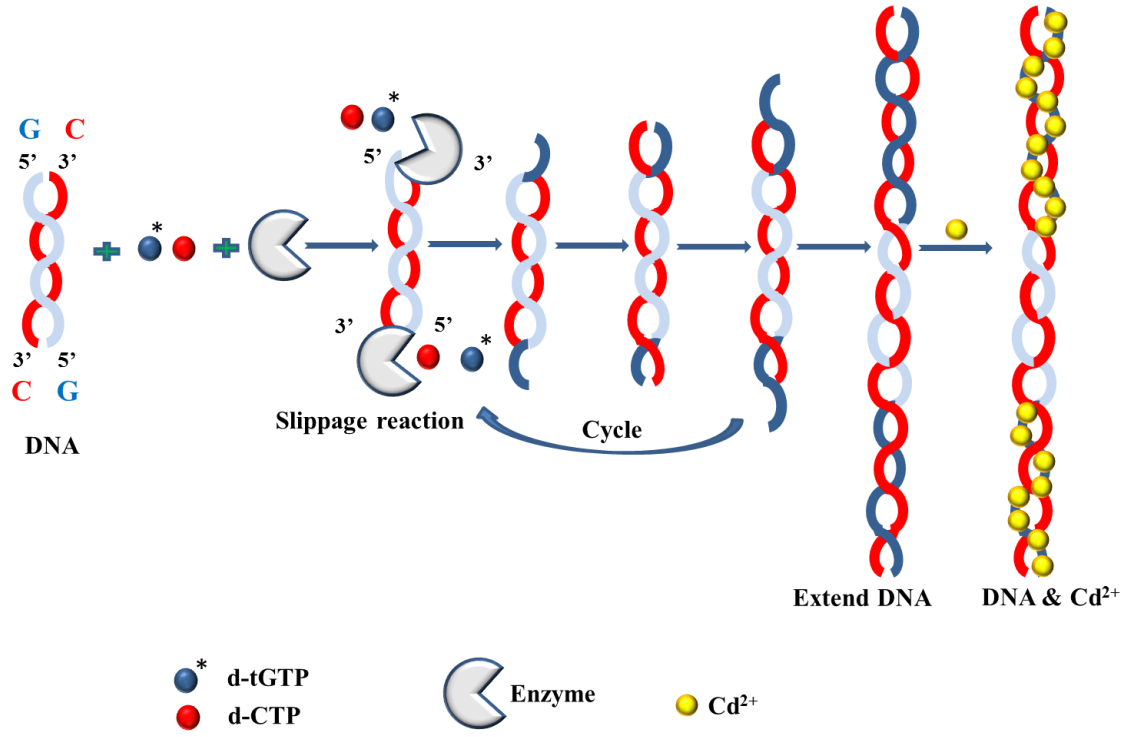

Scheme 1. Synthetic route for the synthesis of a thio-functionalized long DNA duplex using slippage extension reaction and subsequent metal binding to give a coordination polymer.

To reach this goal, it is first necessary to synthesise the thio-modified nucleotide, 2'-deoxy-6-thioguanosine (**d-tGTP)** as it is the essential building block for enzymatic DNA synthesis. Therefore, the next paragraph gives some introductory details about the different methods of nucleotide synthesis.

4.1.1 Modified triphosphates

A nucleoside triphosphate (NTP) consists of a nucleoside (base + sugar) and three phosphate groups, α, β and γ, bonded to the ribose at the 5' position, as shown in Figure 1.

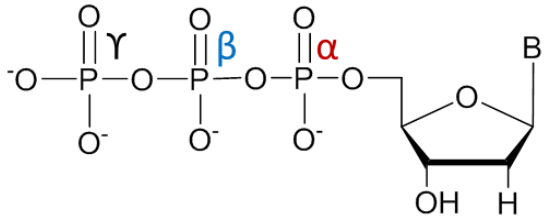

Figure 1. The structure of a nucleoside-5'-triphosphate (NTP), showing the sugar, nucleobase B and the triphosphate unit.

NTPs are involved in several processes in biology such as DNA replication, neurotransmission, translation and transcription.[2] Modified nucleotides have been synthesised for use as antagonists of nucleotide receptors,[3] as inhibitors,[4-6] agonists and substrates of nucleotide-enzyme binding. [7] Therefore, several methods for the synthesis and preparation of nucleotides have been established. Nucleotide synthetic methods commonly depend on the activation of a nucleoside 5'-monophosphate in three reaction steps. The synthesis starts with a nucleoside that is monophosphorylated, followed by activation of the nucleoside 5'-monophosphate as a phosporamidate,[8,9] imidazolidate[10] or morpholidate.[11,12] Finally, a pyrophosphate salt is added to form the triphosphate. Alternatively, a nucleoside-5'-*H*-phosphonate can be converted to its nucleotide *via* a silyl-*H*-phosphonate, followed by the addition of $(NBu_4)_3HP_2O_7$ to give moderate yields of the nucleotide.[13]

Other techniques for the synthesis of nucleotides have relied on the activation of the 5'-position of the nucleoside by 8-quinolyl monophosphate, 2,2,2-tribromoethyl morpholinochloridate or tosylate,[14,15] followed by treatment with tripolyphosphate.

"One-pot, three steps" is the most extensively utilized method for the synthesis of nucleoside-5'-triphosphates using phosphorous(V) chemistry, established by Yoshikawa[16] and developed by Ludwig and others.[17,18] This method includes the formation of the nucleoside dichlorophosphoridate by the addition of phosphoryl oxychloride ($POCl_3$) to the nucleoside. Following that, bis-(tri-*n*-butylammonium) pyrophosphate is added in order to form a cyclic intermediate triphosphate. The final triphosphate is generated by the hydrolysis of the cyclic intermediate triphosphate. Other methods have used the same reaction steps but replaced the pyrophosphate salt with inorganic phosphate.[19] An advantage of both these procedures is that a protecting group is not required on either the ribose unit or the nucleobase and the reaction proceeds in one pot without the need to isolate any intermediates. The characterisation of synthetic triphosphates relies on multiple chromatographic steps and analysis by ^{31}P-NMR and mass spectroscopy.[2] There is also a good method available for the one-pot triphosphate synthesis using phosphorous (III) chemistry.[20] The phosphorylating agent employed in this situation is salicyl chlorophosphite, which forms a phosphite intermediate which is then reacted with pyrophosphate again through an intramolecular cyclization to produce a α–phosphite moiety. This intermediate was oxidized by iodine in aqueous pyridine and forms the cyclic triphosphate species, which can be quickly hydrolysed and give the linear triphosphate.

The attention in this thesis focuses on the synthesis of 2'-deoxy-6-thioguanosine-5'-triphosphate (**d-tGTP**). Most previous reports prepared **d-tGTP** according to the methods that are described above. For example, Ueda *et al*. reported the synthesis of **d-tGTP** by adding 1,1'-carbonyldiimidazol to a solution of tri-n-butylammonium 2'-deoxy-6-thioguanosine-5'-monophosphate to form a diimidazolidate intermediate, followed by the addition of bis-(tri-*n*-butylammonium) pyrophosphate to form **d-tGTP**.[21] **d-tGTP** was also synthesized from 5'-DMT-3'-Bz-N_2-phenylacetyl-2'-deoxyguanosine by the addition of thioacetic acid to form the thioguanosine analogue. After that, treatment with 2-chloro-4H-1,3,2-benzodioxaphosphorin-4-one formed the desired triphosphate.[22-24]

Broom *et al*. reported the synthesis of **d-tGTP** according to Yoshikawa's procedure (see above) to form directly the triphosphate without a protecting group, but at higher reactant concentrations. The 2'-deoxy-6-thioguanosine was treated with $POCl_3$ and

formed a nucleoside dichlorophosphoridate intermediate. Subsequent addition of bis-(tri-*n*-butylammonium) pyrophosphate produced **d-tGTP.**[19]

The above paragraph has described the different synthetic pathways to **d-tGTP,** the next paragraph will look at how this **d-tGTP** can be incorporated into DNA.

4.1.2 The incorporation of 6-thioguanosine into DNA

6-Thioguanine is known as an active anti-acute myelogenous leukemia agent and is generally utilized in the maintenance treatment of childhood acute leukemia.[25] In spite of its recent clinical use, little is understood of the molecular basis for its cytotoxicity although it is hypothesised to be due to its incorporation in DNA.[26] Therefore, there have been a number of basic studies about how enzymes respond to 6-thioguanine, and about -how it affects the structure and stability of DNA. Yoshida *et al*. reported that **d-tGTP** could be incorporated into DNA by extension with polymerase α in the absence of **d-GTP**, using activated DNA as a primer-template.[27] The duplex product containing **d-tG-DNA** was isolated by chloroform: isoamyl alcohol from the reaction mixture, and was characterised by UV-vis absorption which showed the peak at 342 nm characteristic of **d-tG**. Ling and his group showed that **d-tGTP** can be incorporated into the growing DNA-single strand in place of **d-GTP** by human leukemia DNA polymerases α, δ and γ. However, an order of magnitude decrease of efficiency was observed when **d-tGTP** replaced **dGTP.**[28] Later, the same group reported that the Klenow fragment polymerase could be used in place of polymerases α, δ and γ for the same reaction. Subsequently, this DNA was examined as a substrate for type II restriction enzymes and was shown to restrict the ability of some enzymes.[29] Luna *et al*. used the Ling sequence and examined its mutagenic activity and they found that it could produce mutagenic effects.[30] Lahoud and his group reported that in the enzymatic extension sequence, the Sequenase enzyme (from USB, exo$^-$ T7 DNA polymerase, engineered to lack proof-reading ability) was unable to synthesize a full sequence when the **d-GTP** was replaced by **d-tGTP.** They assumed the synthesis was obstructed by a hairpin homologous strand.[31]

However, the above studies have focused on the incorporation of **d-tG** into DNA that has four nucleotides species. Some research also reported the insertion of 6-thioguanosine into RNA. Darlix *et al*. reported the synthesis of poly (**tG**)-poly(**C**) by polymerisation of **d-tGTP** on a poly(**C**) template using RNA polymerase. The homopolymer poly **d-tG** could not be separated from poly(**C**) at room temperature, and the melting temperature of the duplex was measured to be *ca*. 90 °C in 100 mM NaCl.[32]

Broom and his group described another method to synthesis homopolymer poly (t**G**)-poly(**C**).[33] In this technique, poly (**tG**) was synthesized by the reaction of poly (2-amino-6-chlorpurinylic acid) in Tris HCl buffer with hydrogen sulphide gas. The poly (**d-tG**)-poly(**C**) complex was formed by heating a mixture of the single-stranded polynucleotides to 70 ^{o}C for 1 hour in buffer. The melting temperature of this duplex was measured as 40 ^{o}C in 100 mM NaCl, which contrasts sharply with the previous report. A possible explanation is that the polynucleotide duplex was shorter in this case.[33]

4.1.3 The effect of 6-thioguanosine (tG) on the stability of DNA double strands

The incorporation of 6-thioguanosine into a DNA duplex has been reported, as described above.[27,28] Several studies have reported the effects of **tG** incorporation on the stability of the DNA duplex,[34] and it is found that thioguanosine has a local influence on the environmental chemistry of the DNA duplex when the oxygen at position 6 in guanine is replaced with sulphur. This effect was studied by examining the differences in ^{1}H-NMR chemical shifts of every proton of the DNA duplex that contained thioguanosine-cytosine (**tG-C**) base pairs, in place of normal guanosine-cytosine (**G-C**) base pairs. The differences were most pronounced for the imino proton. The large resonance shift of the imino proton of thio**G** relative to the imino proton of **G**, suggested that **tG** exists in the keto form, due to weakened Watson-Crick hydrogen bonds with cytosine as illustrated in Figure 2.[35,36]

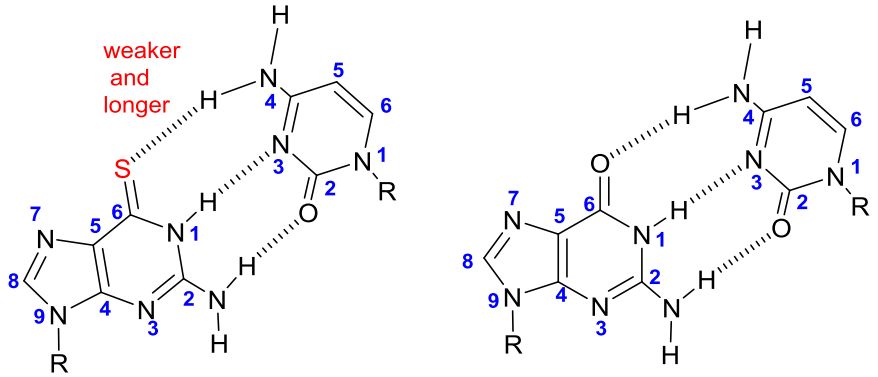

Figure 2. The difference of hydrogen bonds of (**G-C**) bases when the **G** was replaced with **tG.**

The length of the hydrogen bond between thio**G** and **C** is increased because of the large atomic radius of sulphur as well as its lower electronegativity compared to that of oxygen. Additionally, due to the weakened hydrogen bond between **tG** and **C,** the

thiobase pair is opened toward the major groove by about 7°-10°.[34,37] Furthermore, the thermal stability of the DNA duplex is decreased when the **G** base is replaced with thio**G**. [38] The effects of sulphur atom substitution on the dynamics of the DNA duplex are highly localized,[39] a single **tG** base pair in the centre of an oligomer causes only minor global distortion of the DNA duplex.[37] Theoretical studies have examined the effects on DNA stability and structure when 6-thioguanine replaces guanine in DNA.[40,41] Villani has found that the change of the oxygen atom to sulphur in the G-C base pair creates a S-H hydrogen bond that is about 0.5 Å longer than the O-H hydrogen bond,[40] consistent with NMR data.[34,37] Also agreeing with structural studies, theory predicts that substitution of oxygen with sulphur in the **G-C** base pair will raise the energies of the hydrogen bonds, weaken the base pair, and open the major groove.[40,41] These theoretical studies suggest that the differences in the chemistry and biology between normal and thiolated base pairs could be due to different base pair dynamics, as well as energetic and structural changes.[41] Therefore, because of these reasons, the presence of 6-thioguanosine in place of guanosine in DNA leads to a small destabilization of DNA double strand.

4.1.4 Enzymatic synthesis

The synthesis of DNA chains in a test tube was first demonstrated in the 1950s. The enzymatic synthesis of DNA was extensively explored in Kornberg's seminal Nobel Prize-winning work on DNA replication using DNA polymerase. [42-45] DNA polymerase is an enzyme that catalyses incorporation of deoxyribonucleotides into a nucleic acid strand *via* polymerization in the presence of a pre-existing DNA template that directs complementary strand synthesis. This polymerisation is the natural process by which DNA is replicated in cells, and is used in biotechnical applications such as the primer extension process, PCR (polymerase Chain Reaction) and slippage extension. A primer is a single stranded oligonucleotide that is complementary and hybridised with the 3'-terminus of the template strand. Primer extension is a technique that elongates the primer *via* insertion of nucleotides opposite the template using Watson-Crick base pairing. The role of DNA polymerase is to insert the correct nucleoside triphosphate opposite its matching base in the template and to catalyze formation of a phosphodiester bond with that nucleotide.

Scheme 2 illustrates an example of the incorporation of nucleotides against a complementary sequence to form double-stranded DNA. The template sequence in the bottom contains a A, G, C, T, G, A, G, G, and C (9 bases) in the direction from 3’ to 5’. The shorter primer consists of complementary bases T, C, G, A, C and T (6 bases) hybridized to the 3’-end of the template. As seen in Scheme 2, a (C) is added opposite its complementary base (G) on the template sequence by the DNA polymerase. This process continues until the primer is extended to the full length of the template, forming double stranded DNA.

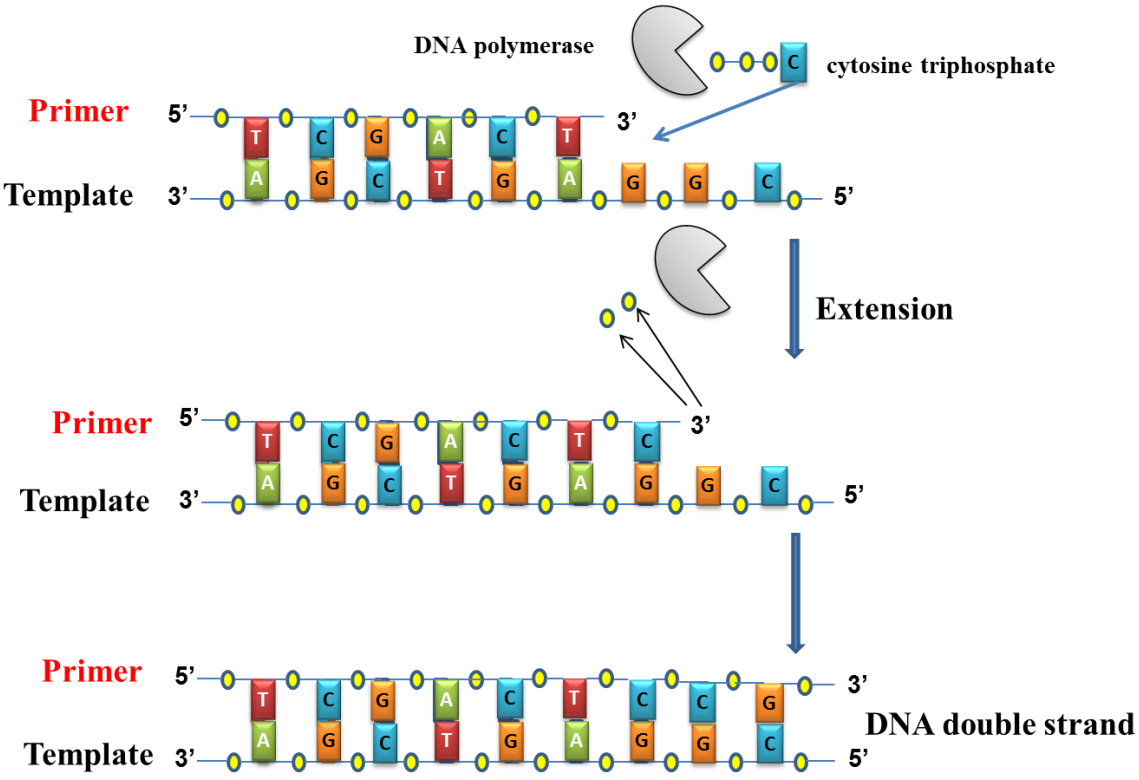

Scheme 2. Schematic illustration of the primer extension process.

All DNA polymerases perform the same function, although they vary in their primary and secondary structures, depending on the organism of origin. From a schematic perspective, they have areas that resemble the form of a human right hand; fingers, palm and a thumb as shown in Figure 3.

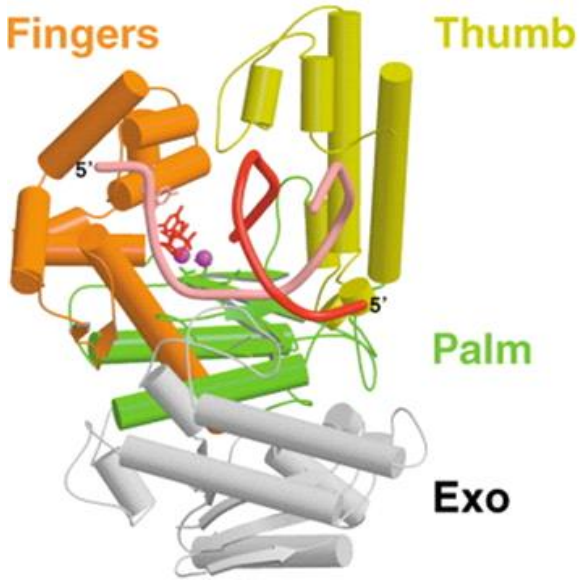

Figure 3. T7 DNA polymerase structure. [46]

The DNA is carried through the polymerases fingers and thumb, when the polymerase binds to the DNA primer-template. The DNA double strand is positioned with the 3'-terminus of the primer beside the thumb. The fingers bring nucleosides triphosphates to the 3'-terminus of the primer. The palm contains the active site that forms the phosphodiester bond between the primer 3'-OH and the triphosphate of the nucleoside.[47] The incoming base will bind to the template if it is identified forming the correct Watson-Crick base pairs. This binding of incoming base to the template causes a conformational modification of the polymerase to bring the active side of the polymerase into the correct position to initiate polymerization.[48] To facilitate the attack of nucleophile, aspartate residues are coordinated to two metal ions, usually Mg^{2+}, within the polymerase active side, which help to stabilize the negatively charged incoming triphosphate. In this mechanism, the proton from 3'-OH of the deoxyribose sugar of the incoming triphosphate was abstracted by an aspartate residue that acts as the general base in order to produce a more reactive nucleophile. Subsequently the α-phosphate of the incoming base is attacked by the activated 3'-oxygen, creating a pentacoordinate transition state among two bases as shown in Figure 4. The divalent metal ion stabilizes the transition state. As a result, a pyrophosphate is released as a leaving group during the breaking of the bond between the α- and the β-phosphate.[49]

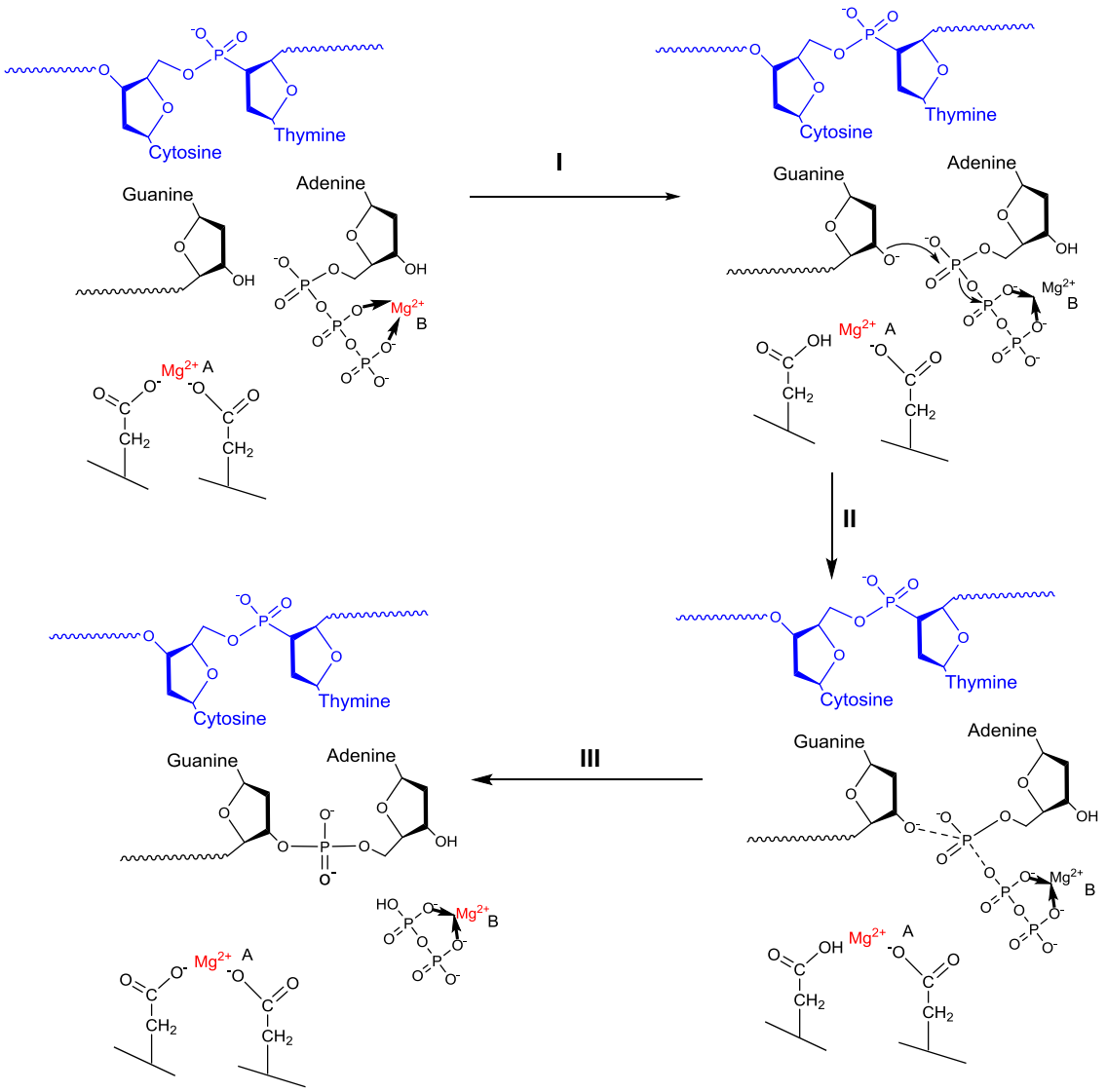

Figure 4. Scheme to demonstrate the chemical mechanism of DNA polymerases.[49,50]

Polymerase Chain Reaction (PCR) is an enzymatic amplification method developed by Mullis[51] in which a large number of copies of a specific DNA sequence are rapidly produced. The PCR reaction can be divided into three steps; firstly, the denaturation step, during which the DNA is heated up to 94°C to melt the duplex by separating it into single strands. The second step is annealing which occurs at 54°C, at which temperature H-bonds between the single stranded template and primer are formed. Subsequently, the DNA polymerase binds and copies the template. Finally, the extension step is run at 72 °C which is ideal for optimal performance of thermophilic polymerases such as Taq polymerase. Hybridization of the complementary primer is stable at this temperature. The DNA polymerase adds the complementary dNTPs to the 3'-terminus of the primer.

These three steps of the PCR reaction produces a single cycle of PCR that could be repeated several times to synthesise millions of copies of DNA.[52]

However, one disadvantage of this method is length limitation of DNA template. DNA polymerases are capable of proficiently amplifying DNA products up to a few thousand base-pairs (2-5 kb) but PCR is less efficient with longer products as the activity of the enzyme is lost. Therefore, enzymatic slippage extension synthesis established in recent years by Kotlyar *et al*. has provided a way for DNA to be grown from a short repeat sequence duplex to a high macromolecular weight up to 10,000 bp in length using DNA polymerases.

4.1.4.1 Slippage Extension

The enzymatic extension of the DNA double strand by several methods has been described in the literature. Primer extension described above is one of the methods that extends a primer to synthesise DNA against a template, creating lengths of DNA determined by the template length. To fabricate DNA of high macromolecular weight, the DNA slippage method can be employed. In this method, DNA is grown from a short repeating sequence duplex using DNA polymerases. Five decades ago, Kornberg's seminal Nobel Prize-winning work on DNA replication reported that short homopolymers such as oligo(**dA**).oligo(**dT**) were expanded to high molecular weight using DNA polymerase I from *E*.coli.[44] This extension was probably due to the slippage synthesis. However, at that time the slippage reaction mechanism was unknown.[45] A few studies have proposed the mechanism of this slippage reaction. The complementary duplex oligonucleotide used to start the slippage extension is known as the primer-template.

One mechanism proposed for the slippage is that one DNA strand slides over the other producing a relocation of the template from the primer toward the 5'direction and forming overhangs. The 3' ends can be extended to fill in the overhangs, forming an overall sequence extension, as shown in Figure 5 (right side of diagram). Overall, the slippage extension requires disruption and recreation of hydrogen bonds between complementary base pairs within in the duplex. The expansion rate is expected to be independent on the duplex length.[53-55] Other researchers have proposed different mechanisms for extension of repetitive sequences such as hairpin−coil transition,[56,57]

duplex elongation at melting equilibrium, [58,59] template switching,[60] bulge migration,[61-63] the formation of terminal hairpin and the self-priming extension model.[64]

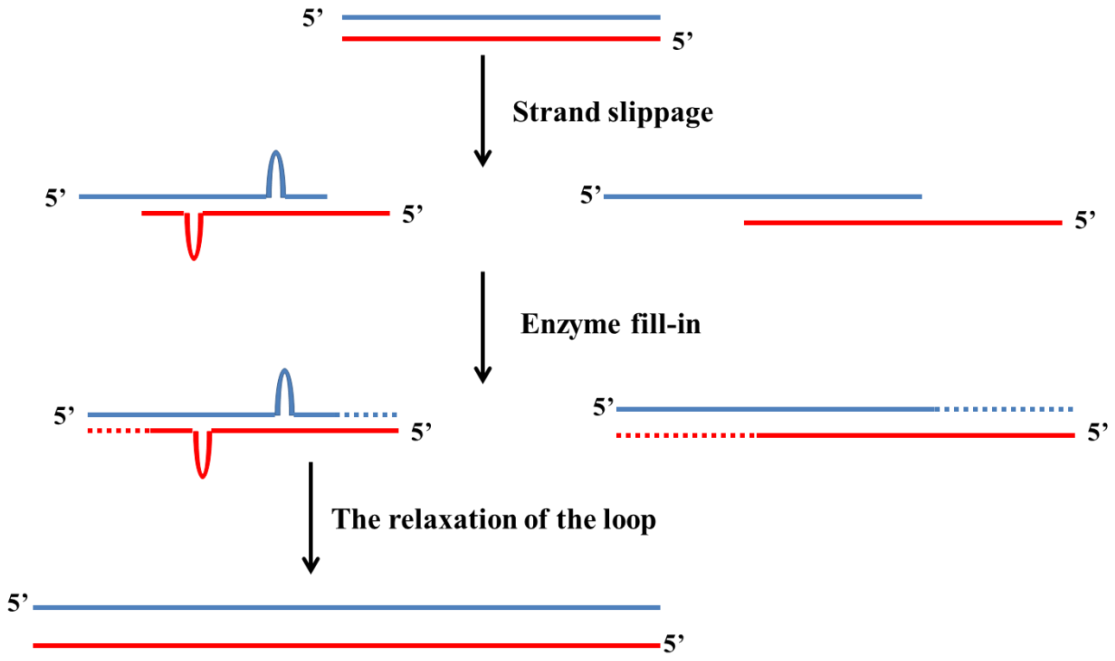

Figure 5. Models for slippage mechanism.

However, the most convincing mechanism was proposed by Kotlyar and co-workers,[1] who have reported the extension of a poly(**dG**).poly(**dC**) primer-template up to 10,000 base pairs using the Klenow exo$^-$ polymerase. In this mechanism, the 3'-end of DNA is bound to the enzyme and forms a short loop *de novo* due to a shift of nucleotides within the polymer towards the 5'direction as shown in Figure 5 (left side of diagram). The enzyme then fills in the overhang with dNTPs to make a complementary duplex. Subsequently, the loop relaxes after the enzyme dissociates from the DNA strand and after that the reaction cycle is repeated. Extended poly (**dA**).poly (**dT**) sequences were also generated up to 3000 base pair lengths by Kotlyar using Klenow exo$^-$ polymerase.[65] The same enzyme was also used to extend trinucleotide units such as CAG/CTG.[54,66] Ijiro and his group have taken advantage of the slippage reaction to deposit platinum metal on long DNA polymers consisting of poly(**dG**).poly(**dC**) and poly-[(**AT**)] in order to produce new properties of DNA that might have potential applications in nanotechnology.[67] In addition, Kotlyar *et al*. used the slippage extension to grow small Ag nanoparticles on a poly(**dA**)-poly(**dT**) DNA duplex that induced chioptical properties.[68]

Therefore, in this chapter, the enzymatic slippage reaction will be used to investigate the extension of a poly(**dG**)$_{10}$.poly(**dC**)$_{10}$ primer-template using Klenow exo$^-$polymerase and the modified thioguanosine triphosphate. Metal ions will be then added to the extended polymer, in order to create a one dimension coordination polymer.

4.2 Results and discussion

The conversion of **d-tG** to its corresponding triphosphate, **d-tGTP** was achieved and the desired triphosphate was purified by MPLC and HPLC, and characterised by ^{31}P- NMR, ES-MS and UV-visible spectroscopy. The enzymatic synthesis of extended DNA duplexes which incorporate **d-tGTP** was examined using a range of different polymerase enzymes. Long DNA duplexes containing **d-tG** were characterised by agarose gel electrophoresis, UV-visible spectroscopy and atomic force microscopy (AFM). Subsequently, cadmium ions were added to study their binding properties to the thio-modified DNA and were characterised by UV titration and denaturation experiments. The overall work in this chapter is summarised in Scheme 3 below, and discussed in the following sections.

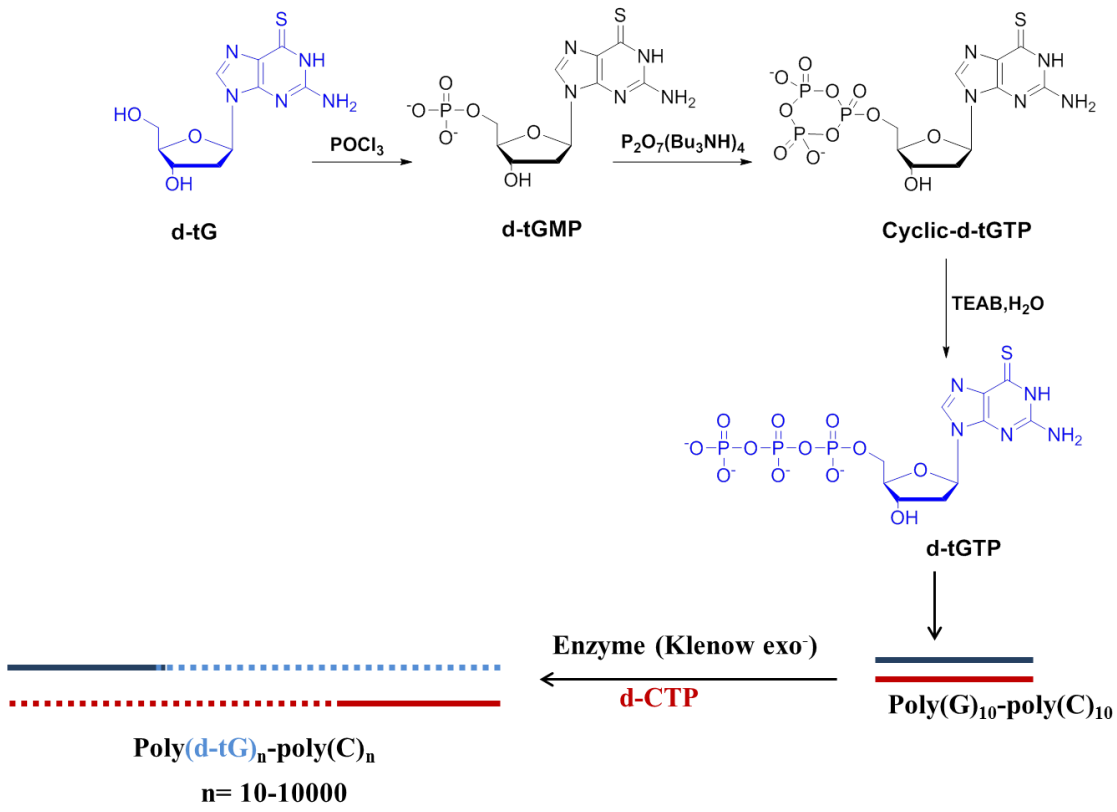

Scheme 3. Synthetic route for the synthesis of a thiomodified-long DNA duplex using **d-tGTP** *via* the slippage extension reaction.

4.2.1 Synthesis of modified nucleotide d-tGTP

2'-Deoxy-6-thioguanosine-5'-triphosphate (**d-tGTP)** was synthesised according to the procedure developed by Broom[19] *via* the conversion of **d-tG** to its corresponding triphosphate. Although **d-tGTP** is commercially available this synthesis was performed due to the high cost of the compound. The advantages of using the Broom method is that it is quick and convenient without the need for a protecting group of the nucleobase 2-NH_2 and ribose secondary 3'-OH that are normally sensitive to phosphorylation.[19] Therefore the conversion of **d-tG** into its triphosphate **d-tGTP** was performed using a phosphorylation reaction (phosphorus(V) chemistry) in three steps as shown in Scheme 4.

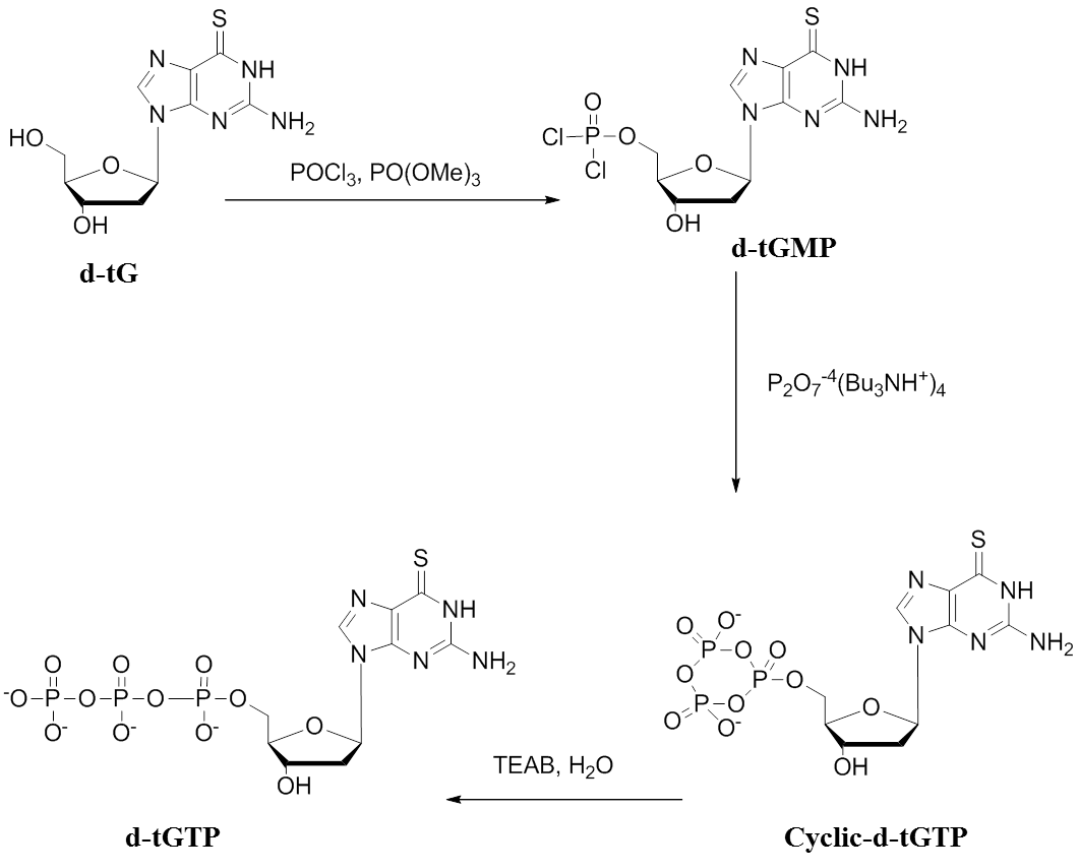

Scheme 4. Synthesis of **d-tGTP.**

In the phosphorylation reaction, trimethylphosphate $PO(OMe)_3$ was used to dissolve **d-tG** with gentle warming. Phosphoryl oxychloride ($POCl_3$) has to be extra dry before addition to the $PO(OMe)_3$ solution, as any moisture could hinder the phosphorylation reaction. The phosphorodichloridate intermediate was formed after the $POCl_3$ was added. Then the addition of tri-n-butylammonium pyrophosphate to the reaction mixture

led to the formation of the cyclic triphosphate. The cyclic triphosphate is quickly broken into the linear triphosphate during hydrolysis using triethylammonium hydrogen carbonate (TEAB) buffer. Anionic exchange on a MPLC column (sepharose media) was used to monitor and purify the **d-tGTP** from the crude reaction, see Figure 6.

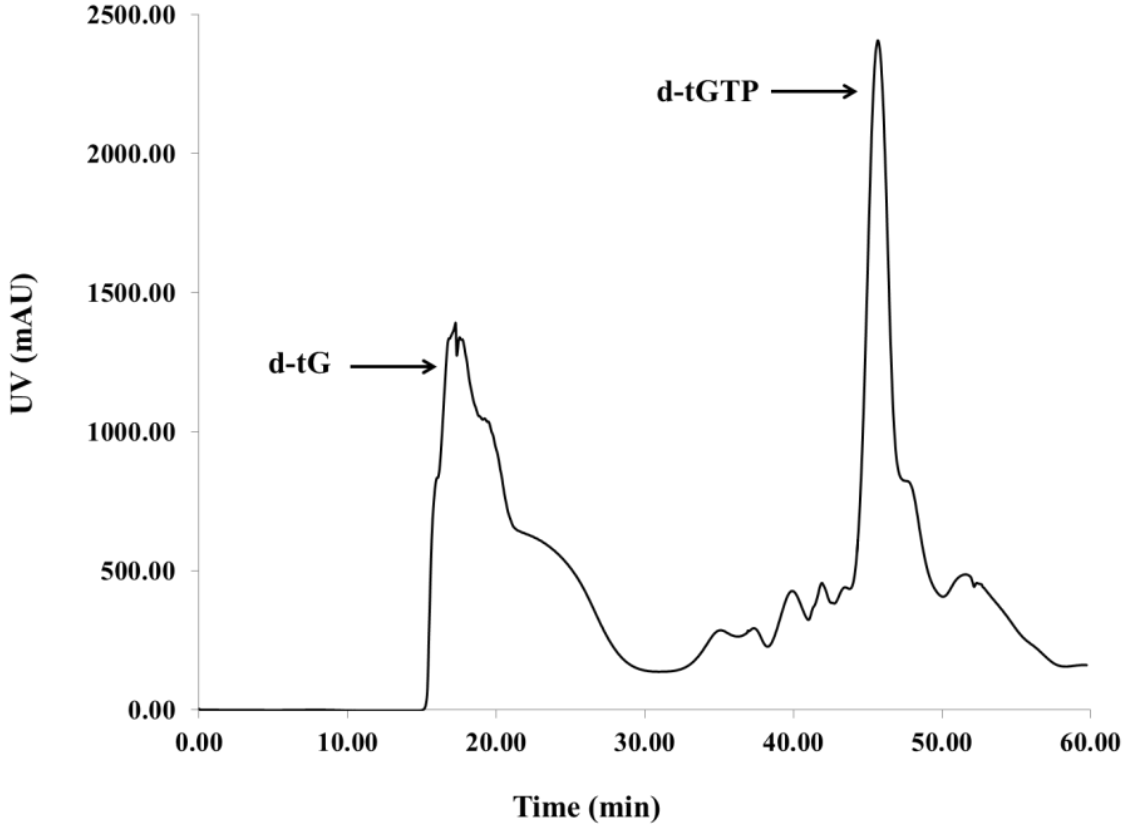

Figure 6. MPLC traces for **d-tGTP** synthesis.

In the MPLC trace (recorded at 280 nm) of the crude reaction mixture, two major components were identified as shown in Figure 6**.** The first major peak which eluted at ~20 min was associated with the unreacted starting material, **d-tG** as it carries no charge. This was confirmed by collecting the peak and comparing its UV-vis and MS data with the start material. The second major peak was observed at a longer retention time of ~48 min, which was expected to be the desired triphosphate **d-tGTP**. The smaller peaks at about 40 min related to the monophosphate, **d-tGMP** and as expected the intensity is very small due to its conversion into the triphosphate. The peak at ~48 min was collected and examined by ^{31}P-NMR spectroscopy which revealed three resonances; a triplet at δ -21.90 ppm from the β phosphorus, a doublet at δ -10.69 ppm

which is associated with the α phosphorus and a second doublet at δ -5.91 ppm corresponding to the γ phosphorus. Therefore the ^{31}P-NMR data confirmed the formation of **d-tGTP**.

However, the ^{31}P-NMR spectrum also showed that in addition to the three peaks a strong singlet at δ -20.81 ppm was observed. Previous work deduced that this peak belongs to unreacted pyrophosphate.[69] Pyrophosphate has a comparable charge to the triphosphate, shown in Figure 7, and so is likely to elute at around the same time as **d-tGTP** during purification by MPLC. Therefore, further purification by HPLC is required to remove the pyrophosphate. Reverse phase HPLC was carried out using a mixed solvent system of 0.1 M TEAB buffer and acetonitrile, employing a solvent gradient of 0-30% buffer over 30 min.

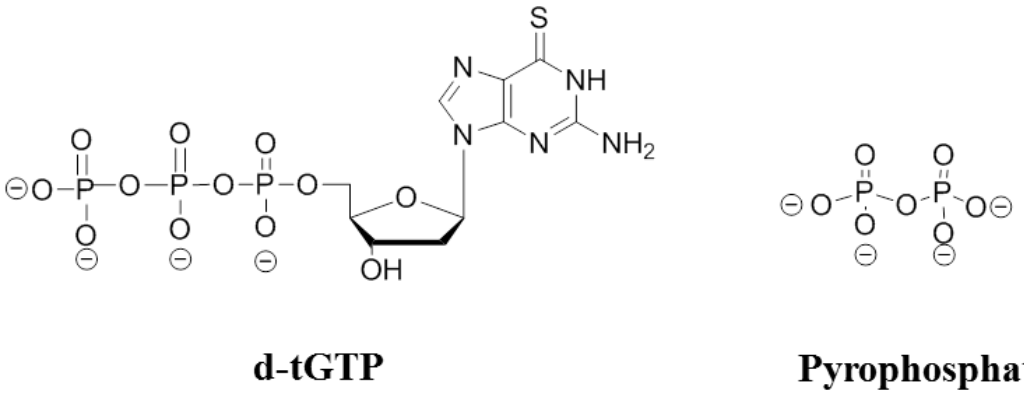

Figure 7. The structure of **d-tGTP** and the pyrophosphate group that has similar charge to triphosphate.

The pyrophosphate eluted first, at 13 min as it has a higher polarity than **d-tGTP.** The **d-tGTP** was then eluted at a longer retention time, 16 min. The **d-tGTP** peak was collected and then re-analysed for purity using the same HPLC system, see Figure 8. This now showed a single peak at 16 min confirming the purity of **d-tGTP**.

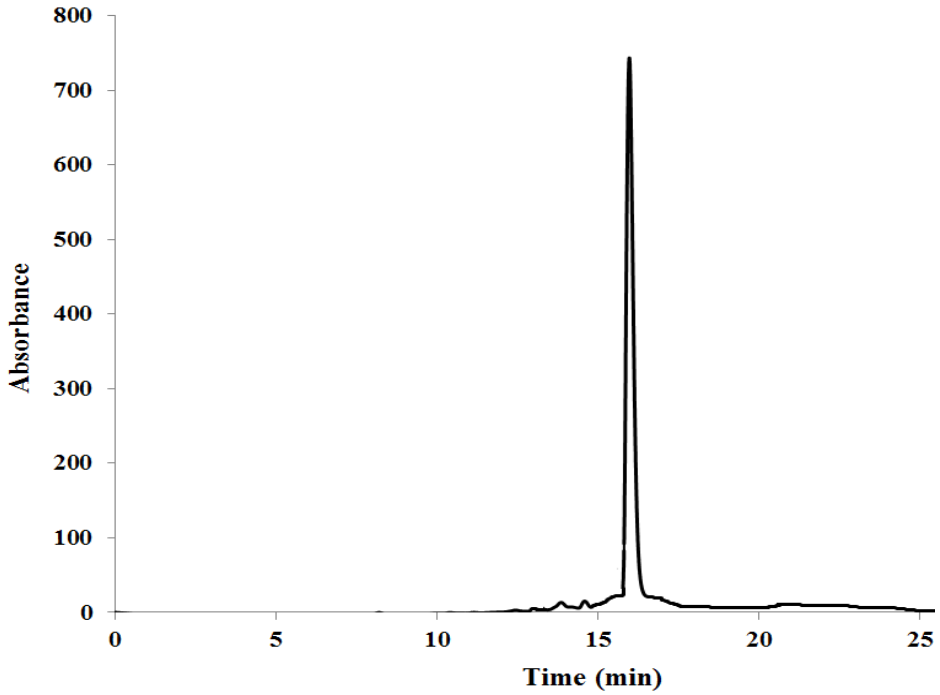

Figure 8. HPLC of pure **d-tGTP.**

The ^{31}P-NMR spectrum of the purified **d-tGTP** only showed the three expected peaks of a nucleotide at: -10.69 ppm (d, 1P, α), -21.90 ppm (t, 1P, β) and -5.91 ppm (d, 1P, γ) as illustrated in Figure 9.

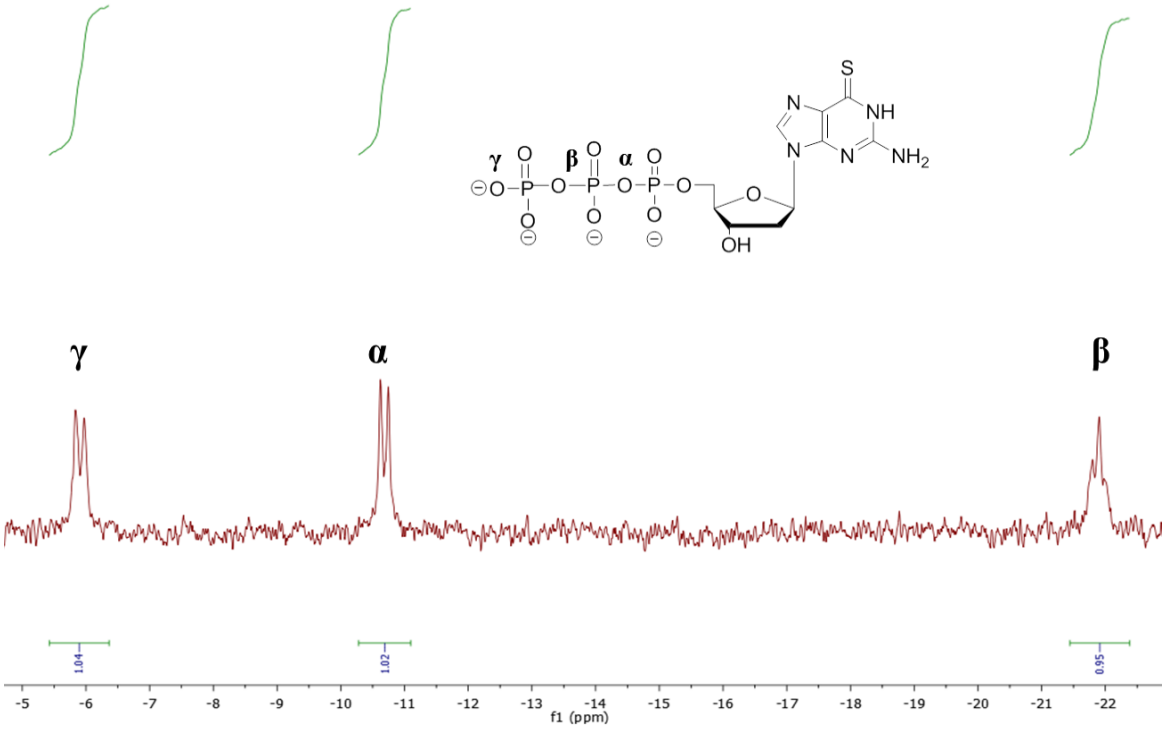

Figure 9. ^{31}P-NMR of **d-tGTP**.

The identity of **d-tGTP** was also confirmed by ES-MS mass spectrometry. The calculated m/z for **d-tGTP**, $C_{10}H_{16}N_5O_{12}P_3S$ $(M-H)^-$ is 521.9651 and the found peak was at 521.9809. Further characterisation was carried out by UV-vis spectroscopy of an aqueous solution of the purified **d-tGTP,** showing the characteristic peaks at 260 and 345 nm due to the thio-nucleobase.[70] Figure 10 shows a comparison of the absorption spectra of **d-tGTP** and **d-tG,** and indicated that the addition of the triphosphate group to the nucleoside does not have any significant influence on the wavelength of the maximum absorption, λ_{max} was 345 nm for **d-tG** and 344 nm for **d-tGTP.**

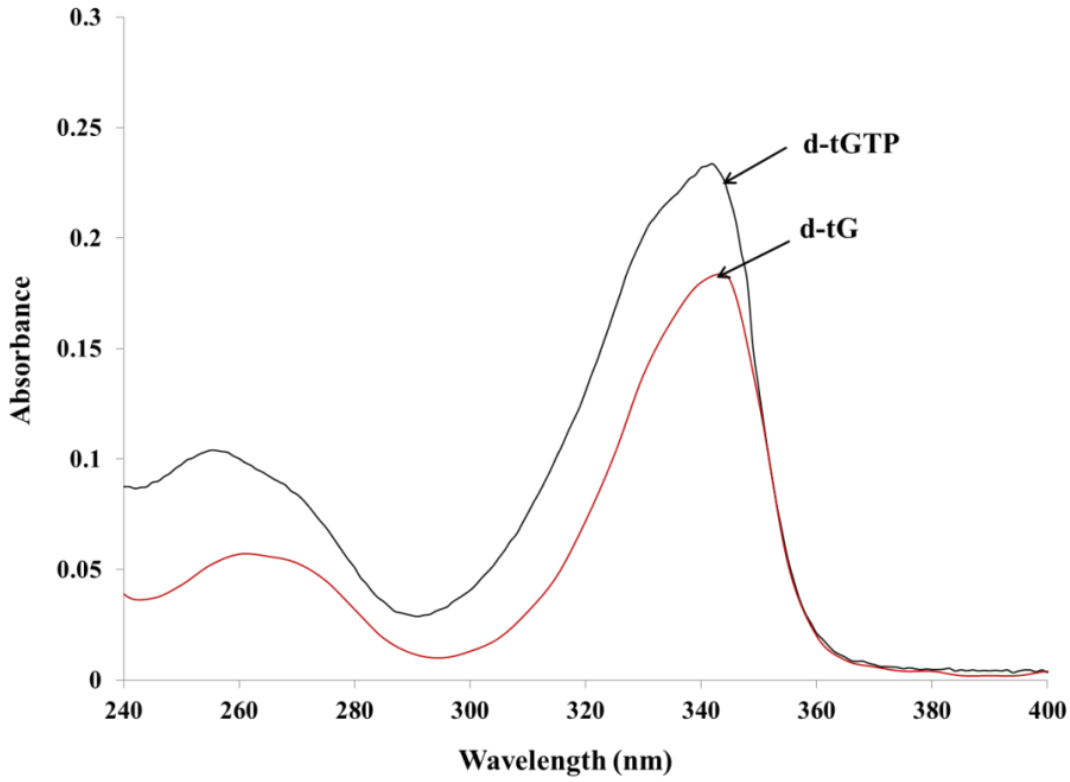

Figure 10. Comparsion of the UV-vis spectra for compounds **d-tG** and **d-tGTP** in aqueous solution.

The above findings indicated that the synthesis and purification of the modified triphosphate, **d-tGTP** were achieved. The incorporation of **d-tGTP** into DNA using short primer-template sequences and the enzymatic slippage extension reaction to form long DNA double strands was then investigated in the next stage of this work.

4.2.2 Slippage extension reaction

The enzymatic slippage reaction was performed according to Kotlyar's method,[1] by employing poly $(\mathbf{dG})_{10}$ - poly $(\mathbf{dC})_{10}$ as the template/primer. Our standard procedure for the extension reaction required **d-GTP, d-tGTP, d-CTP** and reaction buffer. The slippage extension was started by adding a polymerase; Klenow exo$^-$ polymerase, Taq polymerase, Bsu polymerase or *E. coli* polymerase I. These polymerases, especially the Klenow exo$^-$ polymerase have been reported as an efficient enzyme for the slippage extension reaction.[1] To identify the role of these polymerases, we need to further study and understand what these polymerases are. Klenow exo$^-$ polymerase is a fragment of DNA polymerase I that lacks both nick transition 5'>3' and proofreading 3'>5' exonuclease activity. Therefore it could accept modified nucleotides and prevent excision during reaction. This enzyme can work at quiet high temperatures but becomes inactive at 75 °C. Taq polymerase is structurally very similar to Klenow exo$^-$ but is thermodynamically stable and can act at higher temperatures and only loses its activity at 94 °C. Bsu polymerase has been chosen as it has a similar function to Klenow exo$^-$ polymerase. *E. coli* polymerase I ((PolI) can perform the slippage extension reaction, known since the early work of Kornberg.[45] In our lab, we have successfully used both PolI and BSu to extend poly $(\mathbf{dG})_{10}$- poly $(\mathbf{dC})_{10}$ to yield kilo base pair lengths of DNA. However, these enzymes had lower rates of extension than the Klenow exo$^-$ fragment. There are only limited publications that discuss why these enzymes have been used for the slippage extension reaction and hence the need to try a range of enzymes in the studies here.

4.2.2.1 Slippage test reactions with standard 2'-deoxyguanosine-5'-triphosphate (d-GTP)

Our standard **d-GTP** experiment is started by adding the Klenow exo$^-$ polymerase to the enzymatic reaction mixture. Figure 11 demonstrates that Klenow exo$^-$ polymerase extends the oligonucleotide primer/template poly$(\mathbf{dG})_{10}$-poly$(\mathbf{dC})_{10}$ at room temperature to form long double stranded DNA using the natural nucleotide triphosphates **d-CTP** and **d-GTP**.

The length of the poly (**dG**)-poly (**dC**) homopolymers that are produced can be controlled, as previously described by Kotlyar.[1] As shown in Figure 11; the DNA length's increased with incubation time, as observed by Kotlyar.[1] After 15 minutes, a band at approximately 500 base pair was observed whereas at 135 minutes, around 6,000 base pair DNA was seen.

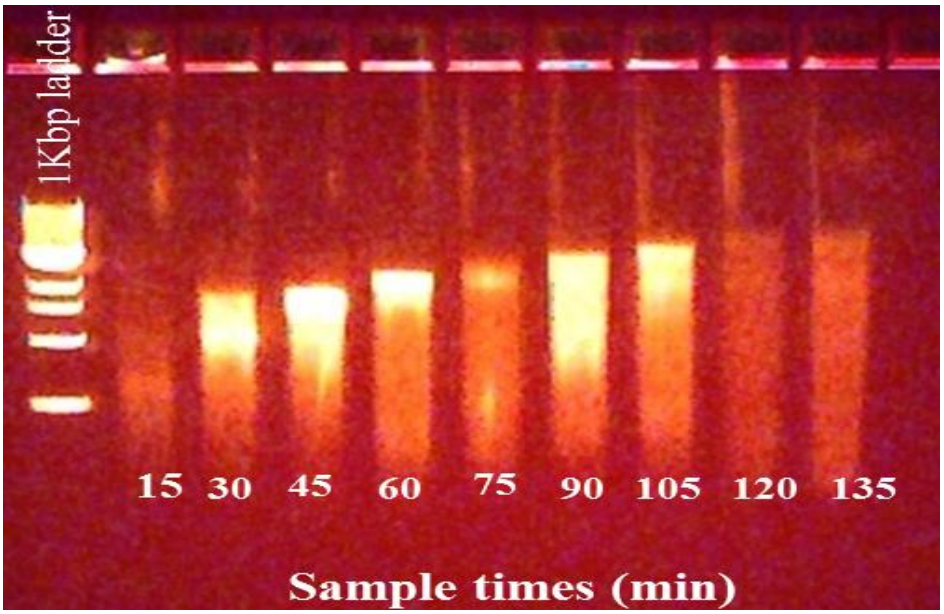

Figure 11. Lonza FlashGel^{TM}cassette (1.2 % agarose) showing progress of the slippage extension reaction of poly (**dG**)-poly(**dC**) using **d-GTP** at room temperature with time. Lane 1 = 1Kb ladder. Lanes 2-9 = products of enzymatic slippage of poly (**dG**)-poly(**dC**), that illustrate the increase in the length of DNA with time.

The reaction was then repeated using the same protocol however it was carried out at a slightly elevated temperature of 37 ^{o}C .The results in Figure 12 demonstrated that there was a clear increase in DNA length, as a thick band of about 10,000 base pair was observed, even after only 30 minutes.

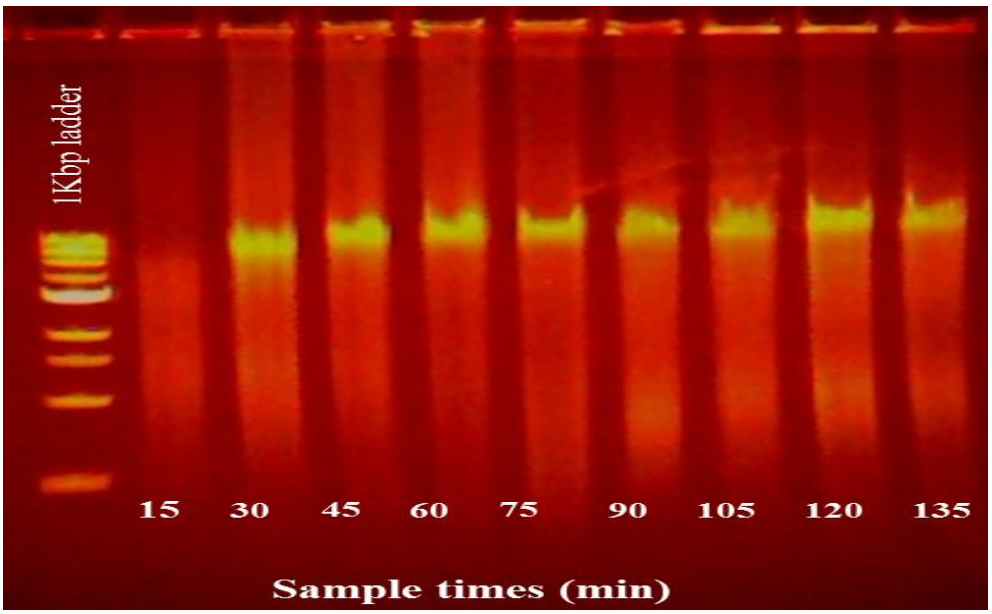

Figure 12. Lonza FlashGel^{TM}cassette (1.2 % agarose) showing progress of the slippage extension reaction of poly (**dG**)-poly(**dC**) using **d-GTP** at 37 °C with time Lane 1 = 1Kb ladder. Lanes 2-9 = products of enzymatic slippage of poly (**dG**)-poly (**dC**), that illustrated the increase of DNA length with time.

Therefore the band from the 135 min sample was recovered from the gel, using a Lonza 1.2 % agarose recovery gel. The collected sample was then analysed by UV-vis as seen in Figure 13.

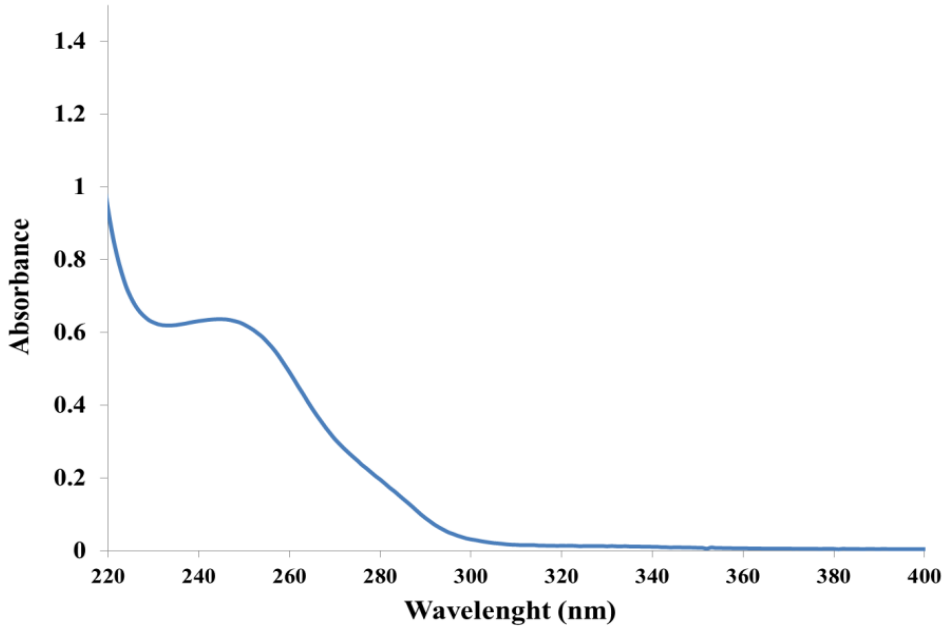

Figure 13.UV absorption of long details of DNA duplex containing about 10,000 base pair of homogeneity lengths of **d-G** and **d-C**.

UV-vis of an aqueous solution of the recovered poly(**dG**)-poly(**dC**) **[d-G-DNA]** showed the characteristic DNA base absorption peak at ~250 nm related to the poly(**dG**)-poly(**dC**) band as determined by Inman and his group.[71]

Topographical imaging of the **d-G-DNA** was carried out by AFM in order to probe its size and morphology. This was carried out by depositing the **d-G-DNA** from solution onto mica substrates, and imaging in tapping mode. The AFM image showed clear evidence of the presence of individual duplex DNA molecules (see Figure 14, red arrow) aligned on the surface, as well as examples of bundles of DNA molecules (see Figure 14, blue arrow). Line profile measurements of the individual DNA molecules on the surface found the structures to typically range in height from 1.5 nm–1.9 nm, whilst the bundled DNA structures were found to typically be 2.03-2.3 nm in height. The length of the DNA molecules shown in Figure 14 were estimated to range from 1.73 μm –2.28 μm in length. This corresponds to the molecules consisting of 5000–7000 base pairs (assuming each base pair unit is 0.34 nm in length). This is somewhat shorter than the 10,000 base pairs suggested by the gel data. One possible explanation is that the gel is not separating the various lengths of product for this particular DNA sequence because of aggregation of DNA strands under the conditions employed for electrophoresis. On the other hand, these are separated during the molecular combing process for sample deposition during AFM preparation. However, a similar AFM image of **d-G-DNA** has been reported by Kotlyar and his group who found that no self-folding and lengths up to 2.70 μm was observed. [65]

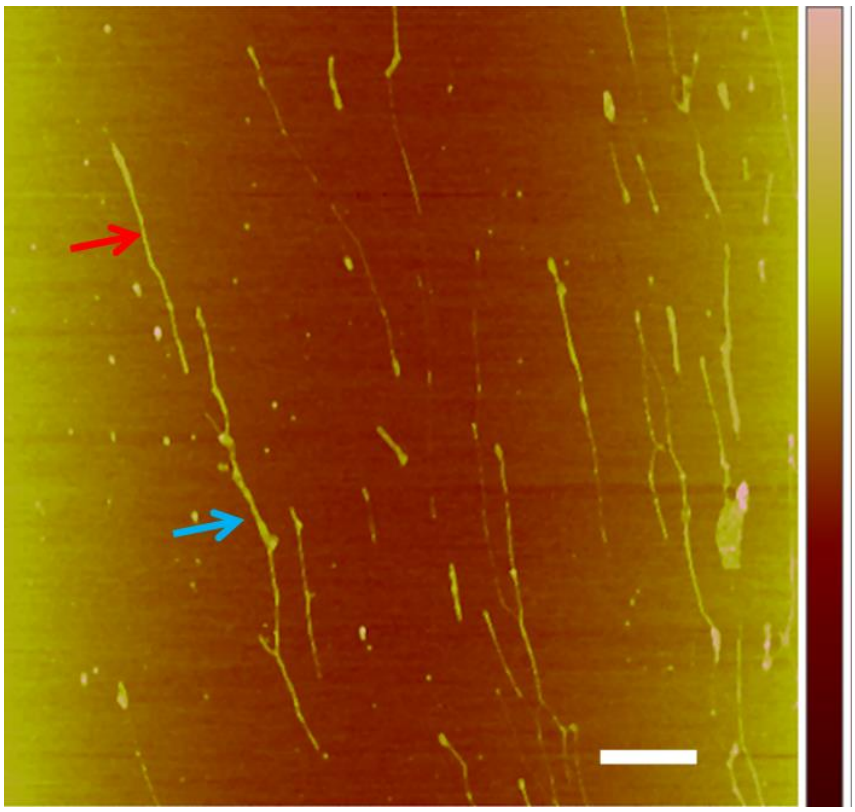

Figure 14. AFM height images of **d-G-DNA**. Scale bar = 500 nm and the height scale = 10 nm. Red arrow indicated the presence of individual duplex DNA molecules, blue arrow indicated bundles of DNA molecules.

4.2.2.2 Slippage extension reactions with 2'-deoxy-6-thioguanosine-5'-triphosphate (d-tGTP)

The slippage extension reaction, using the same protocol as for the synthesis of **d-G-DNA** was repeated with the thio-modified nucleotide triphosphate, **d-tGTP** instead of **d-GTP**. The slippage extension reaction was carried out at room temperature and at 37 °C, using **d-tGTP** with Klenow exo$^-$ polymerase and the products were monitored by agarose electrophoresis. The gels showed no sign of extension at either temperature, therefore, different reaction conditions were attempted to perform the extension, and these included changes to the concentration of triphosphate, template and polymerase in the reaction. However, despite multiple attempts, no efficient extension to the same level as observed for the incorporation of **d-GTP** was observed. On the other hand, at the optimised conditions of 50°C for 24 hours a narrow band, see lane 4 of Figure 15A, indicates that the extension reaction has produced some **d-tG** modified DNA (**d-tG-DNA**). From the gel in Figure 15A, there is clearly some extension of the

template up to approximately 300 bp. The modified DNA is clearly longer than the template (10 bp) and is retained in the gel for longer; see the free template in lane 2. These results for **d-tGTP** extension showed that the Klenow exo$^-$ polymerase could extend the DNA template to around 300 bp, but that no further extension occurred even at considerably longer reaction times, more than 24 hours.

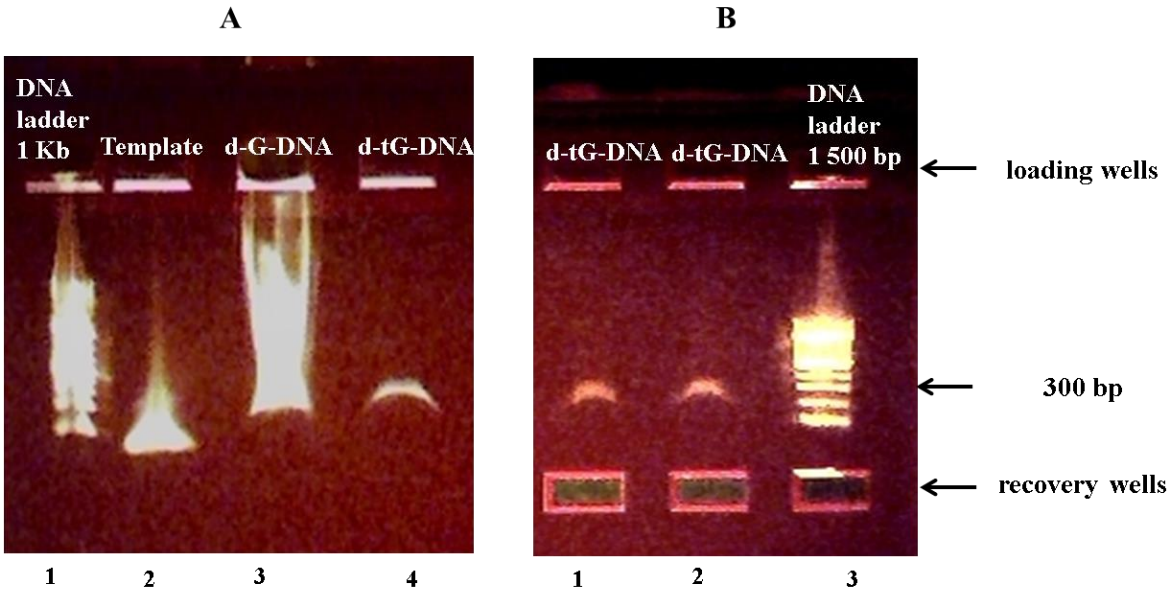

Figure 15. Lonza FlashGel^{TM} electrophoresis characterisation of the enzymatic slippage extension reaction of poly (**dG**)-poly(**dC**) using **d-tGTP** at 50 °C in 1.2 % agarose gel. (A) shows the image of the slippage reaction of **d-tGTP**, lane 1 = 1 Kb DNA ladder, lane 2 = free template, lane 3 = **d-G-DNA** and lane 4 = product of enzymatic slippage of poly (**dG**)-poly(**dC**) using **d-tGTP (d-tG-DNA).** (B) the recovery Lonza FlashGel^{TM} (1.2 % agarose) of **d-tG-DNA.** Lane 3= 1500 bp ladder, lane 1 and 2 = **d-tG-DNA.**

In a second gel electrophoresis experiment the **d-tG-DNA** was recovered from the gel using a recovery Lonza FlashGel^{TM}, with a short DNA ladder of about 1500 bp was used to calibrate mobility as shown in Figure 15B. The DNA ladder was loaded in the well number 3 and the sample was loaded in wells 1 and 2 in the upper tier of a Lonza cassette. Voltage was applied to the Lonza cassette, and the samples started to migrate. Before the desired sample reached the recovery well in the lower tier (shown in Figure 15B), the voltage was turned off and the excess buffer was removed from the wells. Subsequently, the Lonza recovery buffer was loaded into the wells. The voltage then restarts and the bands were run until they reached the wells, where they were recovered from the gel.

UV-vis of an aqueous solution of the recovered [**d-tG-DNA]** from the Lonza gel showed the characteristic peaks at 250 and 345 nm respectively, see Figure 16.[70] This absorption is similar to results of **(d-tG)$_4$** that are described in chapter 3, see Figure 16. The difference in the absorption of **d-tG-DNA** at 250 nm and **(d-tG)$_4$** at 260 nm is the presence of the cytosine in the **d-tG-DNA** structure whereas in the case of **(d-tG)$_4$** the only base is **d-tG**.

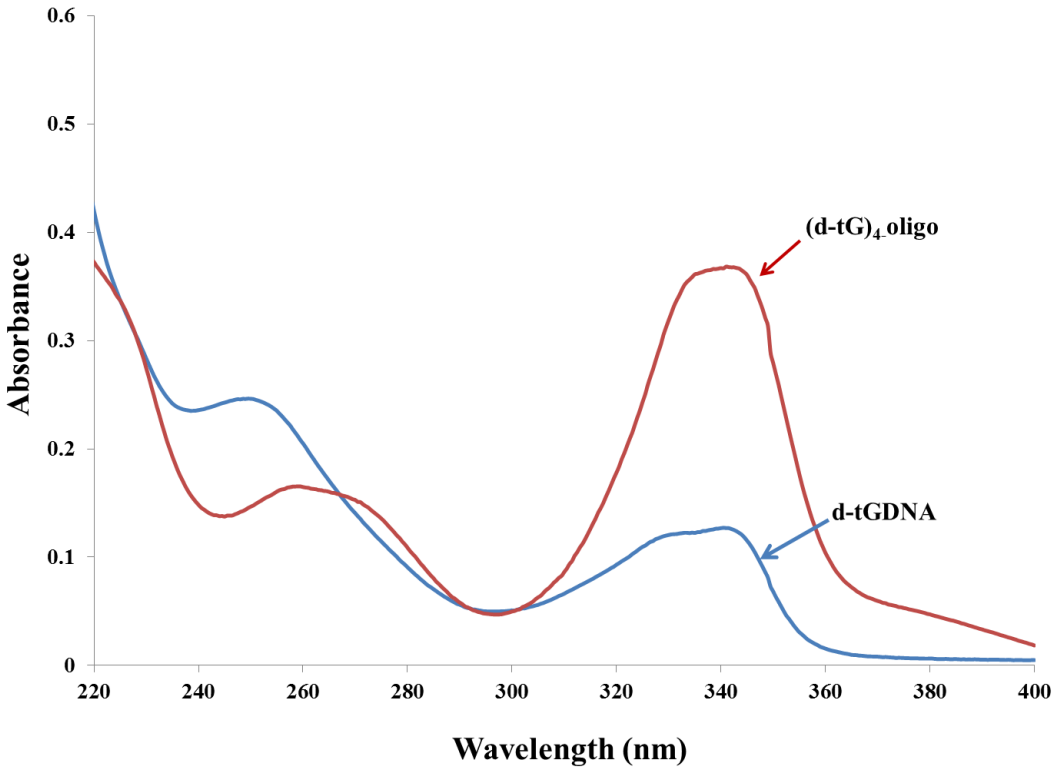

Figure 16. UV comparison between **d-tG-DNA (**blue line**)** and **(d-tG)$_4$ (**red line**).**

In an effort to improve the yield of the enzymatic synthesis of **d-tG-DNA** the enzymes *Taq* polymerase, polymerase I and Bsu polymerase were tested for their ability to extend the poly **(dG)**$_{10}$-poly**(dC)**$_{10}$ primer with **d-tGTP** to higher lengths. However, there was no indication that these polymerases could promote slippage extension at temperatures up to 50 °C any better than Klenow exo$^-$ polymerase.

Topographical imaging of the **d-tG-DNA** was carried out by AFM in order to probe its size and morphology in a similar way as for **d-G-DNA** described earlier. This was carried out by depositing the **d-tG-DNA** from solution onto mica substrates, and imaging in tapping mode AFM. The AFM image showed the presence of DNA

deposited onto the surface. Its morphology was different to that of **d-G-DNA** and appeared as bundles, branched networks and dots. These features are common when the sample is deposited at a high concentration,[72] as shown in Figure 17. However, when the sample was diluted, AFM images showed only small dots on the surface and there was no sign of linear extended DNA. This is not unexpected, due to the relatively short length of the recovered sample, around 300 bp which equates to approximately 0.1 μm. At this length it is difficult to see DNA by AFM due to the limits of the technique on soft biological materials.

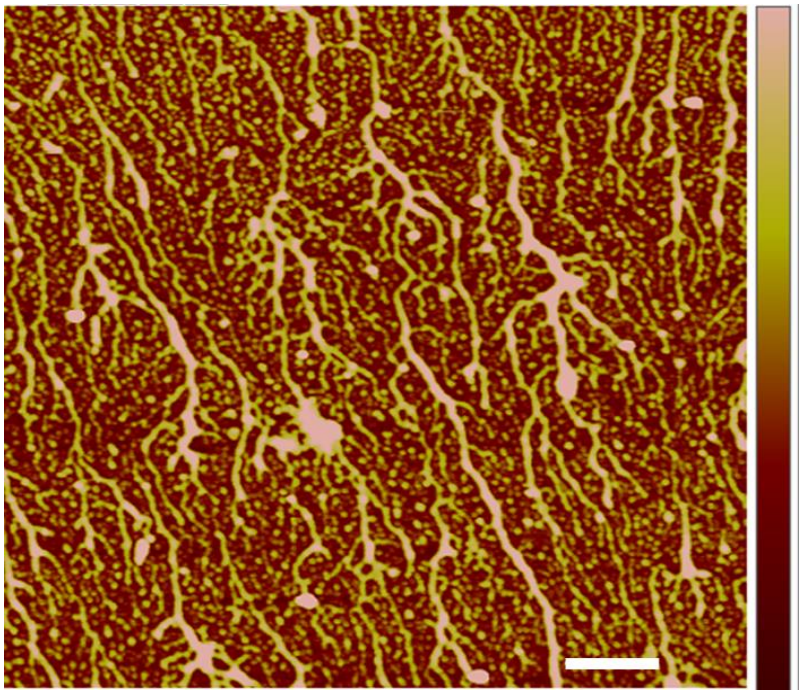

Figure 17. AFM height images of **d-tG-DNA**. Scale bare = 300 nm and the height scale= 10 nm.

Having established the synthesis and characterisation of long thio-DNA duplexes, attention was then turned towards investigations into the metal ion binding properties of **d-tG-DNA**.

4.3 Metal binding and characterisation

In Chapter 3 the interaction of the **(d-tG)$_2$**, **(d-tG)$_3$**, **(d-tG)$_4$** and **(d-tG)$_5$** oligomers with divalent metal ions was discussed, with particular emphasis on the binding of Cd^{2+}. In this section, we will examine how the long DNA duplex containing thioguanosine

interacts with Cd^{2+} and whether this forms a one dimensional coordination polymer similar to that observed for Cd^{2+} with mercaptopurine.[73]

4.3.1 UV titration of d-G-DNA with cadmium ion

The first experimental method that was used to investigate the binding of metal ions by **d-G-DNA** was a UV titration experiment. Titration of **d-G-DNA** with cadmium (II) nitrate showed that upon addition of Cd^{2+}, the absorption at 250 nm gradually decreased, as shown in Figure 18 A. This is probably due to the binding of Cd^{2+} by the guanine base through N7 as well as to the cytosine base *via* N3, as previously reported by Thomas.[74] To understand more about the binding of cadmium (II) to DNA, the absorption data at 250 nm were plotted for a series of ligand to metal ratios as shown in Figure 18 B. Within experimental error, the absorbance does not vary systematically for [metal] / [base] ratios of 0–2, probably because initially the Cd^{2+} binds to the phosphate group of the DNA backbone as previously reported by Dupuis.[75] Therefore, the base pair absorbance at 250 nm is not perturbed. For [metal] / [base] ratios of about 3-7 the absorbance drops markedly, probably due to increasing the Cd^{2+} concentration causing deprotonation of the **G-C** base pairs. It was previously noted by Thomas *et al.*[74] that binding of Cd^{2+} to genomic DNA raised the bulk solution pH as H^{+} was released by increased Cd^{2+} concentration, which is consistent with this proposal. Then, at [metal] / [base] ratios of more than 7 the curve appears to level off because the increase of Cd^{2+} did not affect on the binding site of the base any more.

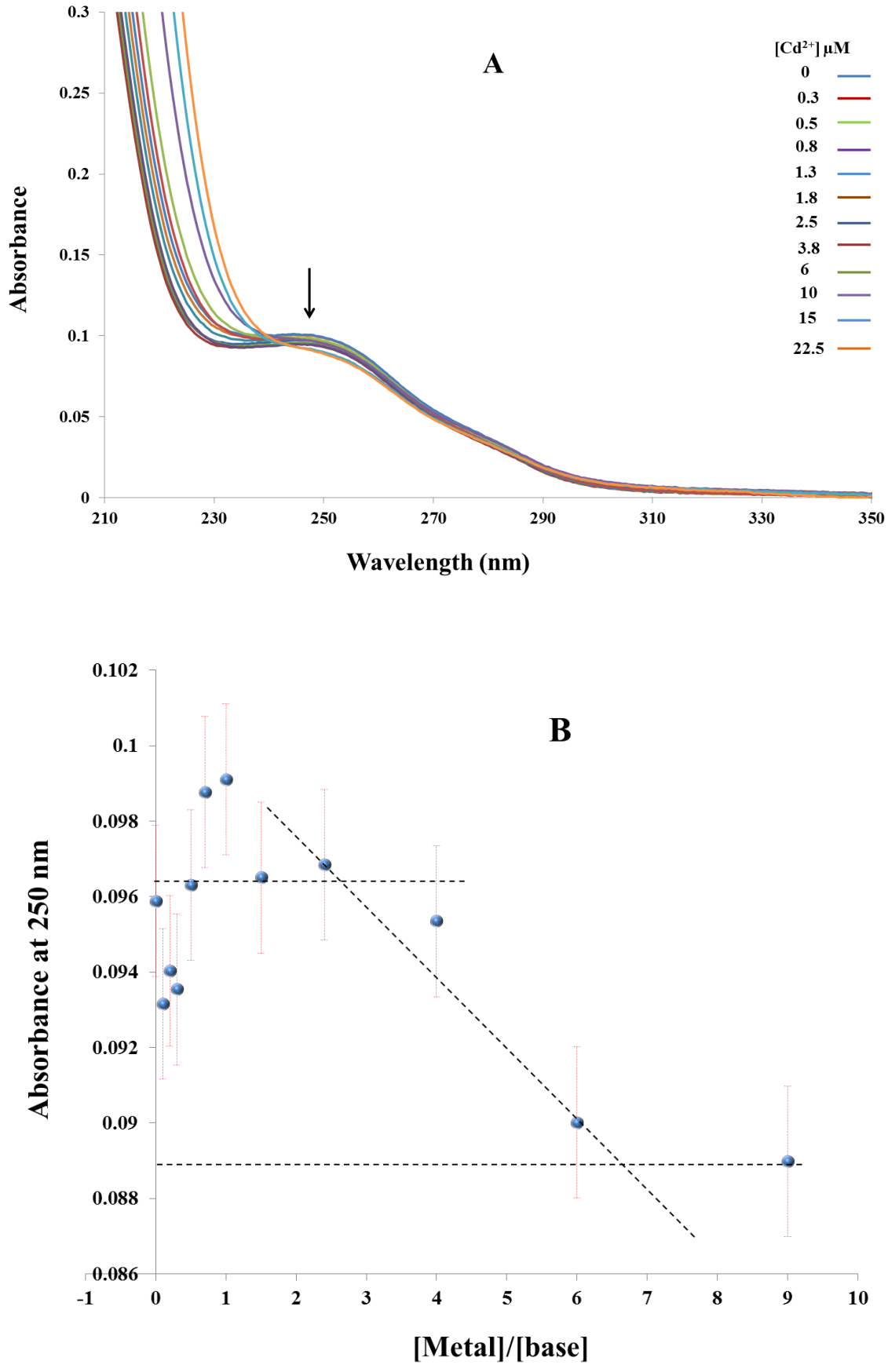

Figure 18. Absorption titration spectrum of **d-G-DNA (**2.5 µM**)** with cadmium nitrate in aqueous solution (**A**), Binding curve of **d-G-DNA** and Cd^{2+} at 250 nm (**B**) (fixed value ± 0.002).

4.3.2 UV titration of d-tG-DNA with cadmium nitrate

In order to achieve the formation of a one dimension coordination polymer based on the thioguanosine systems studied in this work, Cd^{2+} was added to a **d-tG-DNA** solution. The UV titration of **d-tG-DNA** with cadmium (II) nitrate showed that during the addition of Cd^{2+}, the absorbance at 345 nm gradually decreased while the absorbance at 250 nm increased as seen in Figure 19. It also appears that the 345 nm absorption band blue-shifts to higher energy with a maximum at 319 nm. However, it could be conceived that this is in fact the appearance of a new band. This variation is similar to that observed when the pH of **d-tG** solution is lowered by the addition of NaOH (see chapter 2, Figure 7). Hence, an increase in Cd^{2+} concentration is equivalent to a rise in pH which causes deprotonation of **d-tG** and gives some indication of the binding interactions involved between the metal and nucleobase.[74]

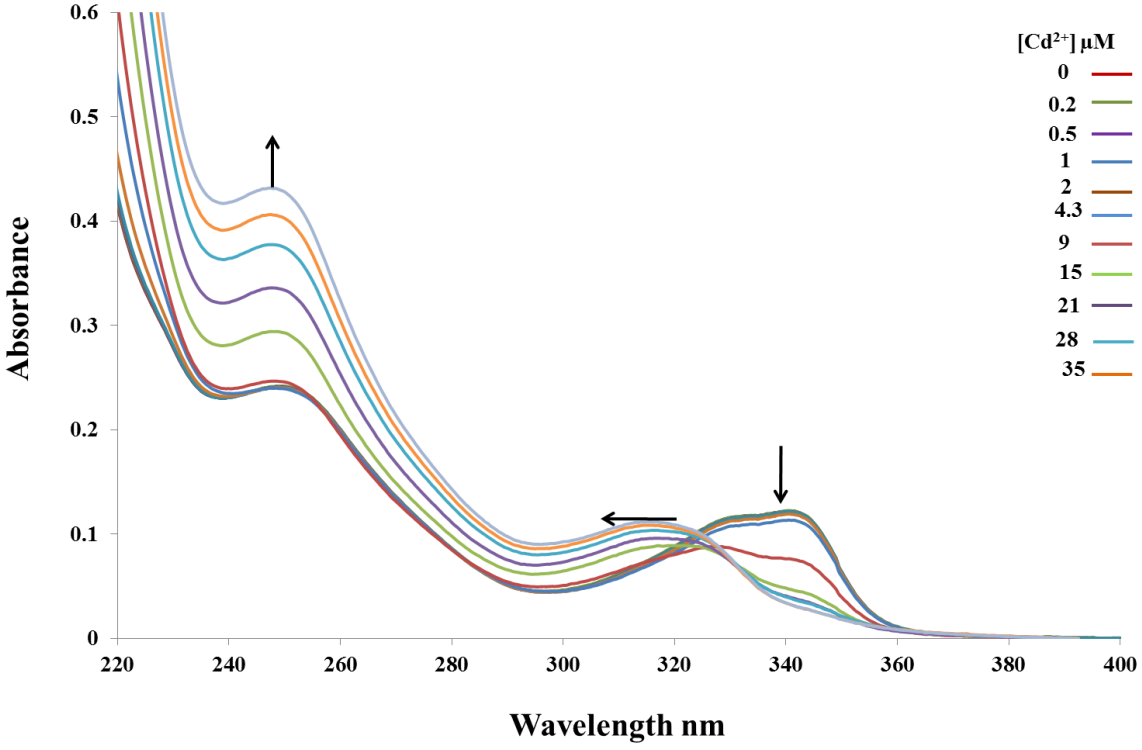

Figure 19. Absorption titration spectrum of **d-tG-DNA (**2.5 µM**)** with cadmium nitrate in aqueous solution.

The plot of the absorbance at λ = 345 nm against base to metal ratio, shown in Figure 20, can be divided into three regimes and provides some insights into the possible binding modes. First, the absorbance is constant for [metal] / [thiobase] ratios of 0 - 0.5. This is likely to be due to the binding of Cd^{2+} by the phosphate groups along the backbone of the **d-tG-DNA**, and so does not strongly perturb the **d-tG** absorption**.** Second, the absorbance decreases for [metal] / [thiobase] ratios of 0.5 - 6, this is likely to be due to **d-tG** deprotonation which is then coupled to Cd^{2+} binding to N7 and S6 of the 6-thioguanosine. This is in agreement with the monomer studies detailed in Chapter 2. Finally, at [metal] / [thiobase] ratios > 6 the absorbance does not change greatly as the Cd^{2+} has no more possible sites for interaction with the modified DNA.

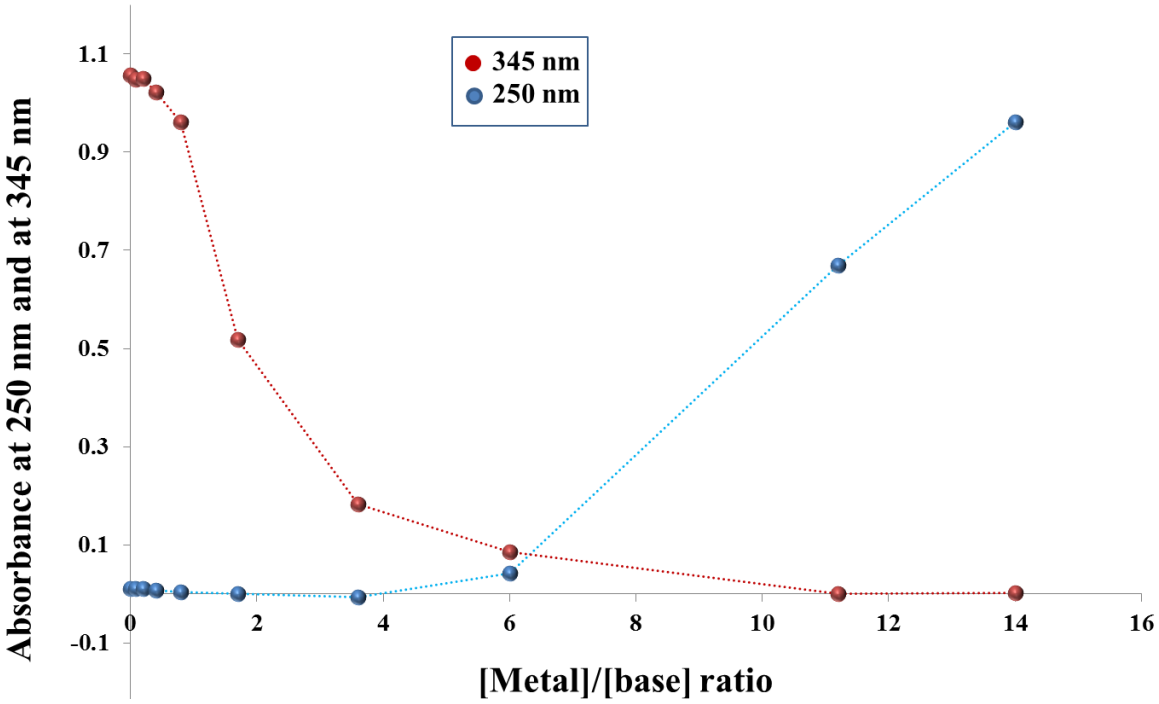

Figure 20. Binding curve of **d-tG-DNA** and Cd^{2+} at 345 and 250 nm.

The variations in absorbance for the same titration, but recorded at 250 nm, were dramatically different, as seen in Figure 20. There is no change in absorption until the [metal] / [thiobase] ratio is greater than 5, but at higher ratios there is a strong increase in absorbance. This indicates that the binding of Cd^{2+} up to a [metal] / [thiobase] ratio of 5-6 does not significantly perturb the base-pair stacking interactions within the modified DNA.

However, the observed hyperchromism at higher cadmium concentration implies that some destacking of the base pairs occurs once the [metal] / [thiobase] ratio reaches at least 5, and continues to increase as the metal concentration is increased. This was not observed for unmodified DNA (Figure 18 shows a decrease in absorption), and suggests that a significant change in the conformation of the **d-tG-DNA** occurs upon complexation with Cd^{2+}. This can be accounted for by the simple difference in the guanosine base, as the C6-oxygen having been replaced by sulphur in the modified polynucleotide.

4.3.3 Melting temperature studies of d-G-DNA and d-tG-DNA

In a further attempt to understand the behaviour of the modified polynucleotide upon complexation, a comparison of the stability of the **d-G-DNA** and **d-tG-DNA** helices were first investigated through melting temperature studies. To determine the effect of **d-tG** on the stability of the DNA duplex, the melting temperature was measured for both modified and unmodified DNA. Figure 21 compares the thermal denturation profiles for ~ 300 bp segments of **d-tG-DNA** (red line) and **d-G-DNA (**blue line), both recovered from a Lonza™ gel as previously described. Both samples were heated up to 95 ºC at 0.1 per min while the absorbance at 260 nm was monitored. Both DNA samples were very stable and an upper absorption plateau was not reached by 95 ºC in both cases. However, in Figure 21, the absorbance for **d-tG** raises more strongly than **d-G,** in particular at lower temperatures, 60-75 ºC. This observation indicates that by replacing every **d-G** with **d-tG** in DNA, leads to the destablisation of the duplex structure, in a manner similar to that previously reported by Santos.[37]

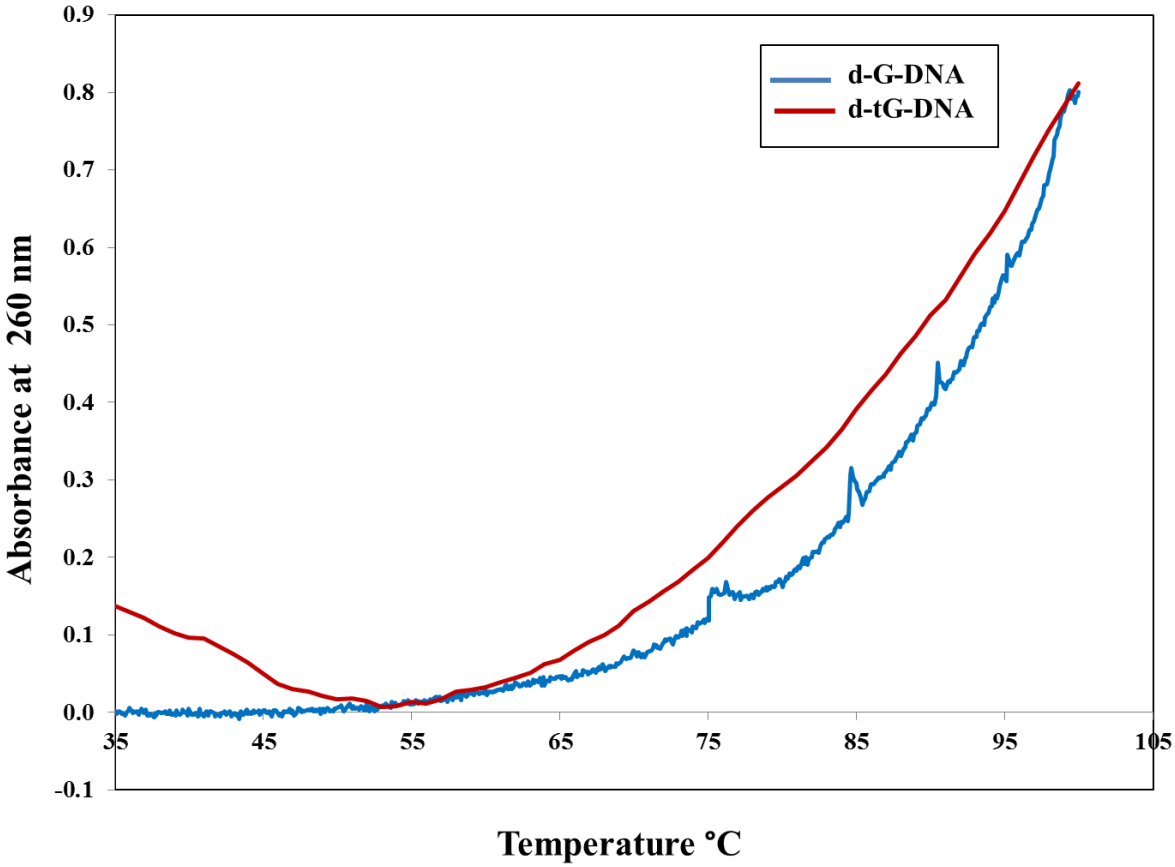

Figure 21. Thermal denaturation of **d-G-DNA** (blue line) and **d-tG-DNA** (red line).

4.3.3.1 Melting temperature studies of d-G-DNA and d-tG-DNA after addition of cadmium ions

Likewise, the stability of long unmodified DNA duplexes after the addition of cadmium ions was investigated through melting temperature studies. Figure 22 compares the thermal denturation profile for **Cd-d-G-DNA** (green line) and free **d-G-DNA** (blue line), the **Cd-d-G-DNA** sample was that from the final UV /vis titration experiment. Both samples were heated up to 95 ºC while the absorbance at 260 nm was monitored. In Figure 22, the **Cd-d-G-DNA** melting-temperature profile increases uniformly across the whole temperature range, suggesting a very stable complex which undergoes little denaturation, even at temperatures over 95 ºC. On the other hand, the melting temperature profile for **d-G-DNA** starts to increase at temperatures below 55 ºC. These

findings suggest that a more stable complex is formed after addition of metal ions to **d-G-DNA**.

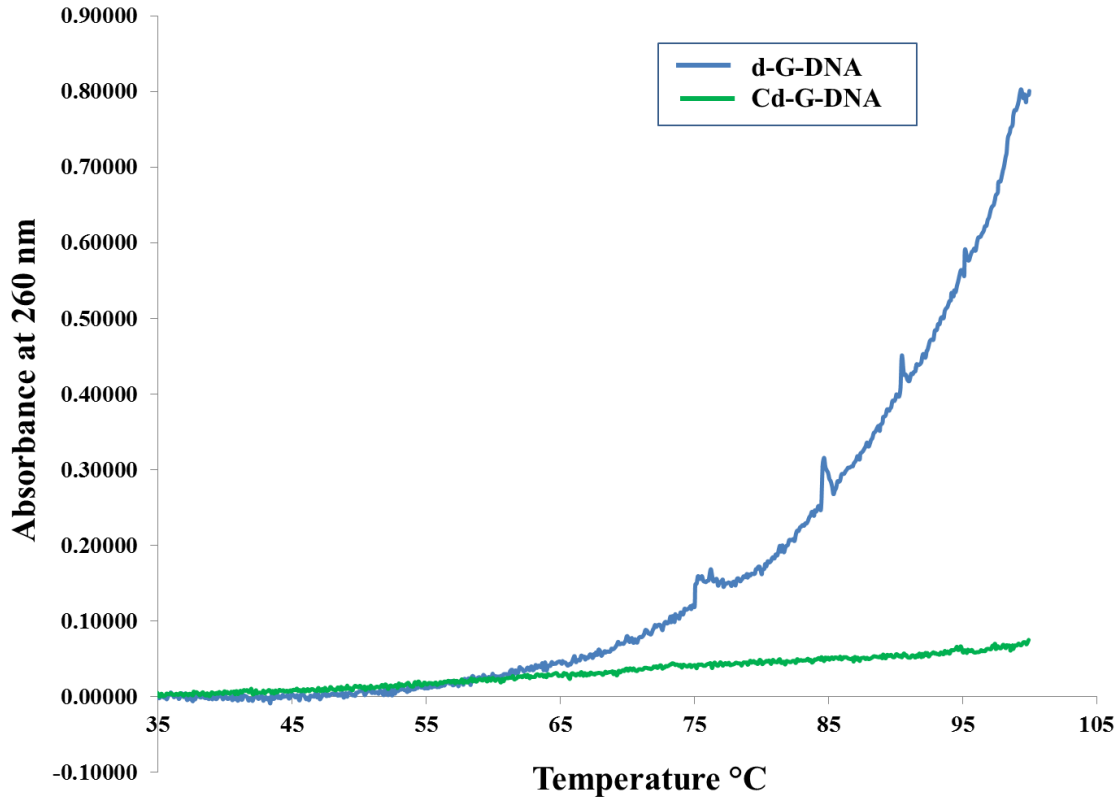

Figure 22. Tm comparison between **d-G-DNA (**blue line**)** and **Cd-d-G-DNA (**green line**)**.

Similar studies with the modified polynucleotide **d-tG-DNA** and its cadmium complex **Cd-d-tG-DNA** were also performed**.** In general the results were very similar to the unmodified case. Once again the melting-temperature profile of **Cd-d-tG-DNA** increases uniformly across the whole temperature range, suggesting a very stable complex which undergoes little denaturation, even at temperatures over 95 ºC, as shown in Figure 23. On the other hand, the melting temperature profile for **d-tG-DNA** starts to increase at temperatures around 50 ºC. These results indicated that the addition of cadmium ions to long thio-modified DNA duplexes once again makes their structures more stable.

As the addition of Cd^{2+} to either thio-modified or unmodified **d-G-DNA** increases the stability of the polynucleotide in both cases it is clear that the binding of Cd^{2+} could be by both guanine and thioguanine bases. However, other possible interactions with the duplex through binding to the cytosine bases at position N3 may also have an effect on the duplex stability, as previously reported by Thomas. [74]

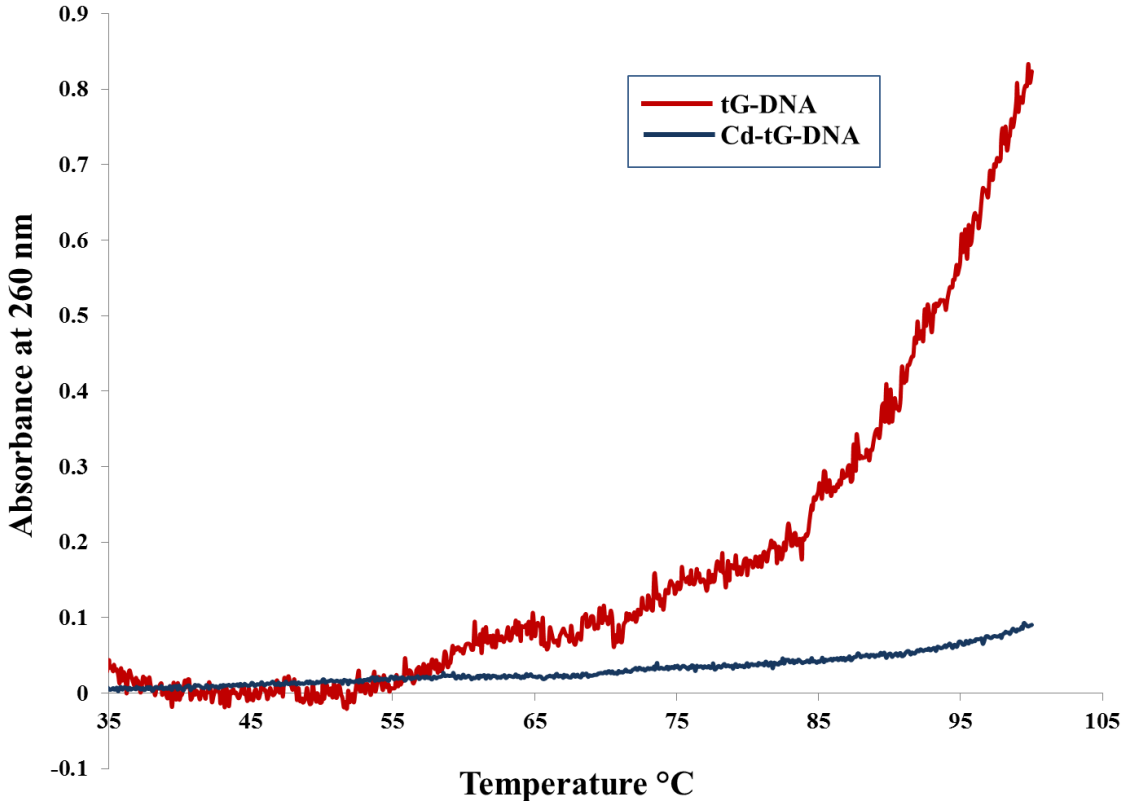

Figure 23. Tm comparison between **d-tG-DNA (**red line**)** and **Cd-d-tG-DNA (**dark blue line**)**.

4.3.3.2 Melting temperature comparison between Cd-d-G-DNA and Cd-d-tG-DNA

As discussed above the addition of cadmium ions to long DNA duplexes increases the stability of the helix. It is expected that **Cd-d-tG-DNA** would be more stable than **Cd-d-G-DNA** when examined by Tm since we anticipate that **d-tG** would be more likely to coordinate metal ions than **dG.** Although the melting temperatures of both systems are over 100 ºC, i.e. no plateau is reached within the experimental conditions employed, see Figure 24, it appeared that within the **d-tG** system there was some evidence that the duplex started to destabilise / denature from around 85 ºC, whilst the unmodified **dG** system did not. Since we cannot determine exact Tm values for these systems, it is impossible to draw concrete conclusions about the stabilizing effects of Cd^{2+} on these two duplexes.

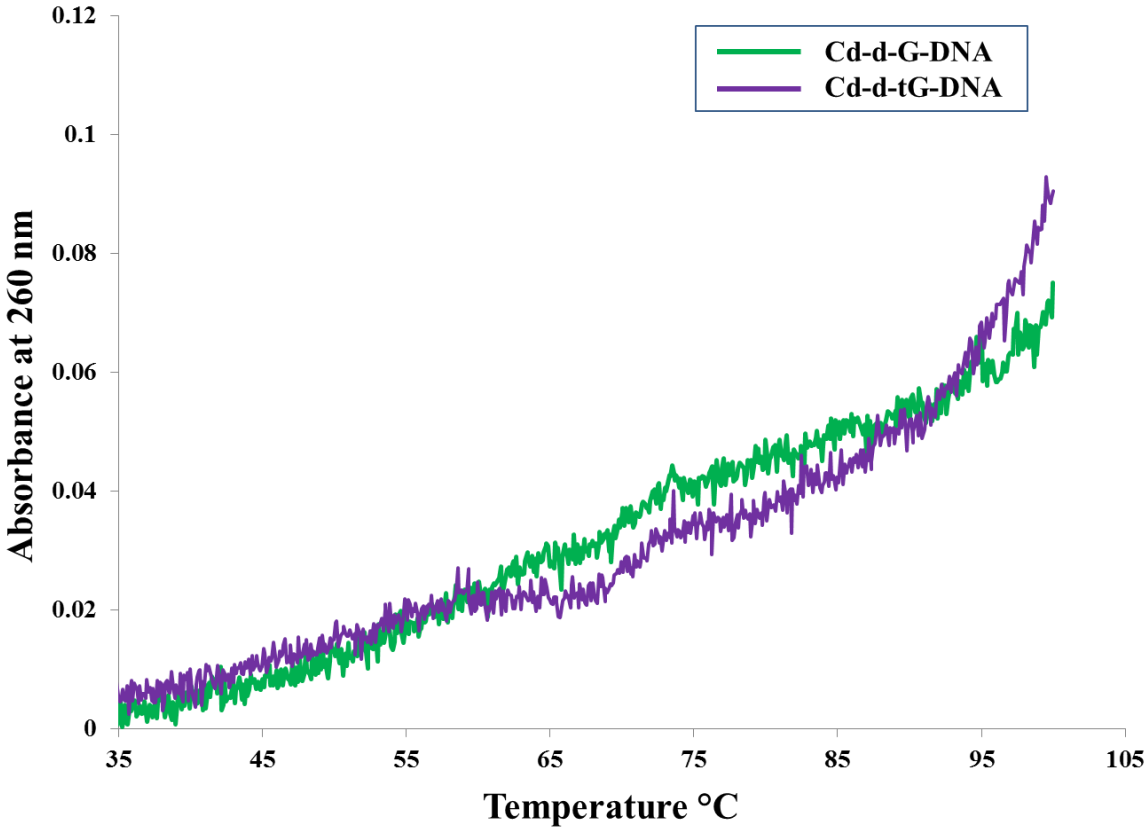

Figure 24. Tm comparison between **Cd-d-G-DNA (**green line**)** and **Cd-d-tG-DNA (**purple blue line**)**.

In summary, the titration studies of long unmodified and modified DNA, **d-G-DNA** and **d-tG-DNA** with Cd^{2+} suggest that the phosphate group is the first binding target for the metal ions, followed by base deprotonation coupled to complexation to the DNA. At high Cd^{2+} concentrations hyperchromism is observed at 260 nm for **d-tG** DNA but not **d-G**, indicating destacking of the bases. We suggest that under these conditions a new structure is formed involving Cd^{2+} binding to **d-tG-DNA** in a different mode. G-rich sequences can form higher order structures stabilized by cations such as quadruplexes or condensed toroids.[76,77] However; the bases should remain well stacked in these structures. Therefore, we suggest that a structure resembling M-DNA (see Chapter 1) is formed here, in which Cd^{2+} binds between the bases in a pair. Because Cd^{2+} forms octahedral complexes, the bases would destack to accommodate this preferred geometry.

4.4 Conclusion

In summary, 2'-deoxy-6-thioguanosine-5'-triphosphate (**d-tGTP**) was successfully synthesised from **d-tG** according to the method described by Broom.[19] **d-tGTP** was effectively incorporated into short primer-template of poly (**dG**)$_{10}$-poly (**dC**)$_{10}$ and extended *via* the enzymatic slippage reaction using Klenow exo$^-$ polymerase to fabricate thio-modified DNA **d-tG-DNA** of up to 300 bp in length. The **d-tG-DNA** was shown to be less stable than **d-G-DNA** through denaturation experiments. Subsequently, the addition of cadmium ions to thio-modified DNA suggested a structure resembling M-DNA (coordination polymer) is formed, in which Cd^{2+} binds between the two bases in a pair. The resulting metal coordination polymer was more stable than the metal free polymer.

4.5 Experimental

Unless otherwise stated, reagents were used without extra purification. Reagents were purchased from Sigma-Aldrich, New England Biolabs and Eurofins MWG Operon.

Synthesis of 2'-deoxy-6-thioguanosine-5'-triphosphate

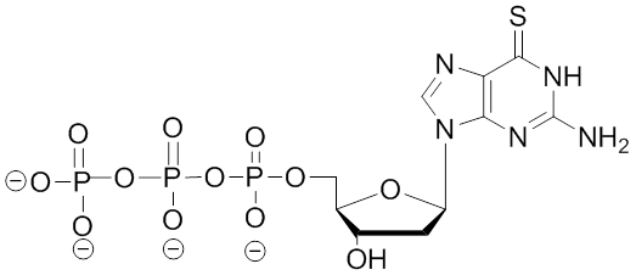

2'-Deoxy-6-thioguanosine (56.6 mg, 0.2 mmol) was dried in the vacuum oven at 50 ºC in the presence of phosphorus pentoxide for overnight. After 24 h the nucleoside was dissolved in trimethyl phosphate (1 ml), and then the solution was cooled in ice bath and stirred for 10 mins, after which phosphoryl oxychloride (57.5 µl, 0.6 mmol) was added to the reaction mixture. After 3 h, a solution of 0.5 M bis(tri-n-butylammonium) pyrophosphate (4 ml, 2 mmol) in DMF (3 ml) and dry tributylamine (0.6 ml) was directly added to the reaction mixture. After 1 min, 1 M aqueous triethylammonium hydrogen carbonate buffer (pH 7.5; 20 ml) was added and the mixture was stirred for 1 h. Yield = 0.044 mmol, 22 %. ^{31}P-NMR (D_2O): δ = -5.91 ppm (s, 1P, γ-P), -10.69 ppm (s, 1P, α-p), -21.90 ppm (s, 1P, β-P). ES-MS: m/z (negative mode) 521.9809 (Calcd. for $C_{10}H_{16}N_5O_{12}P_3S$ $(M-H)^-$ 521.9651).

Gel electrophoresis

The DNA synthesis products were electrophoresed on 1.2 % Lonza FlashGel^{TM}cassettes (Lonza Rockland, Inc). For recovering DNA samples, 1.2 % Recovery Lonza FlashGel^{TM}cassette was used. The fluorescent DNA stain in the Lonza gels was unidentified as it is proprietory. To characterise key properties of the dye, it was extracted from the gel into aqueous solution by soaking, and the absorption and emission spectra were measured. UV shows two maximum wavelengths around 300 nm

and 490 nm, whereas florescence had a maximum around 540 nm. From these data, we suggest the dye which Lonza may use is SyBr Gold Dye.

Slippage reaction-General procedure

A standard reaction was carried out in nanopure water containing 10 x reaction buffer, 15 mM of normal dNTP and 15 mM modified dNTP and 10 µM primer-template. The reactions were initialised by addition of polymerase 5 u/µl and proceeded for the stated times.

[a] For Klenow exo$^-$ polymerase using natural dNTP, the incubation was at room temperature and 37 ^{o}C, whereas when using modified dNTP, the incubation was at 50 ^{o}C.

[b] For Taq polymerase, the reaction was incubated at 55 ^{o}C.

[c] For Bsu polymerase and E.coli polymerase I, the incubations were at 37 ^{o}C.

The reactions were quenched by the addition of an equal volume of 40 mM EDTA.

UV spectra and titrations

UV spectra and titrations were recorded with a Cary100 Bio UV-visible spectrophotometer using 1 cm pathway of quartz cuvettes, using extinction coefficients for 2'-deoxyguanosine of ε = 11700 l mol^{-1} cm^{-1} and for 2'-deoxy-6-thioguanosine of ε = 24900 l mol^{-1} cm^{-1}. For UV titrations with Cd^{2+}, the preparation of the samples was as described in Table 1. The measurements were carried out at two wavelengths 260 nm and 345 nm.

DNA duplex	Thiobase con	Cd^{2+}con
G-DNA	2.5 µM	100 µM
d-tG-DNA	2.5 µM	150 µM

Table 1. Preparations of samples for the different UV experiments carried out of DNA duplex with cadmium nitrate.

AFM measurements

AFM images in Tapping Mode™ were performed in air on a Multimode Nanoscope IIIa (Veeco Instruments Inc., Metrology Group, Santa Barbara,CA). Alignment of **d-G-DNA** and **d-tG-DNA** was achieved by applying 5 µL of DNA samples onto a freshly cleaved mica surface. The droplet was left to stand for about 2 mins before being blown flat with gentle stream of nitrogen gas.

Melting temperature measurements

Melting profiles were obtained with a Cary100 Bio UV-visible spectrophotometer using 1 cm pathway quartz cuvettes. The measurements were carried out at different concentrations of free **d-G-DNA** and **d-G-DNA** with cadmium ions, and also free **d-tG-DNA** and **d-tG-DNA** with cadmium ions. Firstly, the melting temperature of free **d-G-DNA** and **d-tG-DNA** were measured at 1 µ M each in water and were heated at 95 °C at wavelength 260 nm. Then the melting temperature of UV titration sample of **d-G-DNA** with cadmium ions and UV titration sample of **d-tG-DNA** with cadmium were measured at the same temperature and wavelength.

References

(1) Kotlyar, A. B.; Borovok, N.; Molotsky, T.; Fadeev, L.; Gozin, M. *Nucleic Acids Res.* **2005**, *33*, 525.

(2) Gillerman, I.; Fischer, B. *Nucleosides Nucleotides & Nucleic Acids* **2010**, *29*, 245.

(3) El-Tayeb, A.; Qi, A. D.; Muller, C. E. *Journal of Medicinal Chemistry* **2006**, *49*, 7076.

(4) Liu, X. H.; Takahashi, H.; Harada, Y.; Ogawara, T.; Ogimura, Y.; Mizushina, Y.; Saneyoshi, M.; Yamaguchi, T. *Nucleic Acids Research* **2007**, *35*, 7140.

(5) Tomikawa, A.; Seno, M.; Sato-Kiyotaki, K.; Ohtsuki, C.; Hirai, T.; Yamaguchi, T.; Kawaguchi, T.; Yoshida, S.; Saneyoshi, M. *Nucleosides Nucleotides* **1998**, *17*, 487.

(6) Furman, R. R.; Hoelzer, D. *Seminars in Oncology* **2007**, *34*, S29.

(7) Domaoal, R. A.; McMahon, M.; Thio, C. L.; Bailey, C. M.; Tirado-Rives, J.; Obikhod, A.; Detorio, M.; Rapp, K. L.; Siliciano, R. F.; Schinazi, R. F.; Anderson, K. S. *Journal of Biological Chemistry* **2008**, *283*, 5452.

(8) Simoncsits, A.; Tomasz, J. *Nucleic Acids Research* **1975**, *2*, 1223.

(9) Tomasz, J.; Simoncsits, A.; Kajtar, M.; Krug, R. M.; Shatkin, A. J. *Nucleic Acids Research* **1978**, *5*, 2945.

(10) Hoard, D. E.; Ott, D. G. *Journal of the American Chemical Society* **1965**, *87*, 1785.

(11) Vanboom, J. H.; Crea, R.; Luyten, W. C.; Vink, A. B. *Tetrahedron Letters* **1975**, 2779.

(12) Moffatt, J. G.; Khorana, H. G. *Journal of the American Chemical Society* **1961**, *83*, 649.

(13) Sun, Q.; Edathil, J. P.; Wu, R.; Smidansky, E. D.; Cameron, C. E.; Peterson, B. R. *Organic Letters* **2008**, *10*, 1703.

(14) Davisson, V. J.; Davis, D. R.; Dixit, V. M.; Poulter, C. D. *Journal of Organic Chemistry* **1987**, *52*, 1794.

(15) Wu, W. D.; Bergstrom, D. E.; Davisson, V. J. *Journal of Organic Chemistry* **2003**, *68*, 3860.

(16) Yoshikawa, M.; Kato, T.; Takenishi, T. *Tetrahedron Letters* **1967**, *8*, 5065.

(17) Ruth, J. L.; Cheng, Y. C. *Mol. Pharmacol.* **1981**, *20*, 415.

(18) Ludwig, J. *Acta Biochimica Et Biophysica Hungarica* **1981**, *16*, 131.

(19) Mishra, N. C.; Broom, A. D. *Journal of the Chemical Society-Chemical Communications* **1991**, 1276.

(20) Ludwig, J.; Eckstein, F. *The Journal of Organic Chemistry* **1989**, *54*, 631.

(21) Ueda, T.; Miura, K.; Kasai, T. *Chemical & Pharmaceutical Bulletin* **1978**, *26*, 2122.

(22) Xu, Y. Z.; Zheng, Q.; Swann, P. F. *Tetrahedron* **1992**, *48*, 1729.

(23) Ludwig, J.; Eckstein, F. *Journal of Organic Chemistry* **1989**, *54*, 631.

(24) Krynetskaia, N. F.; Feng, J. Y.; Krynetski, E. Y.; Garcia, J. V.; Panetta, J. C.; Anderson, K. S.; Evans, W. E. *Faseb Journal* **2001**, *15*, 1902.

(25) Kovach, J. S.; Rubin, J.; Creagan, E. T.; Schutt, A. J.; Kvols, L. K.; Svingen, P. A.; Hu, T. C. *Cancer Research* **1986**, *46*, 5959.

(26) Elion, G. B. *Angewandte Chemie-International Edition in English* **1989**, *28*, 870.

(27) Yoshida, S.; Yamada, M.; Masaki, S.; Saneyoshi, M. *Cancer Res.* **1979**, *39*, 3955.

(28) Ling, Y. H.; Nelson, J. A.; Cheng, Y. C.; Anderson, R. S.; Beattie, K. L. *Mol. Pharmacol.* **1991**, *40*, 508.

(29) Ling, Y. H.; Chan, J. Y.; Beattie, K. L.; Nelson, J. A. *Molecular Pharmacology* **1992**, *42*, 802.

(30) Uribe-Luna, S.; QuintanaHau, J. D.; MaldonadoRodriguez, R.; EspinosaLara, M.; Beattie, K. L.; Farquhar, D.; Nelson, J. A. *Biochemical Pharmacology* **1997**, *54*, 419.

(31) Lahoud, G.; Timoshchuk, V.; Lebedev, A.; Arar, K.; Hou, Y. M.; Gamper, H. *Nucleic Acids Res.* **2008**, *36*, 6999.

(32) Darlix, J. L.; Fromageo.P; Reich, E. *Biochemistry* **1973**, *12*, 914.

(33) Amarnath, V.; Broom, A. D. *Biochemistry* **1976**, *15*, 4386.

(34) Somerville, L.; Krynetski, E. Y.; Krynetskaia, N. F.; Beger, R. D.; Zhang, W. X.; Marhefka, C. A.; Evans, W. E.; Kriwacki, R. W. *Journal of Biological Chemistry* **2003**, *278*, 1005.

(35) Dhavan, G. M.; Lapham, J.; Yang, S.; Crothers, D. M. *Journal of Molecular Biology* **1999**, *288*, 659.

(36) Li, Y.; Zon, G.; Wilson, W. D. *Proceedings of the National Academy of Sciences* **1991**, *88*, 26.

(37) Bohon, J.; de los Santos, C. R. *Nucleic Acids Res.* **2003**, *31*, 1331.

(38) Saenger, W. *in Springer Advanced Texts in Chemistry* Springer-Verlag, New York, 1984.

(39) Karran, P.; Bignami, M. *BioEssays* **1994**, *16*, 833.

(40) Villani, G. *Journal of Physical Chemistry B* **2009**, *113*, 2128.

(41) Spackova, N.; Cubero, E.; Sponer, J.; Orozco, M. *Journal of the American Chemical Society* **2004**, *126*, 14642.

(42) Schachman, H. K.; Adler, J.; Radding, C. M.; Lehman, I. R.; Kornberg, A. *The Journal of biological chemistry* **1960**, *235*.

(43) Josse, J.; Kaiser, A. D.; Kornberg, A. *The Journal of biological chemistry* **1961**, *236*.

(44) Radding, C. M.; Josse, J.; Kornberg, A. *The Journal of biological chemistry* **1962**, *237*.

(45) Kornberg, A.; Bertsch, L. L.; Jackson, J. F.; Khorana, H. G. *Proceedings of the National Academy of Sciences of the United States of America* **1964**, *51*.

(46) Beard, W. A.; Wilson, S. H. *Structure* **2003**, *11*, 489.

(47) Zhao, G., Guan. Y *Acta Biochim.Pol* **2010**, *42*, 722.

(48) Biles, B. D.; Connolly, B. A. *Nucleic Acids Res.* **2004**, *32*, e176.

(49) Berdis, A. J. *Chemical Reviews* **2009**, *109*, 2862.

(50) Borsenberger, V.; Kukwikila, M.; Howorka, S. *Organic & Biomolecular Chemistry* **2009**, *7*, 3826.

(51) Mullis, K. B.; Faloona, F. A. *Methods in Enzymology* **1987**, *155*, 335.

(52) Erlich, H. A.; Gelfand, D.; Sninsky, J. J. *Science (New York, N.Y.)* **1991**, *252*, 1643.

(53) Karthikeyan, G.; Chary, K. V. R.; Rao, B. J. *Nucleic Acids Res.* **1999**, *27*, 3851.

(54) Ji, J. P.; Clegg, N. J.; Peterson, K. R.; Jackson, A. L.; Laird, C. D.; Loeb, L. A. *Nucleic Acids Research* **1996**, *24*, 2835.

(55) Paiva, A. M.; Sheardy, R. D. *Biochemistry* **2004**, *43*, 14218.

(56) Ogata, N.; Miura, T. *Nucleic Acids Res.* **1998**, *26*, 4652.

(57) Ogata, N.; Morino, H. *Nucleic Acids Res.* **2000**, *28*, 3999.

(58) Ogata, N. *Biochimie* **2007**, *89*, 702.

(59) Miura, T. *Viva Origino* **2003**, *31*, 46.

(60) Tuntiwechapikul, W.; Salazar, M. *Biochemistry* **2001**, *41*, 854.

(61) Kurihara, H.; Nagamune, T. *Biotechnology Progress* **2004**, *20*, 1855.

(62) Lyons-Darden, T.; Topal, M. D. *Nucleic Acids Res.* **1999**, *27*, 2235.

(63) Ogata, N.; Miura, T. *Biochemistry* **2000**, *39*, 13993.

(64) Kato, T.; Liang, X. G.; Asanuma, H. *Biochemistry* **2012**, *51*, 7846.

(65) Borovok, N.; Molotsky, T.; Ghabboun, J.; Cohen, H.; Porath, D.; Kotlyar, A. *Febs Letters* **2007**, *581*, 5843.

(66) Schlötterer, C.; Tautz, D. *Nucleic Acids Res.* **1992**, *20*, 211.

(67) Tanaka, A.; Matsuo, Y.; Hashimoto, Y.; Ijiro, K. *Chem. Commun.* **2008**, 4270.

(68) Molotsky, T.; Tamarin, T.; Ben Moshe, A.; Markovich, G.; Kotlyar, A. B. *Journal of Physical Chemistry C* **2010**, *114*, 15951.

(69) Murphy, P. J., Williams, D.M, Harris, V.H *Organophosphorus reagents:A practical approach in chemistry.*; Oxford University Press Inc: Oxford University Press Inc, 2004.

(70) Santhosh, C.; Mishra, P. C. *Spectrochimica Acta Part a-Molecular and Biomolecular Spectroscopy* **1993**, *49*, 985.

(71) Inman, R. B.; Baldwin, R. L. *Journal of molecular biology* **1964**, *8*.

(72) Zhao, F.; Xu, J.; Liu, S. *Thin Solid Films* **2008**, *516*, 7555.

(73) Amo-Ochoa, P.; RodrÃ-guez-Tapiador, M. I.; Castillo, O.; Olea, D.; Guijarro, A.; Alexandre, S. S.; GÃ³mez-Herrero, J.; Zamora, F. *Inorganic Chemistry* **2006**, *45*, 7642.

(74) Duguid, J. G.; Bloomfield, V. A.; Benevides, J. M.; Thomas, G. J. *Biophysical Journal* **1995**, *69*, 2623.

(75) Alex, S.; Dupuis, P. *Inorganica Chimica Acta* **1989**, *157*, 271.

(76) Biffi, G.; Tannahill, D.; McCafferty, J.; Balasubramanian, S. *Nat Chem* **2013**, *5*, 182.

(77) Stevens, M. J. *Biophysical Journal* **2001**, *80*, 130.

Chapter 5 Conclusions and Future Directions

This chapter summarises the main findings of this thesis and proposes several recommendations and suggestions for the continuation of this project in the future.

5.1 Conclusions

This project has focused on thio-modified guanine base as a monomer, and incorporated into single-strand oligomers and into long DNA double strand polymers. These modified thioguanosine molecules (monomer, oligomer and polymer) were treated with metal ions which resulted in the formation of coordination complexes. In Chapter 2, **d-tG** has been successfully synthesised from **d-G** and has been compared with commercially available **tG** (ligand) for its ability to bind with a range of metal ions. The binding of ligand to metal ions resulted in the formation of coordination complexes with three ligands to one metal in the case of Co^{2+} and Ni^{2+} which was confirmed by x-ray crystallography. On the other hand, in the case of Cd^{2+}, the binding ratio was shown to be two ligands to one metal. However, ES-MS of the Cd-complex did show another possible binding ratio of three ligands to one Cd^{2+} and also evidence of a larger extended structure containing four ligands and two Cd^{2+} centers. This supports the theory that the Cd-complex with **tG** may form the desired 1D coordination polymer.

The crystal structure of the cadmium complex was not obtained; future work could include the examination of different conditions of solvent and techniques to grow the crystal structure with the view to form a 1D-coordination polymer.

Chapter 3 investigated the binding ability of Cd^{2+} by more than one thio-guanine base by the synthesis of 2, 3, 4, and 5 base oligomers *via* solid phase DNA synthesis. Subsequently the guanosine oligomers were converted into 6-thioguanosine oligomers *via* an on-column thiolation reaction. The binding results of thio-guanosine oligomers with Cd^{2+} have shown the binding within the complex is two thiobases coordinated to one Cd^{2+} in the case of the dimer and tetramer. For the trimer and pentamer, the binding ratio studies showed more than one binding species in the solution. Future work could include an investigation into the optimisation of thio- oligomer crystal growth, and

evaluation of its complexation with metal ions. In addition, the synthesis of more than 5 thio-base oligomers for example 9, 12 and 16 bp may be worth investigating.

In order to synthesise a long thio-DNA polymer, **d-tG** was converted into its corresponding triphosphate **d-tGTP** *via* phosphorus (V) chemistry. The afforded triphosphate, **d-tGTP** was then compatible for enzymatic extension reaction using a suitable polymerase. The **d-tGTP** was then effectively incorporated into a short primer-template of poly $(\mathbf{dG})_{10}$-poly $(\mathbf{dC})_{10}$ and extended through the enzymatic slippage reaction by Klenow exo$^-$ polymerase to produce thio-modified DNA **d-tG-DNA** of up to 300 bp in length. By studying the stability of **d-tG-DNA** compared to **d-G-DNA** through DNA denaturation experiments, it was found that the **d-tG-DNA** was shown to be less stable than **d-G-DNA**. Subsequently, the titration studies of long modified DNA, **d-tG-DNA** with Cd^{2+} suggest that the phosphate group is the first binding target for the metal ions, followed by base deprotonation coupled to complexation to the DNA. These findings suggested that a structure comparable to M-DNA is formed, in which Cd^{2+} binds between the two bases in a pair. The resulting Cd^{2+}-coordination polymer was shown to be more stable than the metal free polymer **d-tG-DNA.** The characterisation of this structure was unfortunately outside the scope of this thesis, but could be studied in the future.